NUREG/CR-3700

Decay of Buoyancy Driven Stratified Layers With Applications to Pressurized Thermal Shock (PTS)

Prepared by T. G. Theofanous, H. P. Nourbakhsh, P. Gherson, K. Iyer

School of Nuclear Engineering
Purdue University

Prepared for
U.S. Nuclear Regulatory
Commission

GPO Printed copy price: $6.50

NUREG/CR-3700
R4

Decay of Buoyancy Driven Stratified Layers With Applications to Pressurized Thermal Shock (PTS)

Manuscript Completed: February 1984
Date Published: May 1984

Prepared by
T. G. Theofanous, H. P. Nourbakhsh, P. Gherson, K. Iyer

School of Nuclear Engineering
Purdue University
West Lafayette, IN 47909

Prepared for
Division of Accident Evaluation
Office of Nuclear Regulatory Research
U.S. Nuclear Regulatory Commission
Washington, D.C. 20555
NRC FIN G1047
Under Grant No. NRC-G-04-83-003

SUMMARY

This report consists of two parts. In Part I physically based calculational models are proposed for predicting (a) conditions for stratification due to HPI in a circulating reactor loop (stratification model) and (b) cooldown transients due to HPI in a stagnated primary reactor fluid (thermal mixing model). The integral aspects of these models are confirmed by comparison to the CREARE 1/5-scale data. In part II the thermal mixing model is assessed in an integral as well as in a local sense by comparison to the first round of data from Purdue's 1/2-scale facility. These data are the only available large-scale data at this time and they are an important complement to CREARE's 1/5-scale results in constructing a basis for scale-up to reactor conditions. Facility construction, instrumentation, data reduction techniques and detailed experimental results are also included in Part II.

TABLE OF CONTENTS

ACKNOWLEDGMENTS

This work was supported by NRC Grant 03-003 sponsored by the Office of Nuclear Regulatory Research. We are grateful to Dr. N. Zuber for drawing and supporting our interest in this area and for his stimulating technical discussions, to Dr. D. Ross for his interest in our work, and Mr. J. Reyes for his cooperation and help with all aspects of our effort.

NOMENCLATURE

A	flow area
C	concentration
C_p	heat capacity
D	diameter
Fr_i	actual Froude No. of stream i: $Q_i/A_i/(gD_i(\Delta\rho/\rho))^{1/2}$
$Fr_{i,j}$	superficial Froude No. of flow stream i in cross section j: $Q_i/A_j/(gD_i(\Delta\rho/\rho))^{1/2}$
g	acceleration of gravity
h_i	height of stream i, or heat transfer coefficient on slab i
	plume length
L	width of downcomer
t	time
Q	flow rate
$\dot{Q}_w$	wall heat flux
S	wall slab surface area
T	temperature
U	velocity
V	volume
W	width of stream or of planar plume
x	distance from wall
y	distance from wall (along vertical diameter)

Greek

β	thermal expansion coefficient
ρ	density
τ	time constant for cooldown, Eq. (2)

Subscripts

C	cold stream
CL	cold leg
DC	downcomer
e	entrained in plume
H	hot stream
HPI	high pressure injection
L	loop
M	well mixed mean value, mixing cup
MM	mixed mean (local flow averaged)
p	plume
o	initial
PM	perfectly mixed
T	total
WS	wall surface
1,2	referring to stratified fluid layers

PART I: THE REGIONAL MIXING MODEL

TABLE OF CONTENTS

LIST OF FIGURES

1. Introduction

This Part of the report deals with the prediction of downcomer coolant temperature transients in the presence of stratification in the cold leg due to high pressure injection (HPI). Such thermal stratification is obtained at low (and zero) loop flow and it is not represented in the system codes (TRAC, RELAP5) currently used to simulate transients with Pressurized Thermal Shock (PTS) potential.

In the limit of perfect stratification the heavy (cold) HPI fluid (typically at $\sim 90^{\circ}F$) would flow as a separate stream "sliding" along the bottom of the cold leg and "falling" along the length of the downcomer thus exposing critical vessel wall welds to severe cooling and thermal stresses.

At the extreme of perfect mixing, on the other hand, a loop flow of only a few times that of the HPI would be adequate to drastically reduce the cooling effect of the safety injection. However, at very low loop flows (i.e., $Q_L \sim Q_{HPI}$) severe cooldown transients are predicted on the basis of the "perfect mixing" hypothesis also, i.e.,

$$T_M = \frac{Q_L}{Q_L + Q_{HPI}} T_L + \frac{Q_{HPI}}{Q_L + Q_{HPI}} T_{HPI} \qquad (1)$$

In the case of zero loop flow the temperature, T_M, within the volume which is assumed as perfectly mixed, T_M, will decay exponentially to the HPI value with a time constant τ given by

$$\frac{T_M(t) - T_{HPI}}{T_{LO} - T_{HPI}} = e^{-t/\tau} \qquad \tau = \frac{V_M}{Q_{HPI}} \qquad (2)$$

Taking the cold leg plus the downcomer volume for V_M would yield a time constant of a few hundred seconds, i.e., a rather severe cooldown.

The physically unrealistic and highly conservative nature of the "perfect stratification" assumption has been readily recognized, and early work emphasized the "perfect mixing" (or "control volume," or "time constant") approach [1,2], which appeared to be consistent with the experimental simulations at CREARE obtained with an 1/5-scale cold leg-and-downcomer configuration.

The existence and implications of "partial stratification," whose behavior is *not* bounded by the two extremes considered above, were first discussed by Theofanous and Nourbakhsh [3]. Using flow regime stability criteria it was possible to demonstrate that for typical high pressure injection in a stagnated loop a well-mixed cold leg could not exist. The implied cold leg stratification, was then shown to induce a recirculating flow pattern extending to the bottom of the lower vessel plenum and of the loop seal. The effect is to "activate" these relatively large additional volumes, thus substantially increasing the cooldown time constant. Furthermore the degree of stratification (i.e., the temperature difference between the cold and hot streams) which is consistent with this flow pattern was found to be rather small. These trends were confirmed with

subsequent tests with the 1/5-scale facility at CREARE which was modified to incorporate the lower plenum, loop seal, and pump volumes [7]. A quantitative interpretation of these test results in terms of a more integrated, and refined, version of the original, "regional mixing," model [3], is given in Sections 3.1 and 3.2 of this paper. Predictions for a full-scale PWR are presented in Section 3.3.

The modeling approach in the "regional mixing model" is to mechanistically integrate local flow and mixing behavior into an overall system response. In addition to the 1/5-scale model comparisons of Section 3, it is important to experimentally support the computational model with regards to its accurate representation of local phenomena (plume decay, counter-current flow accommodation of the cold leg exit) as well as with regards to its applicability to full-scale. This topic is covered in Part II of this report.

Actual PTS transients [4,5] exhibit rather complicated HPI and loop flow histories. Periods of high loop flows (perfect mixing, system code results applicable) are interdispersed with periods of flow stagnation (stratification, "regional mixing model" applicable). Partial stratification is also possible at non-zero loop flow. A procedure for assessing the extent (timing) of such "intermediate" behavior is developed in Section 2.

2. Criteria for Prediction of Stratification

As pointed out earlier [3] for a well mixed condition there must be sufficient loop flow to not only break up the HPI plume but also to produce a stable exit of the resulting flow into the downcomer. The boundary of stability is expressed in terms of the local Froude number by [3]:

$$Fr_{CL} = 1 \tag{3}$$

which is the degenerate case of the more general condition

$$Fr_1^2 + Fr_2^2 = 1 \tag{4}$$

expressing the stationarity of long waves at the interface of two parallel flowing liquid layers of different density [6]. These conditions are analogous to flow choking (or flooding) in the sense that the two-layer flow cannot be changed gradually through a state where Eq. (4) applies without leading to violent disruption of the flow by internal discontinuities (i.e., hydraulic jump for the case at hand).

The condition expressed by Eq. (3) is applied with the total flow Q_T:

$$Q_T = Q_L + Q_{HPI} \tag{5}$$

at a mixed mean temperature given by Eq. (1), i.e.,

$$\frac{Q_T}{A_{CL}} = \left\{ g\, D_{CL}\, \frac{\rho_M - \rho_L}{\rho_M} \right\}^{1/2} \tag{6}$$

The density ratio may be expressed in terms of the component flows and densities by employing, approximately, "average" expansion coefficients, i.e.,

$$\frac{\rho_M - \rho_L}{\rho_M} \simeq \bar{\beta}_M \, (T_L - T_M) \tag{7}$$

$$\frac{\rho_{HPI} - \rho_L}{\rho_{HPI}} \simeq \bar{\beta}_{HPI} \, (T_L - T_{HPI}) \tag{8}$$

to cast with the help of Eq. (1), Eq. (6) in the form:

$$Fr_{HPI,CL} \simeq \left\{1 + \frac{Q_L}{Q_{HPI}}\right\}^{-3/2} \left[\frac{\bar{\beta}_M}{\bar{\beta}_{HPI}}\right]^{1/2} \tag{9}$$

The effect of β-T nonlinearity, as deduced by exact calculations, is to slightly change the flow ratio exponent in Eq. (9), i.e.,

$$Fr_{HPI,CL} \simeq \left\{1 + \frac{Q_L}{Q_{HPI}}\right\}^{-7/5} \tag{10}$$

The stratification/mixing boundaries expressed by these equations are compared, in Figure 1, with the CREARE 1/5-scale data [1,7,10]. Excellent agreement is noted. Both data and theoretical development were aimed to the $Fr_{HPI,CL}$ range of interest indicated in Figure 1 and the predicted boundary outside this range should be viewed with caution.

Clearly, depending on the imposed conditions, various degrees of stratification may be obtained. We have made no effort to distinguish between them. Rather, from the oscillatory temperature behavior, typically evident even at rather small departures from perfect mixing, an unambiguous classification into the perfectly mixed and stratified (lumping of all degrees) states was made. In this sense, our stratification criteria should be considered as providing a high estimate of the flow ratio, Q_L/Q_{HPI}, necessary for ignoring stratification. This would be particularly true as $Fr_{HPI,CL} \to 0$ yielding drastic increase in mixing both as a result of plume mechanics (see section 3.1) as well as a result of backflow in the injection line itself (see Part II).

However, the above approach is adequate for our purposes. Typically natural circulation flows are in the 150-250 kg/s range, while high pressure injection occurs at ~ 10 kg/s. In terms of our stratification criteria parameters, these values correspond to $Fr_{HPI,CL} \sim 5 \cdot 10^{-2}$ and $Q_L/Q_{HPI} \sim 20$, indicating perfect mixing. That is, for actual reactor conditions stratification would be obtained *only* during flow stagnation.

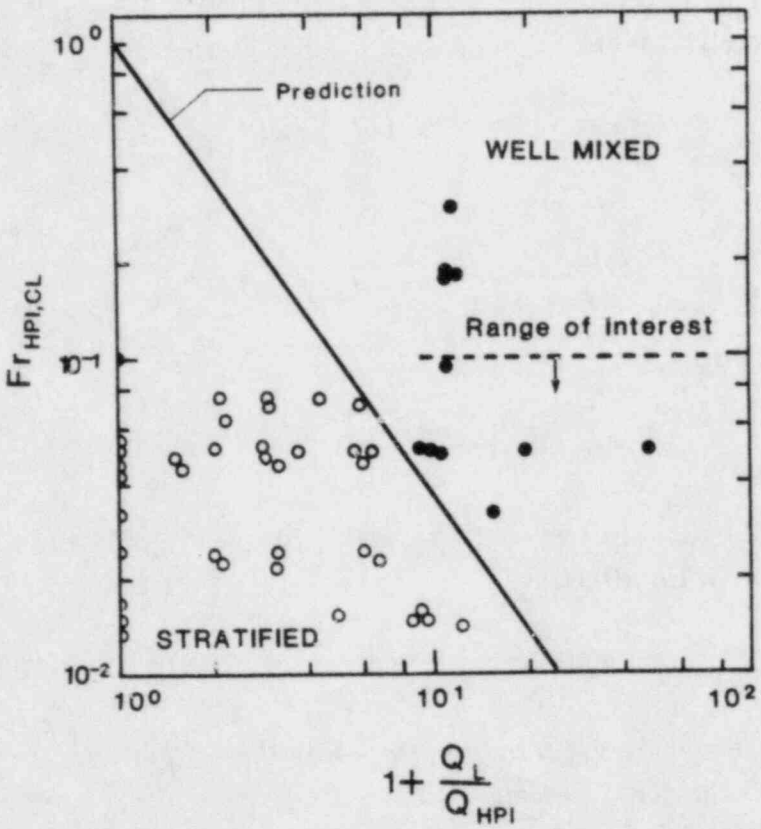

Figure 1. Comparison of theoretical stratification criteria, Eq. (10), with the CREARE 1/5-scale test results.

3. Prediction of Cooldown Transients due to HPI

3.1. The Regional Mixing Model (RMM)

In the previous section, we concluded that for PWR conditions "stratification" under HPI may be considered synonymous with interruption of loop natural circulation ("stagnation"). The RMM was devised to address this condition of interest. The conceptual model and calculational procedure are explained with the help of Figure 2. As we argued previously [3, 11], due to the large volume of the whole system, compared to the HPI flow rate (i.e, long time constant), and except for a short-duration initial transient associated with the establishment of the overall circulation pattern, the temperatures decay slowly compared to the fluid particle residence time in the cold stream portion of the circuit. The whole process may then be viewed as a decay (by mixing-entrainment) of highly buoyant jets (plumes) in a slowly varying ambient. That is,

temperatures of cold layers are estimated quasi-statically (i.e., as in snap-shots in time) on the basis of the instantaneous "ambient" temperature which is found as a continuous function of time for the duration of the transient.

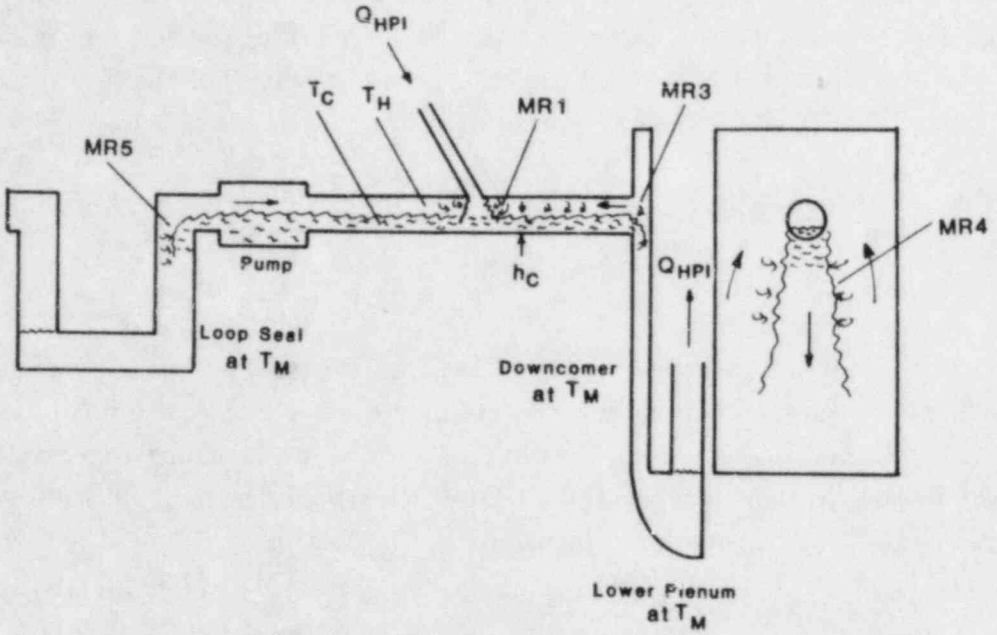

Figure 2. Conceptual definition of the Regional Mixing Model. (MRi is mixing region i.)

This procedure is based on the observation that significant decay of the HPI plume occurs right at the point of injection (MR1) yielding already relatively small degree of stratification in the horizontal portion of the cold leg. The temperature difference between hot and cold streams is further reduced by mixing in the regions near the entrance to the loop seal and downcomer volumes. Thus, from an overall energy balance point of view these volumes as well as that of the lower plenum are taken as well mixed, at T_M. Taking into account the heat conducted from the metal walls, $\dot{Q}_W$, the T_M transient may be found from:

$$\rho V_T C_P \frac{dT_M}{dt} = \dot{Q}_W - Q_{HPI}\ \rho C_P\ (T_M - T_{HPI}) \tag{11}$$

$$\dot{Q}_W = \sum_i h_i S_i\ (T_{WS_i} - T_M) \tag{12}$$

The wall surface temperature, T_{WS}, is found numerically by solving the conduction equation in an appropriate number of metal slabs (corresponding to the vessel and pipe walls and the thermal shield). The local heat transfer coefficient, h_1, is obtained from an appropriate mixed convection correlation or, a rough constant, and uniform, value may be utilized. The stainless steel vessel wall cladding is also taken into account.

The temperature T_M physically exists, as discussed above, in the major portions of the loop seal, downcomer, and lower plenum. In the cold leg (pump) and in the upper part of the downcomer, however, T_M represents an "average" of the hot and cold stream temperatures, and it can be partitioned by:

$$V' T_M = V_H T_H + V_C T_C \tag{13}$$

$$V' = V_H + V_C \tag{14}$$

V_H includes the volume of the top layer of the cold leg (and pump), as well as an upper section of the downcomer, extending two cold leg diameters below the cold leg centerline (see Part II, Section 5), which is essentially at the hot stream temperature. As neither the volumes, nor the temperatures of the two streams in the cold leg are known, additional constraints are required to complete the partition.

At the point of injection (MR1) the cold plume decay depends upon the injection Froude number (Fr_{HPI}) and the length, h_H, of the plume exposed in the hot stratum. A κ-ϵ-θ' turbulence model [3,8] was utilized to compute this decay. The results for total plume flow (Q_{HPI} plus entrainment) and mixed mean plume temperature are given in Figures 3 and 4. In the area of interest these results may be represented by:

$$\frac{Q_e}{Q_{HPI}} = 0.5176 \left[\frac{h_H}{D_{HPI}}\right]^{1.236} Fr_{HPI}^{-0.414} \tag{15}$$

for: $0.2 < Fr_{HPI} < 1.$ and $0.5 < \frac{h_H}{D_{HPI}} < 4$

$$\frac{T_{MM} - T_H}{T_{HPI} - T_H} = \left[1 + \frac{Q_e}{Q_{HPI}}\right]^{-1} \tag{16}$$

which were utilized, for convenience, in the computations. The stratification in the horizontal travel (MR2) is stable, any additional mixing is neglected, that is,

$$T_C = T_{MM} \tag{17}$$

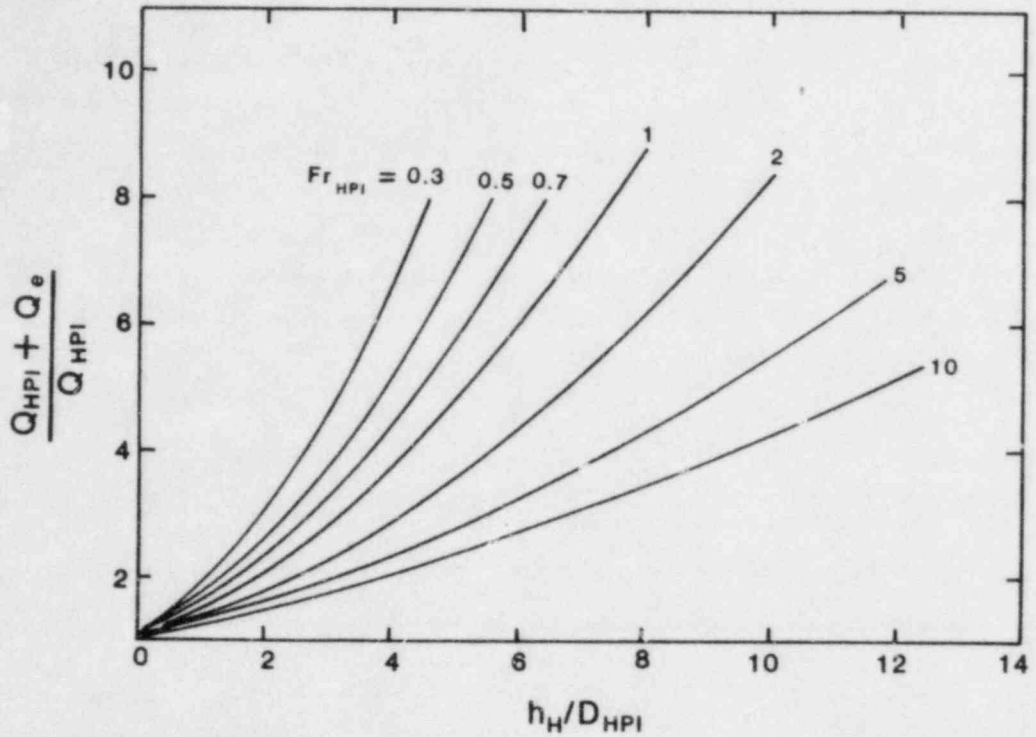

Figure 3 Prediction of total flow in axisymmetric plumes (jets).

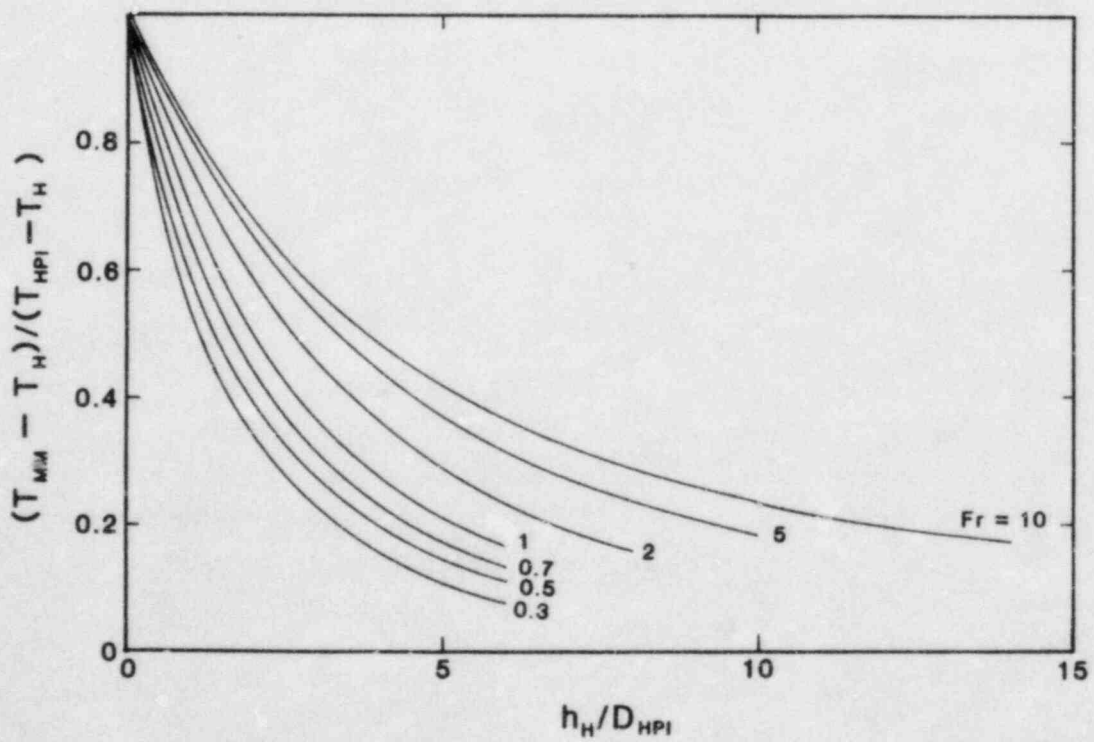

Figure 4. Prediction of mixed mean (radially averaged) temperature for axisymmetric jets (plumes).

The essential control of the overall process, *that is problem closure*, is provided by the counter-current flow condition at the two ends of the cold leg, i.e., the cold stream will accelerate till it reaches a value consistent with plume decay and hot stream entrainment requirements as expressed by the condition of stationarity of long waves, Eq. (4). The algebra for circular cross sections was carried out by Gardner [9] in connection with a different application, and the result indicates a Froude number definition with a length scale expressed as the ratio of the stream cross sectional area and the width, W, of contact between the two streams, i.e.,

$$\frac{(Q_C/A_C)^2}{g\,\frac{A_C}{W}\,\frac{\rho_C - \rho_H}{\rho_C}} + \frac{(Q_H/A_H)^2}{g\,\frac{A_H}{W}\,\frac{\rho_C - \rho_H}{\rho_H}} = 1 \tag{18}$$

The flow areas may be expressed in terms of the stream heights, h_C,h_H, by:

$$A_C = (\pi - \alpha)\frac{D_{CL}^2}{4} + (0.5\,D_{CL} - h_H)\,h_H^{1/2}(D_{CL} - h_H)^{1/2} \quad for\ h_C > \frac{D_{CL}}{2} \tag{19}$$

where,

$$\alpha = arctan\ \{h_H^{1/2}(D_{CL} - h_H)^{1/2}/(0.5\,D_{CL} - h_H)\}$$

and:

$$A_C = \alpha\,\frac{D_{CL}^2}{4} - (0.5\,D_{CL} - h_C)\,h_C^{1/2}(D_{CL} - h_C)^{1/2} \quad \text{for } h_C < \frac{D_{CL}}{2} \tag{20}$$

where,

$$\alpha = arctan\ \{h_C^{1/2}(D_{CL} - h_C)^{1/2}/(0.5\,D_{CL} - h_C)\}$$

while,

$$A_{CL} = A_C + A_H \quad \text{and} \quad D_{CL} = h_H + h_C \tag{21}$$

In the calculations presented here we apply Eq. (18) only at the vessel junction of the cold leg. To make up for this simplification we assume symmetry, i.e., equal amounts of HPI plume entrainment, Q_e obtained from each side of the cold leg. Thus for the left-hand portion of the cold leg the hot and cold streams will each move at a rate of $1/2\ Q_e$ while mass conservation on the right-hand portion requires that:

$$Q_H = \frac{1}{2}\,Q_e \tag{22}$$

$$Q_C = Q_{HPI} + \frac{1}{2} Q_\ell \tag{23}$$

This simplification could be removed (i.e., apply Eq. (18) to both ends of the cold leg) after the role of pump internals is clarified from current 1/2-scale tests at Purdue and CREARE.

Equations (13) to (23) are solved by iteration with the help of the equation of state $\rho=\rho(T)$. For each time of interest, T_M is obtained from Eqs. (11) and (12), values of T_H and h_H are guessed and updated till all equations and in particular the conditions expressed by Eqs. (13) and (18) are satisfied. Convergence is rapid with typical computation CPU times of ~ 50s on the CDC 6600 for a 3,000 s transient.

The temperatures in the downcomer may be estimated on the basis of the temperature transient of the cold stream spilling over the cold leg. Visualization experiments indicate (see Part II) that within ~ 1 cold leg diameter the flow is highly three dimensional with a tendency of the plume to descend closer to the core-side of the downcomer width. From the point of view of fluid temperature in the vicinity of the vessel wall this behavior may be closely bounded by considering two extreme cases: (a) the plume is totally contained between the core barrel and the thermal shield (if present), and the temperature along the vessel wall is nearly uniform and given by T_M, i.e., Eqs. (11) and (12), and (b) the plume occupies the whole width of the downcomer, (that is, it descends as a planar plume, with an initial width obtained, by continuity, from the flow in the cold stream) and decays by entrainment from its sides. The centerline (minimum) temperature of such a plume is estimated from the results of the κ-ϵ-θ' turbulence mixing model shown in Figure 5 [3].

The whole computation has been automated in a user-convenient form in the code REMIX (for REgional MIXing model). The associated documentation is in preparation [12].

3.2. Application to CREARE 1/5-scale Tests

The "Regional Mixing Model" was applied to all 1/5-scale tests carried out with zero loop flow. Typical comparisons of the predictions with the experimental measurements are presented here.

Some of the test runs were carried out with thermally induced buoyancy (initial primary fluid temperature and HPI flow and temperature adjusted to obtain the appropriate Froude number) and some with solute induced buoyancy (HPI flow and salt concentration adjusted to obtain the requisite Froude number, while the temperature was used as a "tracer".) We have chosen for this presentation one from each of these two classes. For the solute-induced buoyancy case (Run 100) the RMM was applied using mass in the place of energy balances and the equivalence between dimensionless

concentration and temperature distributions, i.e., neglecting the density changes due to temperature variations. After the mixing pattern is calculated, the results are converted to thermal dilution, for comparison with the experimental data.

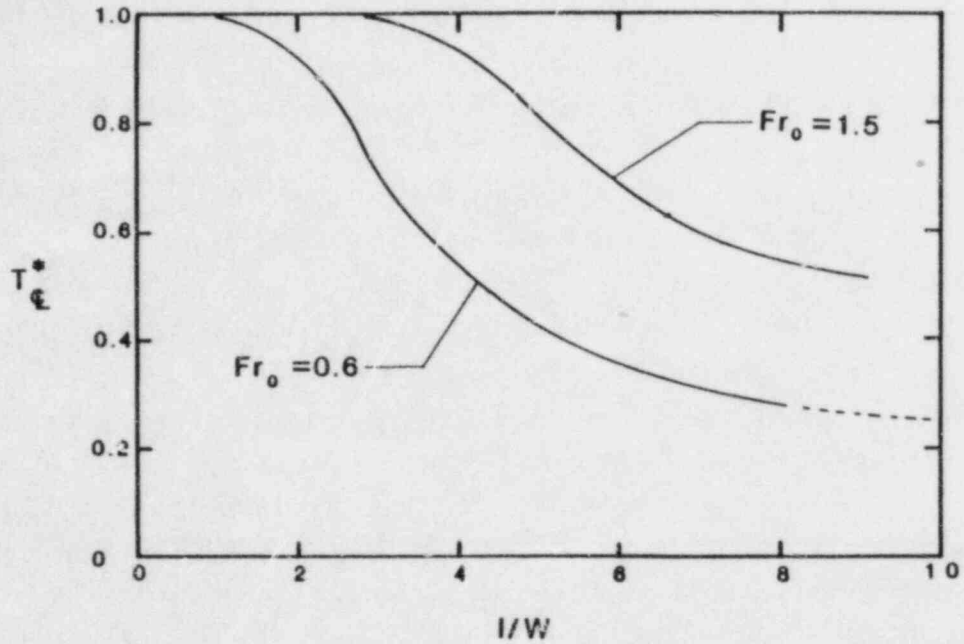

Figure 5. Prediction of centerline temperature in planar plumes, as function of axial position. Fr_0 is based on plume width and velocity at the entrance to downcomer.

Also, the experimental program covered a number of combinations of the loop seal, pump simulator, and lower plenum volumes, attached to the basic, previously used, cold leg/downcomer configuration. In an attempt to reasonably represent these variations in experimental conditions one run was chosen (for these comparisons) with all volumes attached (Run 100) and one having only the lower plenum present (Run 106).

The predictions are compared to the experimental data in Figures 6 to 9. The agreement is uniformly good. Notice that the whole downcomer behavior is closely bounded by the cold stream (T_C) and the mixing cup (T_M) temperatures. That is, within one-to-two cold leg diameters temperatures as low as T_C are found (at the plume centerline), while further below temperatures approach T_M. It should be noted that wall heat (1 inch-thick acrylic downcomer walls, steel lower plenum, etc.) was also taken into account in these calculations, and was found to be significant for the long-duration thermal runs. Due to the low thermal diffusivity of acrylic the results are not sensitive to the value of heat transfer coefficient utilized in Eq. (12). The losses to the environment, which are also important were taken into account.

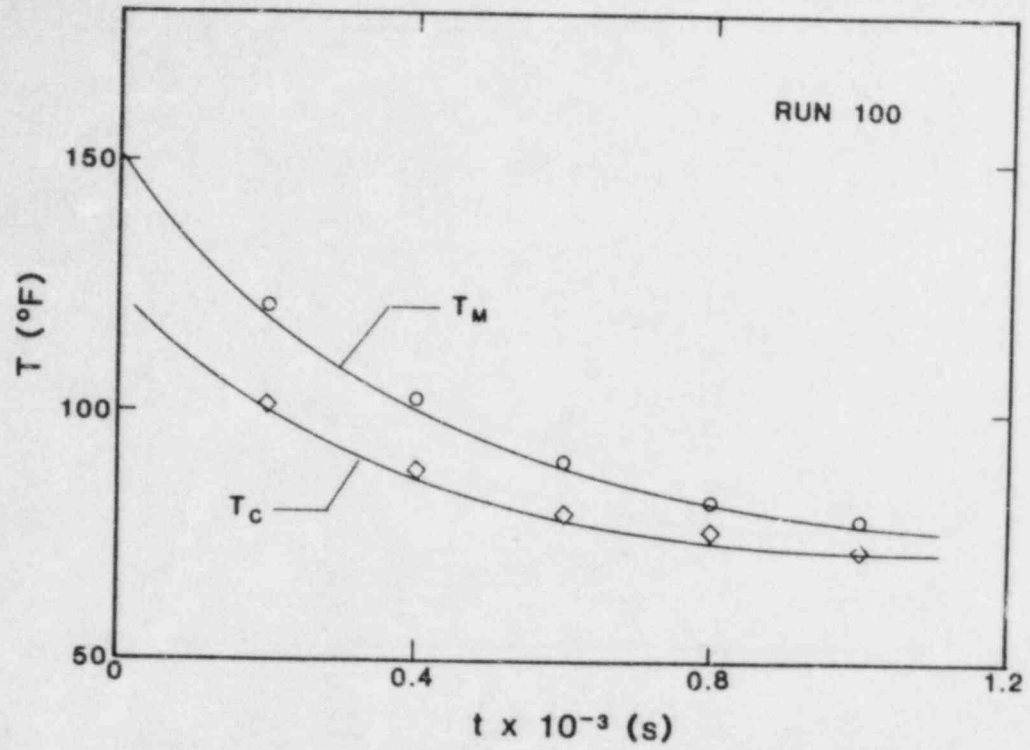

Figure 6. Comparison of RMM prediction with CREARE's 1/5 scale test results. (○ for T_{106}, outflow; □ for T_1, bottom of cold leg.)

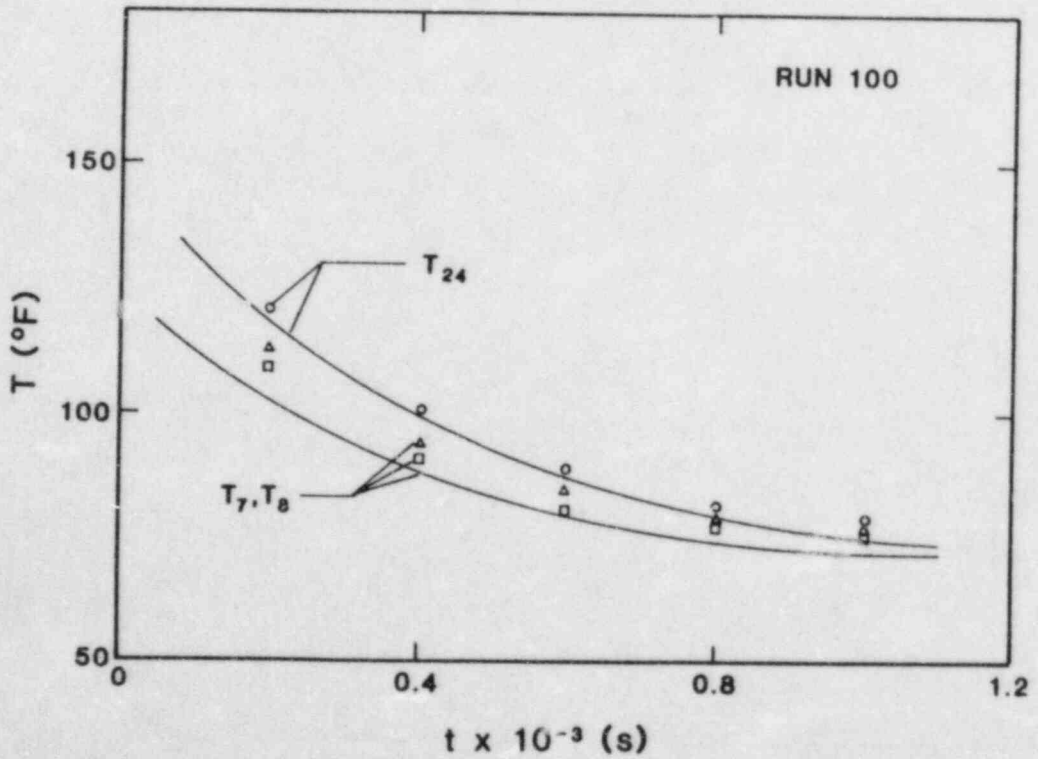

Figure 7. Comparison of RMM prediction with CREARE's 1/5-scale test results. ($T_{7,8}$ at ~ 1D and T_{24} at ~ 6D below the cold leg in the downcomer.)

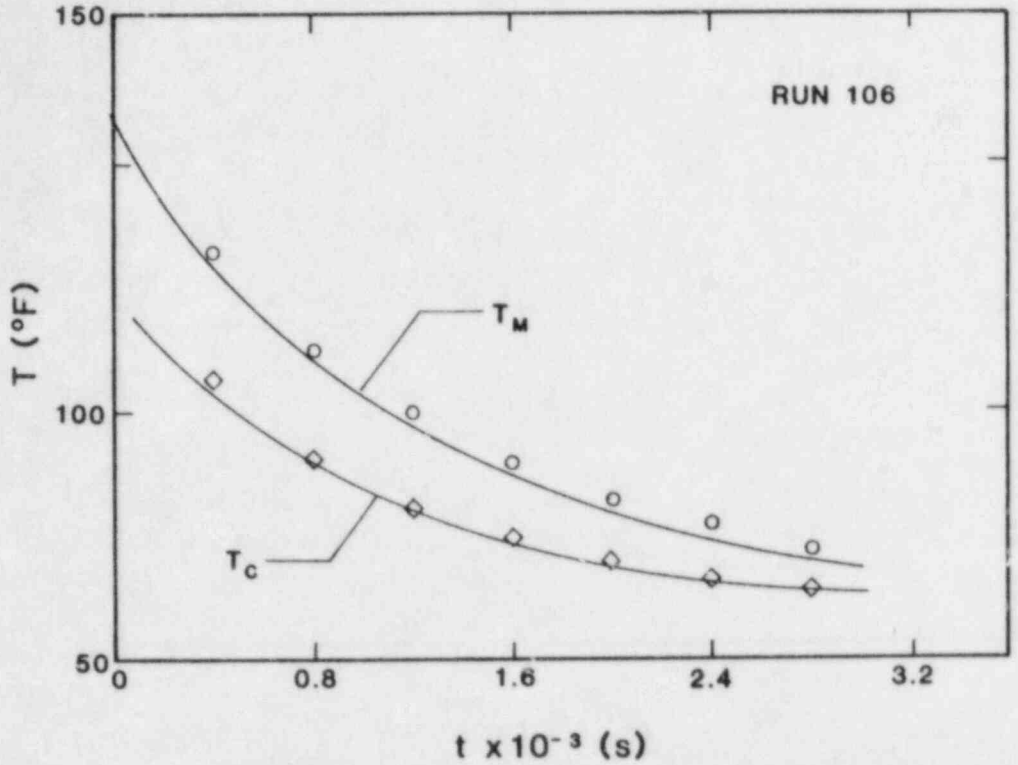

Figure 8. Comparison of RMM prediction with CREARE's 1/5-scale test results. (○ for T_{106}, outflow; □ for T_1, bottom of cold leg.)

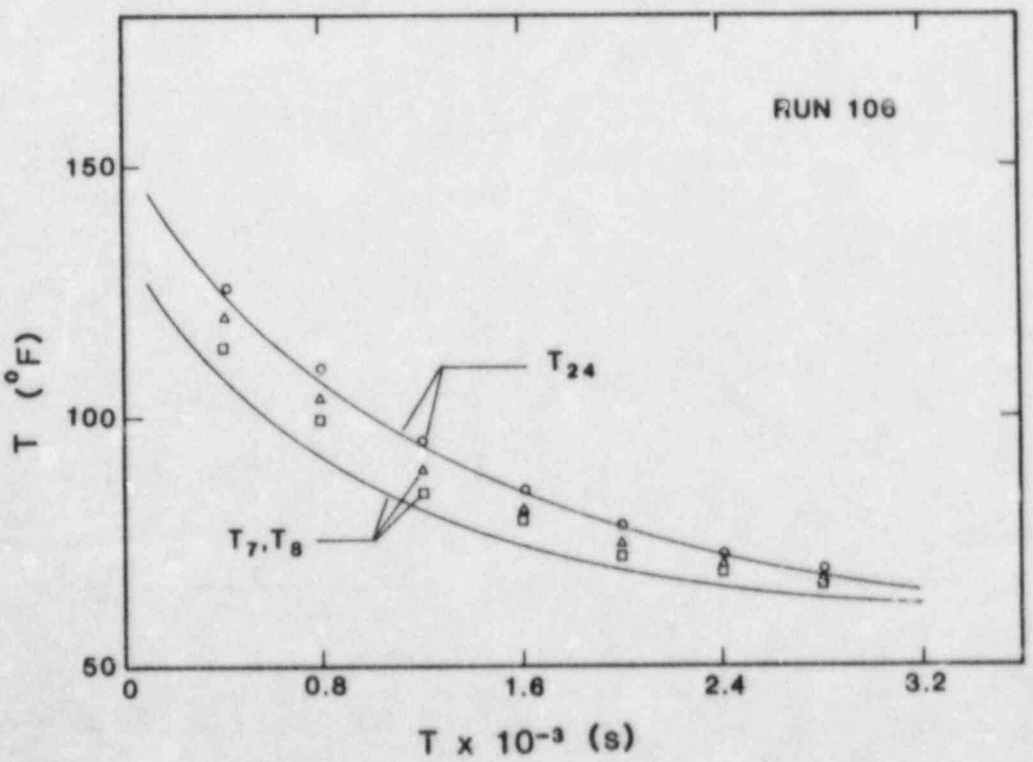

Figure 9. Comparison of RMM predictions with CREARE's 1/5-scale test results. ($T_{7,8}$ at ~ 1D and T_{24} at ~ 6D below the cold leg in the downcomer.)

3.3. Predictions for Full-Scale PWRs.

The RMM is now used to predict the cooldown transient due to HPI in a 3-loop Westinghouse PWR. Loop circulation is *assumed* stopped for the duration of the accident. This calculation is given only as illustration. In actual transients, loop flow due to natural circulation is reestablished periodically.

Metal heat was taken into account, (conduction slabs including the stainless wall cladding), except for the pump and lower plenum internal structures. Results presented here were obtained for a fluid-to-wall heat transfer coefficient kept constant at 500 BTU/hr ft^2 ^oF. A sensitivity study obtained with a value of 100 BTU/hr ft^2 ^oF produced the same results. The overall sensitivity for heat transfer coefficients between 0 and 1000 BTU/hr ft^2 ^oF is less than 10^oF

The fluid temperature transient is shown in Figure 10. The vessel wall temperature profiles as they develop with time are shown in Figure 11. These wall temperatures were based on the mixing cup (T_M) downcomer temperatures and are, therefore, representative of the global vessel wall response. However, as shown in Figure 10 in the entrance region of the downcomer plume fluid temperatures are only 50^oF lower (at the plume centerline) than T_M, hence the *maximum* change in applying these temperature profiles on a local basis would also be ~ 50^oF.

These results are very close to those presented earlier [3] and they indicate that the fluid cooldown would be mild and the imposed vessel wall temperature gradients are rather small.

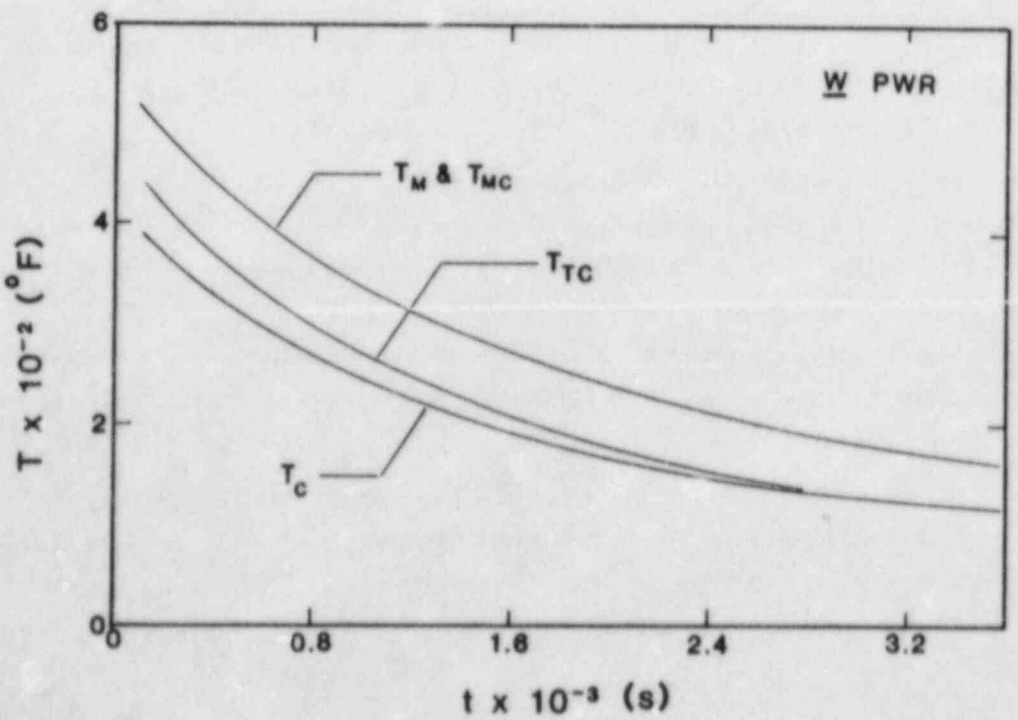

Figure 10 Predicted fluid temperature transients in a 3-loop Westinghouse PWR (T_{TC} and T_{MC} are at top and middle of core elevations in the downcomer).

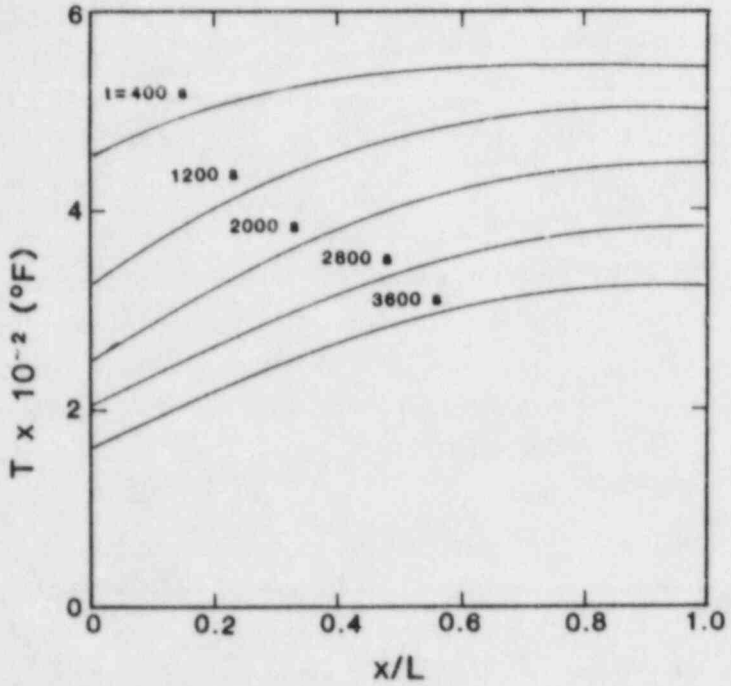

Figure 11 Predicted vessel wall temperature transients for the cooldown transient depicted in Fig. 10.

4. Conclusions

A physically based calculational model is proposed for predicting cooldown transients due to HPI in a stagnated primary reactor fluid. The integral aspects of this model are confirmed by comparison to CREARE's 1/5-scale data.

It is concluded that stratification rather than perfect mixing controls the response. As a consequence of stratification large scale circulations are set up that cause the participation of the HPI with all the primary fluid in the loop seal (one leg and horizontal segment), pump, cold leg, downcomer, and lower plenum. Due to this large thermal inertia the global cooldown is rather slow. Furthermore, it is shown that the stratified layers do not represent precipitously colder regions, and, in general, they follow the global cooldown within ~ 50-100 ^{o}F.

A criterion for the existence of perfect mixing, in the presence of loop flow was developed on the basis of theoretical considerations. The predictions are consistent with CREARE's 1/5-scale results. For typical natural circulation and HPI flows this criterion predicts good mixing, i.e., in practice stratification could only be observed during flow stagnation.

REFERENCES

1. Rothe, P.H. and M.F. Ackerson, "Fluid and Thermal Mixing in a Model Cold Leg and Downcomer with Loop Flow," EPRI Report NP-2312, April 1982.
2. Levy, S. and J.M. Healzer, "Approximate Prediction of Heat Transfer During Pressurized Thermal Shock with No Loop Flow and with Metal Heat Addition," Prepared by S. Levy Inc. for Brookhaven National Laboratory, August 1982.
3. Theofanous, T.G. and H.P. Nourbakhsh, "PWR Downcomer Fluid Temperature Transients Due to High Pressure Injection at Stagnated Loop Flow," Proceedings of Joint NRC/ANS Meeting on Basic Thermal Hydraulic Mechanisms in LWR Analysis, September 14-15, 1982, Bethesda, MD, NUREG/CP-0043, pp. 583-613.
4. Koenig, J.E. et al., "TRAC Analyses of Potential Overcooling Transients at the Calvert Cliff-1 PWR for PTS Risk Assessment," Los Alamos National Laboratory, September 1, 1983.
5. Fletcher, C.D. et al., "RELAP5 Thermal Hydraulic Analysis of Pressurized Thermal Shock Sequence for the Oconee-1 Pressurized Water Reactor," EGG-NSMD-6343, July 1983.
6. Turner, J.S., "Buoyancy Effects in Fluids," Cambridge University Press, 1979.
7. Fanning, M.W. and P.H. Rothe, "Transient Cooldown in a Model Cold Leg and Downcomer," EPRI Report NP-3118, May 1983.
8. Chen, C.J. and W. Rodi, "A Mathematical Model for Stratified Turbulent Flows and its Application to Buoyant Jets," 16th IAHR Congress, Section C.a., San Paulo, Brazil (1975).
9. Gardner, G.C., "Motion of Miscible and Immiscible Fluids in Closed Horizontal and Vertical Ducts," Int. J. of Multiphase Flow, Vol. *3*, pp. 305-318 (1977).
10. Rothe, P.H. and M.W. Fanning, "Thermal Mixing in a Model Cold Leg and Downcomer at Low Flow Rates," EPRI Report NP-2935, March, 1983.
11. Theofanous, T.G., H.P. Nourbakhsh, P. Gherson, and K. Iyer, "Decay of Buoyancy Driven Stratified Layers with Applications to PTS," Proc. of 11th Water Reactor Safety Research Information Meeting, National Bureau of Standards, Gaithersburg, MD, October 24-26, 1983 NUREG/CP-0048, Vol. 2, pp. 91-94.
12. H.P. Nourbakhsh and T.G. Theofanous, "REMIX: A Computer Program for Temperature Transients due to HPI at Stagnated Loop Flow," NUREG/CR-3701.

PART II: PURDUE'S 1/2-SCALE EXPERIMENTS

TABLE OF CONTENTS

LIST OF TABLES

LIST OF FIGURES

LIST OF FIGURES (Continued)

1. Introduction

Natural circulation loop flow is typically 10-20 times larger than High Pressure Injection (HPI). Stratification effects on Pressurized Thermal Shock evaluations, therefore, become relevant for transients that yield loop stagnation (interruption of the natural circulation path) and high primary system pressure. This is the physical situation addressed by our Regional Mixing Model (RMM) [1,2]. The RMM is a fundamentally-based model that integrates "local" plume mixing behavior into an overall system response. A priori application, to the CREARE 1/5-scale (systems) tests indicate good predictive capability (see part I). Comparisons with the limited available, low Froude number, simple plume (planar and axisymmetric) data [2] on the other hand indicate that the model incorporates quantitatively realistic mixing rates at the local level. Yet, encouraging as these comparisons might be, they could not be considered complete. In addition to the considerably more detailed data on "continuous" space-time distributions of temperatures (concentrations) *and* velocities which would be required to test the RMM at the fundamental level, it was noted that certain "scaling" and "injection-geometry" considerations should be addressed [1,2].

There are several related aspects to the "scaling" question. They all originate from the fact that Froude number scaling, in reduced-scale experiments, yields large non-similarities in Reynolds numbers (particularly for low values of $\Delta\rho/\rho$, as for example, in low pressure thermal tests). For instance, the injection Reynolds numbers for the 1/5-scale CREARE runs 100 and 106 (see Part I) were $8.\_ \times 10^3$ and 2.6×10^3 respectively as compared to a value of 8.4×10^4 expected in the reactor. Similarly, the cold stream Reynolds numbers, as deduced from the analysis of Part I, were 2.2×10^3 and 2.7×10^3 respectively as compared to a reactor value of $\sim 3.2 \times 10^5$. The question is whether the implied barely-developed turbulence in the experiment could have caused a significant loss of similitude. In a similar vein, the potential effects on the breakup (entrainment) characteristics of the injected plumes (already shown numerically to be sensitive to the initial level of turbulence [2]) should be considered. Finally, the associated significant reductions (in the experiment) of the momentum fluxes in the various currents (streams) cannot be a priori neglected. Such effects are relevant in impact-like geometries, such as where the injected plume encounters the cold leg boundary or where the cold stream encounters the core barrel as it enters the downcomer, and might be responsible for variations (non-similarity) in local flow regimes and mixing.

The "injection geometry" questions originate in the possibility of backflow into the injection line as dictated by the flow regime stability criteria (see [1] and Part I) at the injector outlet. Such counter-current flow in the injection line would imply, in terms of the RMM, increased contact of the jet with the ambient fluid (i.e. an effective longer axial dimension) and hence increased mixing.

The test facility described herein was designed with these questions in mind. This report details its construction (section 2), instrumentation, data acquisition systems, and reduction techniques (section 3). The experimental program is given in Section 4. Results from the first series of tests in a generic cold leg/downcomer/lower plenum configuration, and their analytical interpretation are given in section 5. A report with results from the second series of tests in reactor specific geometries as represented by Oconee (B&W), Calvert Cliff (CE) and H.B. Robinson (W) will be forthcoming.

2. Experimental Facility

The basic experimental facility consists of a transparent (acrylic) 1/2-scale model of a typical PWR cold leg/downcomer/lower plenum configuration as illustrated in Figures 1-3. The lower portion of the downcomer and of the lower plenum (corresponding to one of the cold legs) are geometrically distorted such as to keep the overall height of the facility manageable, although their total volume is correctly scaled. The injection line indicated is typical of a Westinghouse 3 loop plant (H.B. Robinson). Other injection geometries from representative Combustion Engineering (Calvert Cliff) and Babcock & Wilcox (Oconee) plants, as shown in Figure 4 may also be interchangeably used. For reference purposes, the arrangement of Figure 1 will be called Configuration #0. The reactor-specific arrangements will be referred to by the corresponding reactor vendor and they will include (in addition to the appropriate injection geometry) the pump/loop seal components, as shown in Figure 5 (Configurations *W* and CE), or the lower, inclined, portion of the cold leg (Configuration B&W) as shown in Figure 4. The data reported herein are from Configuration #0.

The buoyancy effect is obtained by the use of salt solutions, such that density changes of up to $\Delta\rho/\rho \sim 18\%$ (i.e. near prototypic) may be obtained easily. For any particular choice of salt concentration in the injection stream, the appropriate Froude number is obtained by selecting the injection flow rate. This solution is filtered, metered, and pumped from the supply tank, through the injection line, into the facility which is initially filled with fresh water. The displaced fluid volume exits through the overflow line and into the receiving tank. With a tank capacity of 275 gallons, a typical run time of ~ 10 to 20 minutes is obtained. The facility has been designed for 7 psig internal pressure, and the overflows shown in Figure 1 were introduced for additional safety.

3. Instrumentation and Data Reduction Techniques

The essential measurements during an experimental run include the injection flow rate and local-instantaneous velocities and concentrations (dilution). The injection flow rate is continuously recorded on a strip chart recorder as the output of a turbine flow meter (Mead Instruments, Model PT 250) calibrated to an uncertainty of 1%.

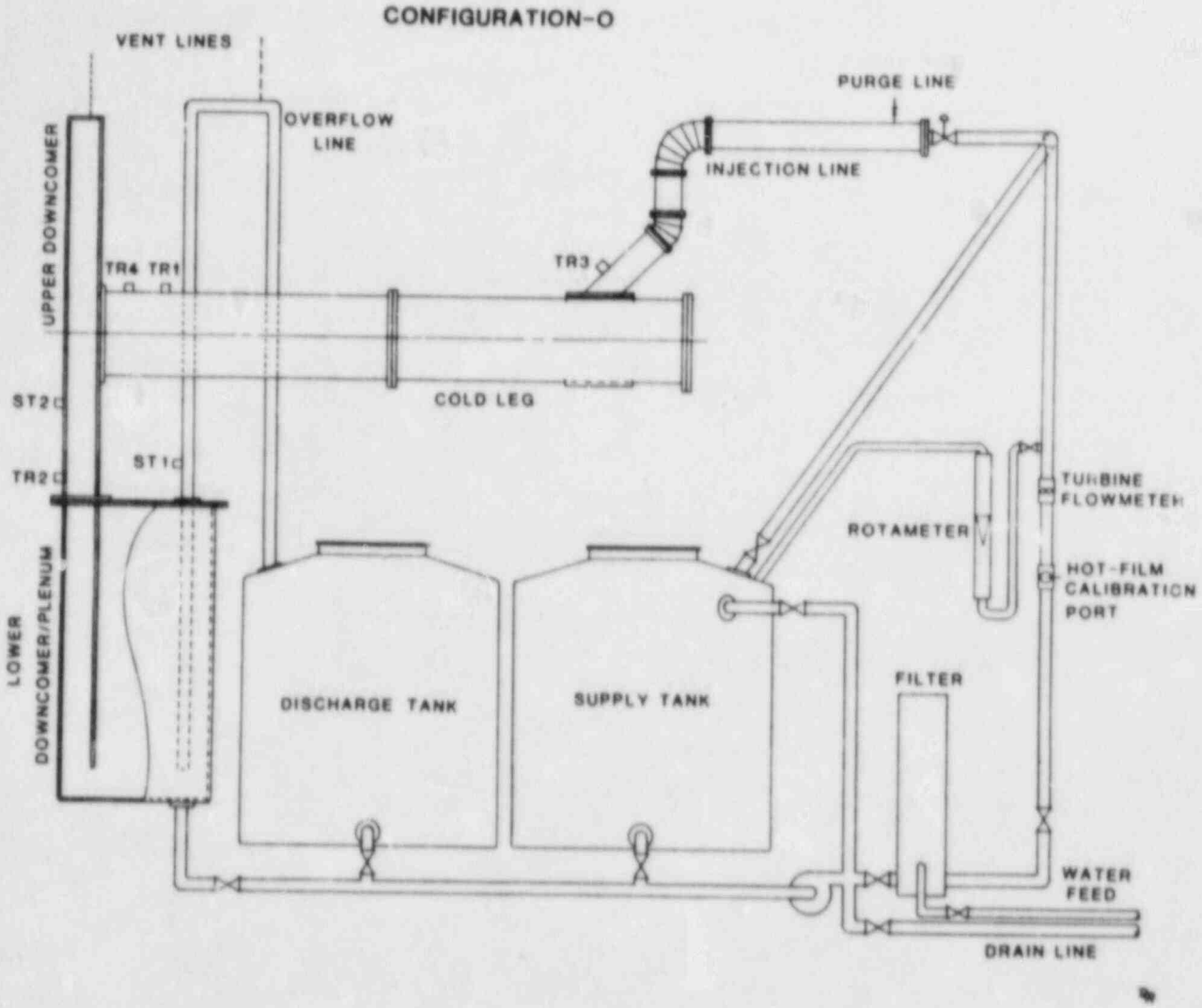

Figure 1. Schematic of the facility -- side view (Configuration 0). Dimensions (D: diameter, l: length, w: width, L: gap, all in m; V: volume in m^3): Cold Leg -- D: 0.343, $l_{HFI\ to\ DC}$: 2.11, $l_{HFI\ to\ blind\ flange}$: 0.76; Injection Line -- D: 0.108, l_{45}: 0.39, l_{vert} : 0.37, l_{horiz} : 1.07; Upper Downcomer -- l: 2.72, w: 1.18, L: 0.127; Lower Downcomer/Plenum -- V 0.912; Supply Tank -- V: 1.05; Discharge Tank V:1.05; Overflow Line -- D: 0.051. Probe locations: TR1,4 (traversing); ST1,2 (stationary).

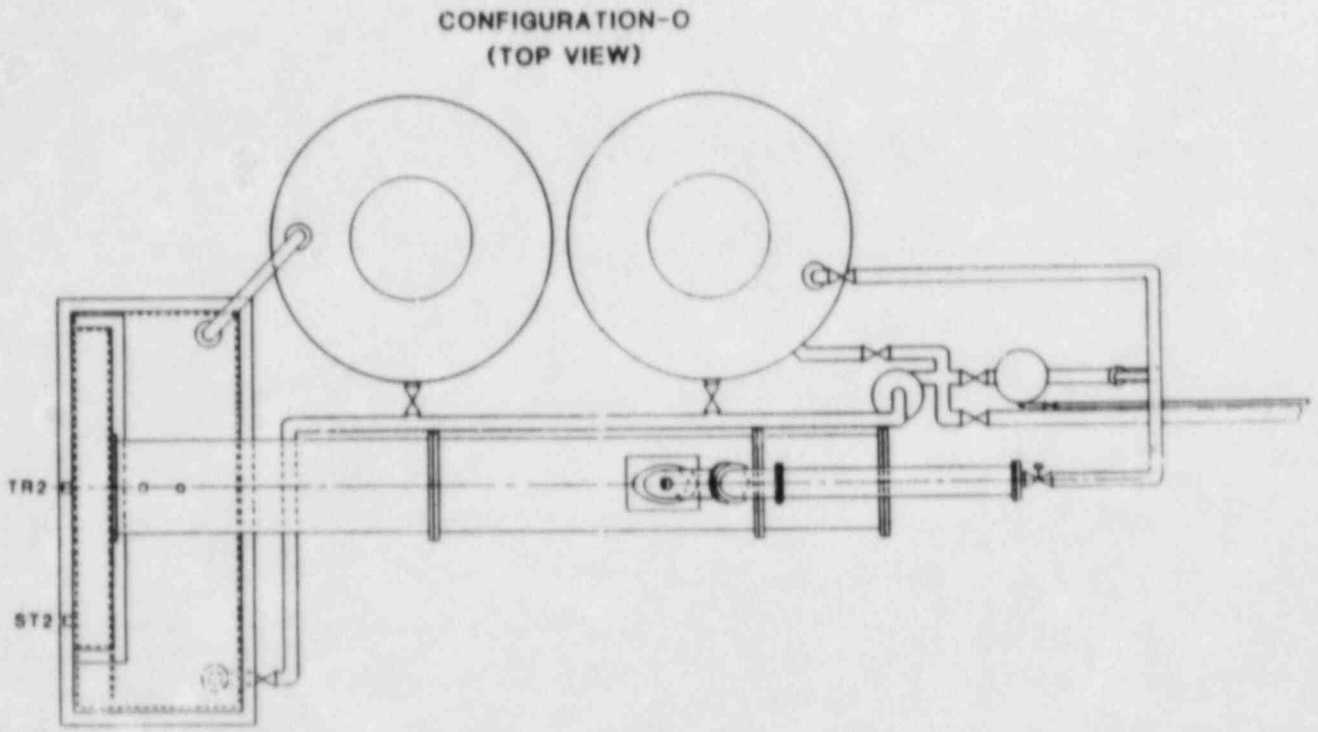

Figure 2. Schematic of the facility -- top view (Configuration 0). See caption of Figure 1 for dimensions.

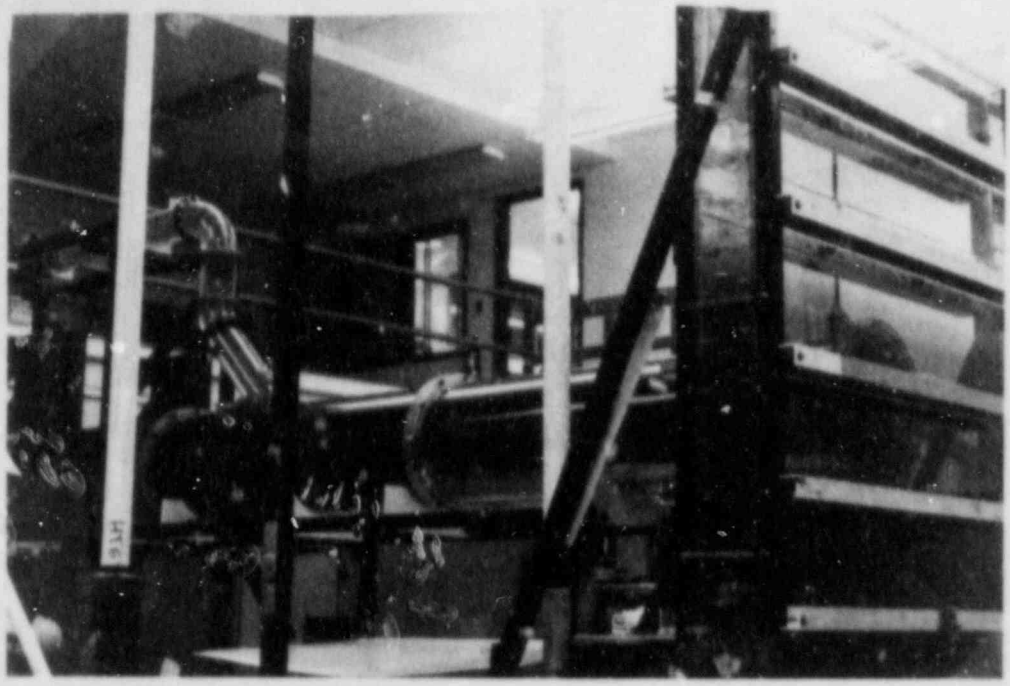

a

b

Figure 3. Photographs of the experimental facility: (a) injection line/cold leg/downcomer, (b) cold leg/downcomer/plenum.

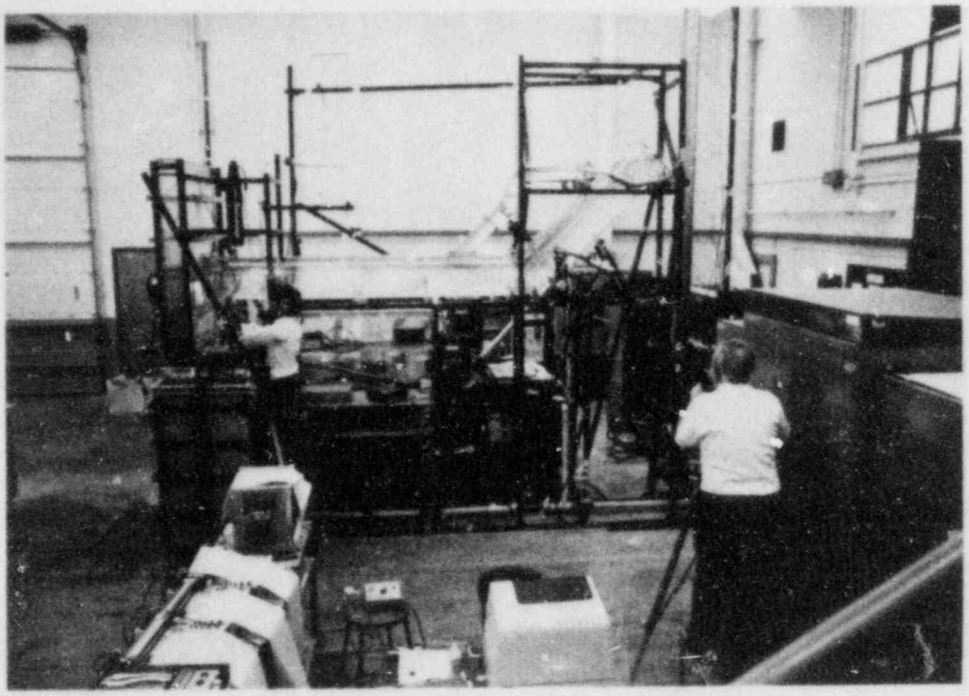

c

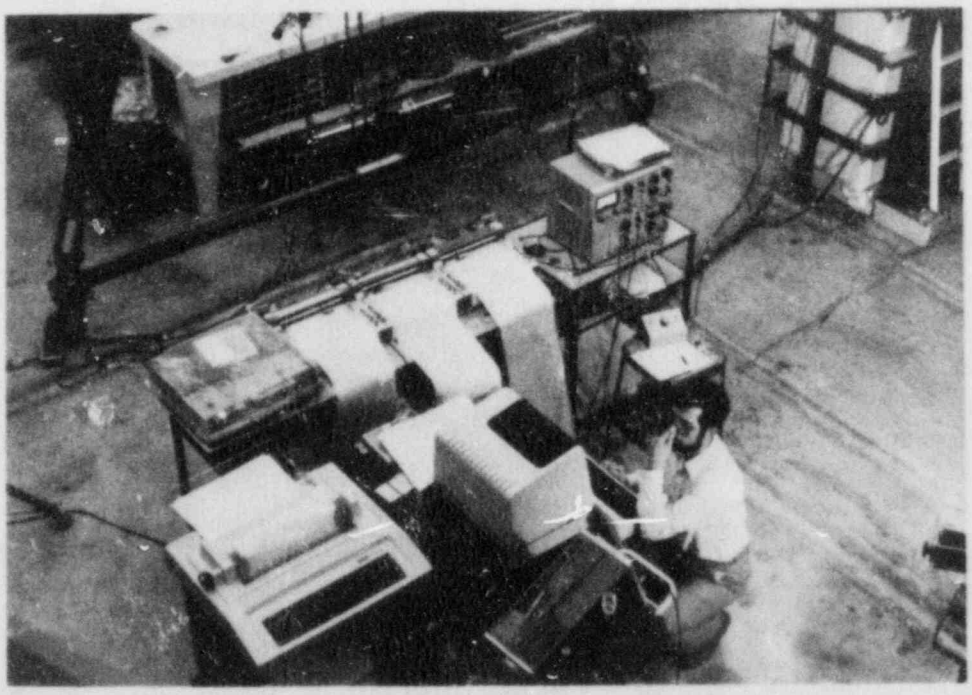

d

Figure 3 (continued). Photographs of the experimental facility: (c) general view (d) instrumentation set-up.

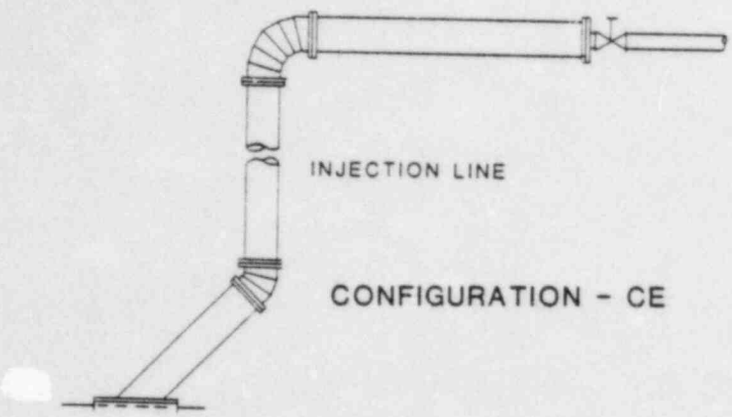

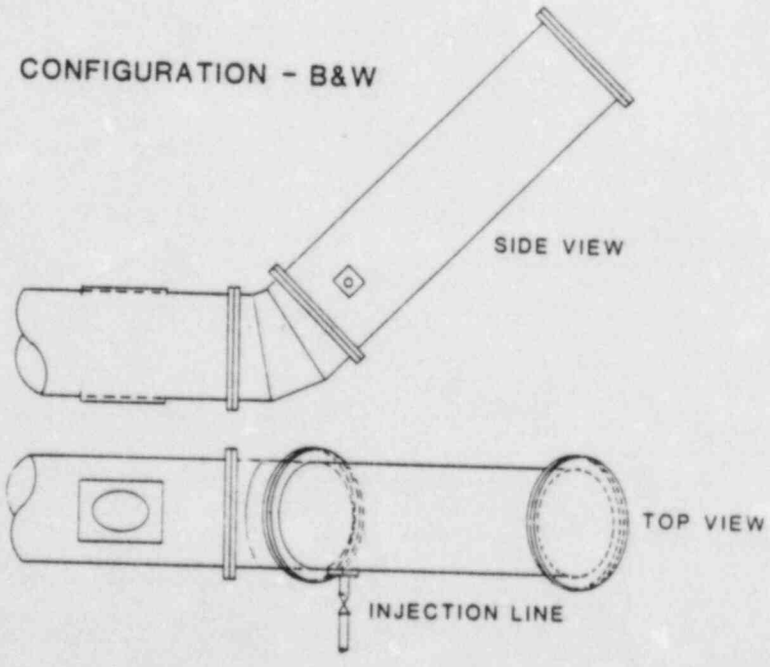

Figure 4. Injector geometries (Notations as in caption of Figure 1). Configuration CE: Injection Line -- D: 0.108, l_{45}: 0.57, l_{vert} : 1.12, l_{horiz} : 1.07. Configuration B&W: Injection line -- D: 0.108; Elbow -- D: 0.343, l: 0.30; Inclined 45° section -- D: 0.343, l: 1.24, $l_{inj\ to\ flange}$: 0.15.

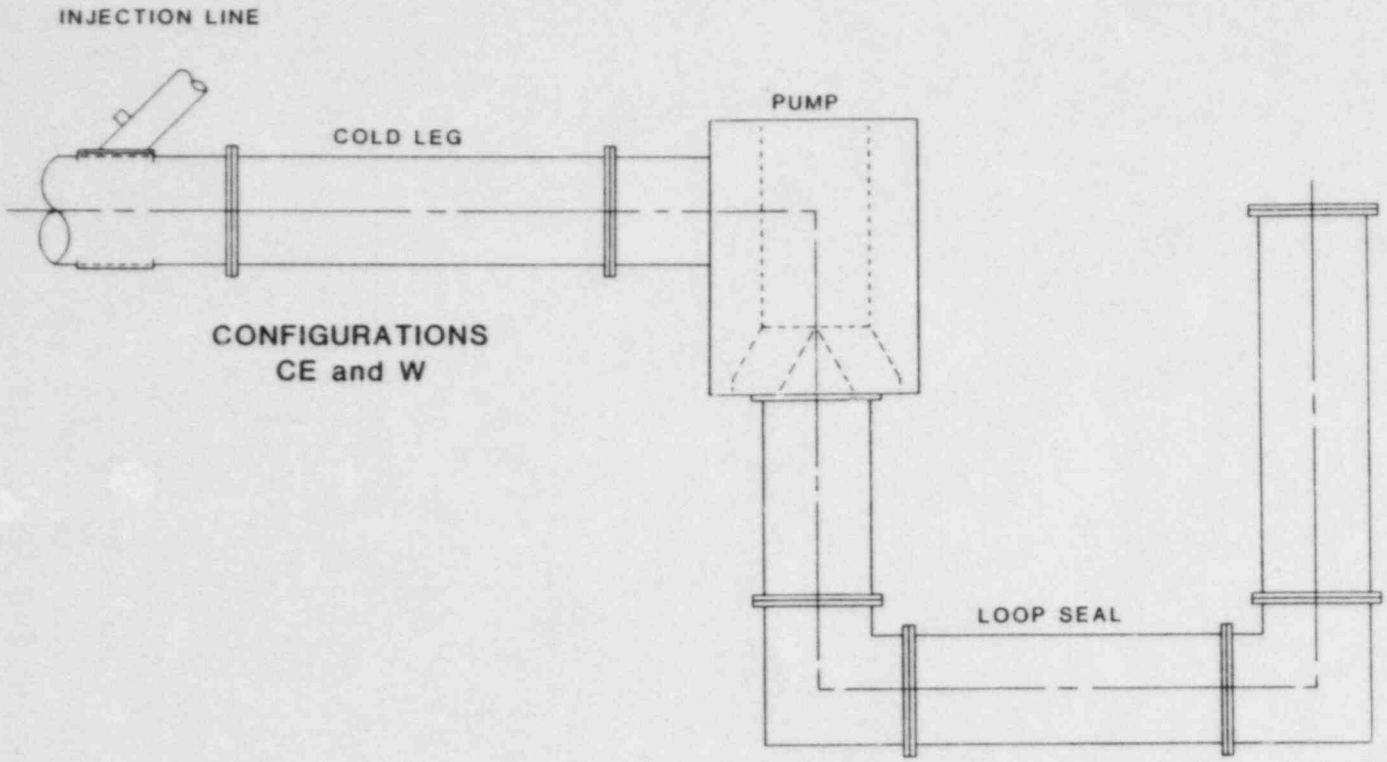

Figure 5. Pump/loop seal assembly. (Notations as in caption of Figure 1). Cold Leg -- D: 0.343, $l_{inj\ to\ pump}$: 1.63; Pump -- V: 0.28; Loop Seal -- D: 0.343, l_{vert} (pump side): 0.98, l_{horiz}: 1.65, l_{vert}: 1.59.

Hot film probes and conductivity probes are employed for the measurement of velocities and concentrations respectively. In the present Configuration #0, such measurements are made by traversing these probes at the exit of the cold leg (along a vertical diameter) and in the downcomer (along the gap) at about 45 cm below the lower cold leg lip, as shown in Figure 1. These will be referred to as locations TR1 and TR2 (for traversing) respectively. A third conductivity probe is intended to record, continuously, the "ambient" (in the RMM sense). This is accomplished by immersing it in the overflow line, position ST1 (for stationary). Another location, ST2, off to the side of the downcomer, as shown in Figures 1 and 2 has also been occasionally used. Provisions for traverses along a diameter of the injection line, near its outlet (location TR3), and along a cold leg diameter somewhat closer to the exit (location TR4), have also been made, but not employed as yet. To avoid interference, and to optimize our data acquisition capability, the hot film and conductivity probes are used separately in each run. That is, for each experimental condition a pair of runs is made. With an excellent reproducibility and facility of operation (~ 3 hours for preparation and run time) this procedure is acceptable and not particularly burdensome.

The hot film probes are TSI model 1212-60NaCl and come specially insulated for longevity in a brine environment. They are used in conjunction with a two-channel TSI anemometer and data conditioning system, Model TSI 1050. The probe is carried within a stainless steel tube (0.95 cm OD) with the sensor element (0.015 cm in diameter) protruding as illustrated in Figure 6.

The probe of position TR1 is operated at an overheat ratio of 4% while for the one at TR2 (typically at higher velocities) an overheat ratio of 2% is used. By slightly heating the water during filling of the facility, a constant temperature, within 0.5°C, may be obtained. The fluid temperature at the sensor is continuously measured by a thermocouple incorporated in the probe support, allowing the temperature compensation of the probe output to be made when necessary. Calibrations are done by placing the probe at the centerline of the recirculation piping (see Figure 1) in series with a rotameter. Stable operation during a run and reproducible calibrations, reflecting small corrections due to density variations, have been consistently obtained. The overall velocity measurement error is estimated as less than ~ 5%.

The conductivity probes employ silver electrodes and they, as well as the amplifiers, are home made and have an estimated frequency response of ~ 1,000 Hz. A probe is carried within a stainless steel tube (0.95 cm OD) with the sensor element (an overall dimension of ~ 1 mm) protruding as illustrated in Figure 6. After considerable development work, the probes are stable with excellent reproducibility in calibrations. The overall concentration measurement error is estimated at less than ~ 3%.

Each stainless steel probe holder (O-ring sealed at the wall) is coupled to a linear traversing device driven by a high torque motor (Japan Servo, Models 8H-6 and 6G5H).

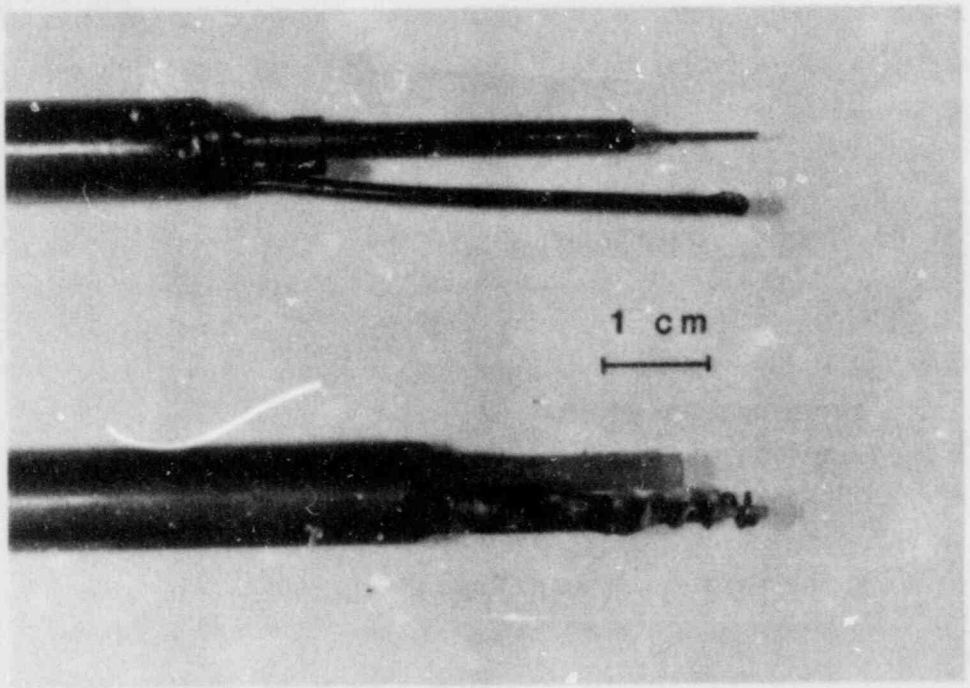

Figure 6. Photograph of the hot-film/thermocouple probe (top) and concentration probe (bottom).

The output of a displacement transducer provides the instantaneous position of the probe, which is continuously recorded along with the probe signal. The whole arrangement is shown in Figure 7.

All data are recorded continuously on three strip chart 2 pen recorders (Watanabe, Model SR 6253), a Lockheed, Model Store 4D 4-channel FM magnetic tape recorder, and after conversion to digital form, to a PDP-11 minicomputer. Only the digital data are used for reductions. The analog records are obtained for visualization of trends during a run, as well as for backup. Both motors are timed to produce a complete traverse in 61 s, and the probes are set in continuous translation throughout a run. The computer samples each probe at 20 ms intervals. For analysis purposes, each traverse is discretized into twelve segments (2.54 cm each for TR1 and 0.85 cm each for TR2), with a total of 256 data points per segment. Mean values and the standard deviation of the fluctuations (i.e. root mean square velocity and concentration fluctuations) around these means are computed for each segment and assigned to a spatial location corresponding to the segment mid-point. Except for a region above the mixing interface where the fluctuations are quite violent, the probe signals are varying slowly, both in space and time, and the above procedure was found as a good compromise between

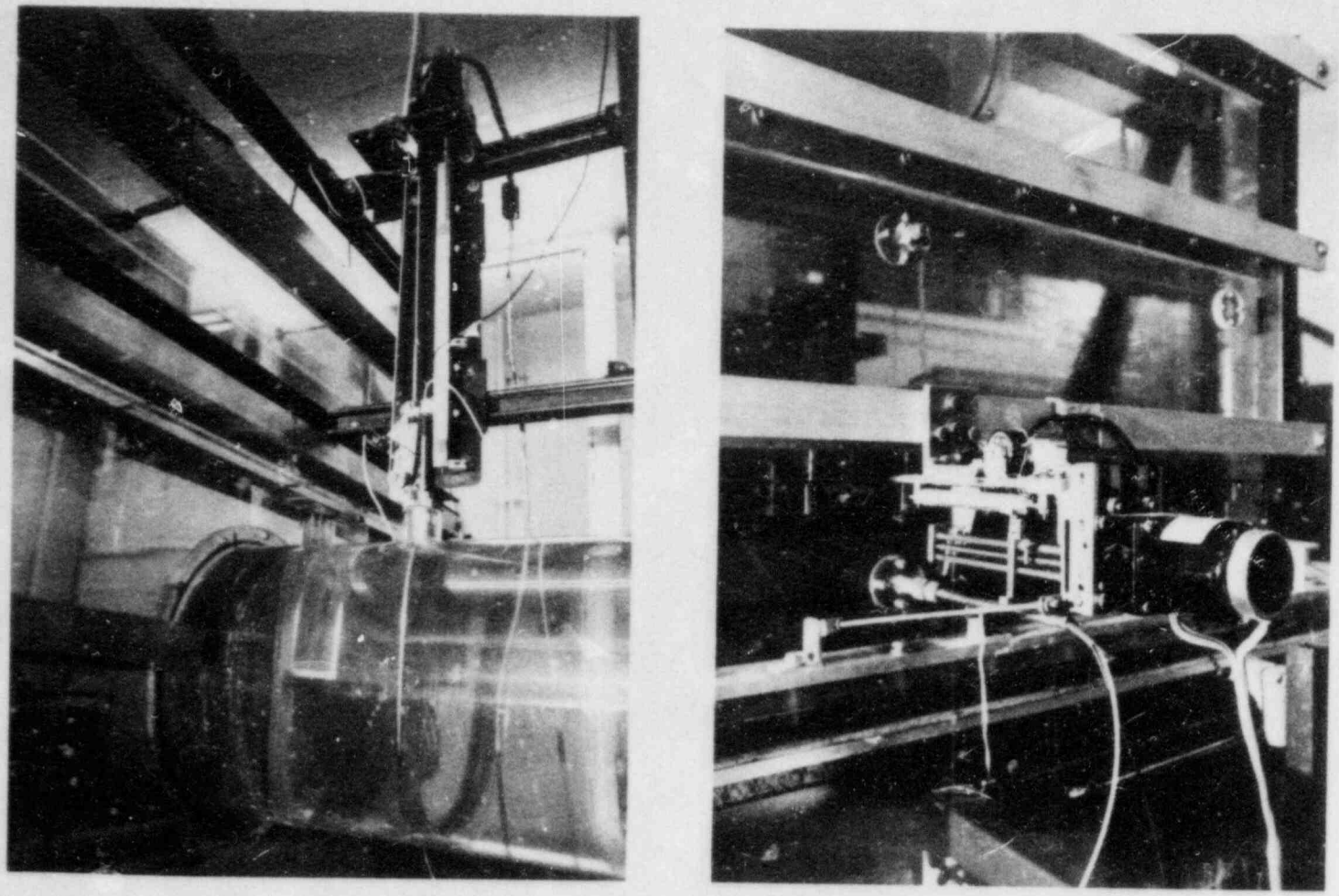

Figure 7. Photograph of the traversing mechanisms in the cold leg (left) and downcomer (right).

quality of statistics on one hand and space-time trend resolution on the other. Sample analog signals are shown in Figure 8. From the so-reduced data, the time-wise variations of each location may be directly constructed. Synchronous, spatial distributions may also be obtained by cross-plotting (interpolating) these results at selected instants in time. Finally, dye injection visualization data are obtained by means of a Panasonic Model NV 8950 audio-video system.

4. Experimental Program

The purpose of this portion of the experimental program is to: (a) Investigate the character of the integral response of the facility, especially with regard to the distorted lower plenum/downcomer components, (b) Demonstrate the instrumentation capability, and (c) Investigate the effect of Froude number variations especially with regard to backflow into the injection line.

Configuration #0 was chosen such that all "cold" stream would flow in one direction (towards the downcomer). This allows an unambiguous approach to goal (a). It is also convenient for goal (b) in that the consistency between velocity and concentration measurements (i.e. water and salt balances) can be directly assessed.

Two Froude number conditions (goal (c)) were chosen. A very low value of $Fr_{HPI} \sim 0.22$, which based upon preliminary flow visualization runs was expected to yield significant penetration (backflow) of "hot" stream fluid into the injection line, and a higher value of $Fr_{HPI} \sim 0.44$ which was found to yield marginal penetration. These two Froude number conditions correspond roughly to CE and W plants respectively.

For convenience, the geometric data and component volumes are summarized in Table 1. The experimental conditions are summarized in Tables 2 to 5. The numbering system refers to the configuration (O, CE, W, B&W), and run number (1,2,3,...), and whether the velocity or the concentration are measured (V or C).

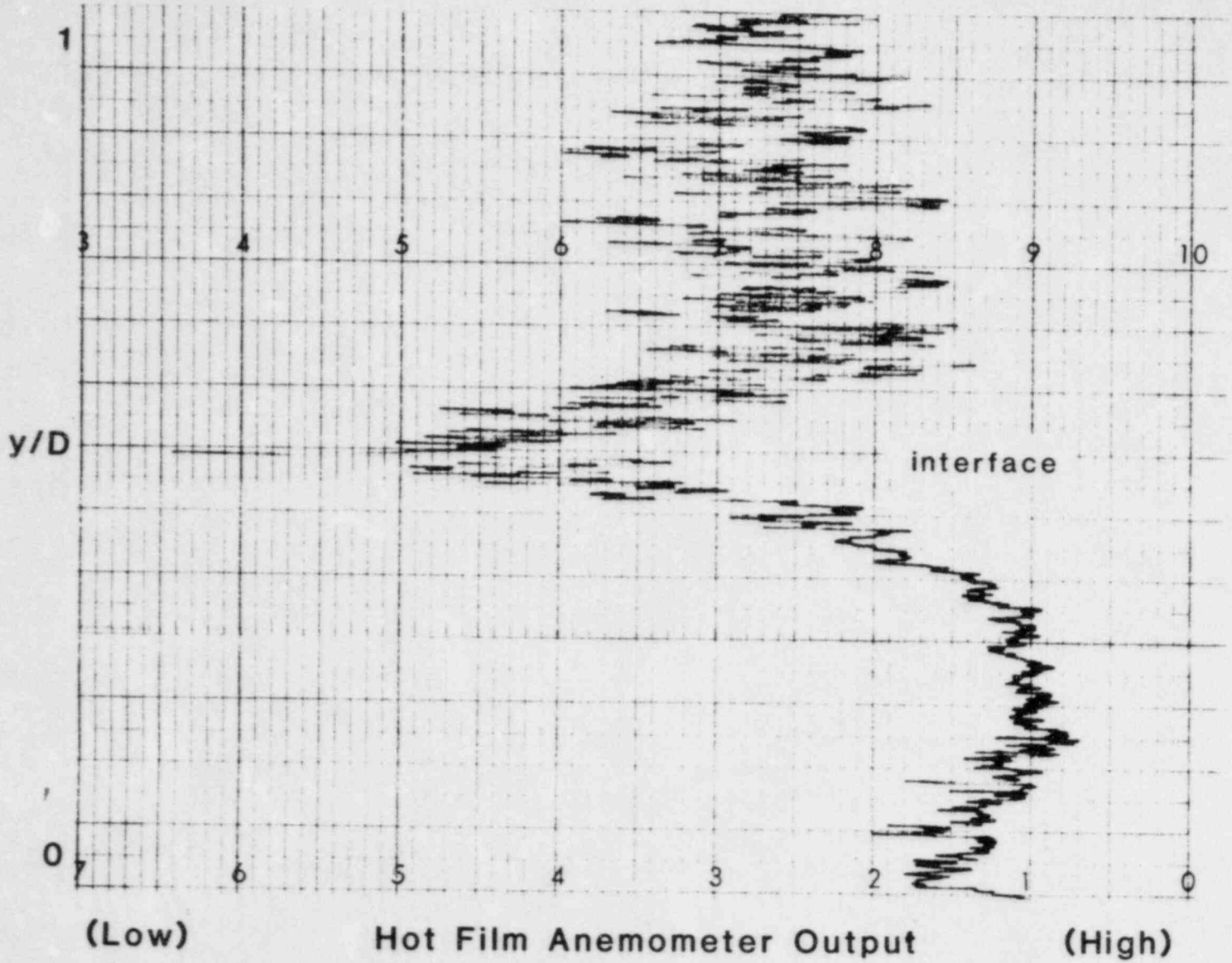

Figure 8a. Typical record on the chart recorder (hot-film probe output).

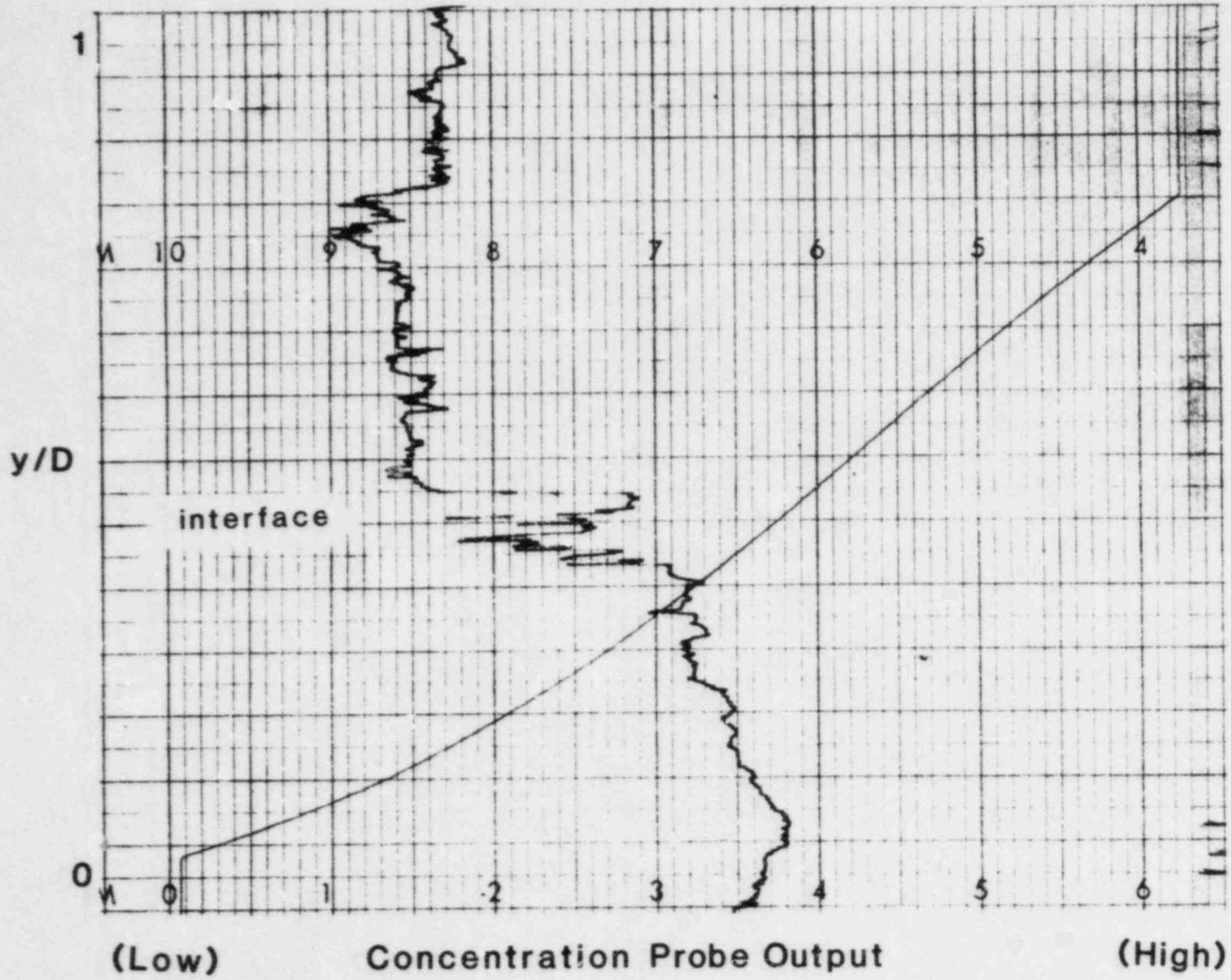

Figure 8b. Typical record on the chart recorder (concentration probe output).

TABLE 1

CONFIGURATION NO:0

COLD LEG	: FIGURE 1
HPI INJECTOR	: FIGURE 1

VOLUMES (M**3)

UPPER DOWNCOMER - ABOVE NOZZLE	: .125E+00
- BELOW NOZZLE	: .320E+00
LOWER DOWNCOMER AND PLENUM	: .900E+00
COLD LEG - UPSTREAM OF INJ.	: .353E-01
- DOWN STREAM OF INJ.	: .195E+00

DIMENSIONS (M)

COLD LEG DIAMETER	: .343E+00
HPI DIAMETER	: .108E+00
DOWNCOMER WIDTH	: .118E+01
DOWNCOMER GAP	: .127E+00
DOWNCOMER PROBE TR2 TO COLD LEG CENTER LINE	: .635E+00
COLD LEG PROBE TR1 TO DOWNCOMER CENTER LINE	: .181E+00

TABLE 2 - RUN 0-1C

TEST CONDITIONS

PARAMETER	NOMINAL	ACTUAL
FLOWS (M**3/S)		
HPI	0.631E-03	0.650-03
LOOP	0.	0.
DENSITIES (KG/M**3)		
HPI (DH)	1097.	1097.
LOOP (DL)	1000.	1000.
DIMENSIONLESS NOS		
HPI FROUDE NO	.215	.221
COLD LEG FROUDE NO	.012	.012
DENSITY RATIO (DH-DL)/DL	.097	.097

TABLE 3 - RUN 0-1V

TEST CONDITIONS

PARAMETER	NOMINAL	ACTUAL
FLOWS (M**3/S)		
HPI	0.631E-03	0.637-03
LOOP	0.	0.
DENSITIES (KG/M**3)		
HPI	1097.	1094.
LOOP	1000.	1000.
DIMENSIONLESS NOS		
HPI FROUDE NO	.215	.220
COLD LEG FROUDE NO	.012	.012
DENSITY RATIO (DH-DL)/DL	.097	.094

TABLE 4 - RUN 0-2V

TEST CONDITION

PARAMETER	NOMINAL	ACTUAL
FLOWS (M**3/S)		
HPI	1.262E-03	1.274-03
LOOP	0.	0.
DENSITIES (KG/M**3)		
HPI (DH)	1097.	1094.
LOOP (DL)	1000.	1000.
DIMENSIONLESS NOS		
HPI FROUDE NO	.430	.441
COLD LEG FROUDE NO	.024	.024
DENSITY RATIO (DH-DL)/DL	.097	.094

TABLE 5 - RUN 0-2C

TEST CONDITIONS

PARAMETER	NOMINAL	ACTUAL
FLOWS (M**3/S)		
HPI	1.262E-03	1.337-03
LOOP	0.	0.
DENSITIES (KG/M**3)		
HPI (DH)	1097.	1097.
LOOP (DL)	1000.	1000.
DIMENSIONLESS NOS		
HPI FROUDE NO	.430	.456
COLD LEG FROUDE NO	.024	.025
DENSITY RATIO (DH-DL)/DL	.097	.097

5. Experimental Results and Interpretations

The complete set of data in both plotted and tabular form may be found in the Appendices. As the qualitative trends are similar, they will be discussed here in terms of a representative sample.

Except for an initial transient (~ 100s), all mean velocity and concentration transients in the cold leg exhibit a monotonic, slow, and smooth, variation, as illustrated in Figure 9. A sample of the resulting, synchronous, spatial distribution is given in Figure 10. The counter-current flow regime, as hypothesized in the RMM, is clearly evident. Since the hot film probe cannot sense the flow direction, some ambiguity exists in selecting the velocity sign for the 1 or 2 data points (low velocities) in the immediate vicinity of the interface. This sign assignment, and choice of interpolated interface position were made such that the integrated velocity profiles, together with the known injection rate, exactly satisfy continuity.

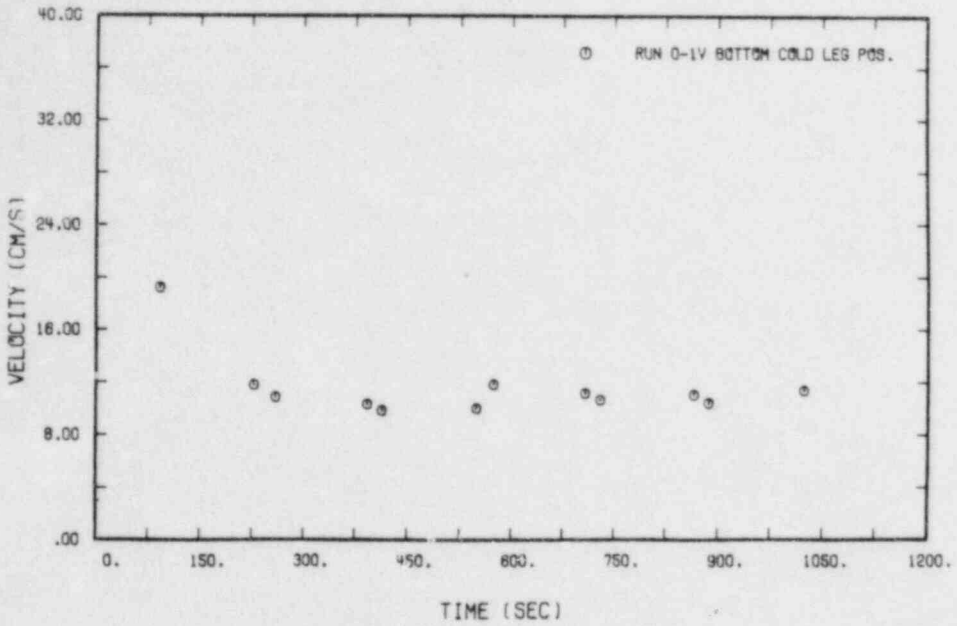

Figure 9a. Velocity transient at the bottom of the cold leg (y/D = 0.074) for Run 0-1V.

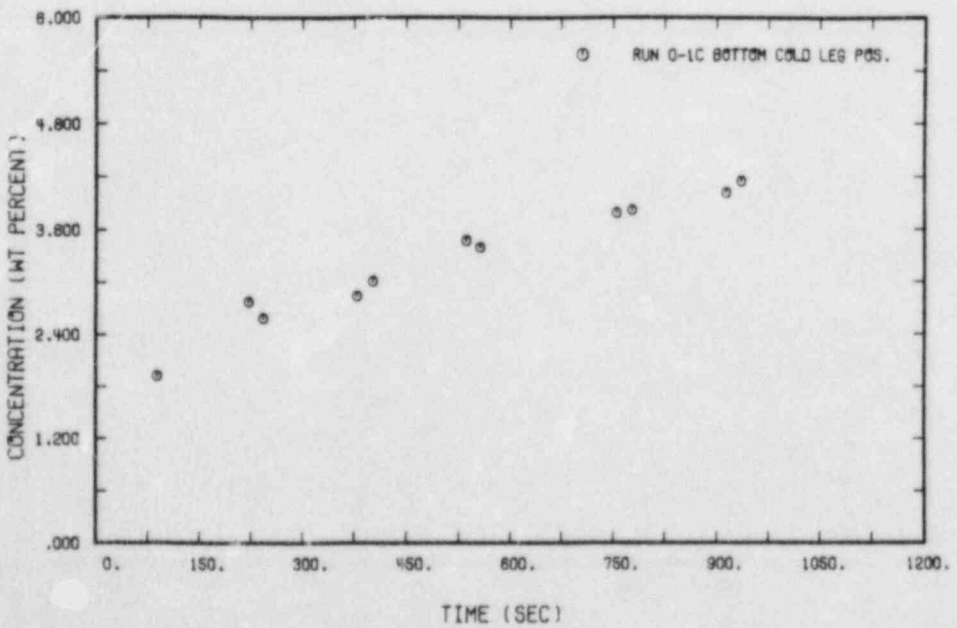

Figure 9b. Concentration transient at the bottom of the cold leg (y/D = 0.074) for Run 0-1C.

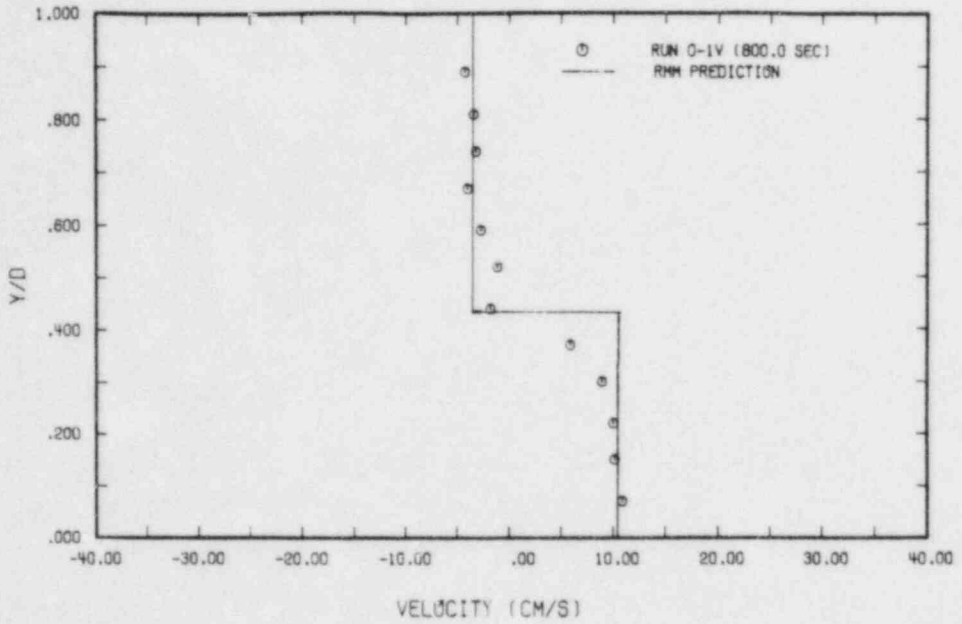

Figure 10a. Velocity profile in the cold leg, at t = 800 sec, Run 0-1V.

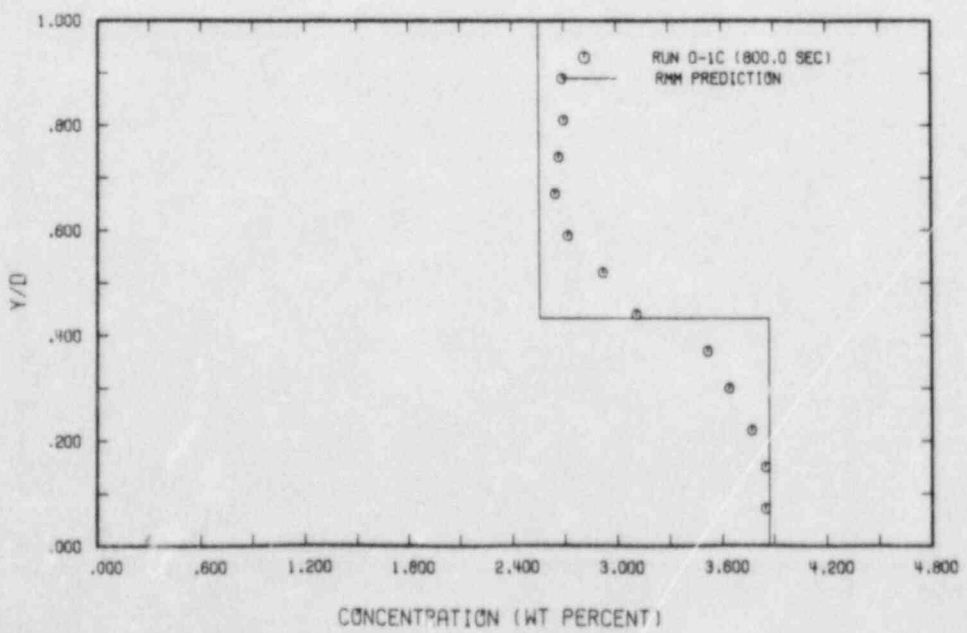

Figure 10b. Concentration profile in the cold leg, at t = 800 sec, Run 0-1C.

With these choices, consistency with the measured concentrations values could be tested by performing a salt balance over the cold leg volume. Since, except for the early portion of the transients, the throughputs are much greater than the rate of accumulation, this test can be conveniently made. The imbalance, expressed as percent of outfow (taken as positive) is shown in Figure 11. The systematic error indicated, we believe, is due to the hot film sensor inability to discriminate the axial component of veocity within the vortex sheet that occupies a narrow region (~ 2 to 4 cm) between the two layers.

The spatial downcomer trends are illustrated in Figure 12. Although the jetting (by deflection) effect along the core barrel wall is evident in the velocity distribution, good radial mixing, and nearly uniform concentration distribution, seem to prevail.

A sample of the intensity of velocity and concentration fluctuation distributions in the cold leg and the downcomer may be found in Figures 13 and 14 respectively. In the "cold" stream, the intensities are limited to values typically expected in single phase flow. In the "hot" stream and particularly in the vicinity of the interface highly energetic fluctuations are noted. Under these conditions, much longer sample records, at a fixed position, would be required to obtain adequate statistics. Such experiments would also provide the data for extracting energy spectra (and length scales) and are planned for the future.

Of particular interest to us was whether the concept of a "well-mixed" ambient in the sense of the RMM (see Part I), would be applicable to our facility. Specifically, we were concerned that due to the distorted lower plenum/downcomer geometry, this concept would not be as favored as it would be in the reactor system. Fortunately, the data indicate otherwise. As seen in Figure 15, the measured "ambient" concentration transient (position 5T1), is in excellent agreement with a straightforward application of Eq. 2 of Part I.

The effect of the Froude number on the entrainment ratio Qe/Q_{HPI} in the mixing region MR1 (Figure 2, Part I) is evident from the experimental data. Using the measured concentration values from the runs 0-1C and 0-2C (Fr_{HPI} = 0.22 and Fr_{HPI} = 0.44 respectively) in Equation 16 (Part I) the entrainment ratio is found to be 4.8 and 2.42 respectively. As we will see below these values are not inconsistent with the predictions of the turbulence model utilized in the RMM. Similarly for the entrance to the downcomer (mixing region 3 of Figure 2, Part I) we deduce an entrainment ratio of ~ 0.8. This value is the same for both runs (i.e., independent of injection Froude number) because the cold stream Froude number seems to always adjust itself to a value near ~ 0.6.

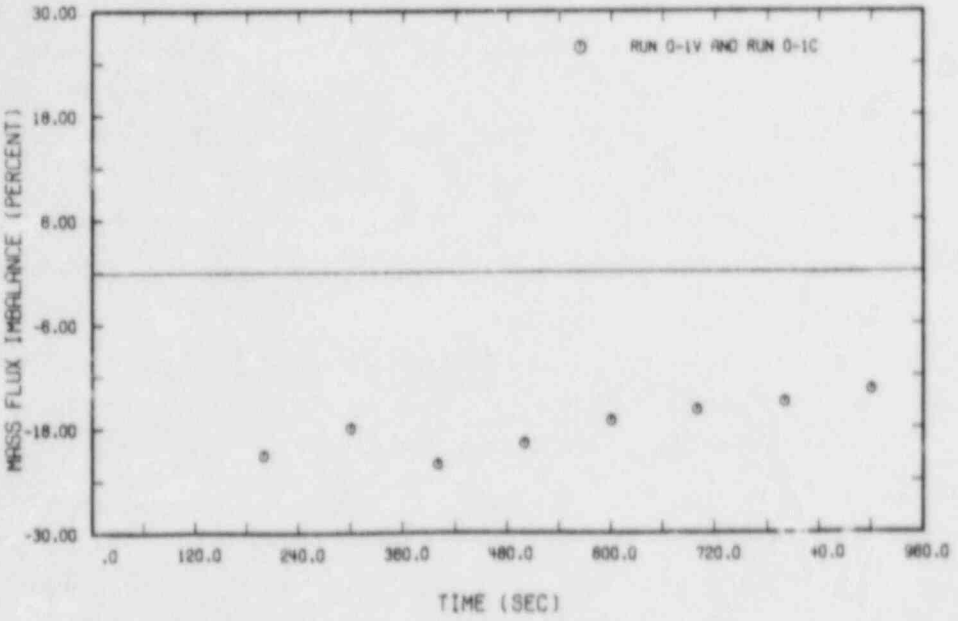

Figure 11a. Mass balance for Runs 0-1C and 0-1V.

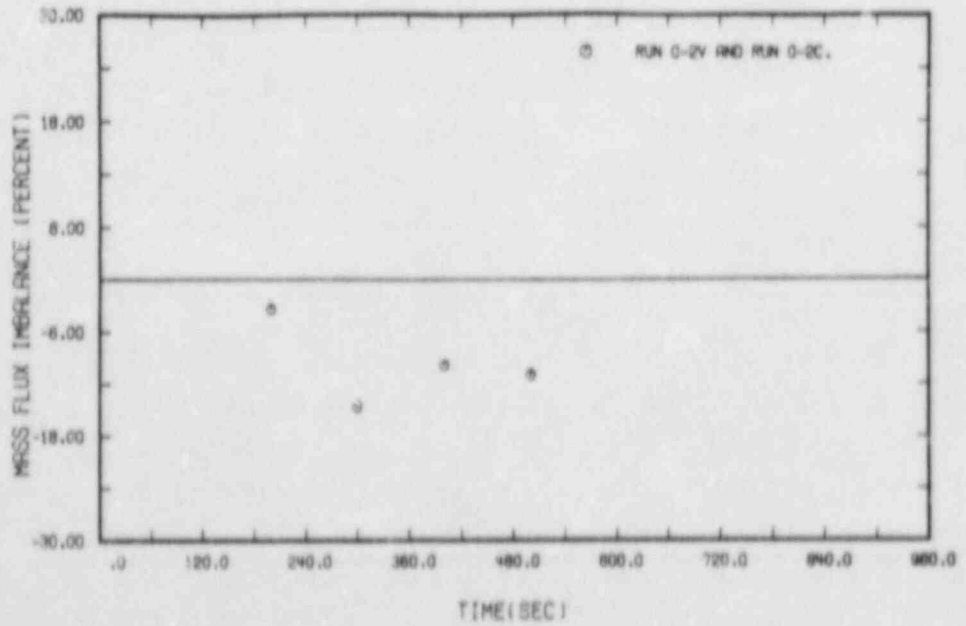

Figure 11b. Mass balance for Runs 0-2C and 0-2V.

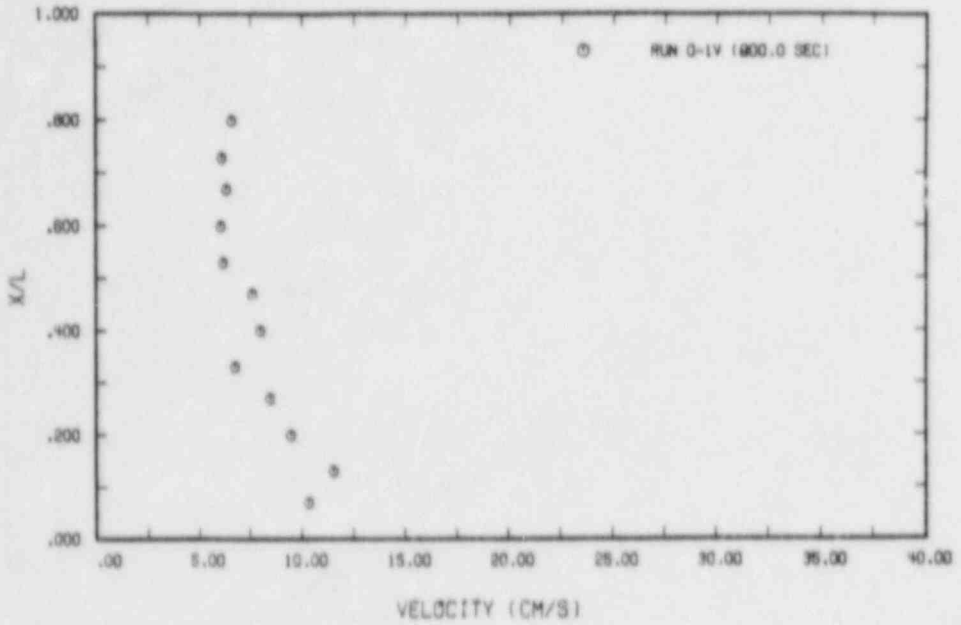

Figure 12a. Velocity profile in the downcomer, at t = 800 sec, Run 0-1V.

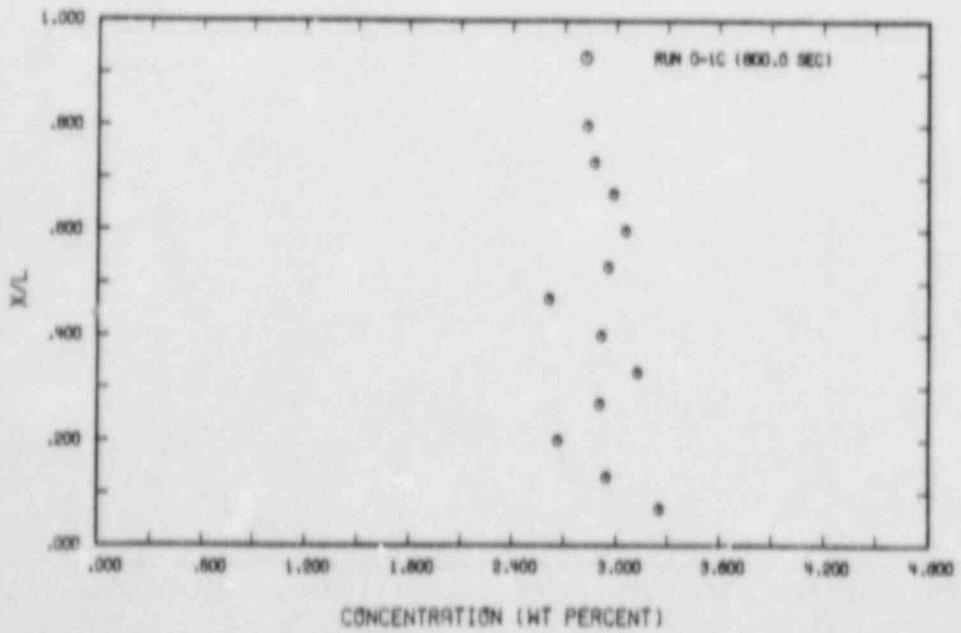

Figure 12b. Concentration profile in the downcomer, at t = 800 sec, Run 0-1C.

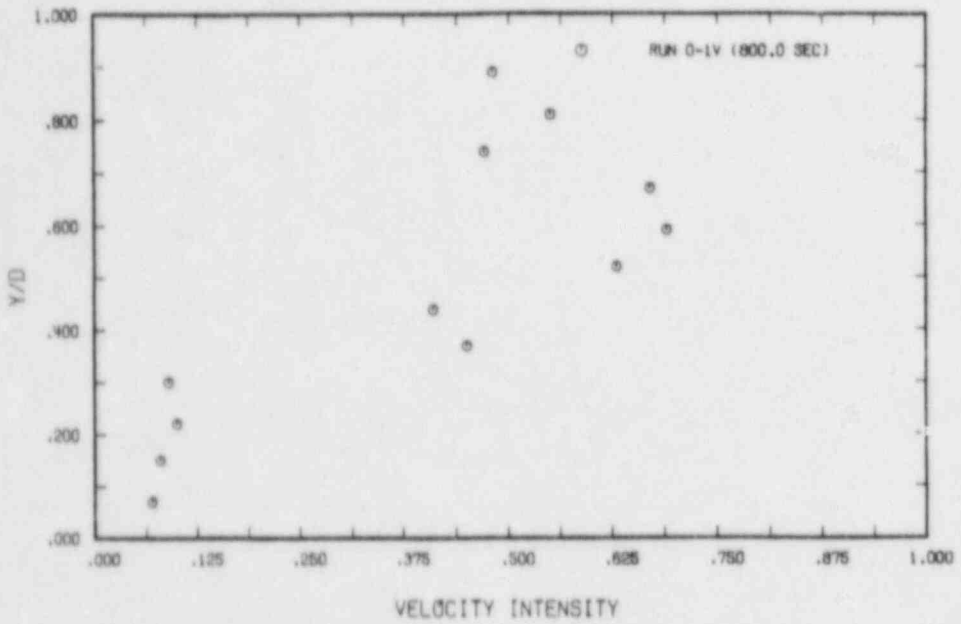

Figure 13a. Velocity fluctuation intensity in the cold leg, t = 800 sec, Run 0-1V.

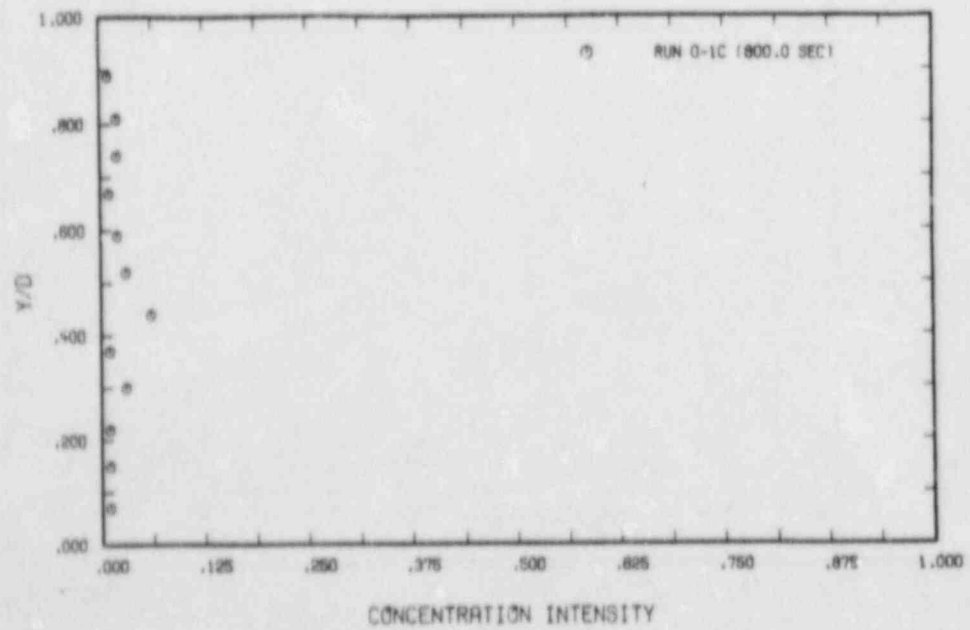

Figure 13b. Concentration fluctuation intensity in the cold leg, at t = 800 sec, Run 0-1C.

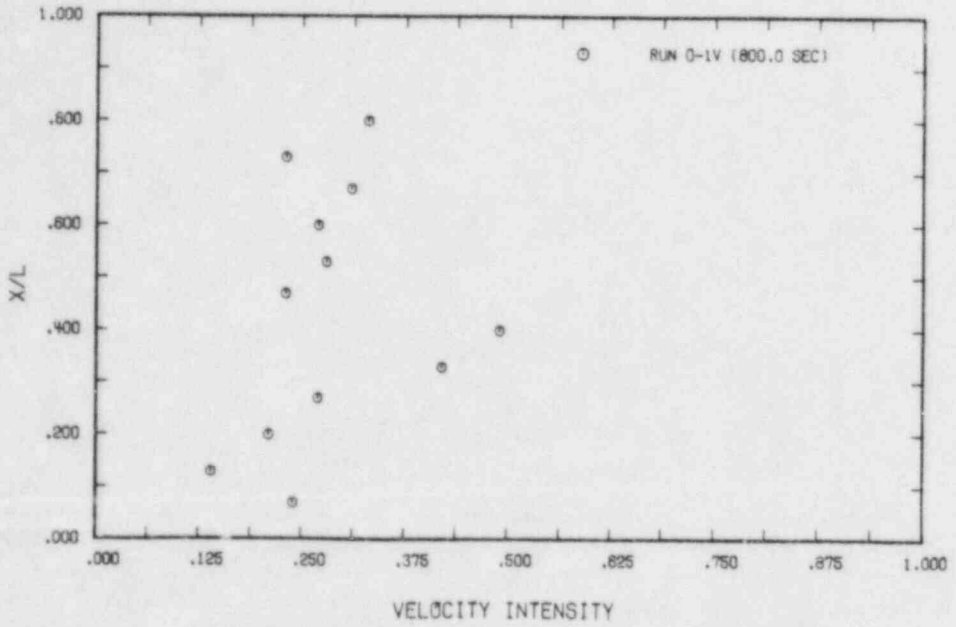

Figure 14a. Velocity fluctuation intensity in the downcomer, t = 800 sec, Run 0-1V.

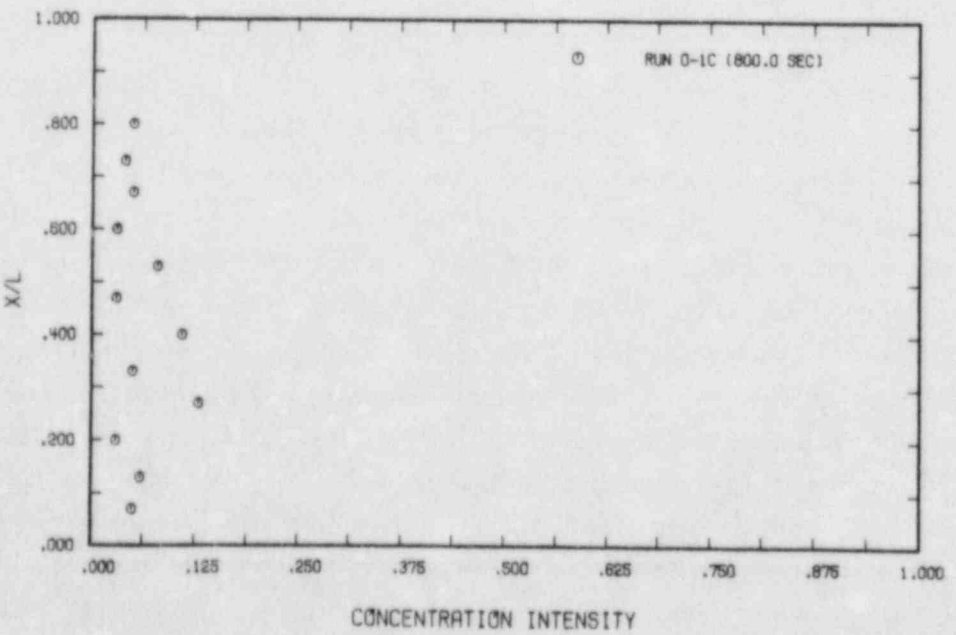

Figure 14b. Concentration fluctuation intensity in the downcomer, t = 800 sec, Run 0-1C.

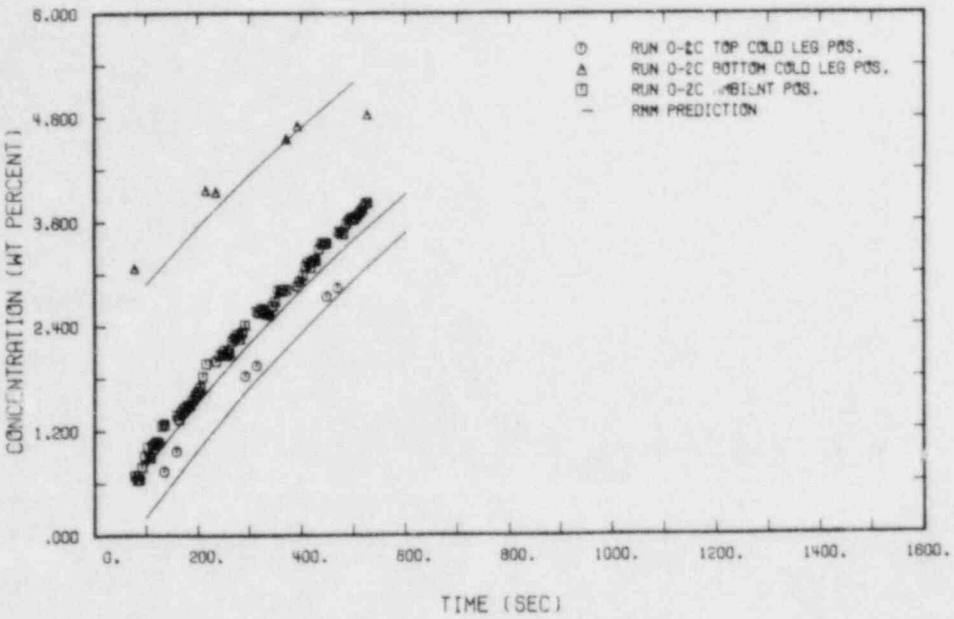

Figure 15. Measured concentration transients versus model prediction, Run 0-2C.

The application of the RMM to the measured space-time concentration and velocity distribution requires a new element, concerned with mixing within the injection line (backflow). In a simple extension of the existing calculational framework, we define an effective plume origin on the basis of the flow visualization data rather than take it at the injector outlet. This effective origin may be taken at the maximum depth of penetration of backflow into the injection line as evidenced by refractive index changes due to mixing of the low salinity solution with the injected brine. This backflow was found to extend by 4 and 2 injection line diameters in Runs 0-1, and 0-2 respectively. Recognizing that over these distances the plumes are restrained, and remain attached to the lower side of the inclined injection line, it would appear that roughly only half of the entrainment estimated for free-fall plumes (of equal length) may be present. Since entrainment is roughly proportional to the plume l/D (see Figure 3 of Part I) a backsetting (from injector outlet) of the effective origin by 2 and 1 diameters respectively would appear reasonable. Adding a free-fall distance (from injector outlet to the cold stream surface) of ~ 1.6 diameters (same for both cases) we obtain 2.6 and 3.6 diameters respectively. The calculated entrainment ratio, corresponding to these lengths is found (Figure 3 of Part I) as 4.8 and 2.5 respectively, in good agreement with the experimental results.

These effective plume origin estimates were utilized in the RMM predictions. Comparison of the calculated space-time distributions with the experimental data of Runs 0-1V, 0-1C, 0-2V, and 0-2C are given in Figure 10a, 10b, 16a and 16b respectively. Very good overall agreement and consistent prediction of both velocity and concentration distributions is noted.

The time variation of the concentrations in the "hot" and "cold" streams is plotted in Figures 15 and 17, along with the RMM predictions. In the model, the upper part of the downcomer extending 2 diameters below the cold leg centerline is considered to be essentially at the "hot" stream temperature (see Part I, Section 3.1). This fact was confirmed experimentally by concentration measurements at position ST2 (see Figures 1 and 2) as well as from visualization runs.

In assessing the quality of these comparisons one should note that these are a priori calculations i.e. the RMM was applied in its original form (published before the existence of the present facility) and no particular effort was made to "tailor" the prediction to the data.

6. Conclusions

The building and proof-testing of Purdue's 1/2-scale HPI mixing facility are complete. Results from the first round of experimental runs and associated analytical interpretations demonstrate that:

(a) The integral response is in accord with the RMM and no ill-effects are produced by the distorted lower downcomer/plenum geometry,

(b) The velocity and concentration measurements are consistent (as determined by appropriate mass balances) and provide an excellent resolution of both space- and time-distributions of velocity and concentration, and

(c) Taking into account an effective origin of the injected plume (due to backflow), as obtained from visualization experiments, the data are in very good agreement with the detailed predictions of the RMM.

Thus based on the first round of the experimental program and in relation to the "scaling" and "injection-geometry" considerations raised in the introduction we may conclude that for the injection conditions of interest to Westinghouse and Combustion Engineering designs (low Fr number injection): (a) backflow in the injection line is important and it can be quantified both experimentally and analytically (as it has been) and (b) the Reynolds number non-similarity found in small-scale experiments is unimportant (i.e. the RMM predicts equally well independently of scale).

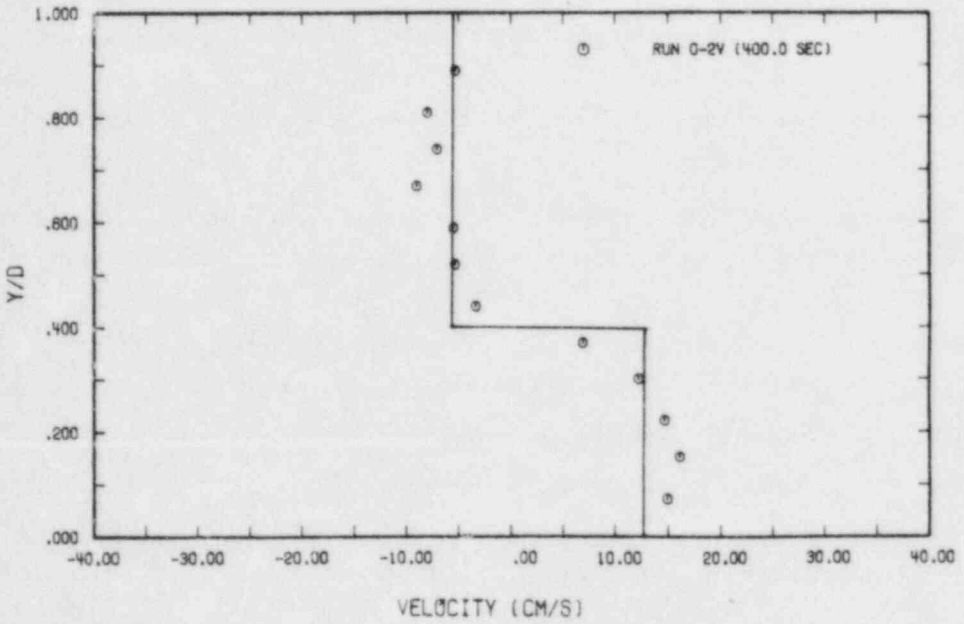

Figure 16a Velocity profile in the cold leg, at t = 400 sec, Run 0-2V.

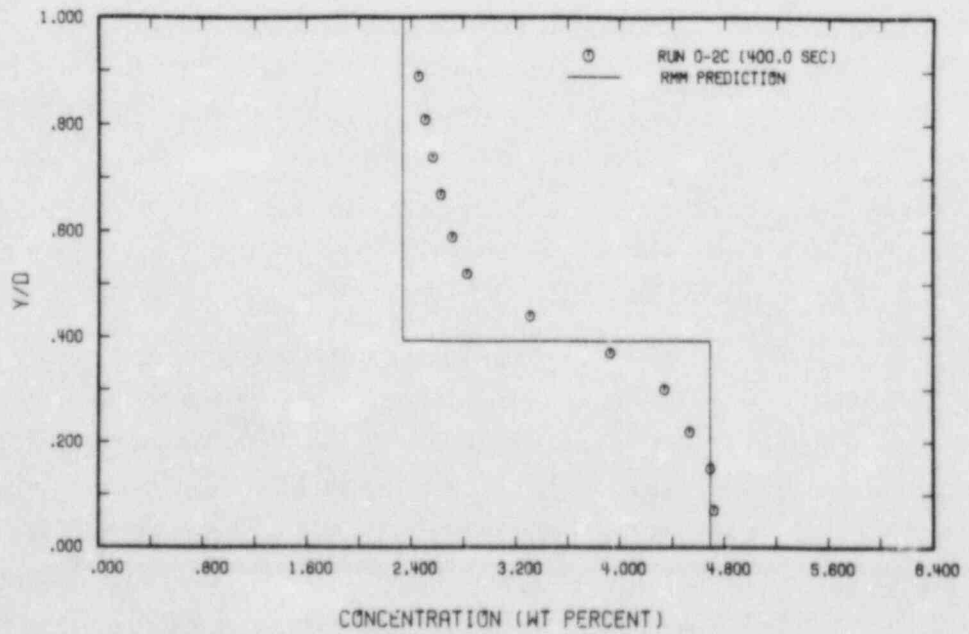

Figure 16b Concentration profile in the cold leg, at t = 400 sec, Run 0-2C.

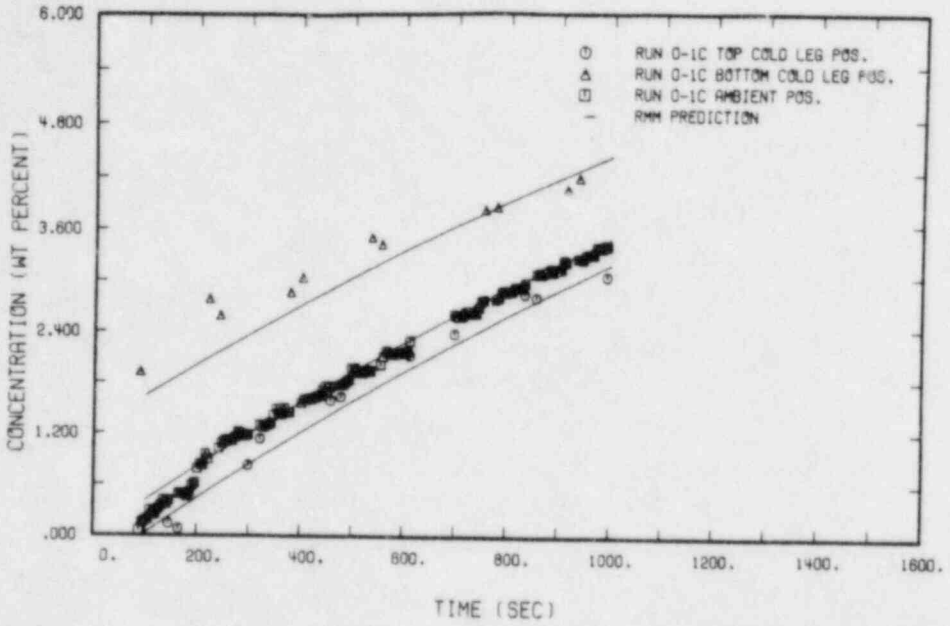

Figure 17. Measured concentration transients versus model prediction, Run 0-1C.

REFERENCES

1 Theofanous, T.G., H.P. Nourbakhsh, P. Gherson, and K. Iyer, "Decay of Buoyancy Driven Stratified Layers with Applications to PTS," Proc. of 11th Water Reactor Safety Research Information Meeting, National Bureau of Standards, Gaithersburg, MD, October 24-26, 1983, NUREG/CP-0048, Vol. 2, pp. 91-94.

2 Theofanous, T.G. and H.P. Nourbakhsh, "PWR Downcomer Fluid Temperature Transients Due to High Pressure Injection at Stagnated Loop Flow," Proc. of Joint NRC/ANS Meeting on Basic Thermal Hydraulic Mechanisms in LWR Analysis, September 14-15, 1982, Bethesda, MD, NUREG/CP-0043, pp. 583-613.

APPENDIX A: PLOTTED RESULTS

LIST OF FIGURES

LIST OF FIGURES (Continued)

Run 0-1C

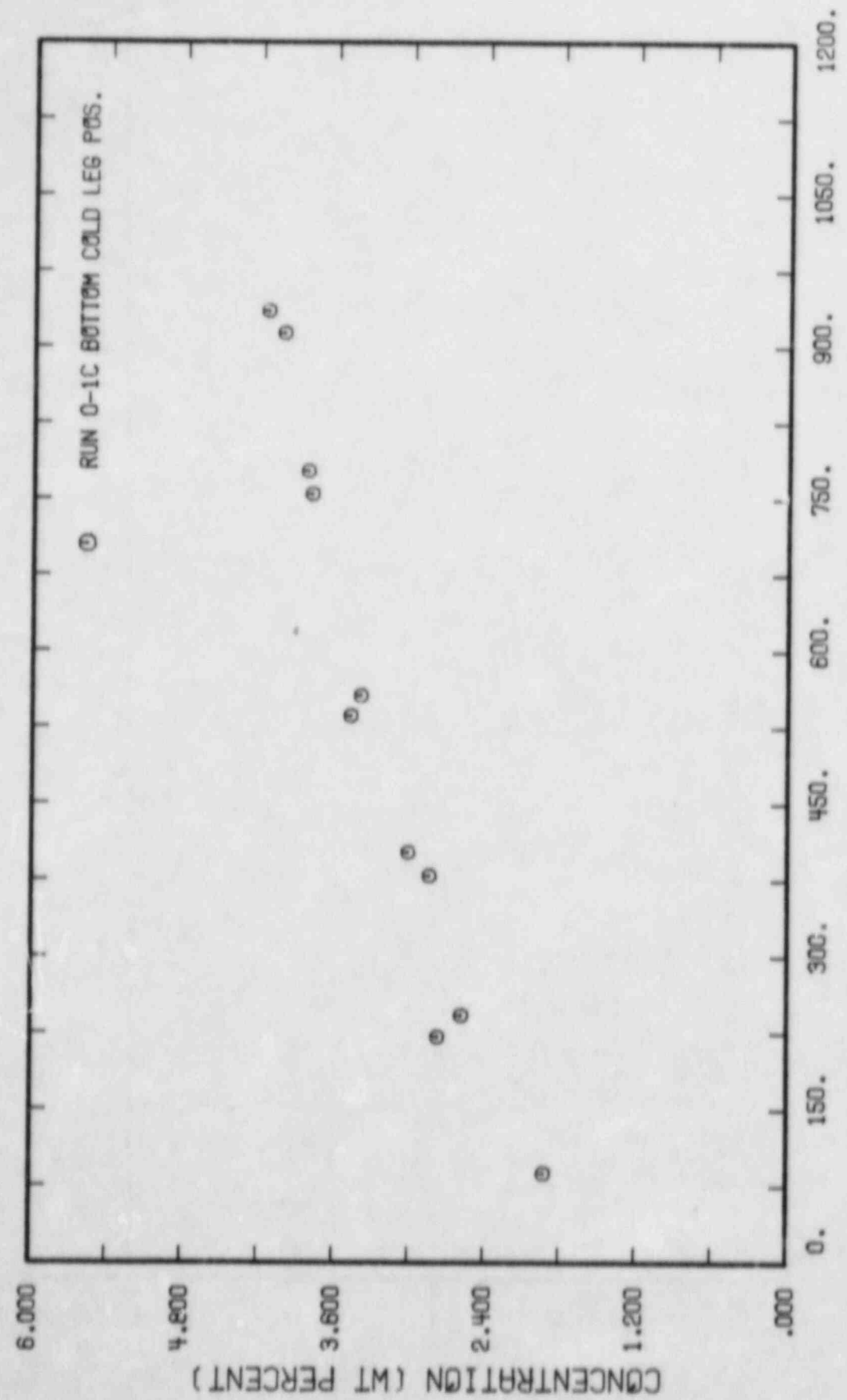
RUN 0-1C BOTTOM COLD LEG POS.
CONCENTRATION (WT PERCENT)
6.000
4.800
3.600
2.400
1.200
.000
0.
150.
300.
450.
600.
750.
900.
1050.
1200.
TIME (SEC)

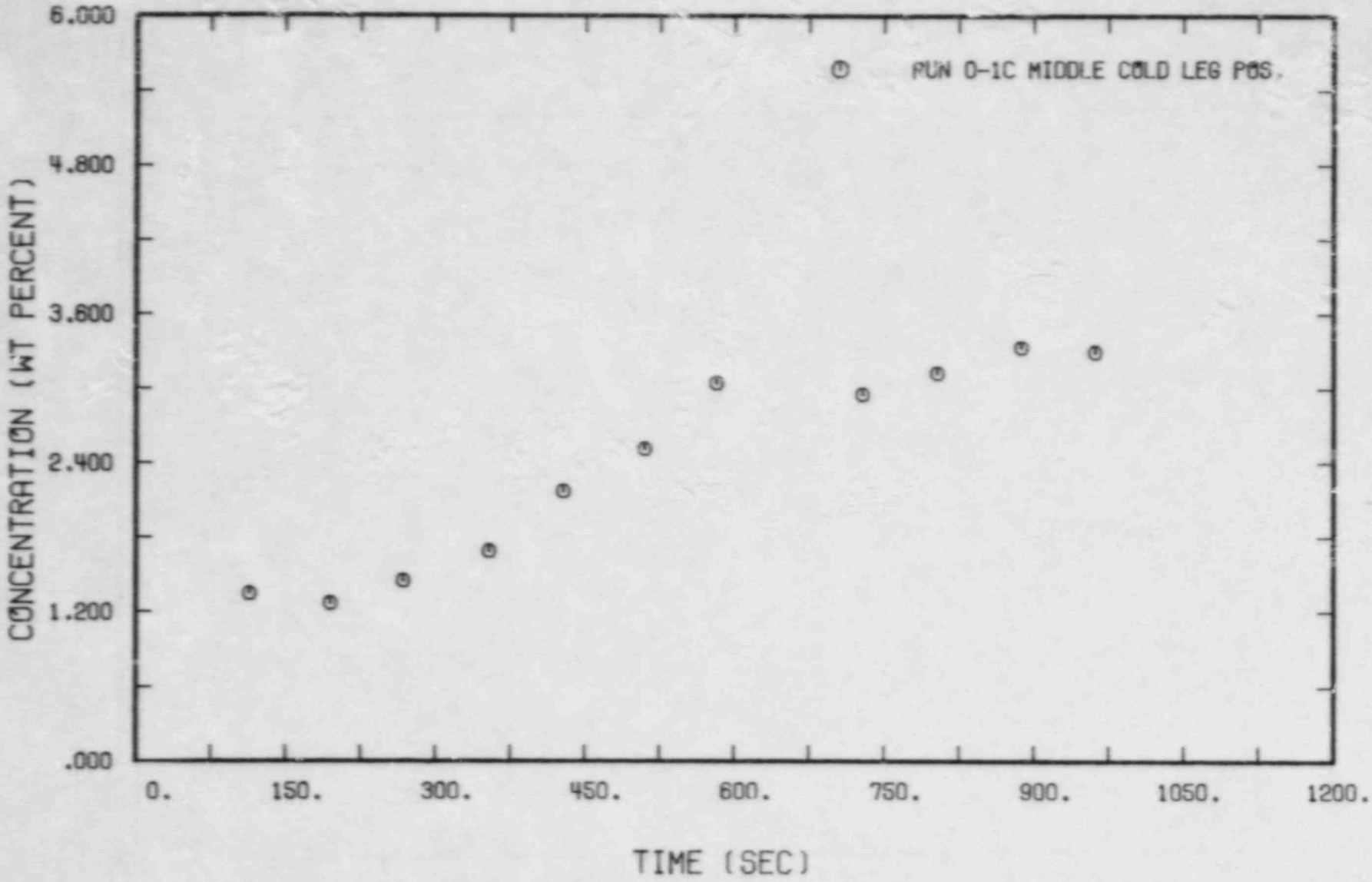
RUN 0-1C MIDDLE COLD LEG POS.
CONCENTRATION (WT PERCENT)
6.000
4.800
3.600
2.400
1.200
.000
0.
150.
300.
450.
600.
750.
900.
1050.
1200.
TIME (SEC)

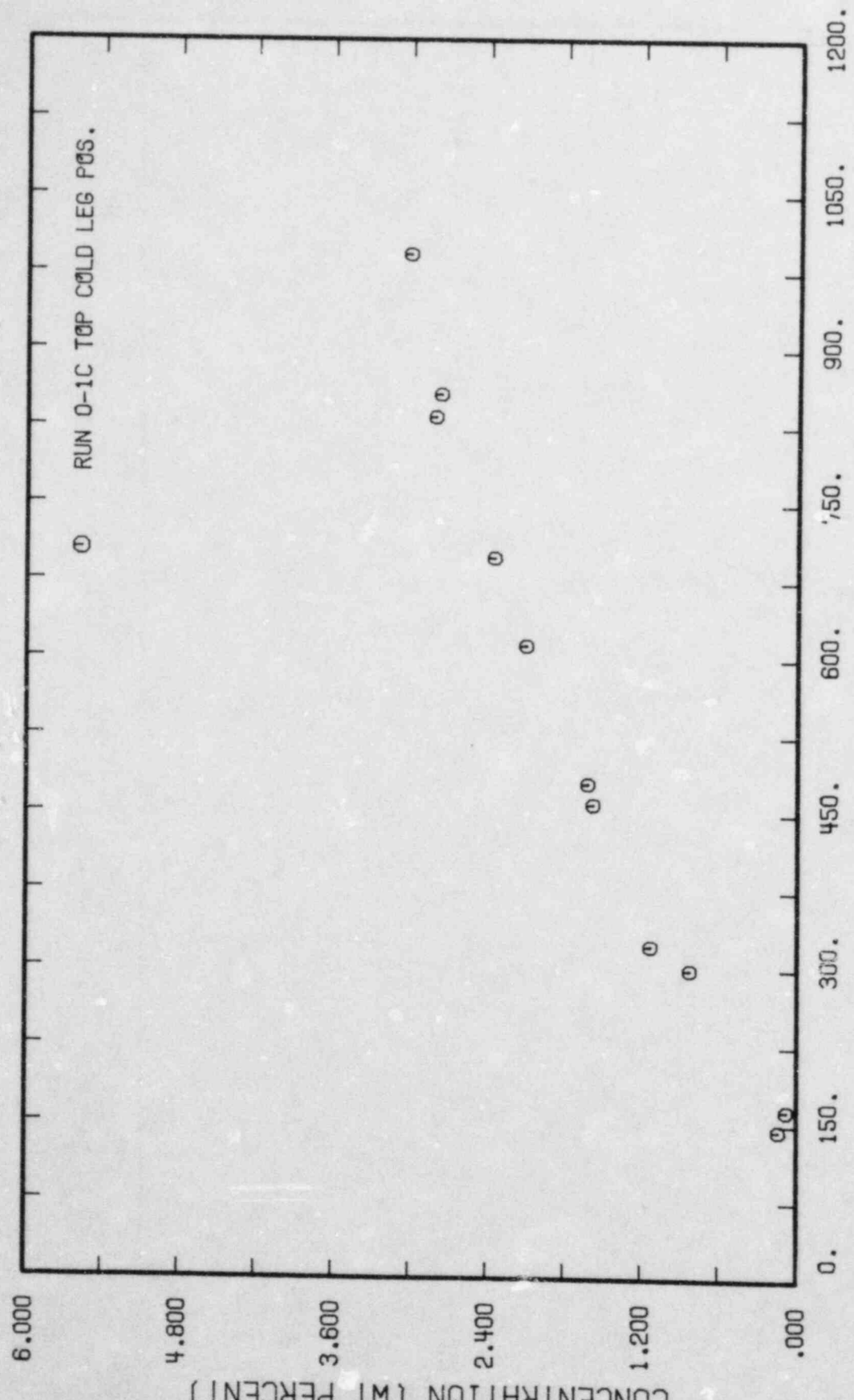
RUN 0-1C TOP COLD LEG POS.
CONCENTRATION (WT PERCENT)
6.000
4.800
3.600
2.400
1.200
.000
0.
150.
300.
450.
600.
750.
900.
1050.
1200.
TIME (SEC)

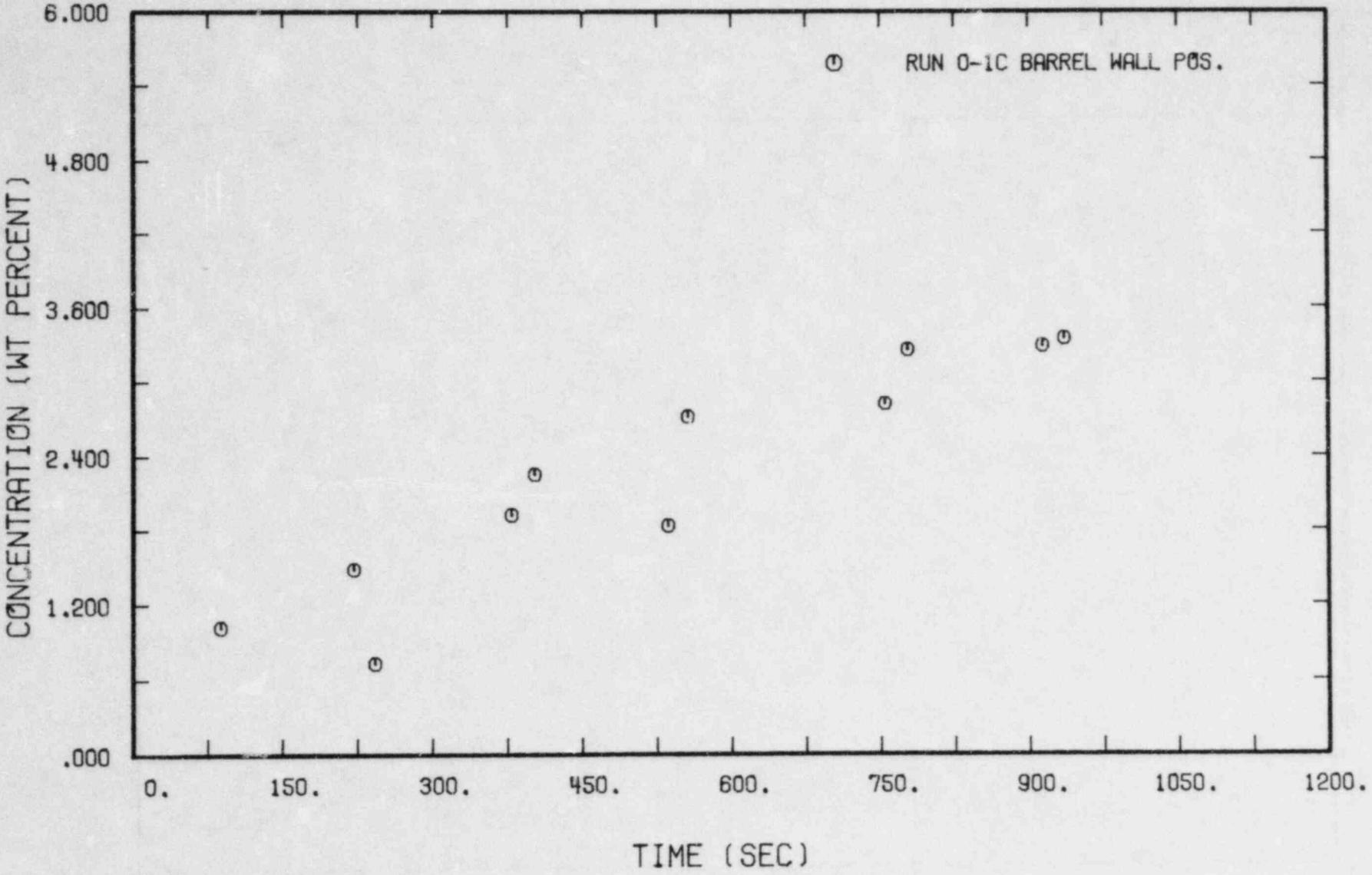
RUN 0-1C BARREL WALL POS.
CONCENTRATION (WT PERCENT)
6.000
4.800
3.600
2.400
1.200
.000
0.
150.
300.
450.
600.
750.
900.
1050.
1200.
TIME (SEC)

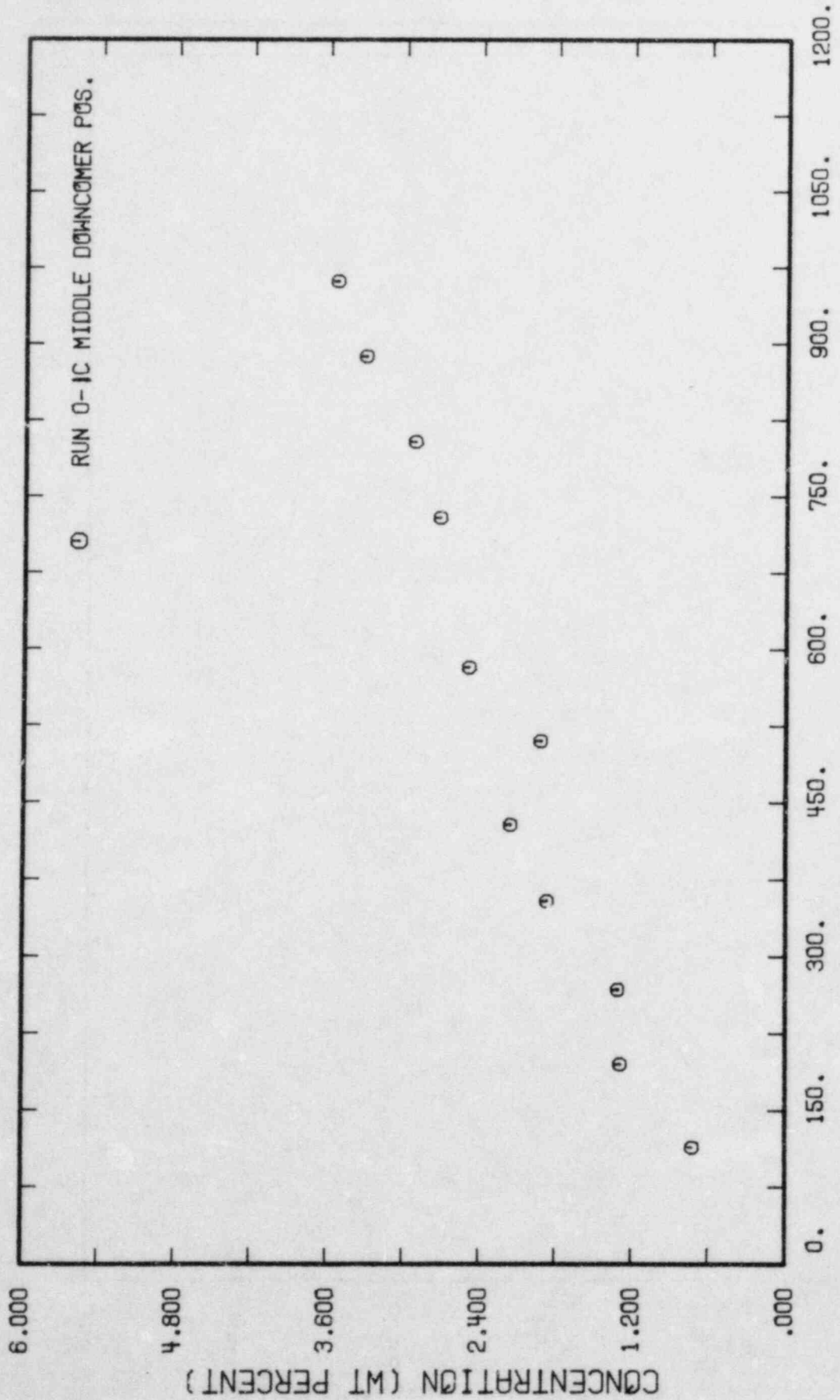
RUN 0-1C MIDDLE DOWNCOMER POS.
CONCENTRATION (WT PERCENT)
6.000
4.800
3.600
2.400
1.200
.000
0.
150.
300.
450.
600.
750.
900.
1050.
1200.
TIME (SEC)

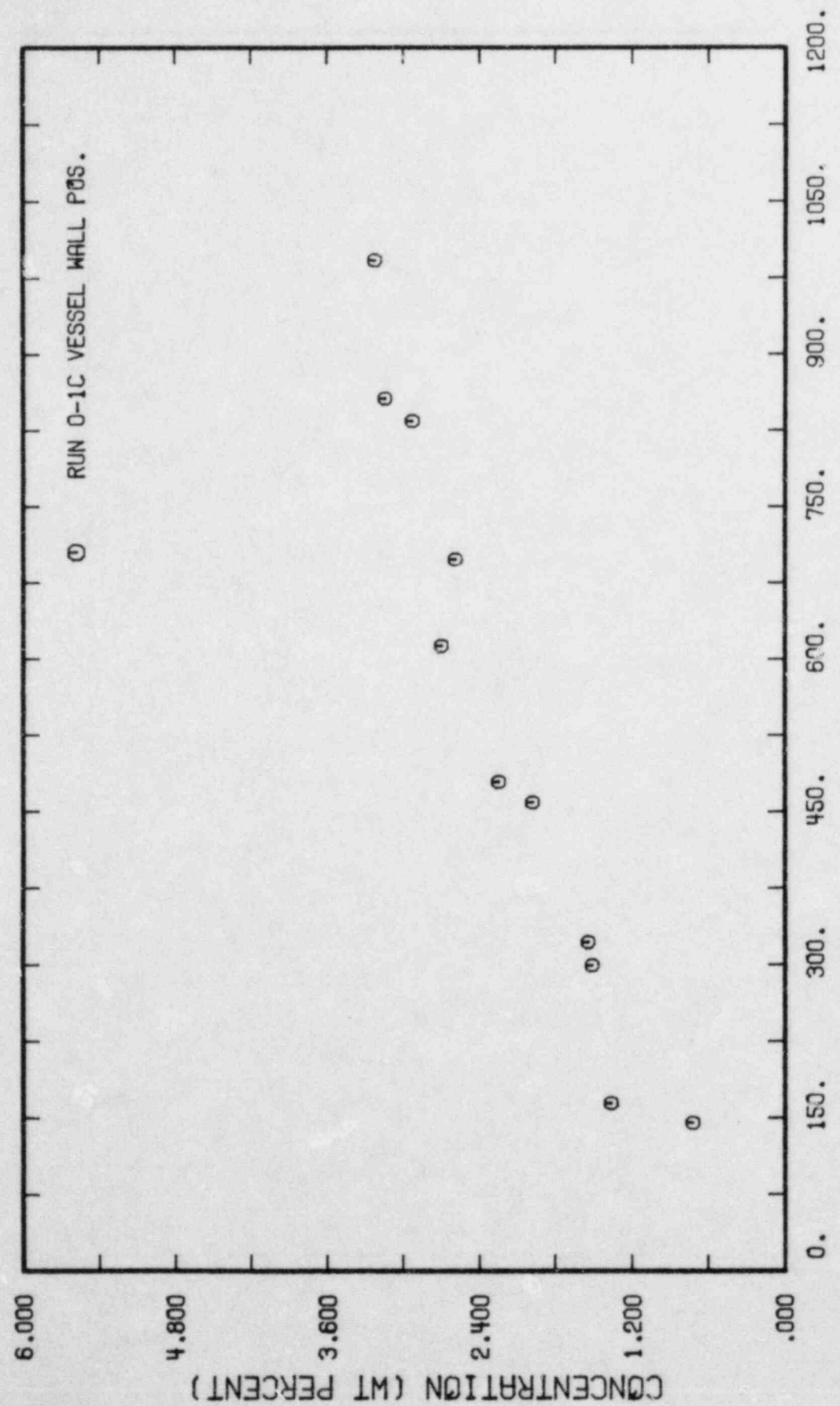
RUN 0-1C VESSEL WALL PØS.
CONCENTRATION (WT PERCENT)
6.000
4.800
3.600
2.400
1.200
.000
0.
150.
300.
450.
600.
750.
900.
1050.
1200.
TIME (SEC)

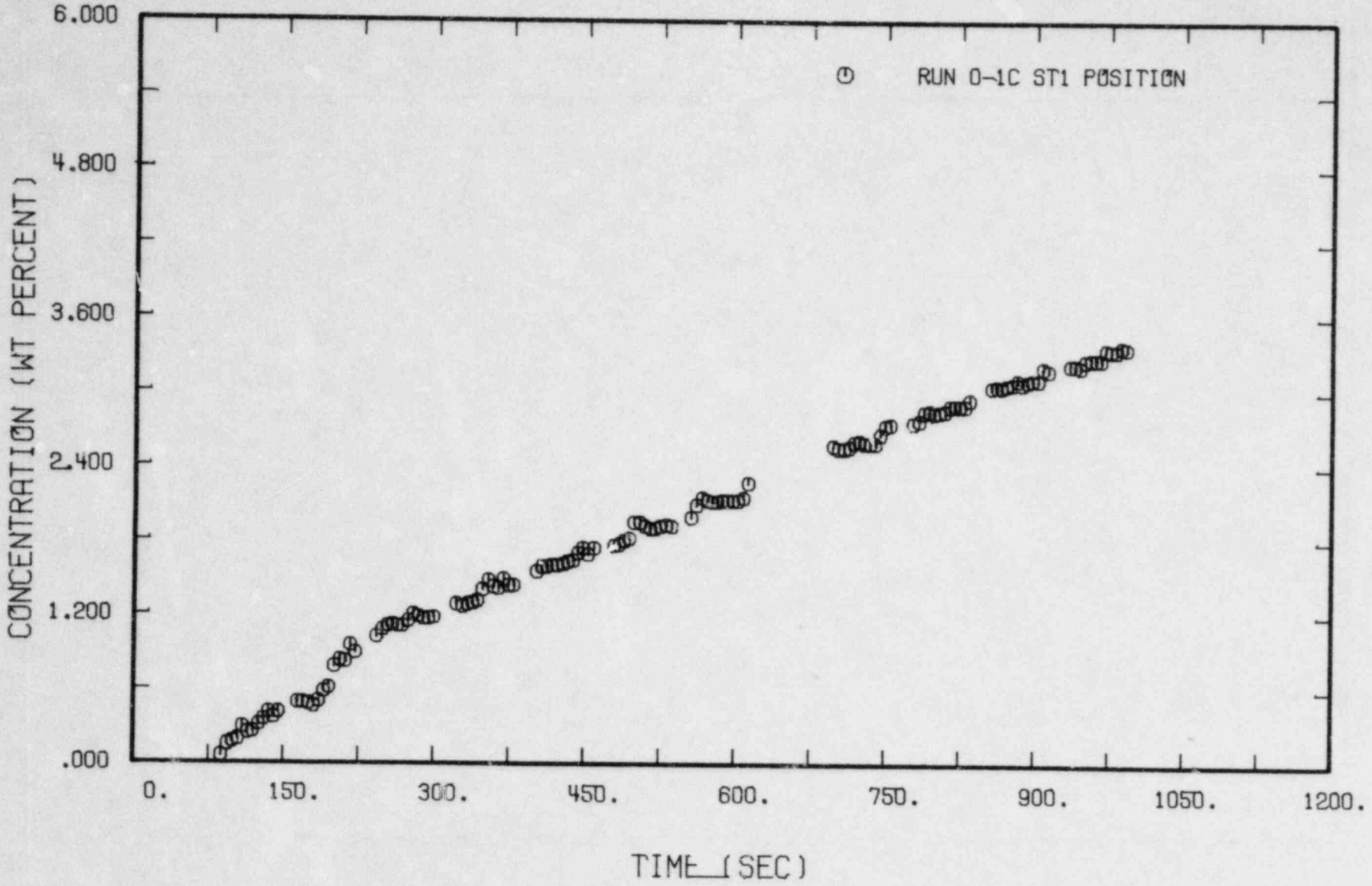
RUN 0-1C ST1 POSITION
CONCENTRATION (WT PERCENT)
6.000
4.800
3.600
2.400
1.200
.000
0.
150.
300.
450.
600.
750.
900.
1050.
1200.
TIME (SEC)

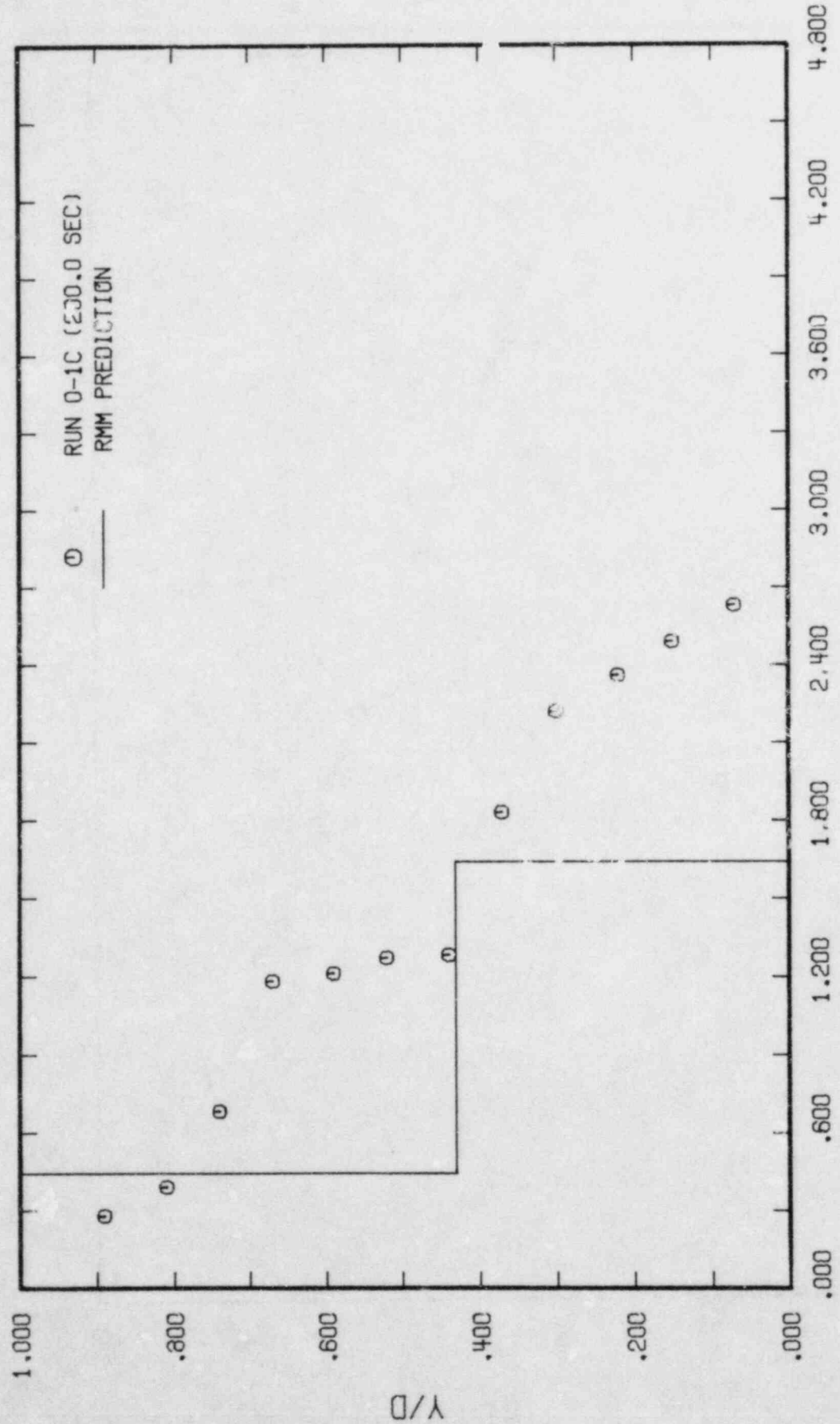
RUN 0-1C (230.0 SEC)
RMM PREDICTION
Y/D
1.000
.800
.600
.400
.200
.000
.000
.600
1.200
1.800
2.400
3.000
3.600
4.200
4.800
CONCENTRATION (WT PERCENT)

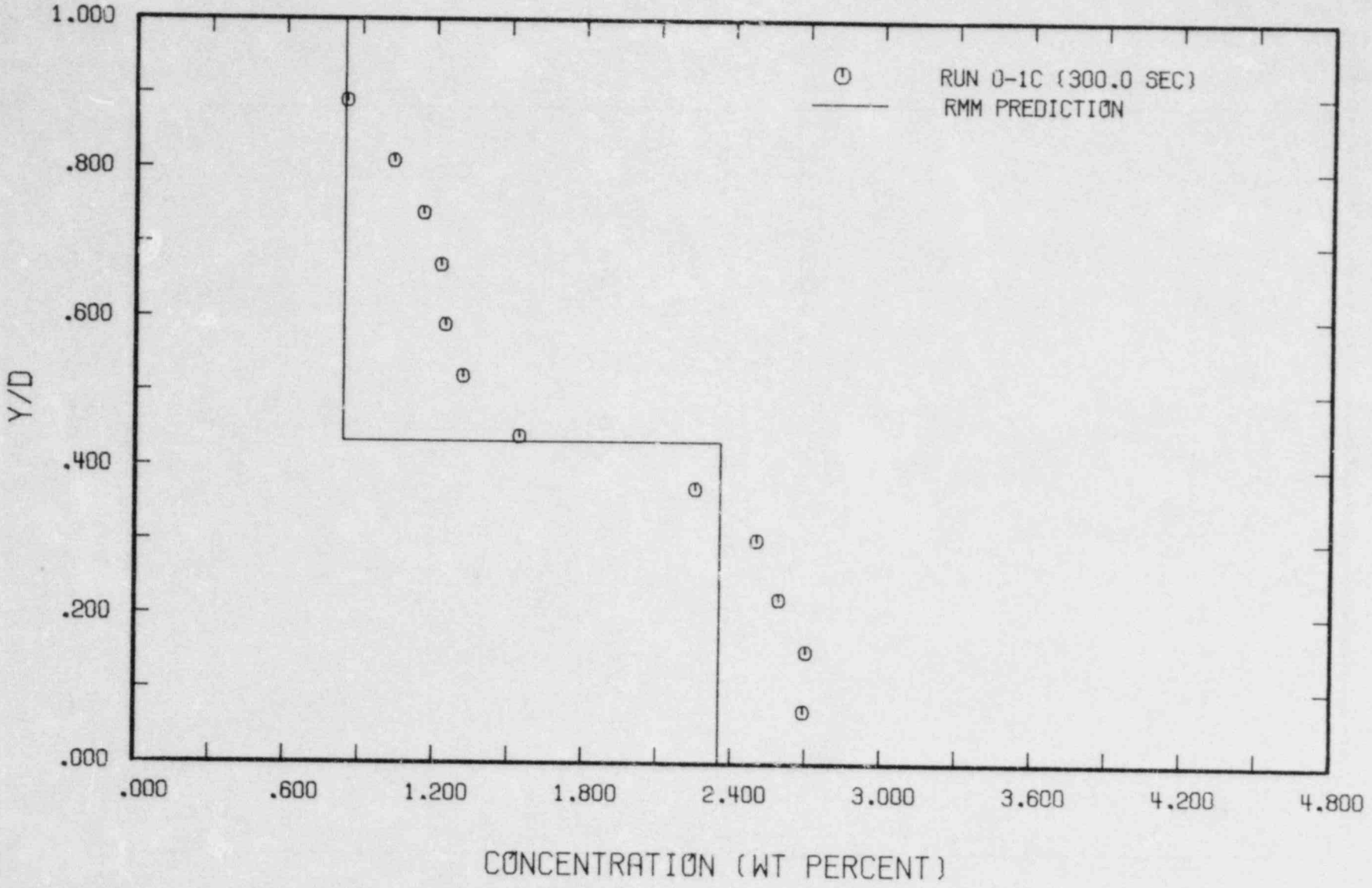
RUN 0-1C (300.0 SEC)
RMM PREDICTION
1.000
.800
.600
.400
.200
.000
Y/D
.000
.600
1.200
1.800
2.400
3.000
3.600
4.200
4.800
CONCENTRATION (WT PERCENT)

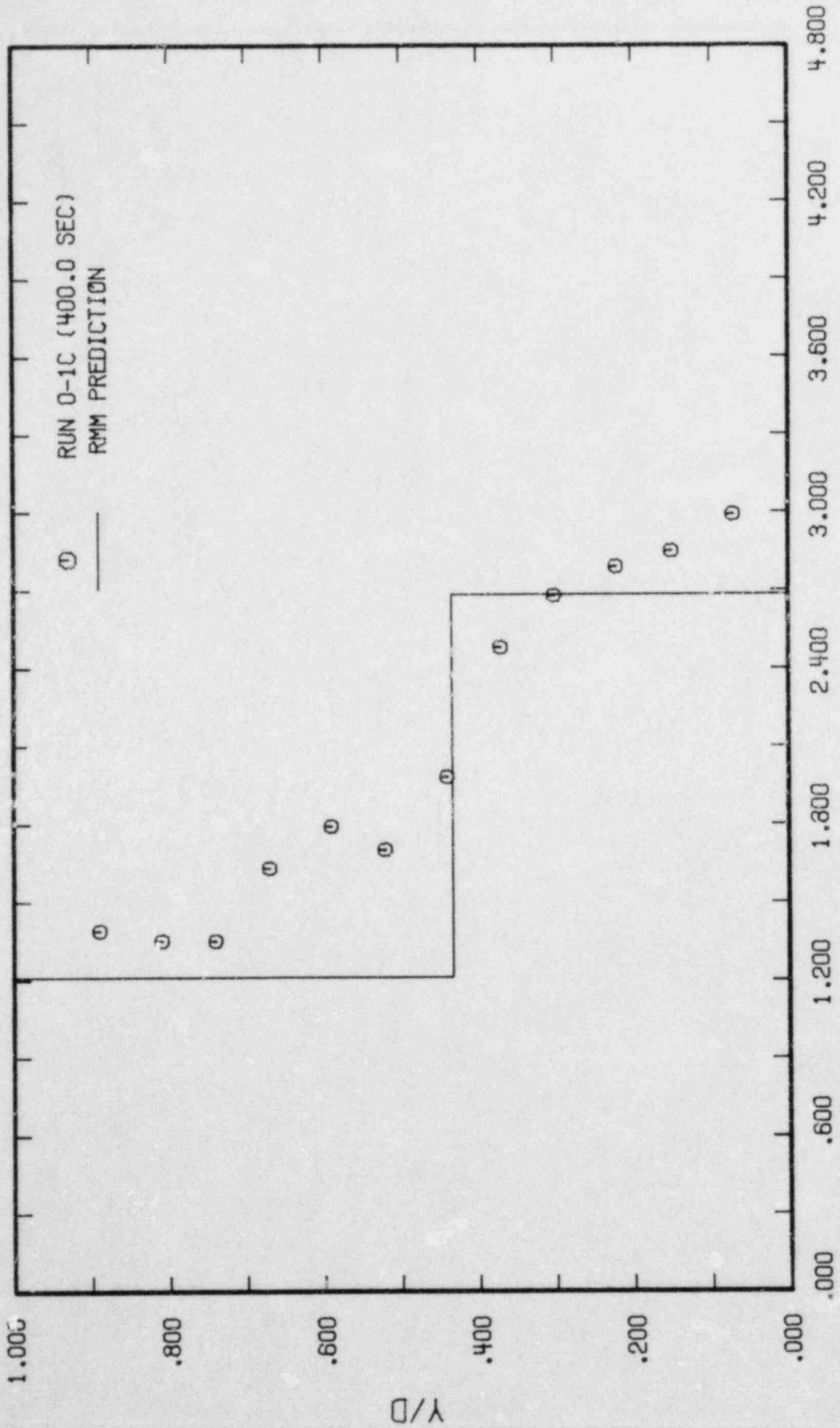
RUN 0-1C (400.0 SEC)
RMM PREDICTION
Y/D
1.000
.800
.600
.400
.200
.000
.000
.600
1.200
1.800
2.400
3.000
3.600
4.200
4.800
CONCENTRATION (WT PERCENT)

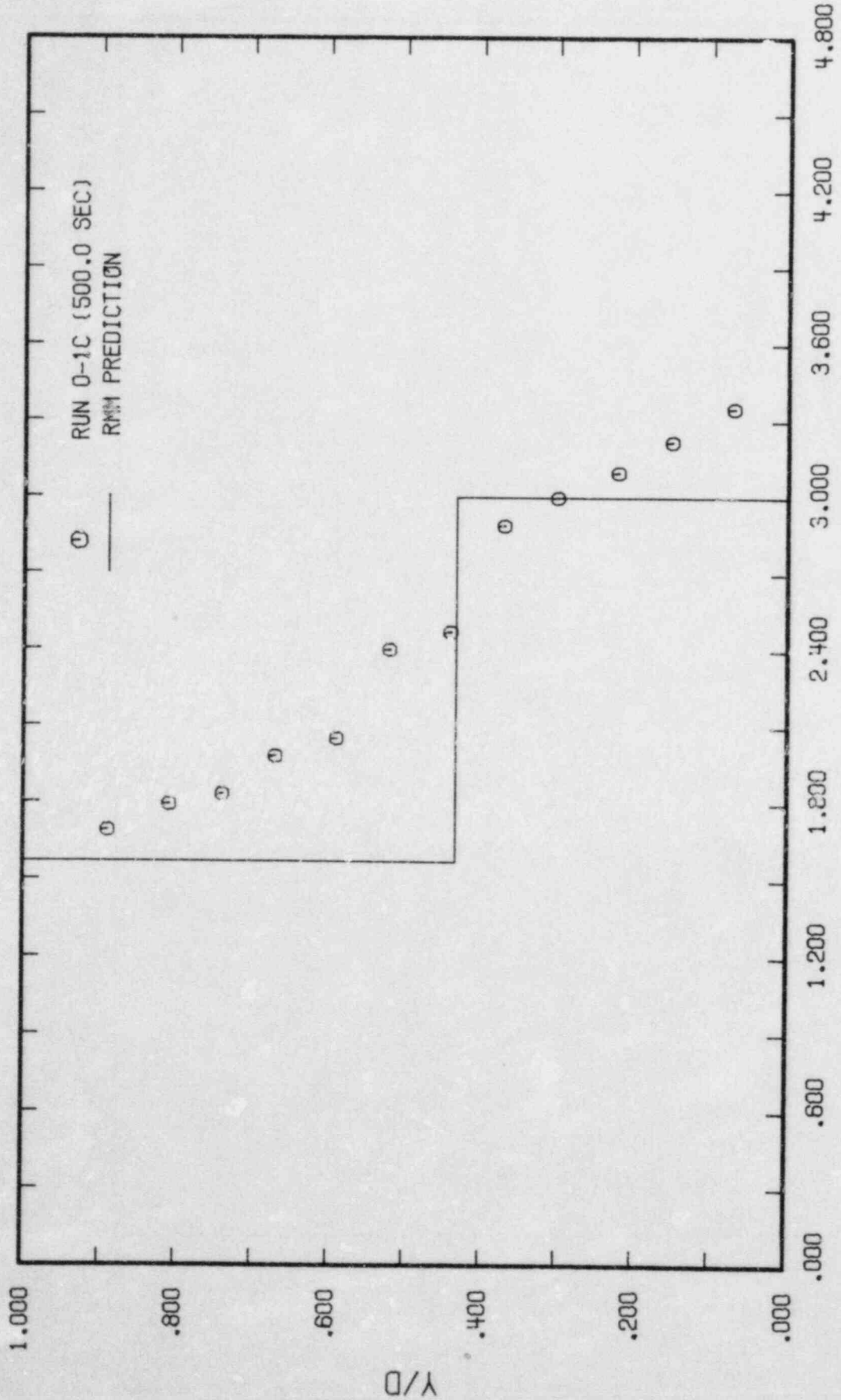
RUN 0-1C (500.0 SEC)
RMM PREDICTION
Y/D
1.000
.800
.600
.400
.200
.000
.000
.600
1.200
1.800
2.400
3.000
3.600
4.200
4.800
CONCENTRATION (WT PERCENT)

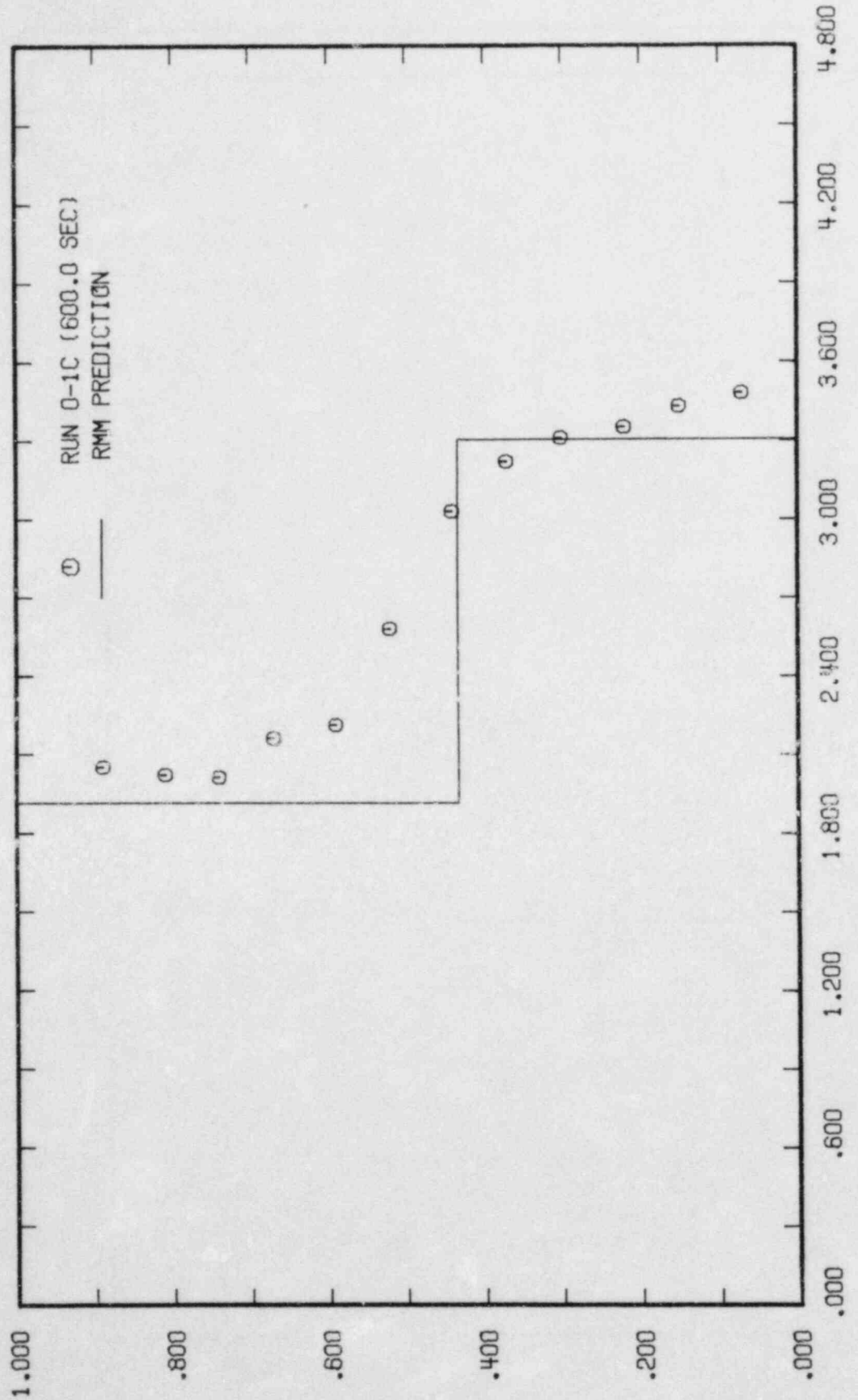
RUN 0-1C (600.0 SEC)
RMM PREDICTION
Y/D
1.000
.800
.600
.400
.200
.000
.000
.600
1.200
1.800
2.400
3.000
3.600
4.200
4.800
CONCENTRATION (WT PERCENT)

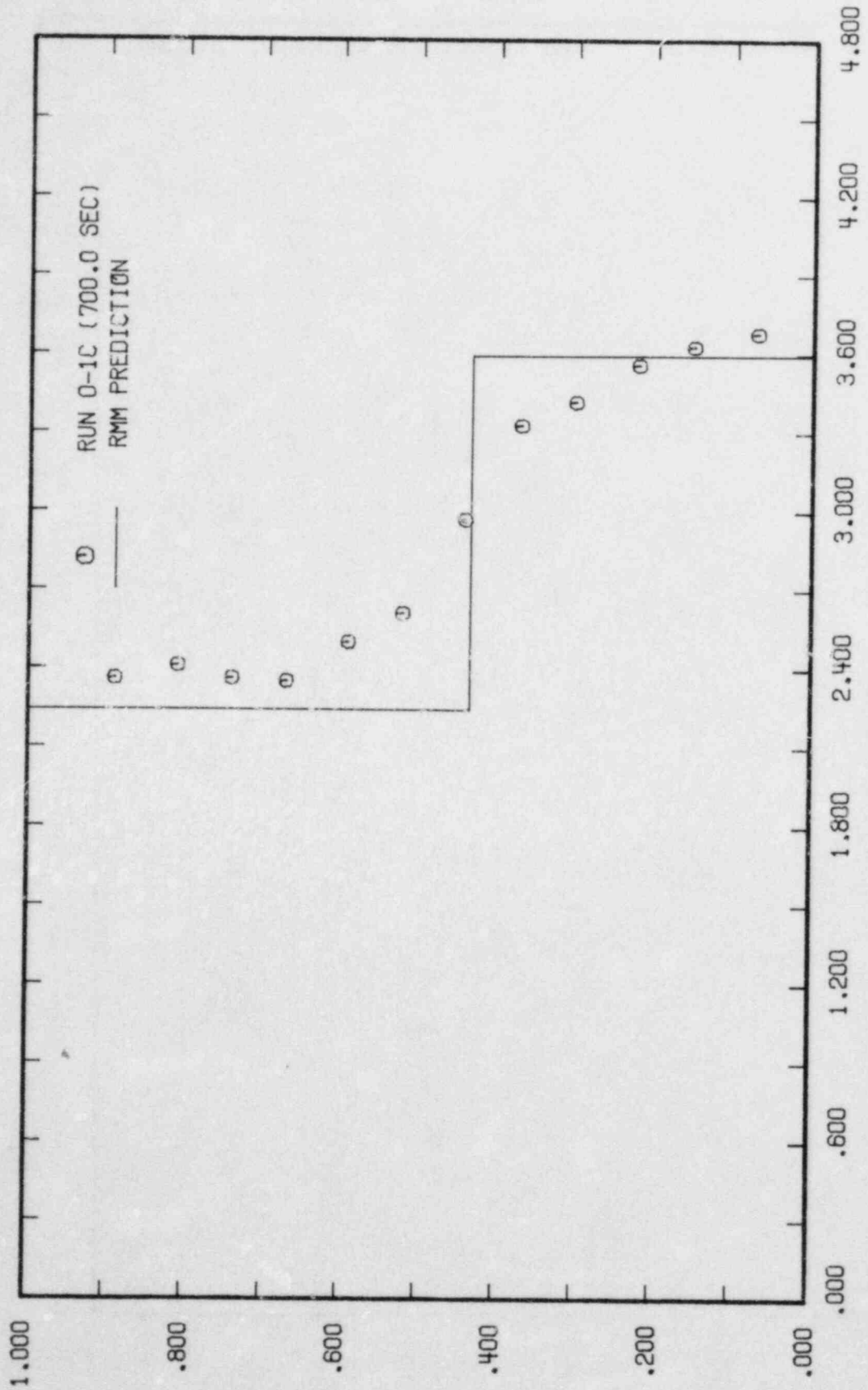
RUN 0-1C (700.0 SEC)
RMM PREDICTION
Y/D
1.000
.800
.600
.400
.200
.000
.000
.600
1.200
1.800
2.400
3.000
3.600
4.200
4.800
CONCENTRATION (WT PERCENT)

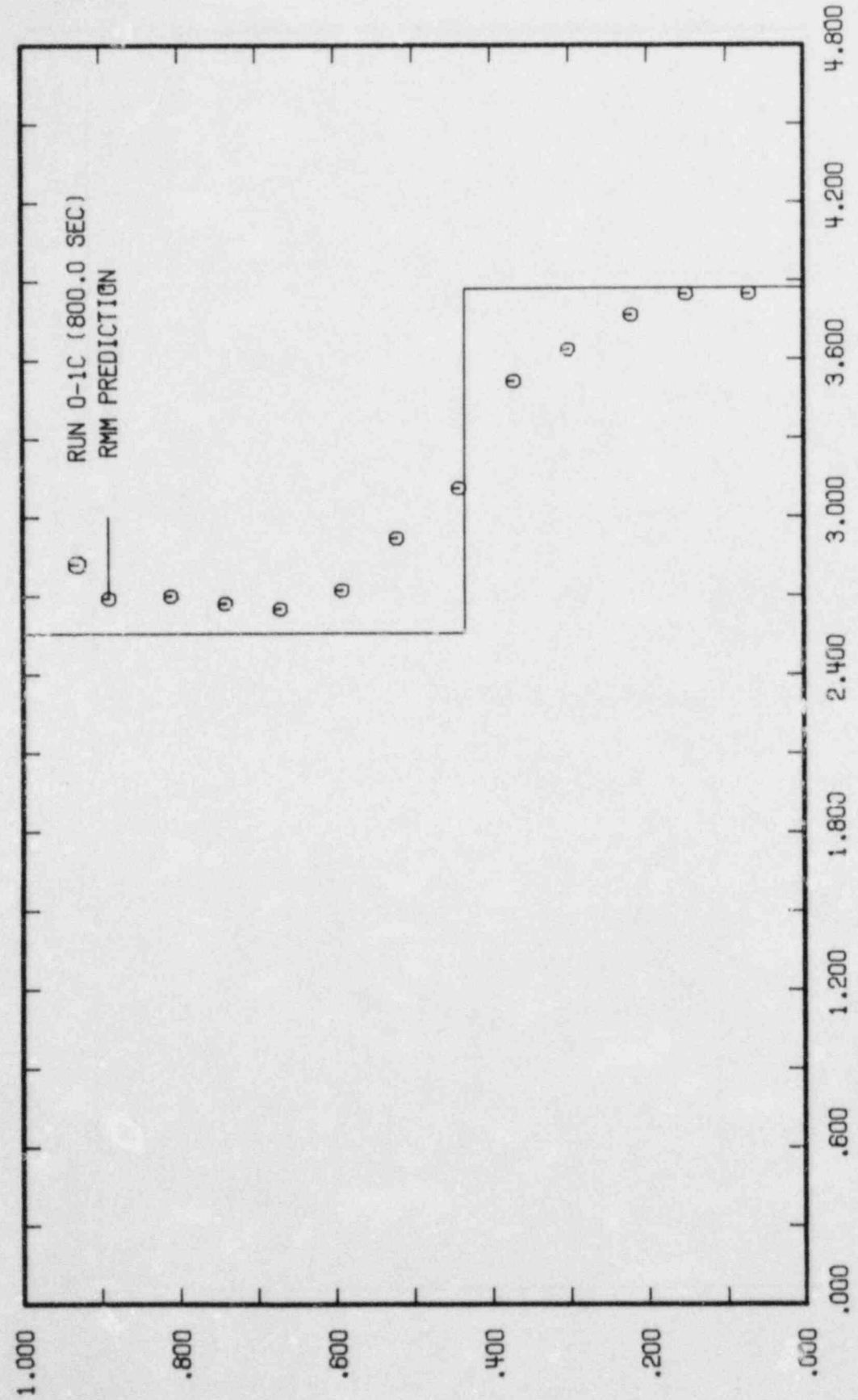
RUN 0-1C (800.0 SEC)
RMM PREDICTION
Y/D
1.000
.800
.600
.400
.200
.000
.000
.600
1.200
1.800
2.400
3.000
3.600
4.200
4.800
CONCENTRATION (WT PERCENT)

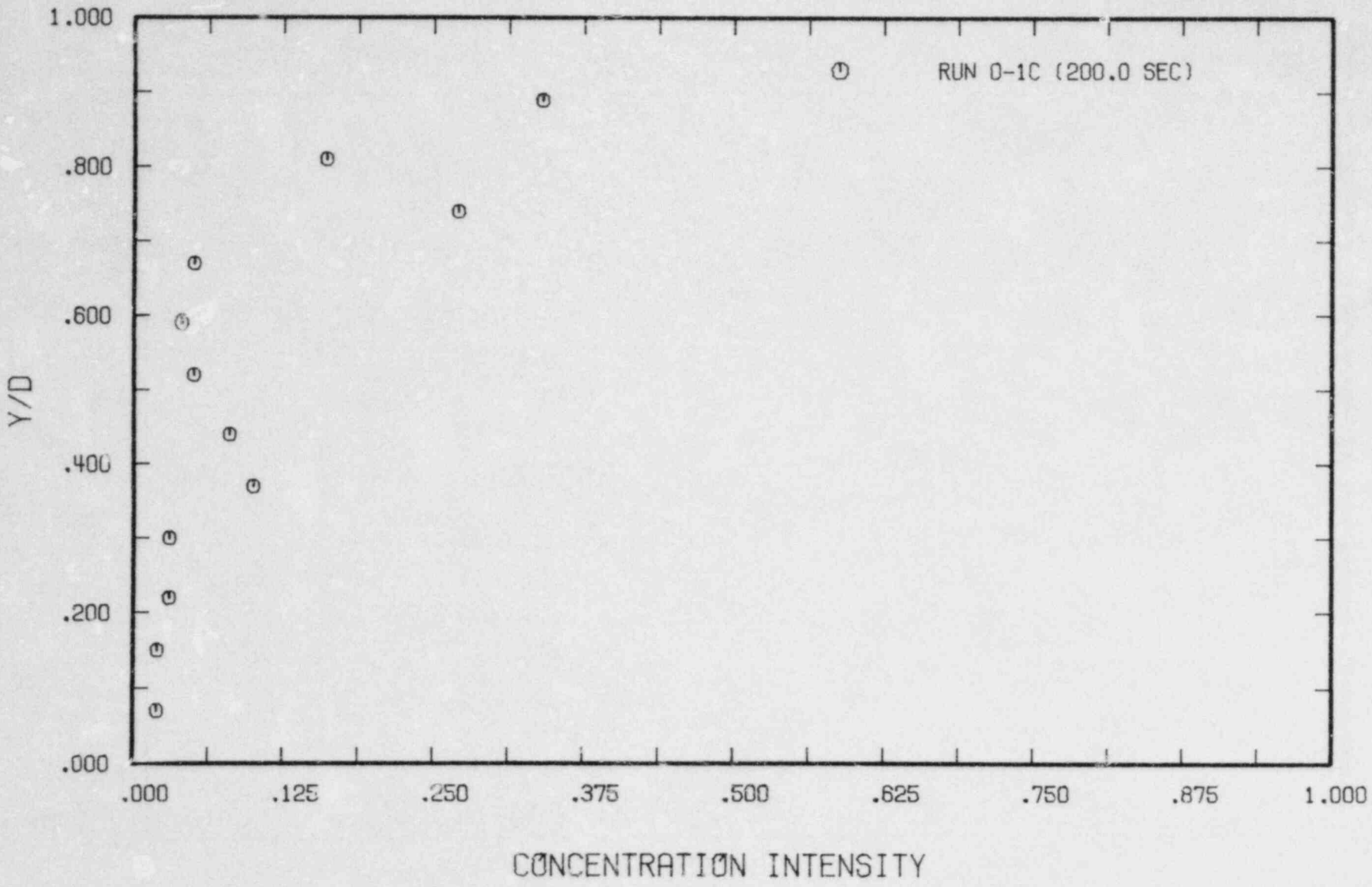
RUN 0-1C (200.0 SEC)
1.000
.800
.600
.400
.200
.000
Y/D
.000
.125
.250
.375
.500
.625
.750
.875
1.000
CONCENTRATION INTENSITY

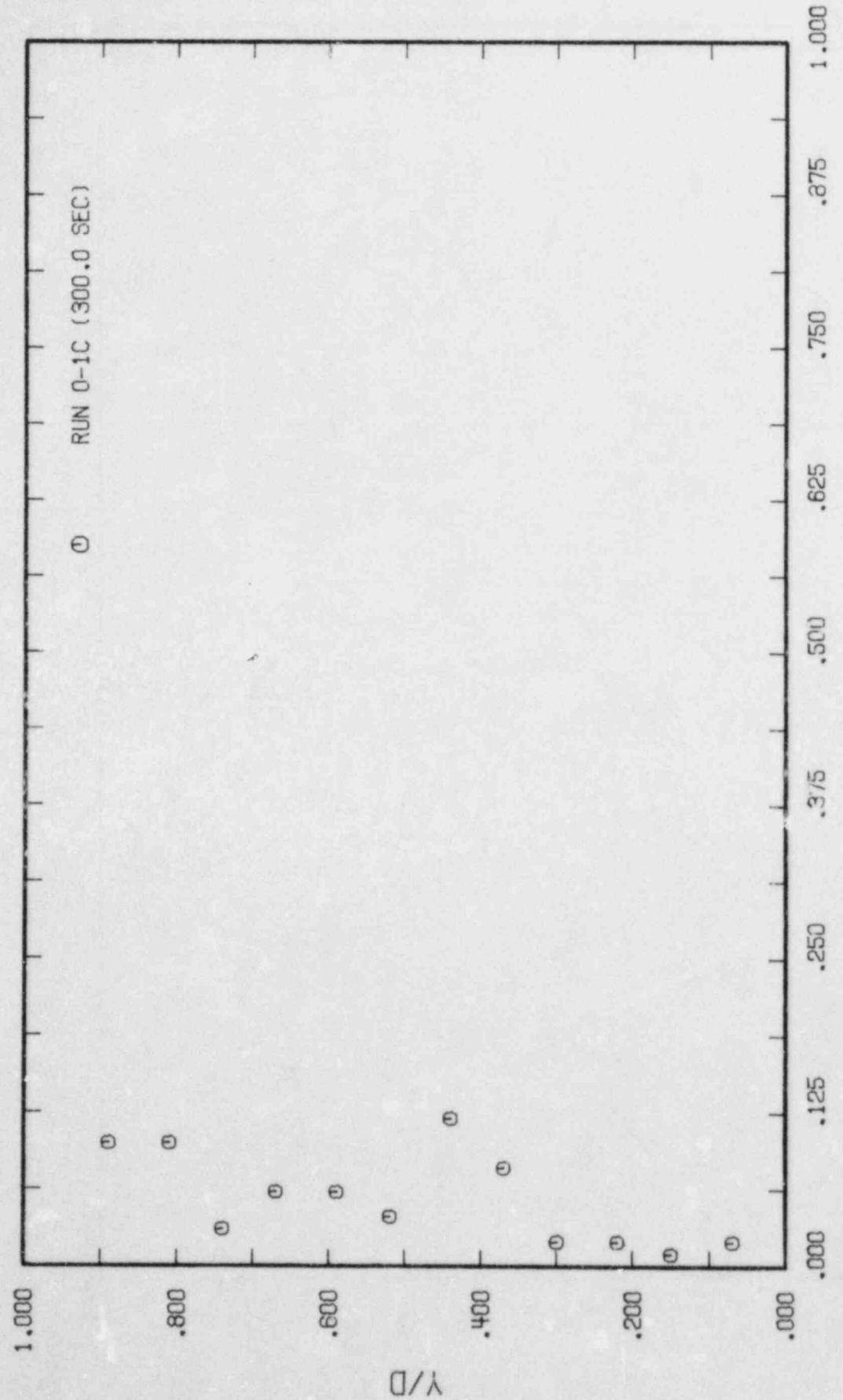
RUN 0-1C (300.0 SEC)
Y/D
1.000
.800
.600
.400
.200
.000
.000
.125
.250
.375
.500
.625
.750
.875
1.000
CONCENTRATION INTENSITY

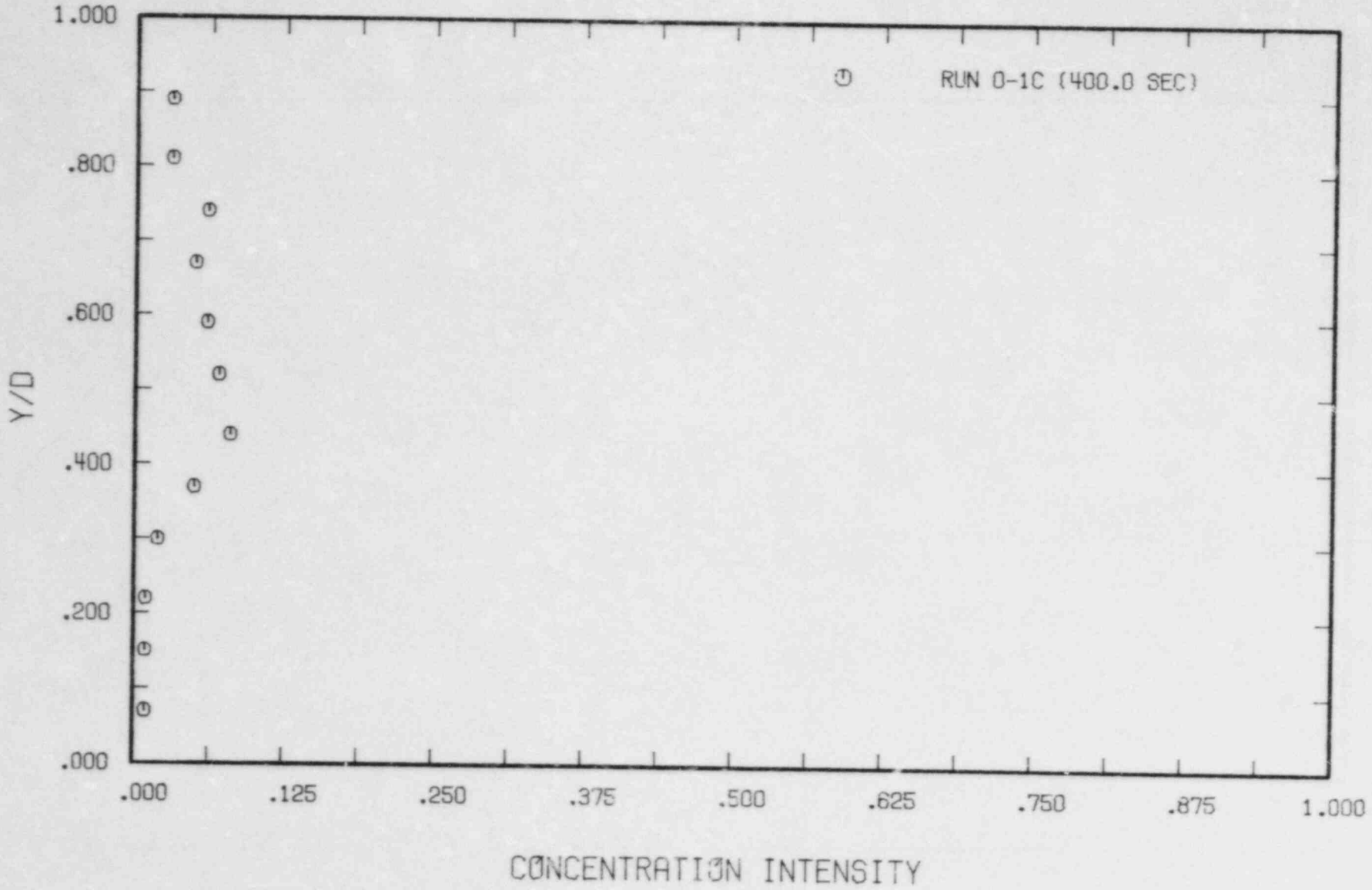
RUN 0-1C (400.0 SEC)
1.000
.800
.600
.400
.200
.000
Y/D
.000
.125
.250
.375
.500
.625
.750
.875
1.000
CONCENTRATION INTENSITY

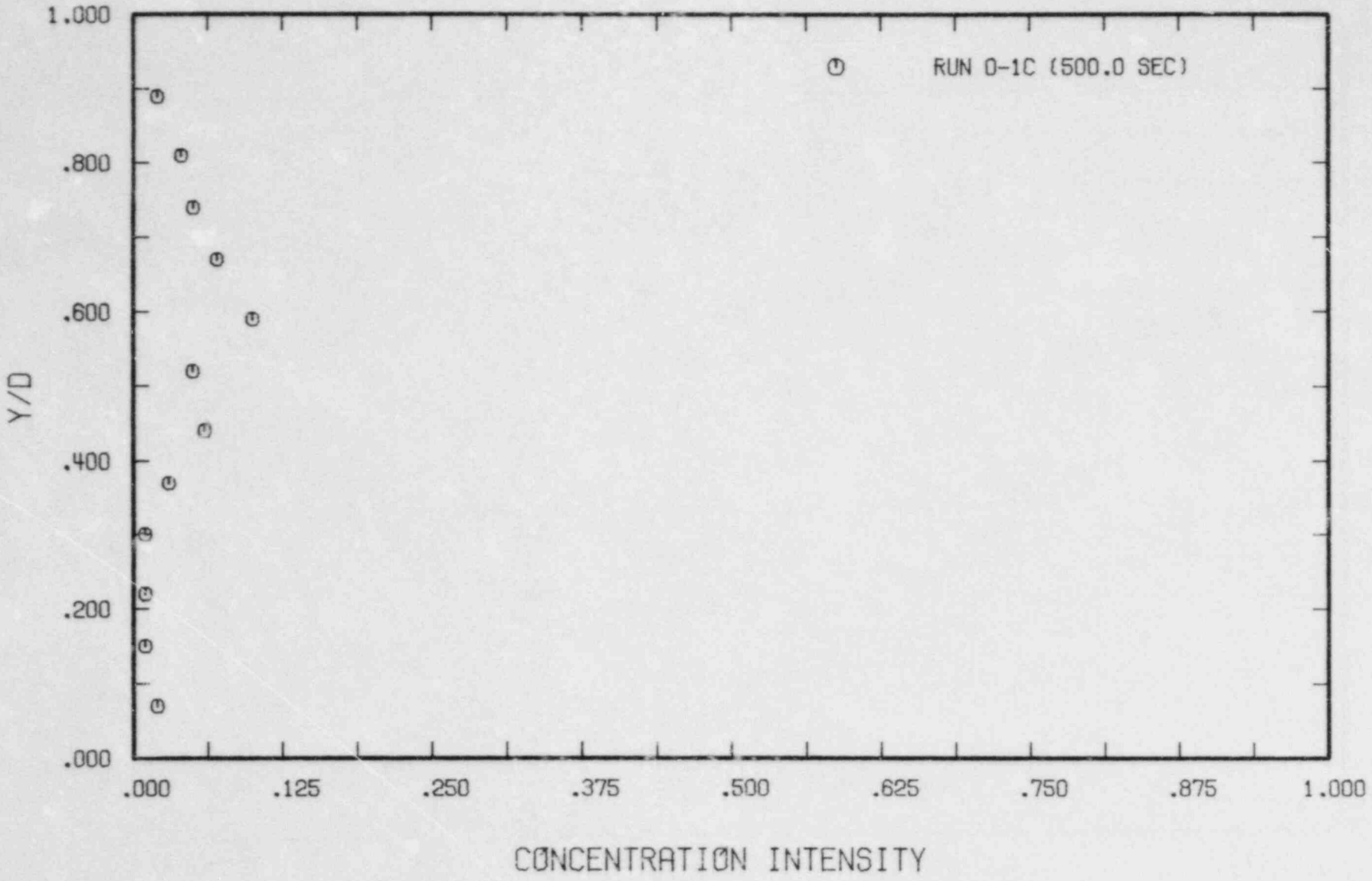
RUN 0-1C (500.0 SEC)
1.000
.800
.600
.400
.200
.000
Y/D
.000
.125
.250
.375
.500
.625
.750
.875
1.000
CONCENTRATION INTENSITY

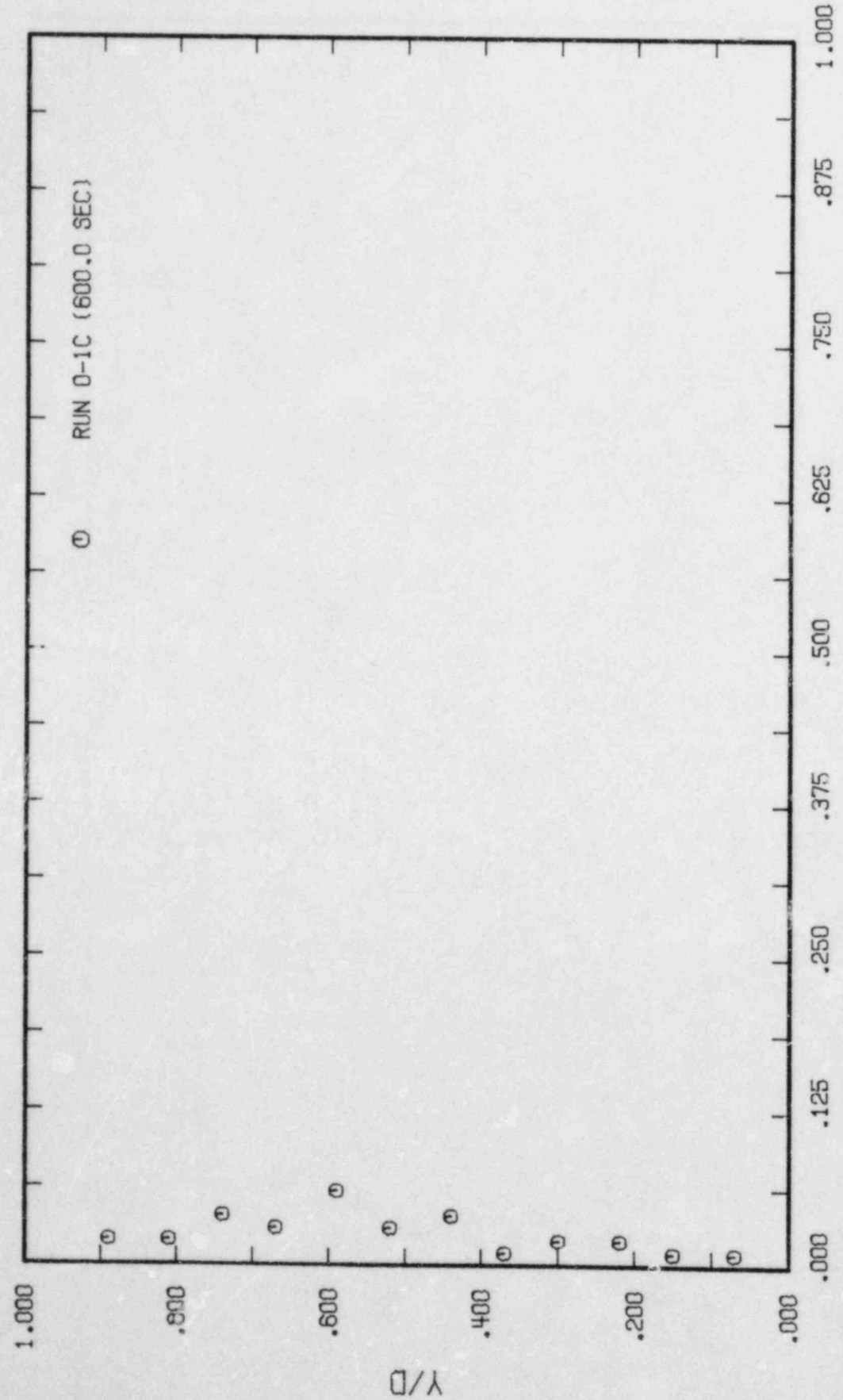
RUN 0-1C (600.0 SEC)
Y/D
1.000
.800
.600
.400
.200
.000
.000
.125
.250
.375
.500
.625
.750
.875
1.000
CONCENTRATION INTENSITY

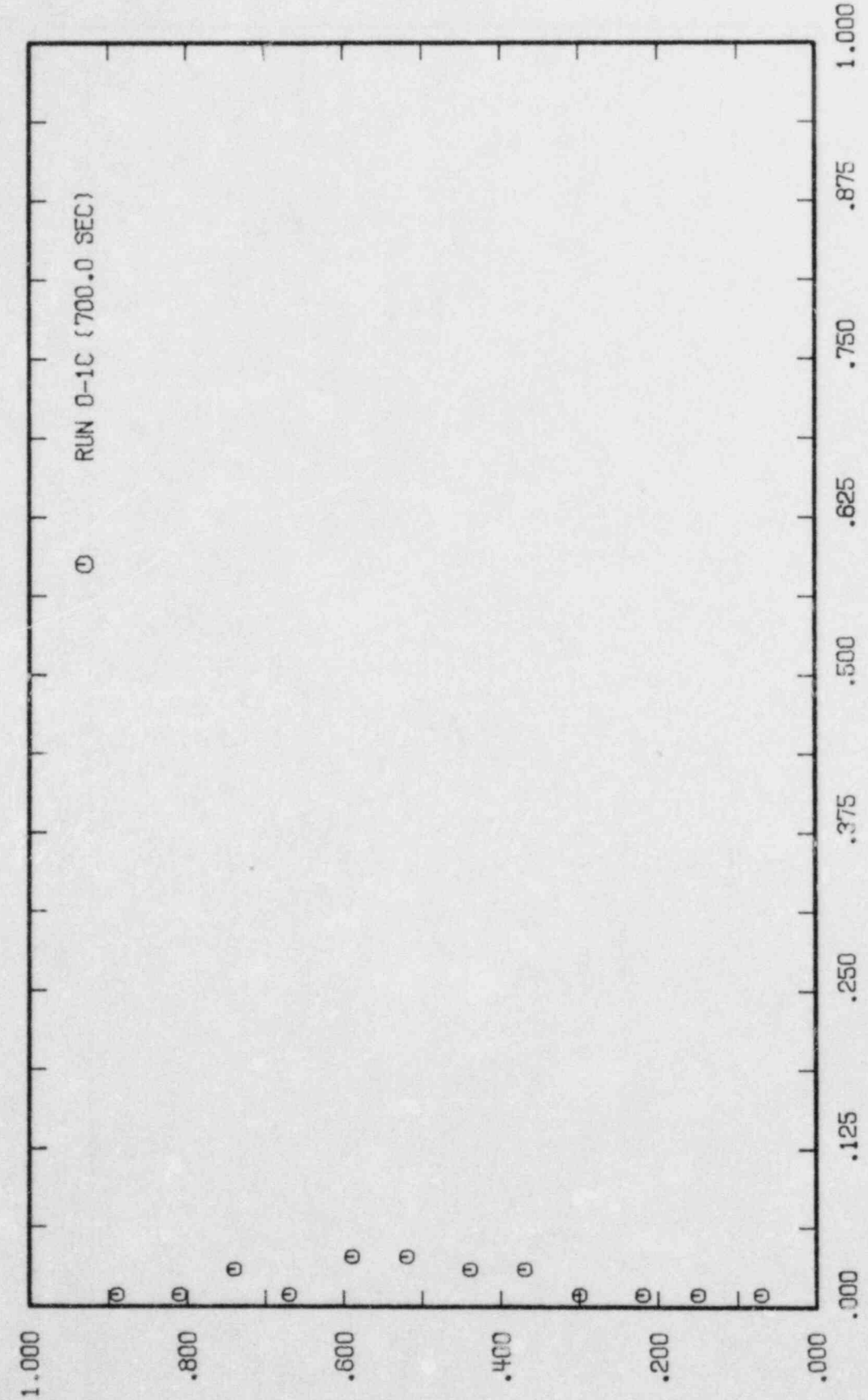
RUN 0-1C (700.0 SEC)
Y/D
1.000
.800
.600
.400
.200
.000
.000
.125
.250
.375
.500
.625
.750
.875
1.000
CONCENTRATION INTENSITY

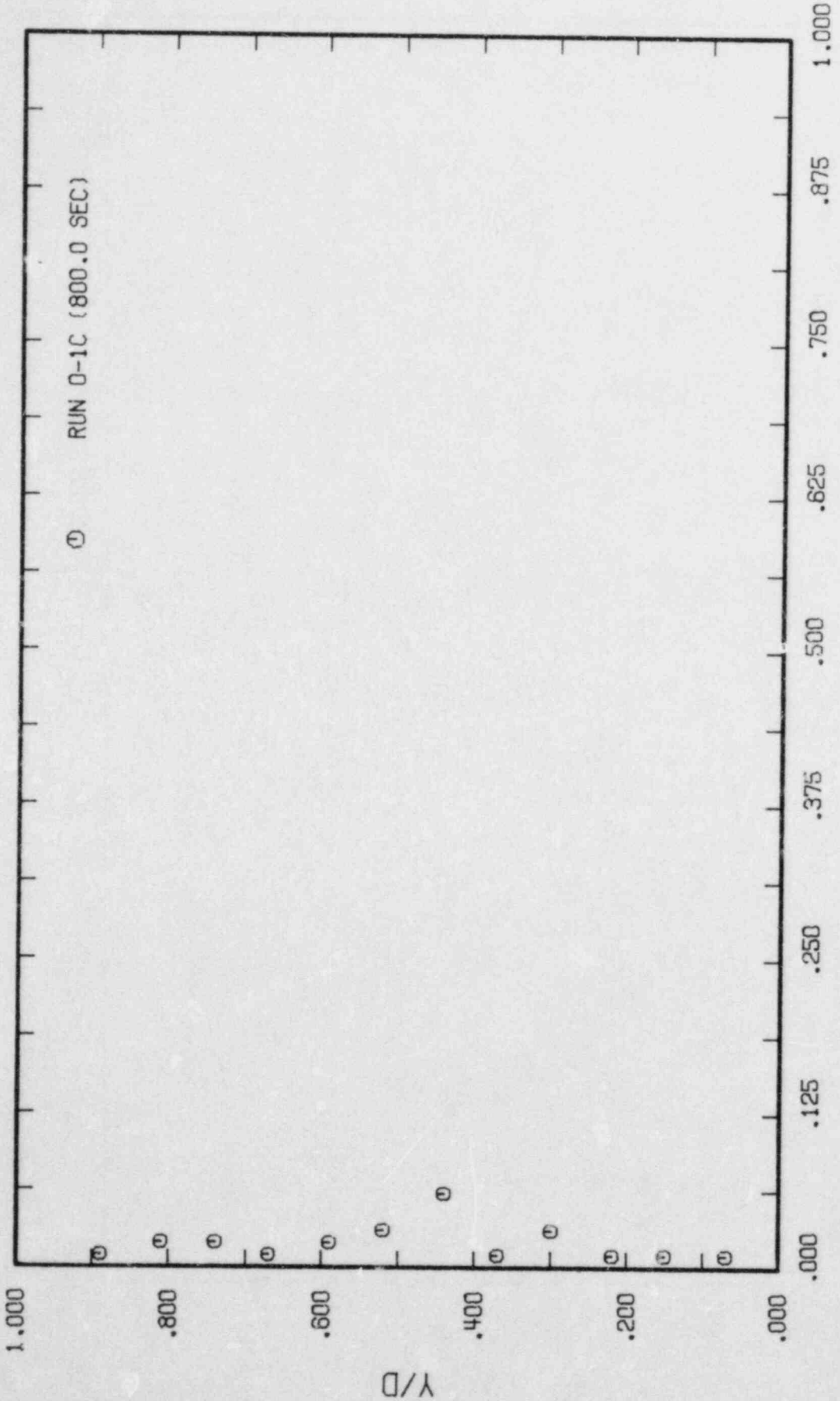
RUN 0-1C (800.0 SEC)
Y/D
1.000
.800
.600
.400
.200
.000
.000
.125
.250
.375
.500
.625
.750
.875
1.000
CONCENTRATION INTENSITY

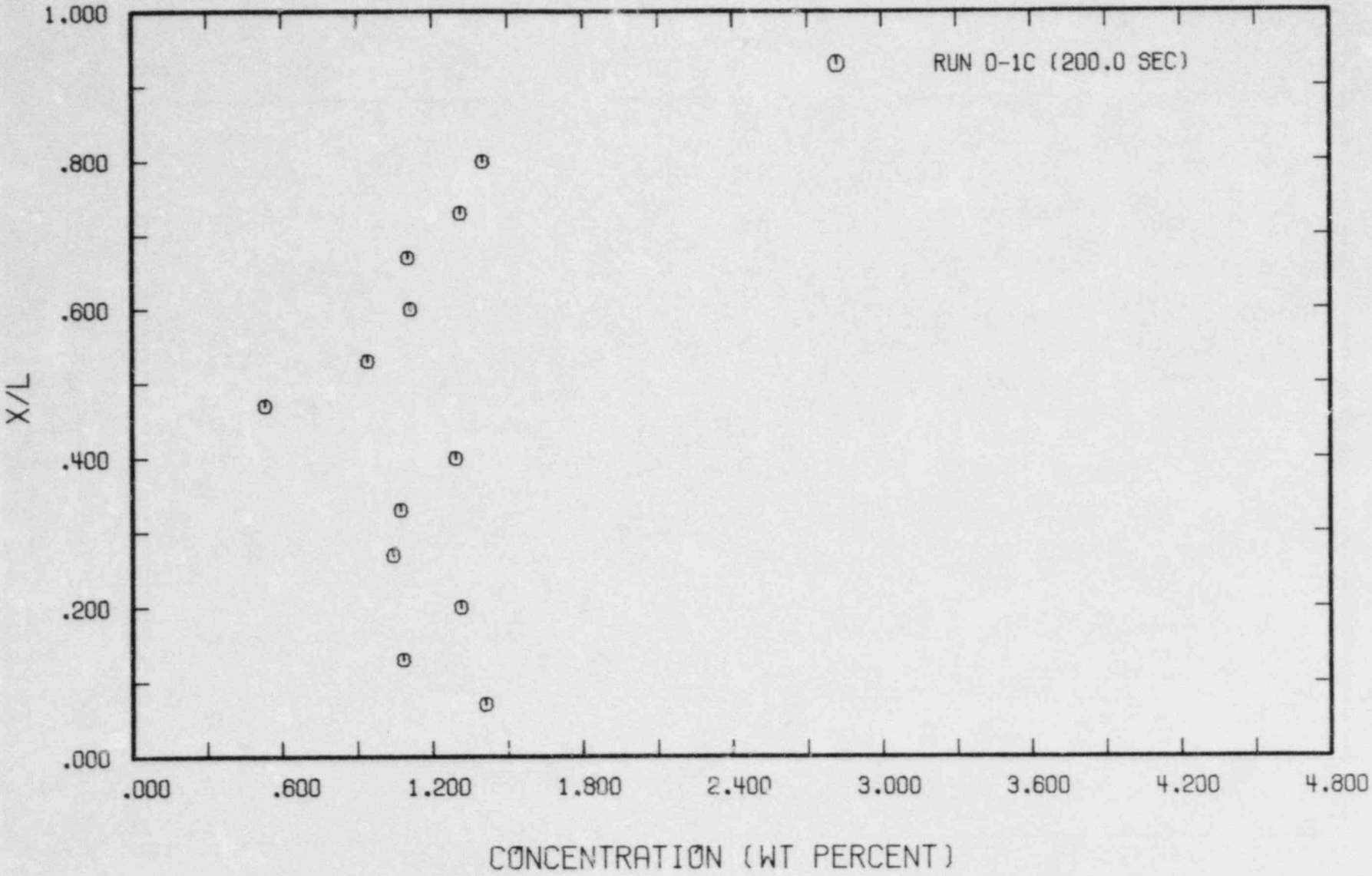
RUN 0-1C (200.0 SEC)
1.000
.800
.600
.400
.200
.000
X/L
.000
.600
1.200
1.800
2.400
3.000
3.600
4.200
4.800
CONCENTRATION (WT PERCENT)

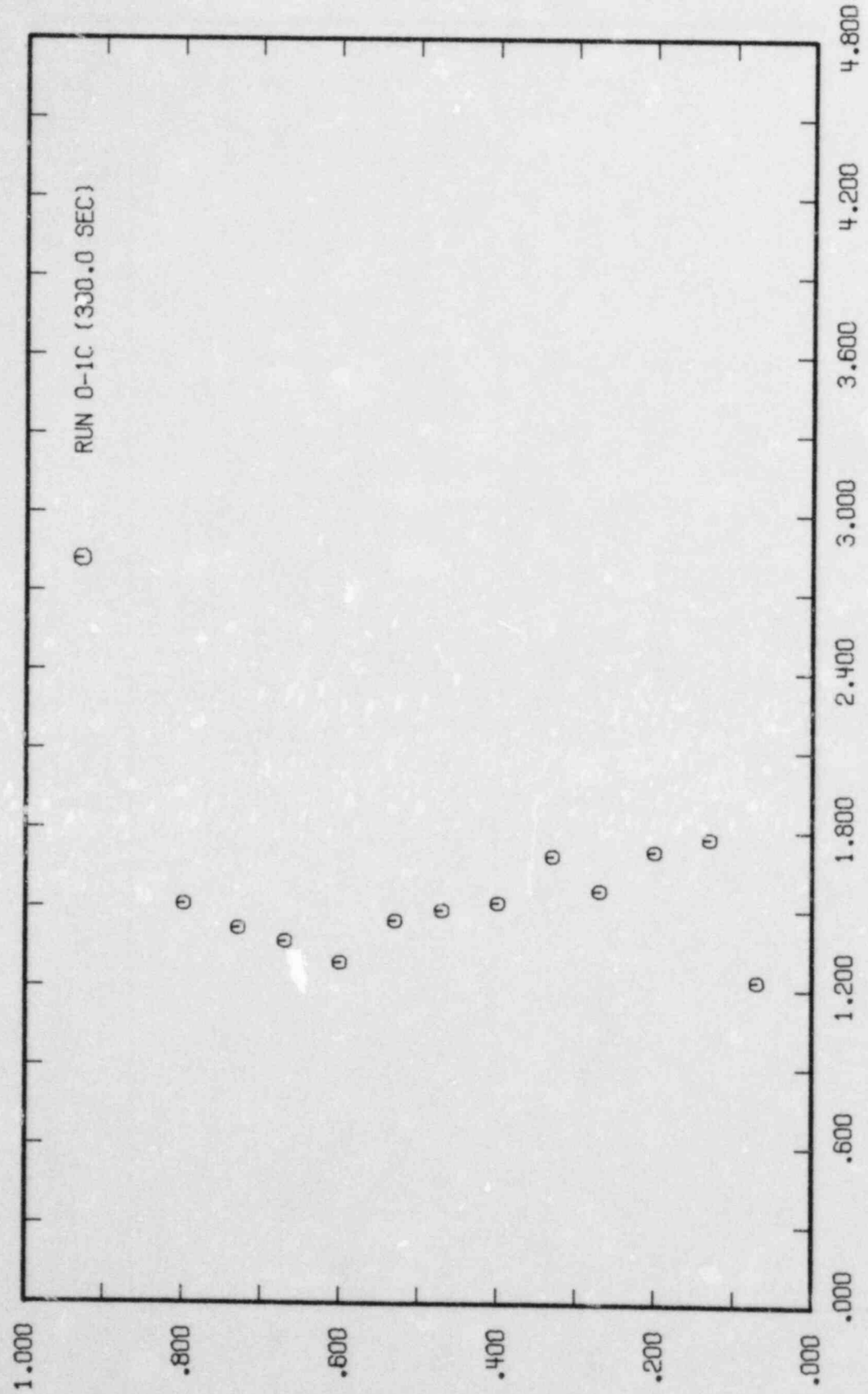
RUN 0-1C (300.0 SEC)
X/L
1.000
.800
.600
.400
.200
.000
.000
.600
1.200
1.800
2.400
3.000
3.600
4.200
4.800
CONCENTRATION (WT PERCENT)

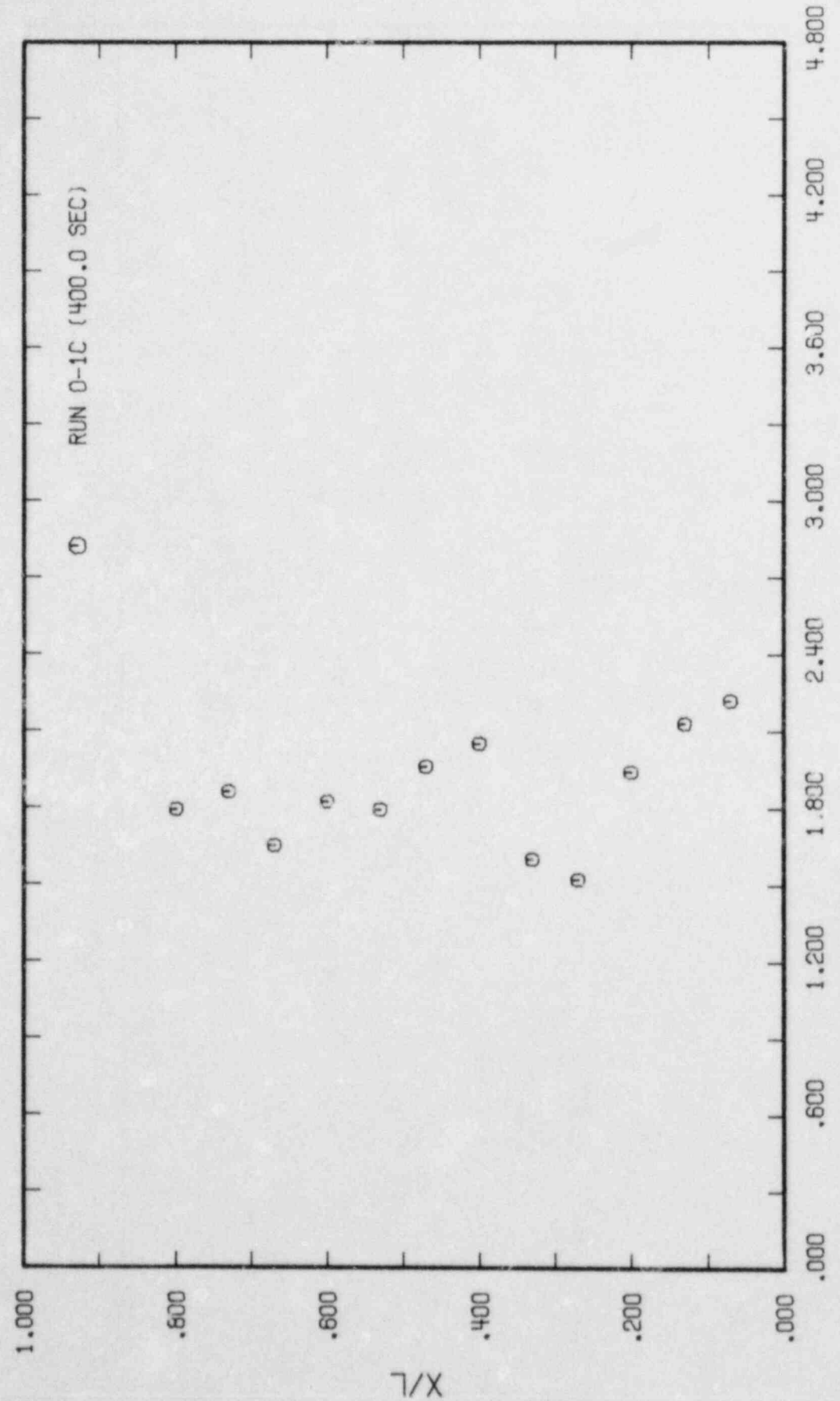
RUN 0-1C (400.0 SEC)
X/L
1.000
.800
.600
.400
.200
.000
.000
.600
1.200
1.800
2.400
3.000
3.600
4.200
4.800
CONCENTRATION (WT PERCENT)

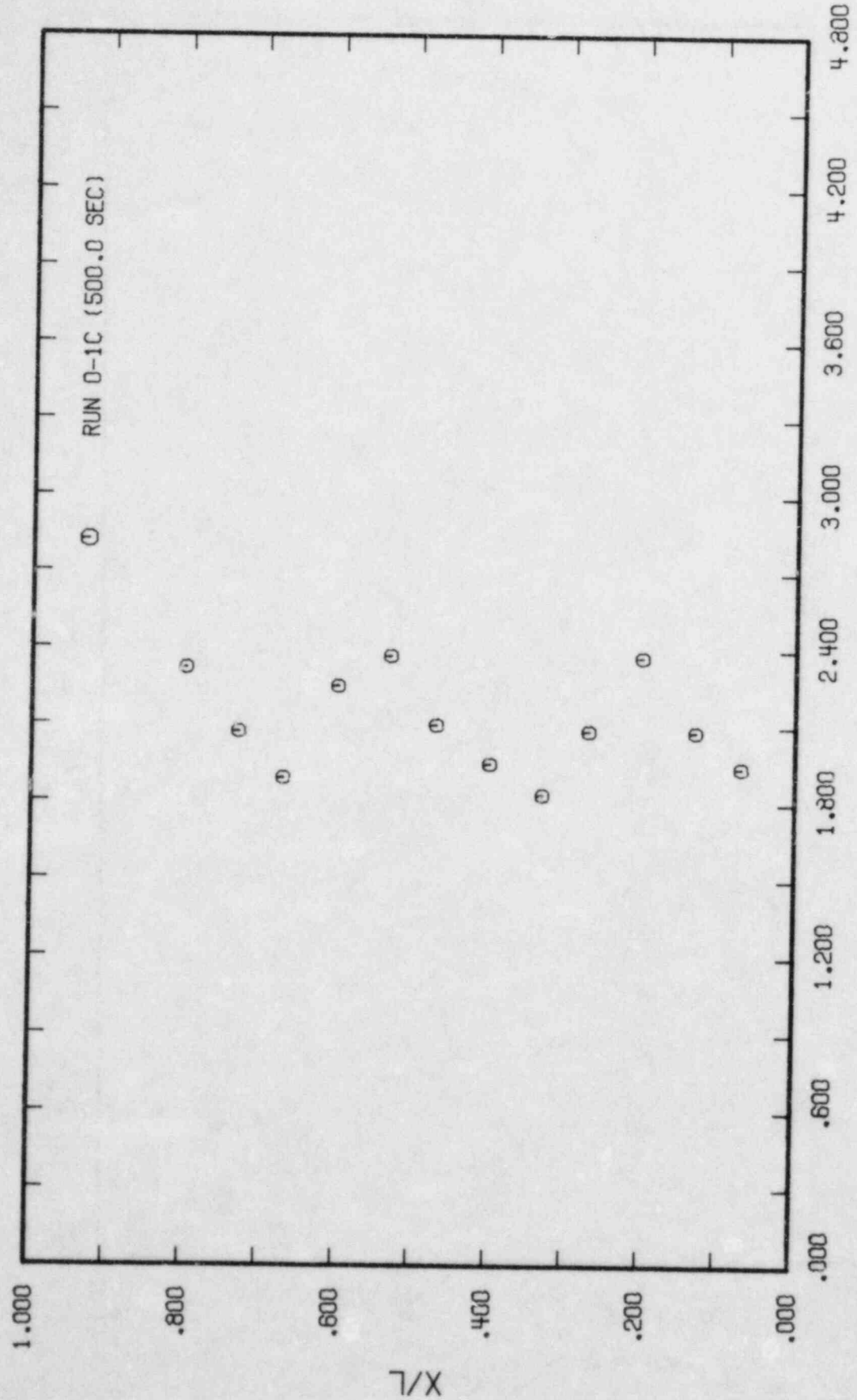
RUN 0-1C (500.0 SEC)
1.000
.800
.600
.400
.200
.000
X/L
.000
.600
1.200
1.800
2.400
3.000
3.600
4.200
4.800
CONCENTRATION (WT PERCENT)

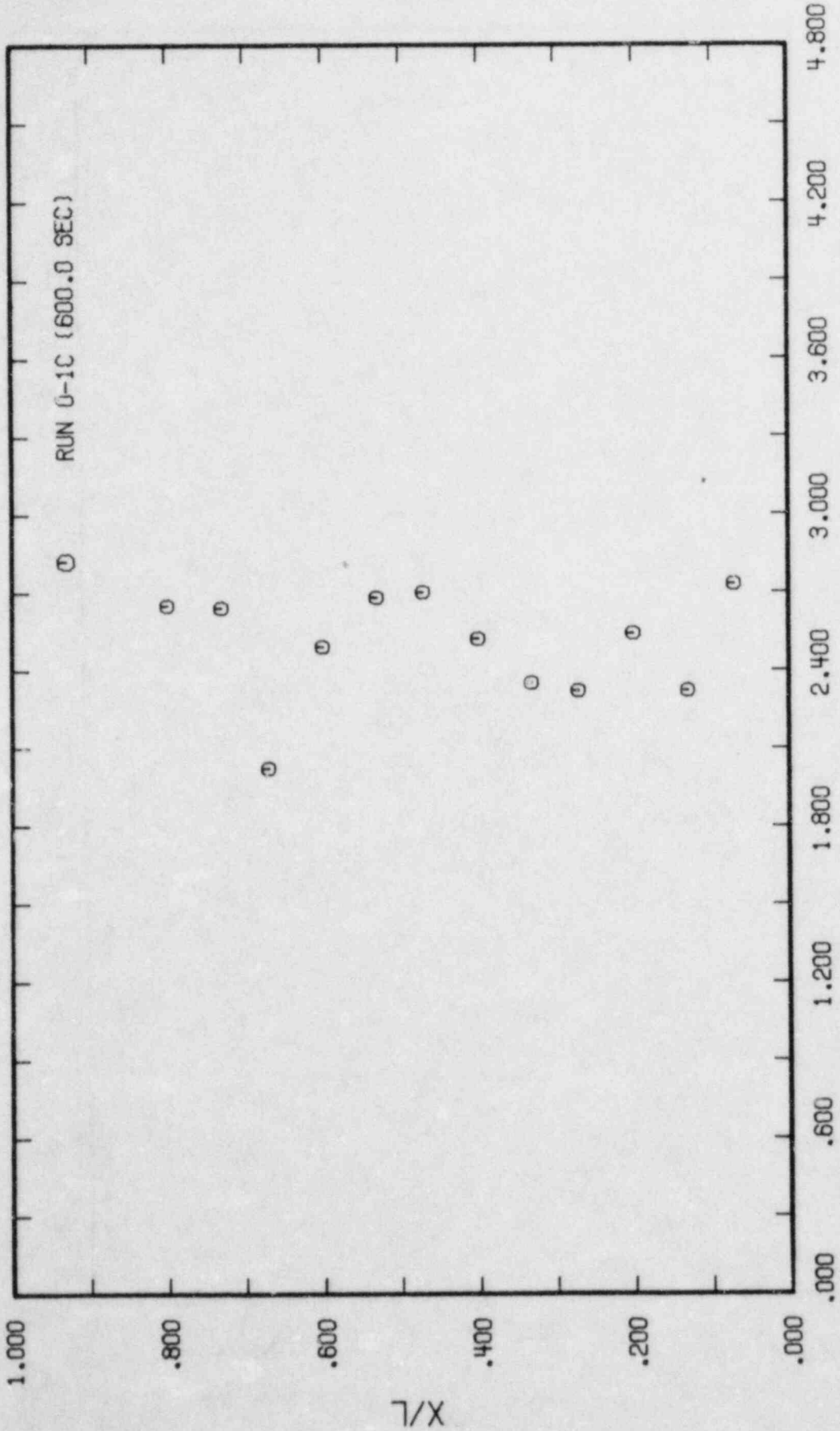
RUN 0-1C (600.0 SEC)
X/L
1.000
.800
.600
.400
.200
.000
.000
.600
1.200
1.800
2.400
3.000
3.600
4.200
4.800
CONCENTRATION (WT PERCENT)

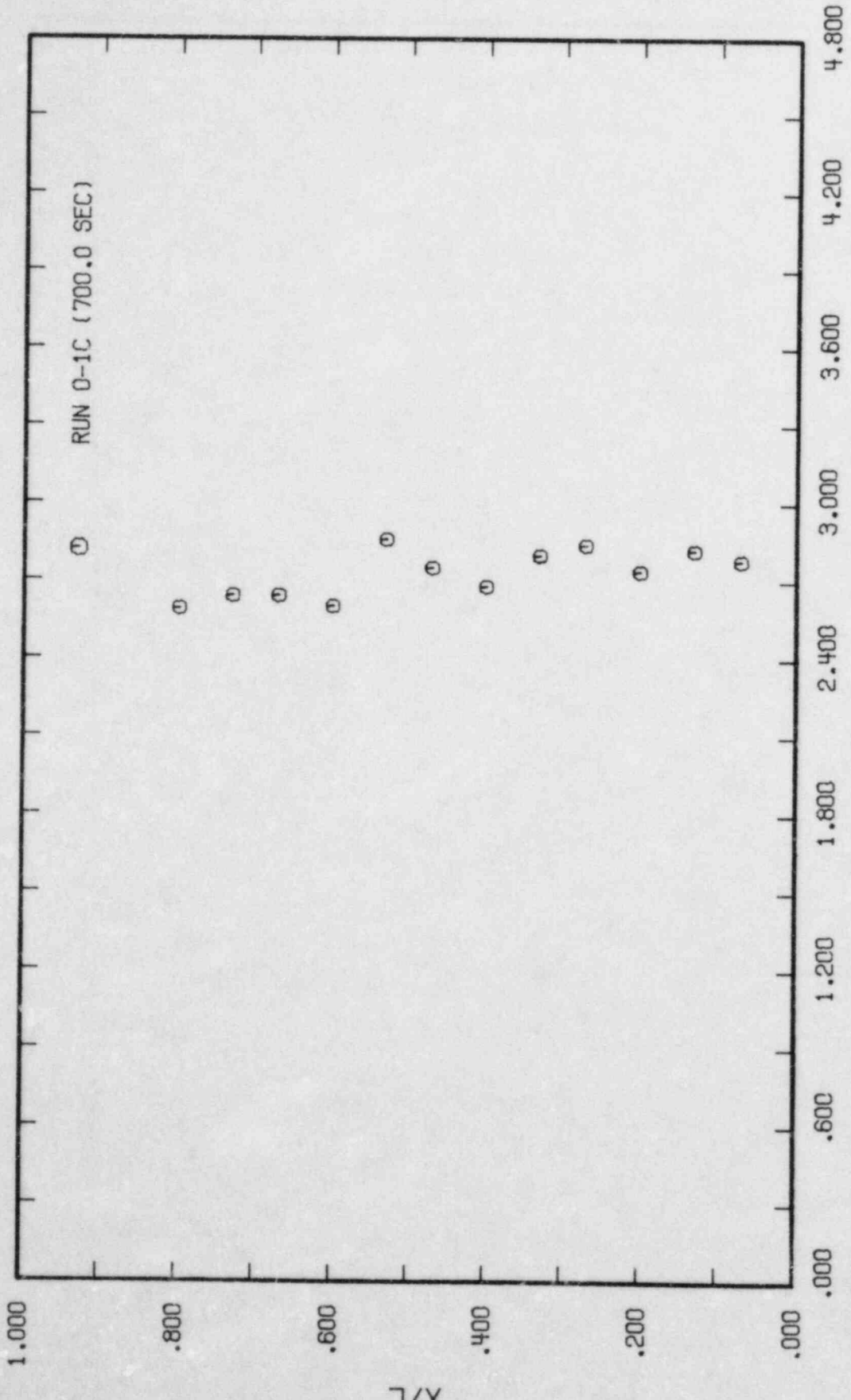
RUN 0-1C (700.0 SEC)
X/L
1.000
.800
.600
.400
.200
.000
.000
.600
1.200
1.800
2.400
3.000
3.600
4.200
4.800
CONCENTRATION (WT PERCENT)

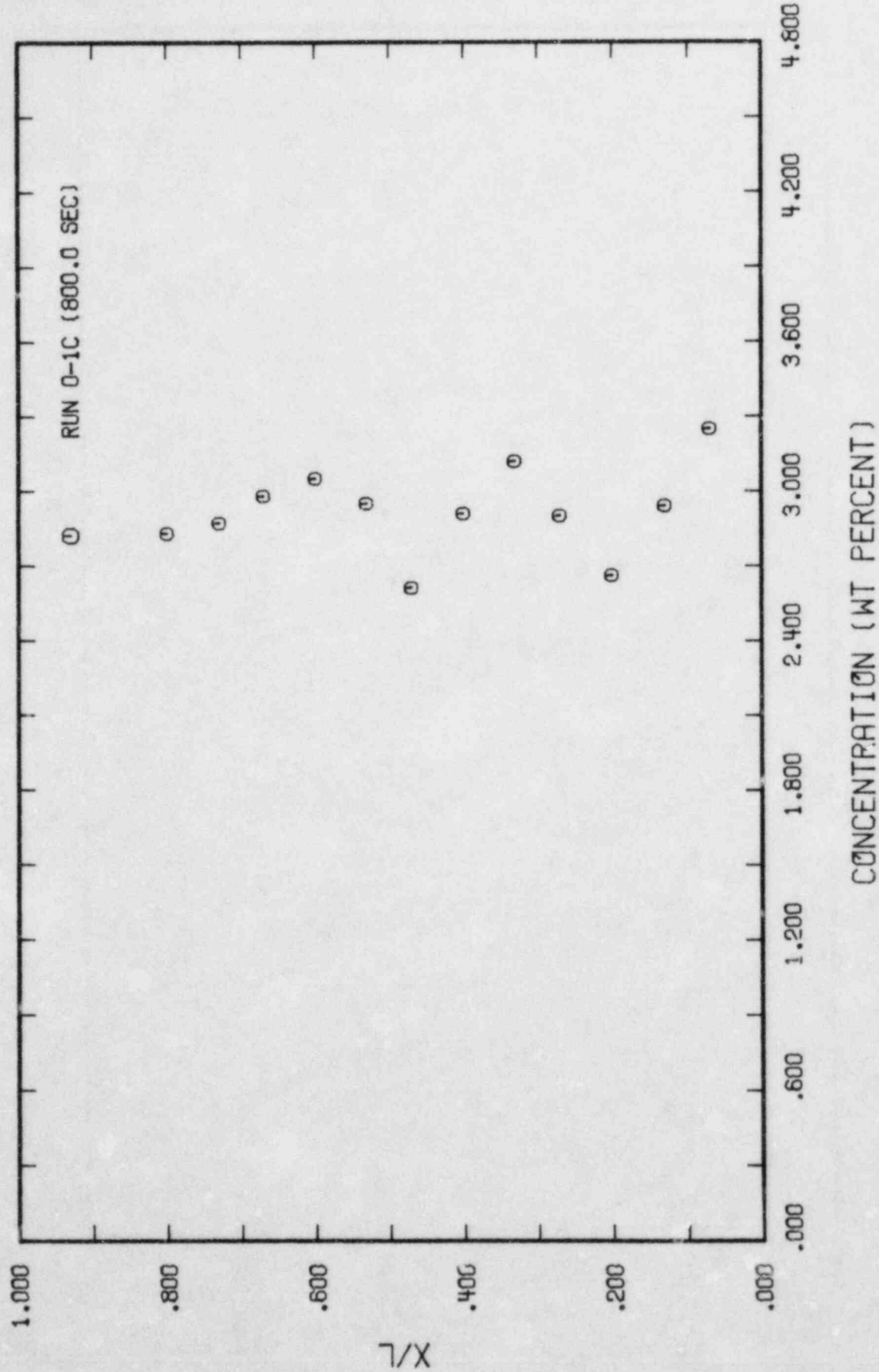
RUN 0-1C (800.0 SEC)
1.000
.800
.600
.400
.200
.000
X/L
.000
.600
1.200
1.800
2.400
3.000
3.600
4.200
4.800
CONCENTRATION (WT PERCENT)

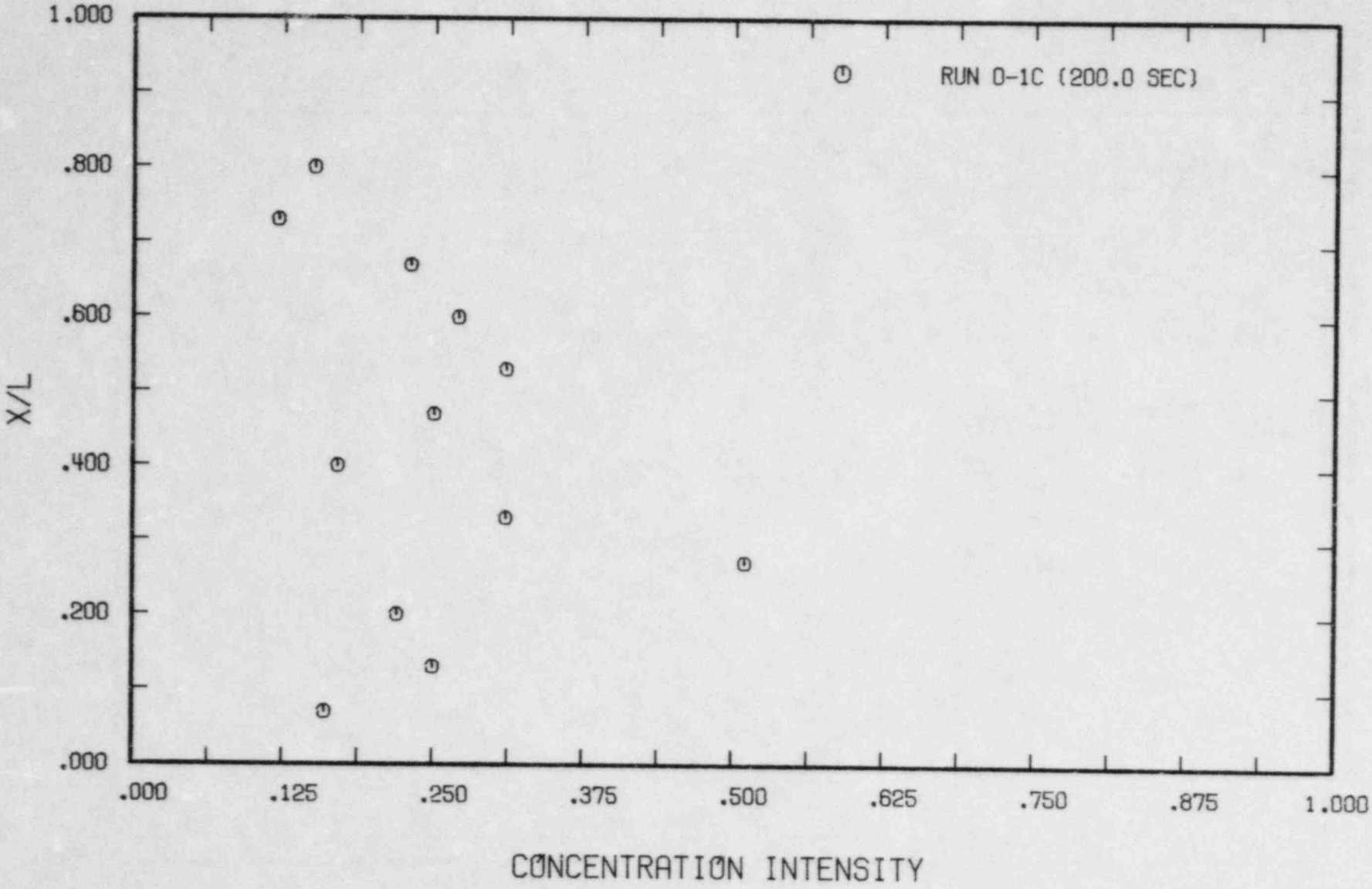
RUN 0-1C (200.0 SEC)
1.000
.800
.600
.400
.200
.000
X/L
.000
.125
.250
.375
.500
.625
.750
.875
1.000
CONCENTRATION INTENSITY

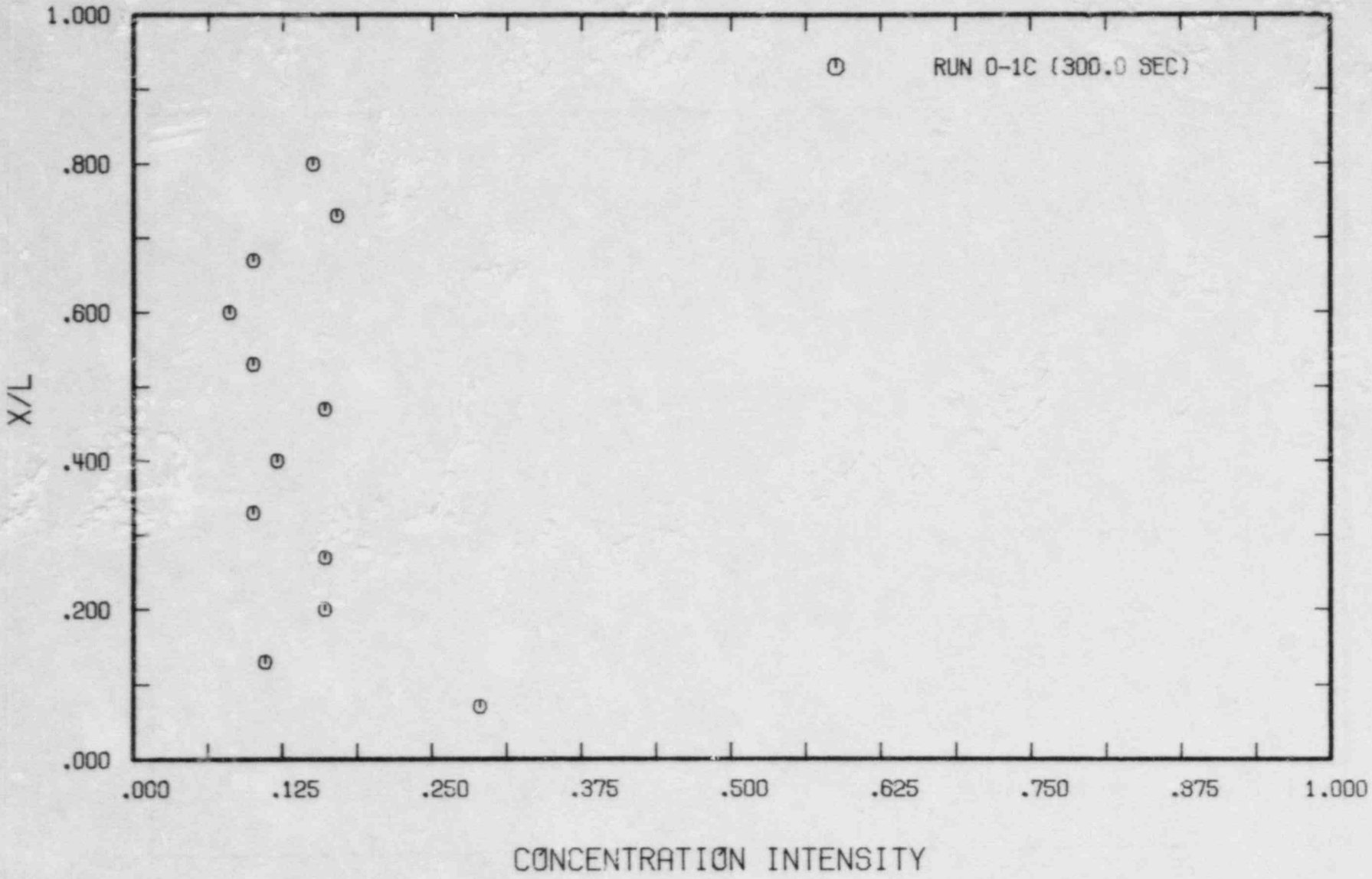
RUN 0-1C (300.0 SEC)
1.000
.800
.600
.400
.200
.000
X/L
.000
.125
.250
.375
.500
.625
.750
.875
1.000
CONCENTRATION INTENSITY

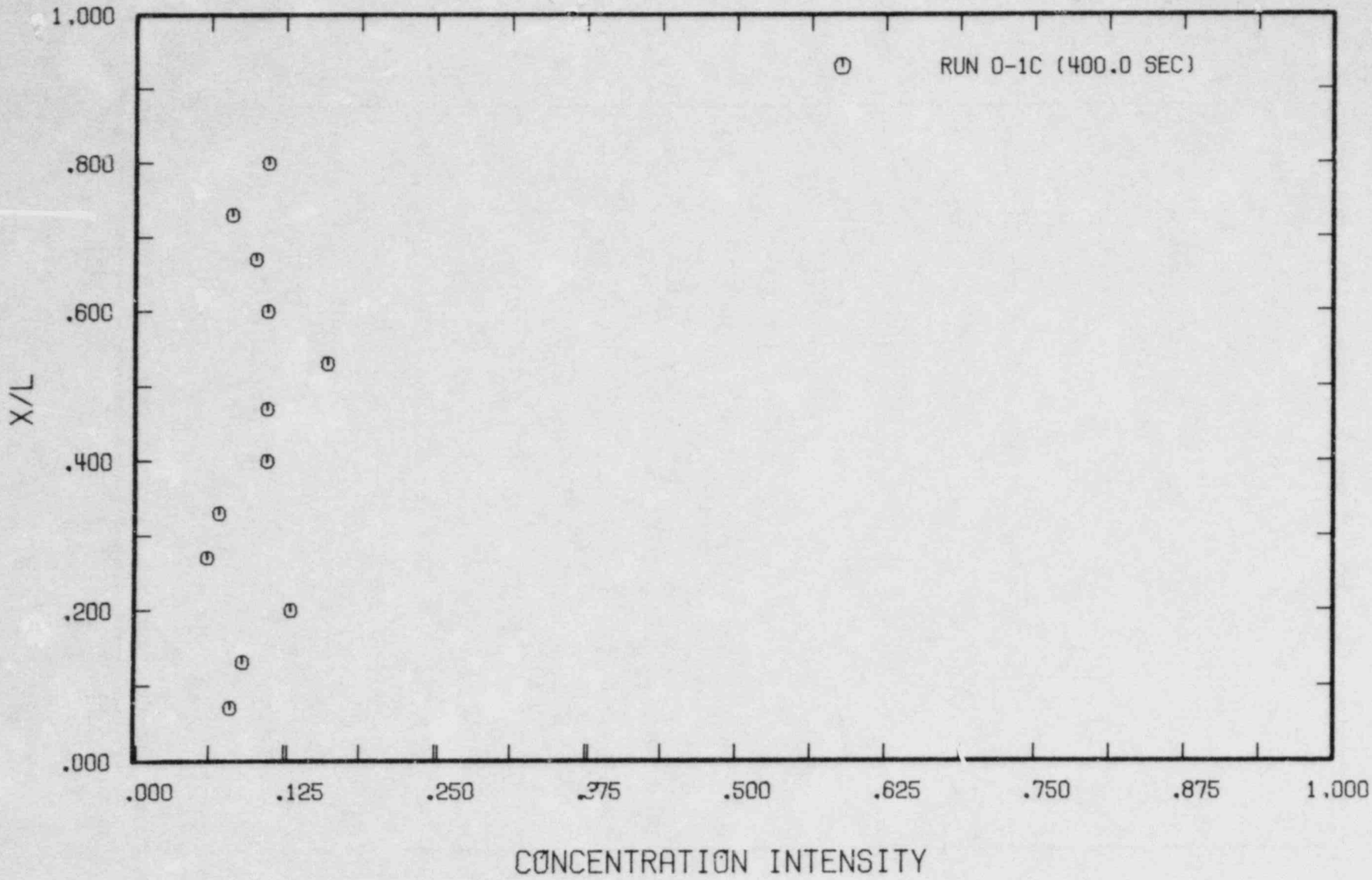
RUN 0-1C (400.0 SEC)
1.000
.800
.600
.400
.200
.000
X/L
.000
.125
.250
.375
.500
.625
.750
.875
1.000
CONCENTRATION INTENSITY

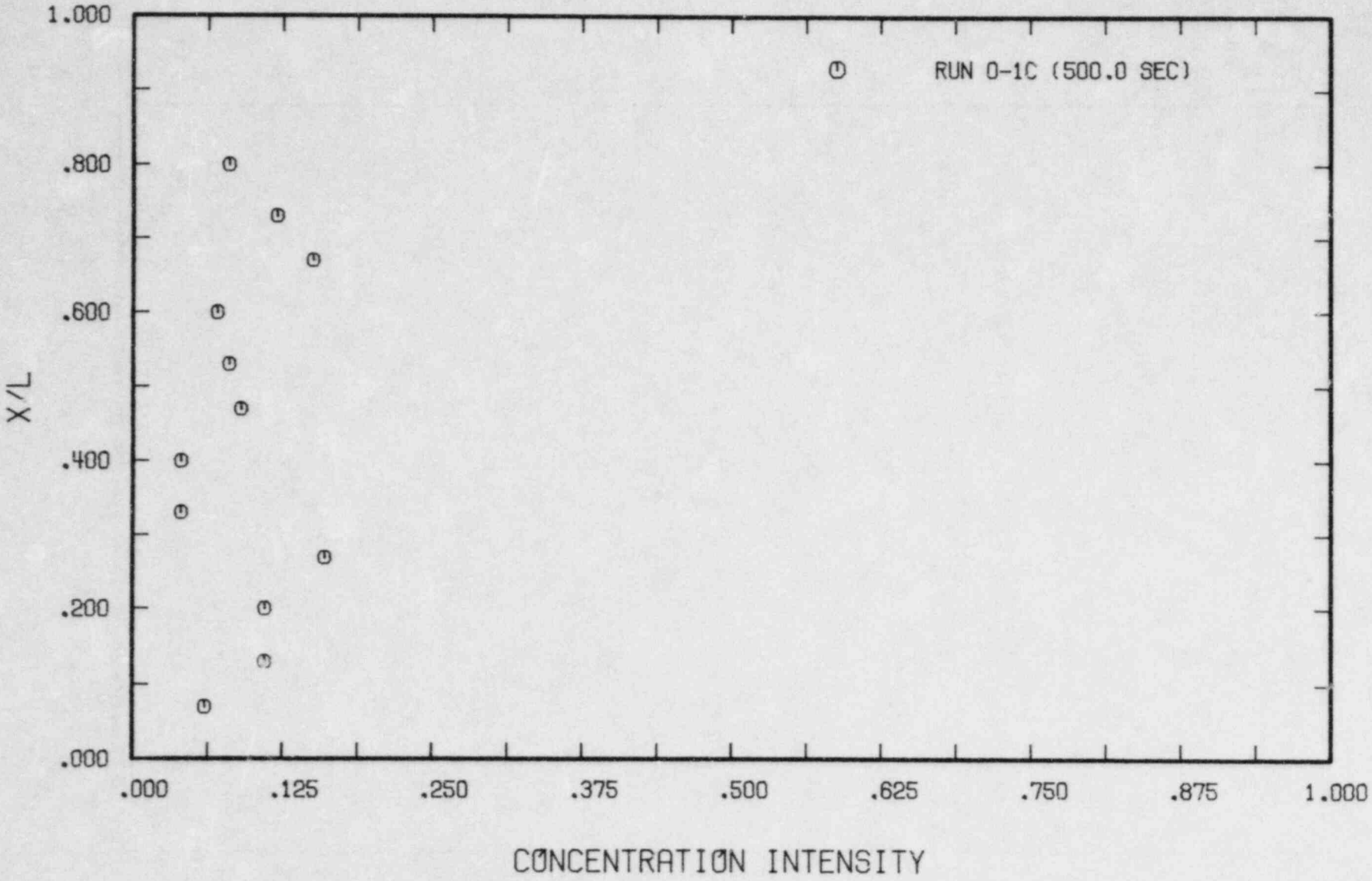
RUN 0-1C (500.0 SEC)
1.000
.800
.600
.400
.200
.000
X/L
.000
.125
.250
.375
.500
.625
.750
.875
1.000
CONCENTRATION INTENSITY

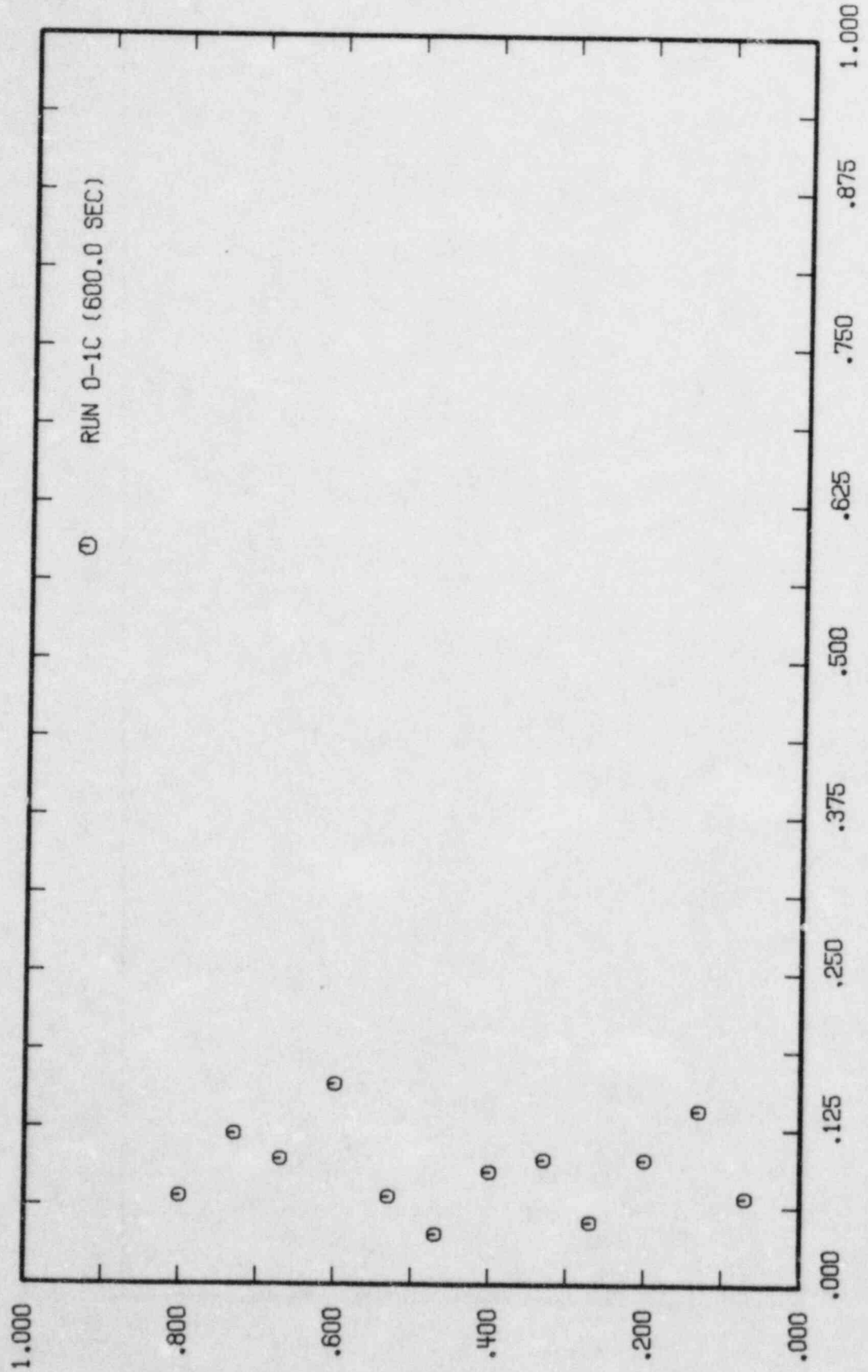
RUN 0-1C (600.0 SEC)
1.000
.800
.600
.400
.200
.000
X/L
.000
.125
.250
.375
.500
.625
.750
.875
1.000
CONCENTRATION INTENSITY

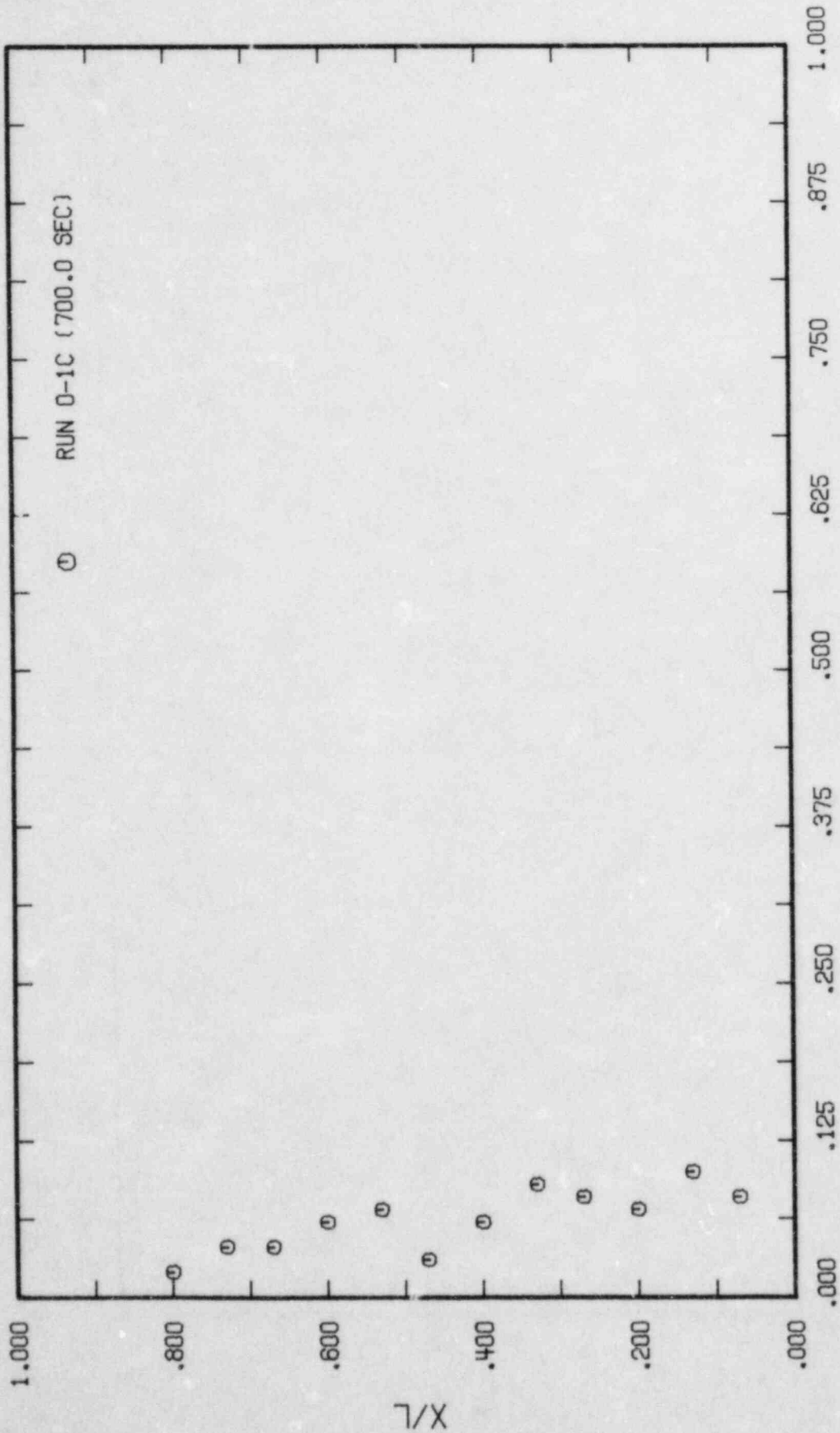
RUN 0-1C (700.0 SEC)
X/L
1.000
.800
.600
.400
.200
.000
.000
.125
.250
.375
.500
.625
.750
.875
1.000
CONCENTRATION INTENSITY

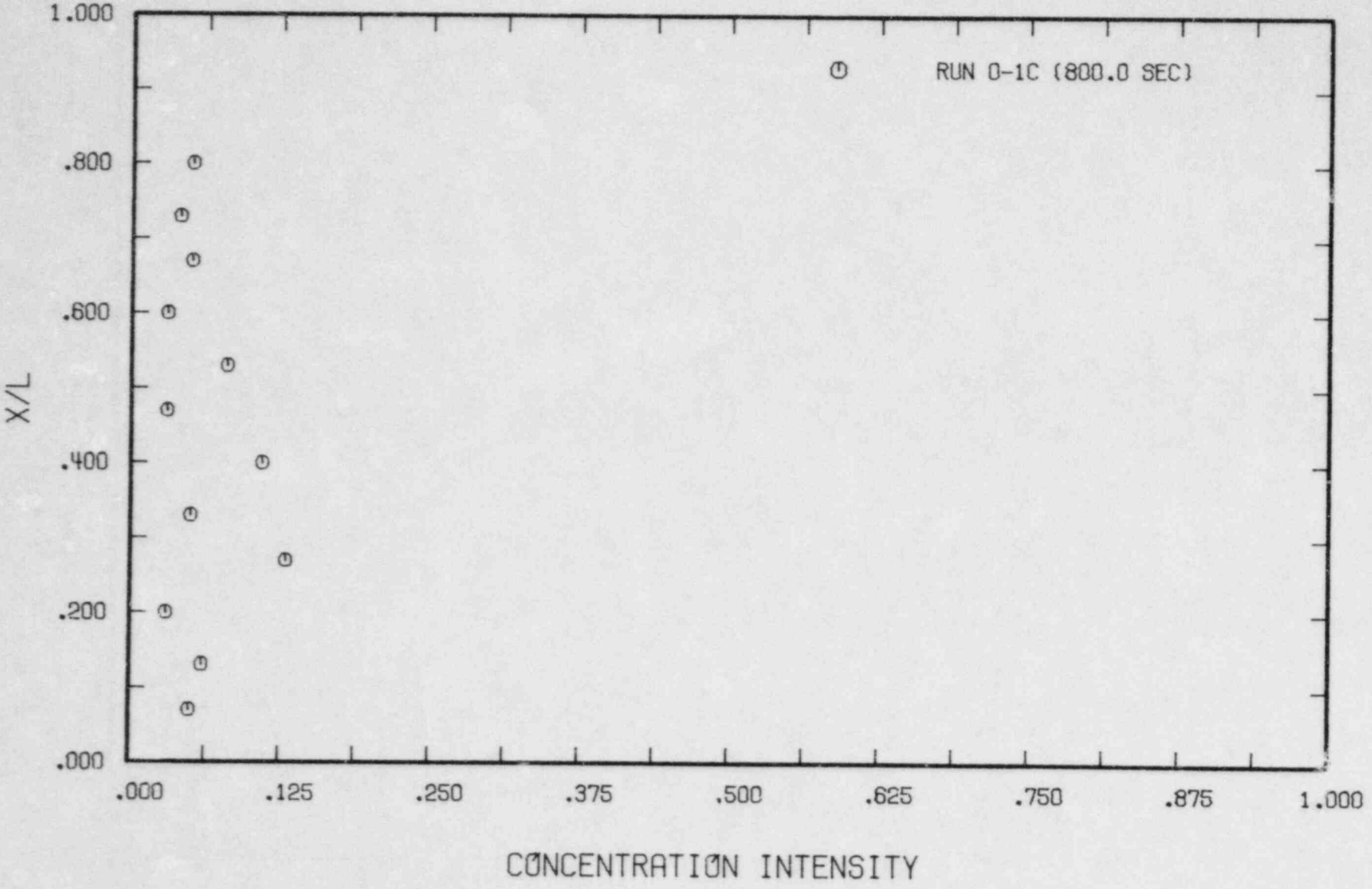
RUN 0-1C (800.0 SEC)
1.000
.800
.600
.400
.200
.000
X/L
.000
.125
.250
.375
.500
.625
.750
.875
1.000
CONCENTRATION INTENSITY

Run 0-1V

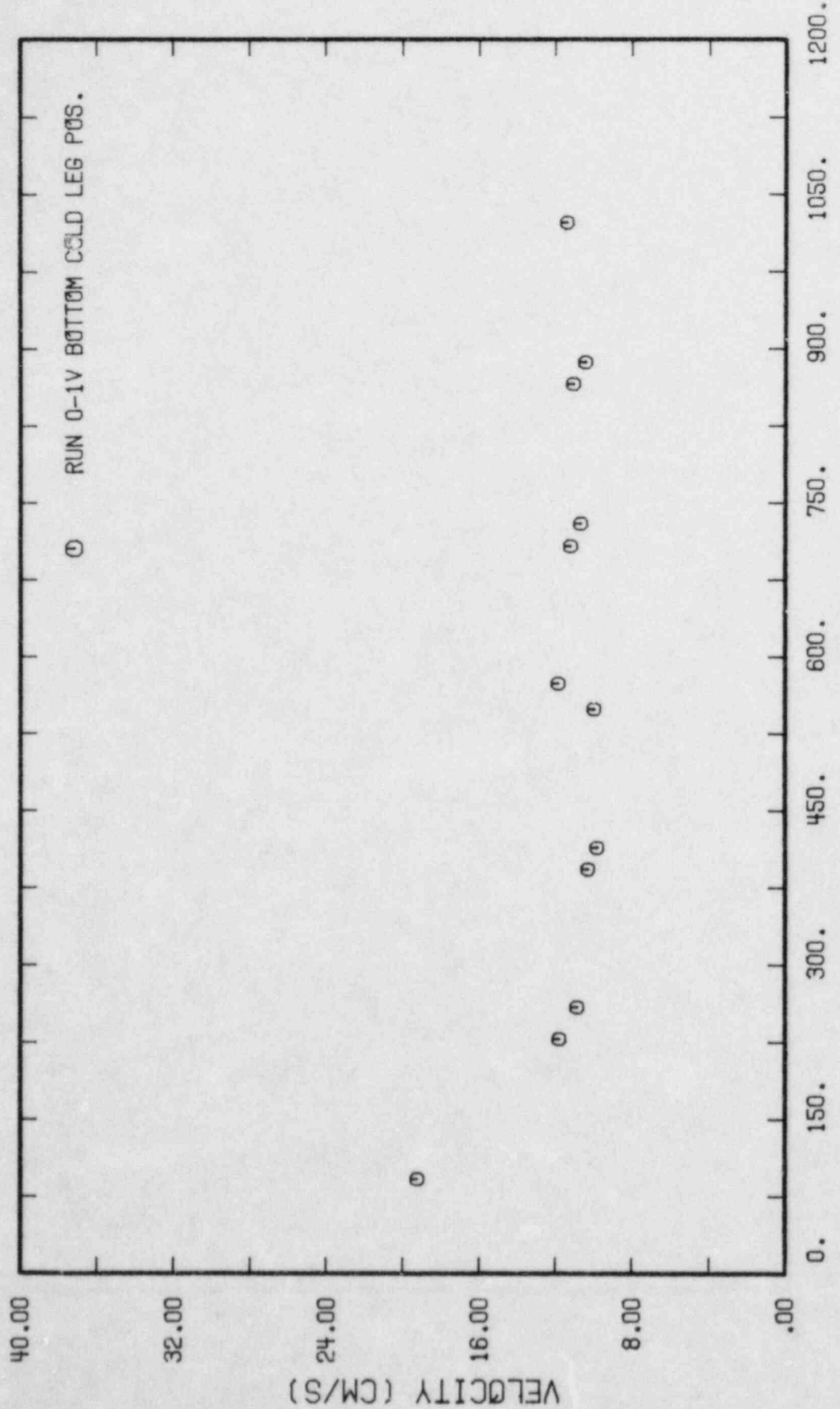
RUN 0-1V BOTTOM COLD LEG POS.
VELOCITY (CM/S)
40.00
32.00
24.00
16.00
8.00
.00
0.
150.
300.
450.
600.
750.
900.
1050.
1200.
TIME (SEC)

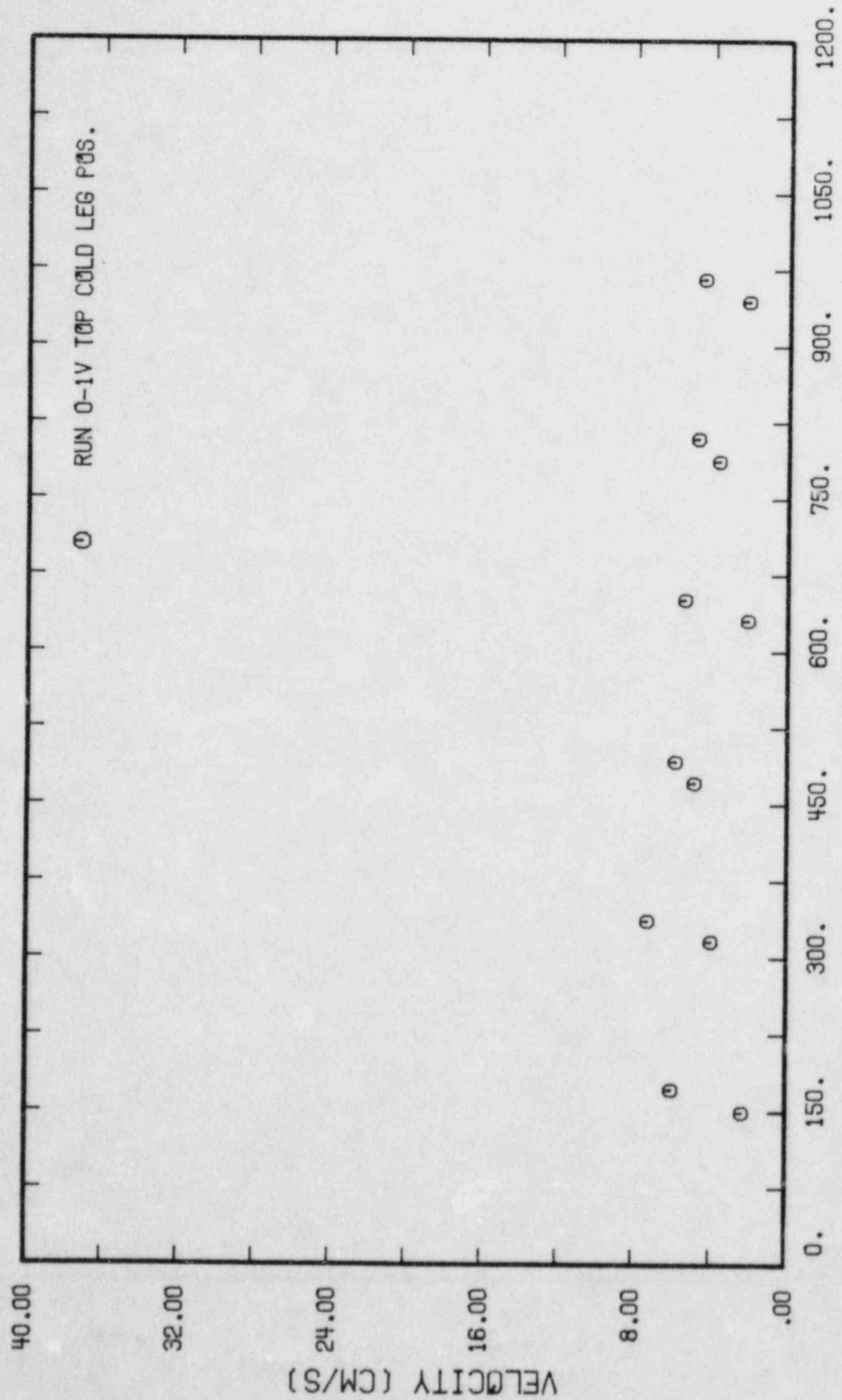
RUN 0-1V TOP COLD LEG POS.
VELOCITY (CM/S)
40.00
32.00
24.00
16.00
8.00
.00
0.
150.
300.
450.
600.
750.
900.
1050.
1200.
TIME (SEC)

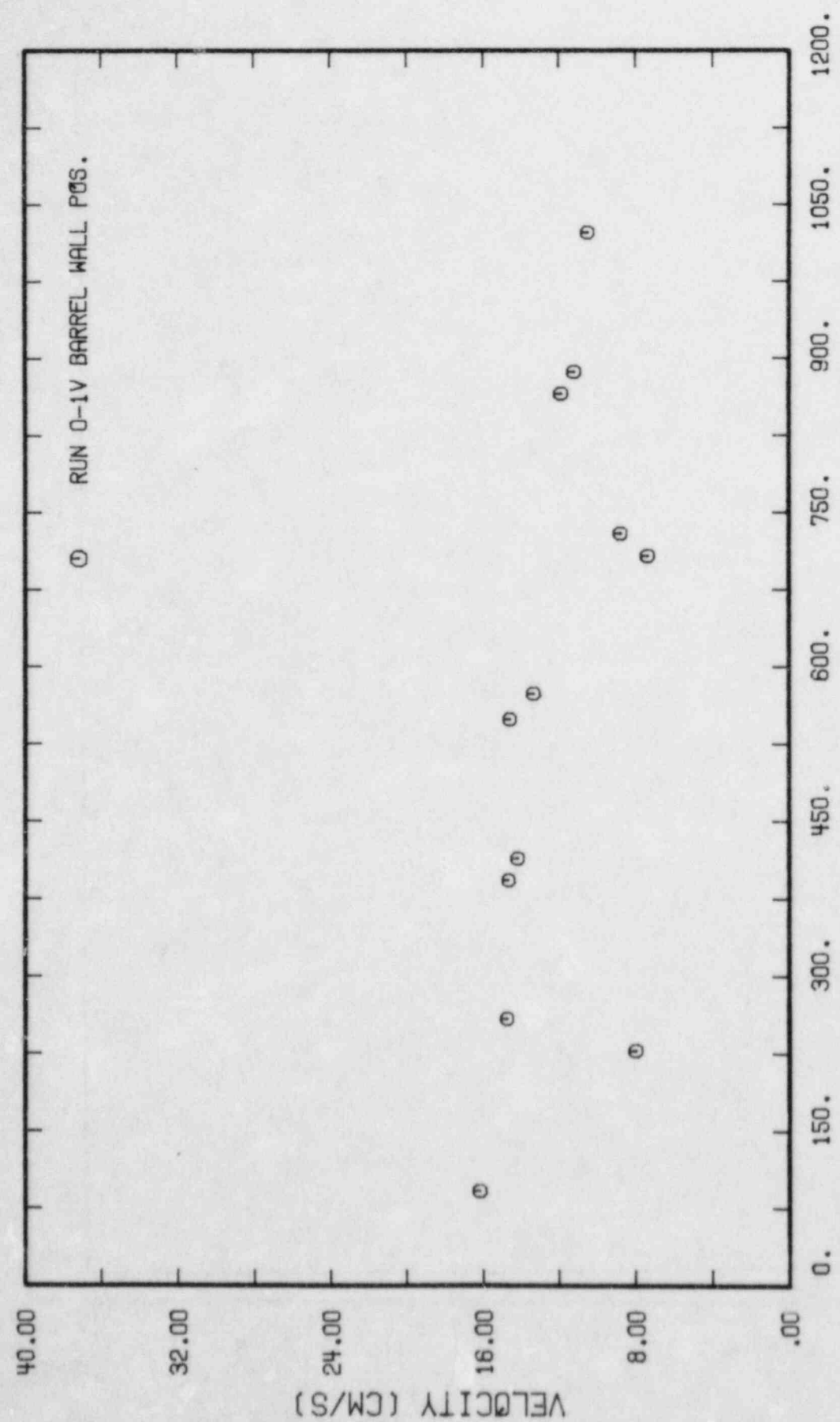
RUN 0-1V BARREL WALL POS.
VELOCITY (CM/S)
40.00
32.00
24.00
16.00
8.00
.00
0.
150.
300.
450.
600.
750.
900.
1050.
1200.
TIME (SEC)

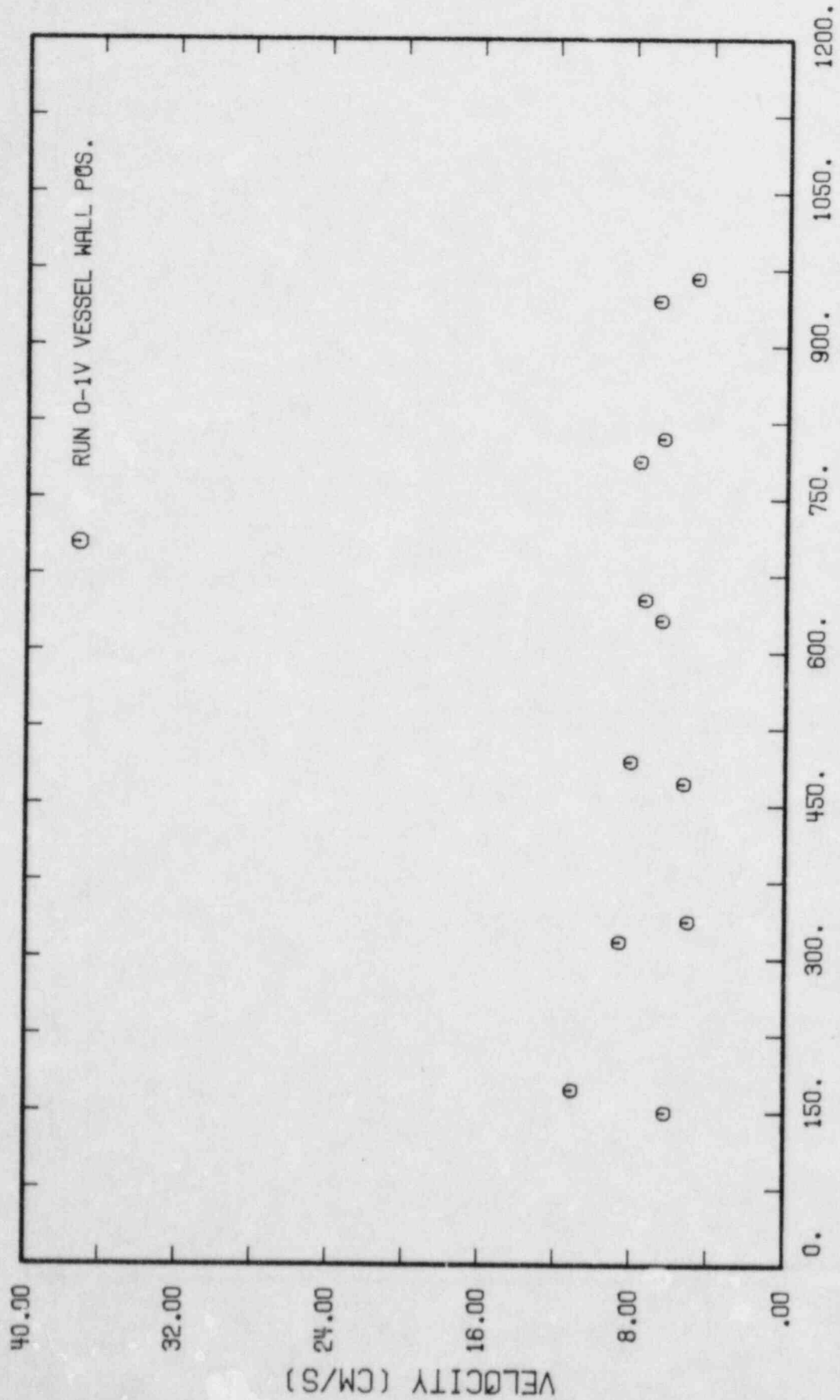
RUN 0-1V VESSEL WALL POS.
VELOCITY (CM/S)
40.00
32.00
24.00
16.00
8.00
.00
0.
150.
300.
450.
600.
750.
900.
1050.
1200.
TIME (SEC)

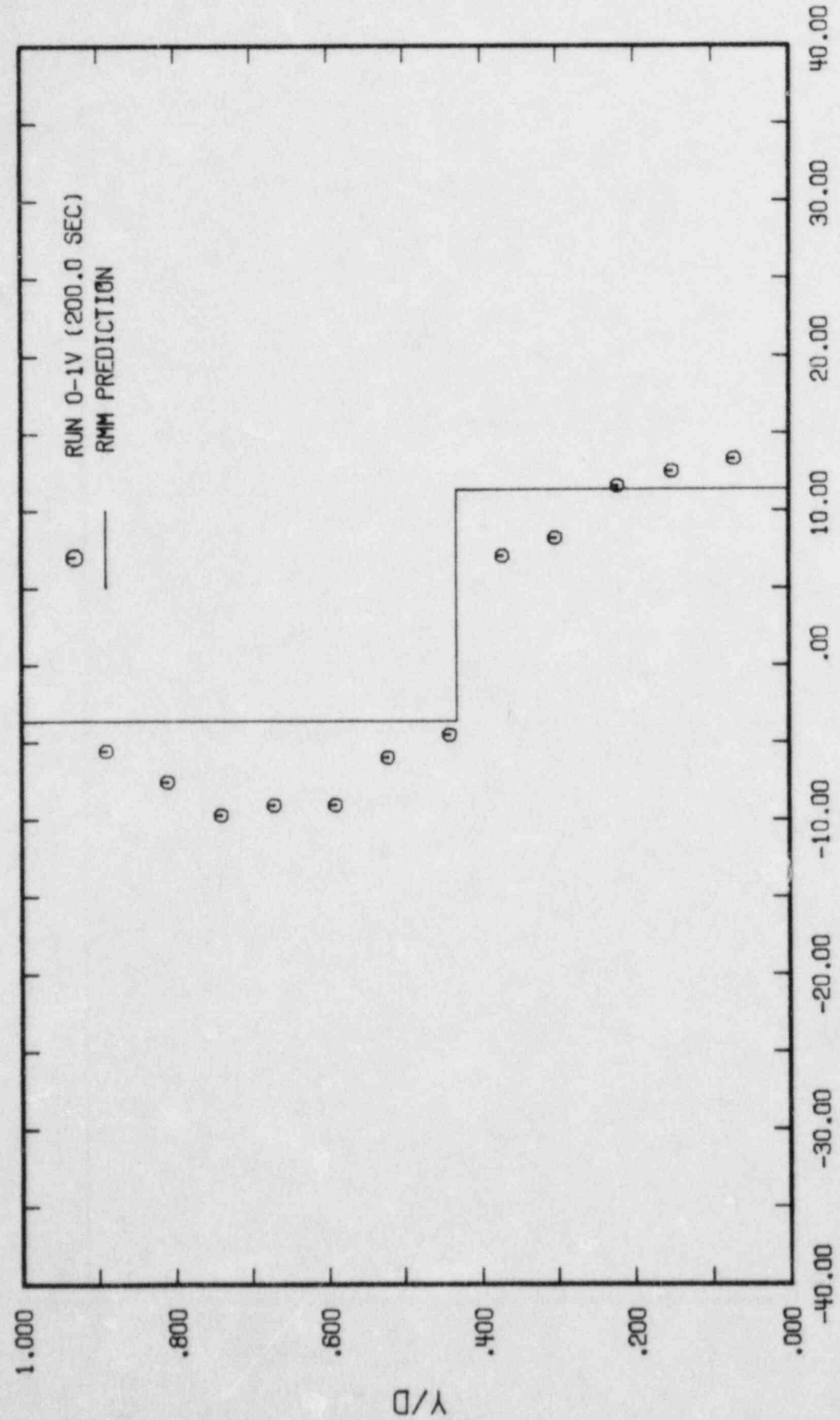
RUN 0-1V (200.0 SEC)
RMM PREDICTION
1.000
.800
.600
.400
.200
.000
Y/D
-40.00
-30.00
-20.00
-10.00
.00
10.00
20.00
30.00
40.00
VELOCITY (CM/S)

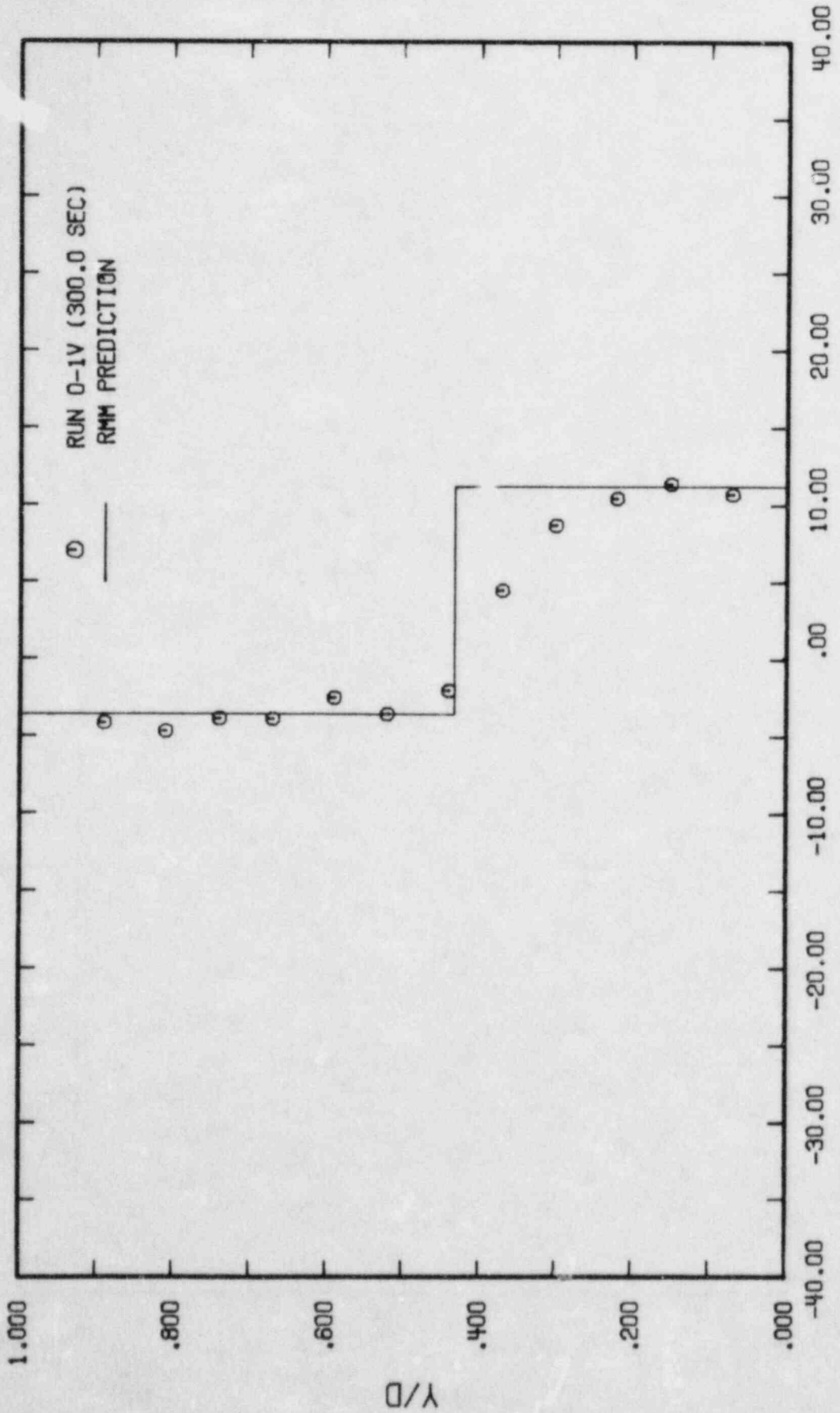
RUN 0-1V (300.0 SEC)
RMM PREDICTION
Y/D
1.000
.800
.600
.400
.200
.000
-40.00
-30.00
-20.00
-10.00
.00
10.00
20.00
30.00
40.00
VELOCITY (CM/S)

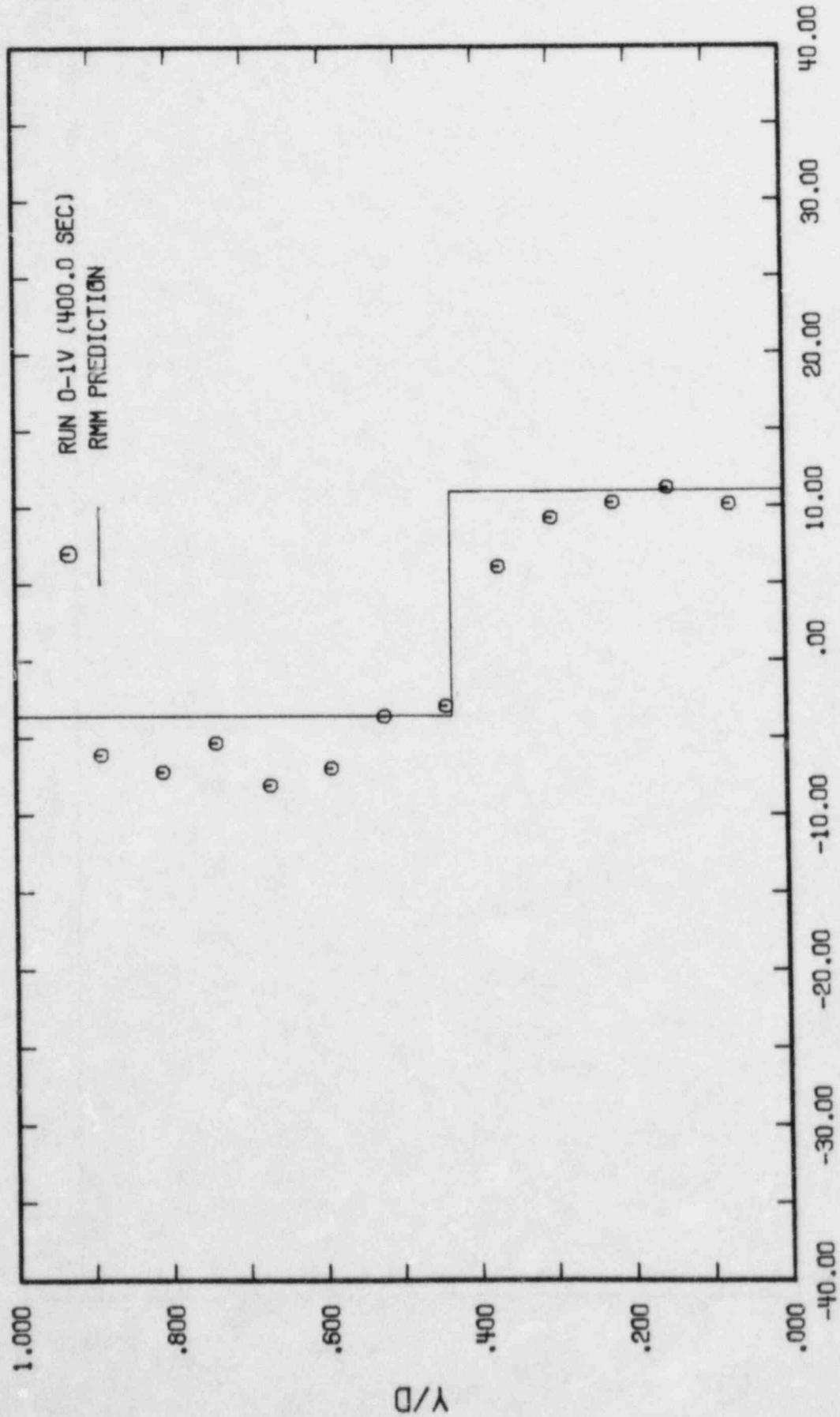
RUN 0-1V (400.0 SEC)
RMM PREDICTION
1.000
.800
.600
.400
.200
.000
Y/D
-40.00
-30.00
-20.00
-10.00
.00
10.00
20.00
30.00
40.00
VELOCITY (CM/S)

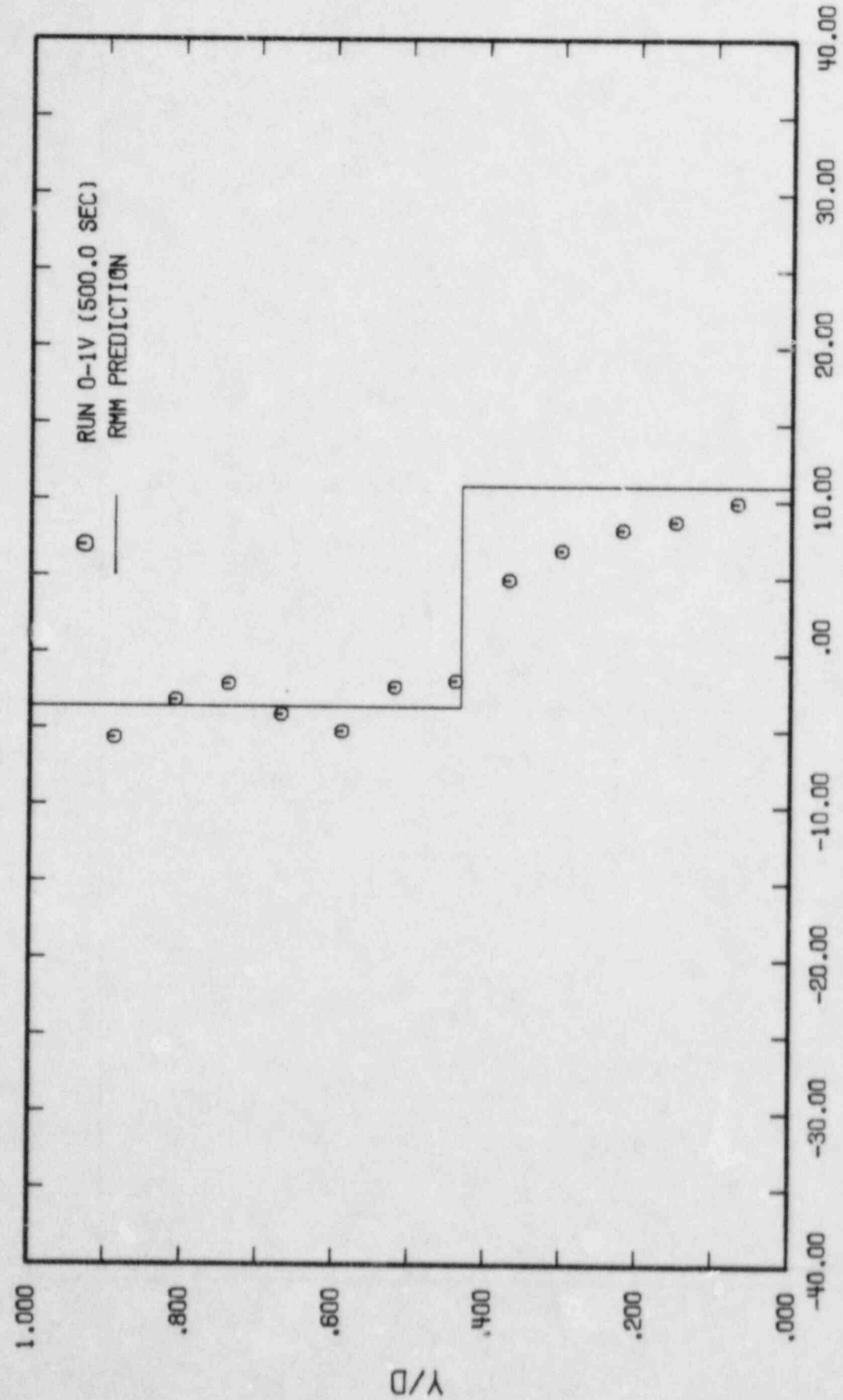
RUN 0-1V (500.0 SEC)
RMM PREDICTION
1.000
.800
.600
.400
.200
.000
Y/D
-40.00
-30.00
-20.00
-10.00
.00
10.00
20.00
30.00
40.00
VELOCITY (CM/S)

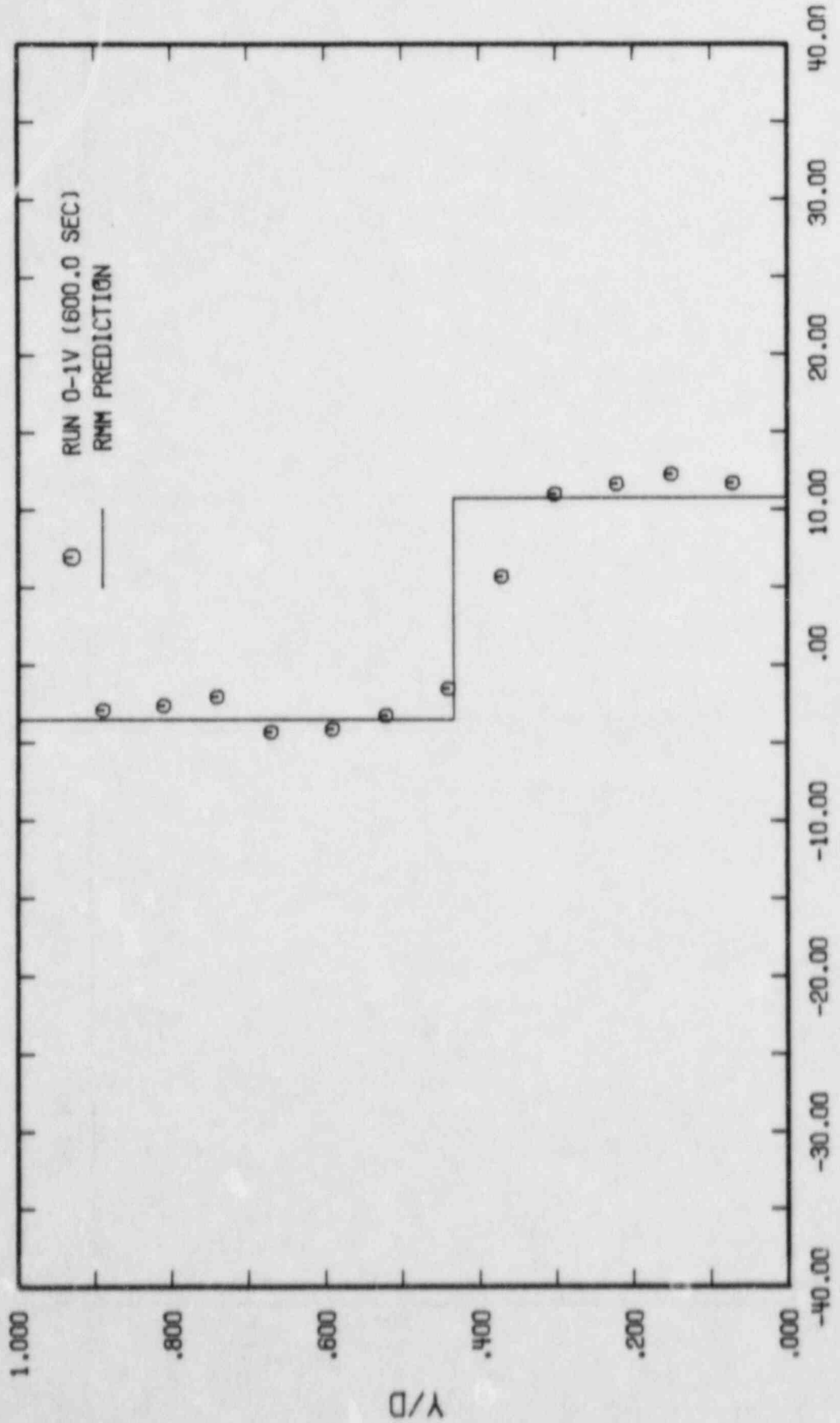
RUN 0-1V (600.0 SEC)
RMM PREDICTION
1.000
.800
.600
.400
.200
.000
Y/D
-40.00
-30.00
-20.00
-10.00
.00
10.00
20.00
30.00
40.00
VELOCITY (CM/S)

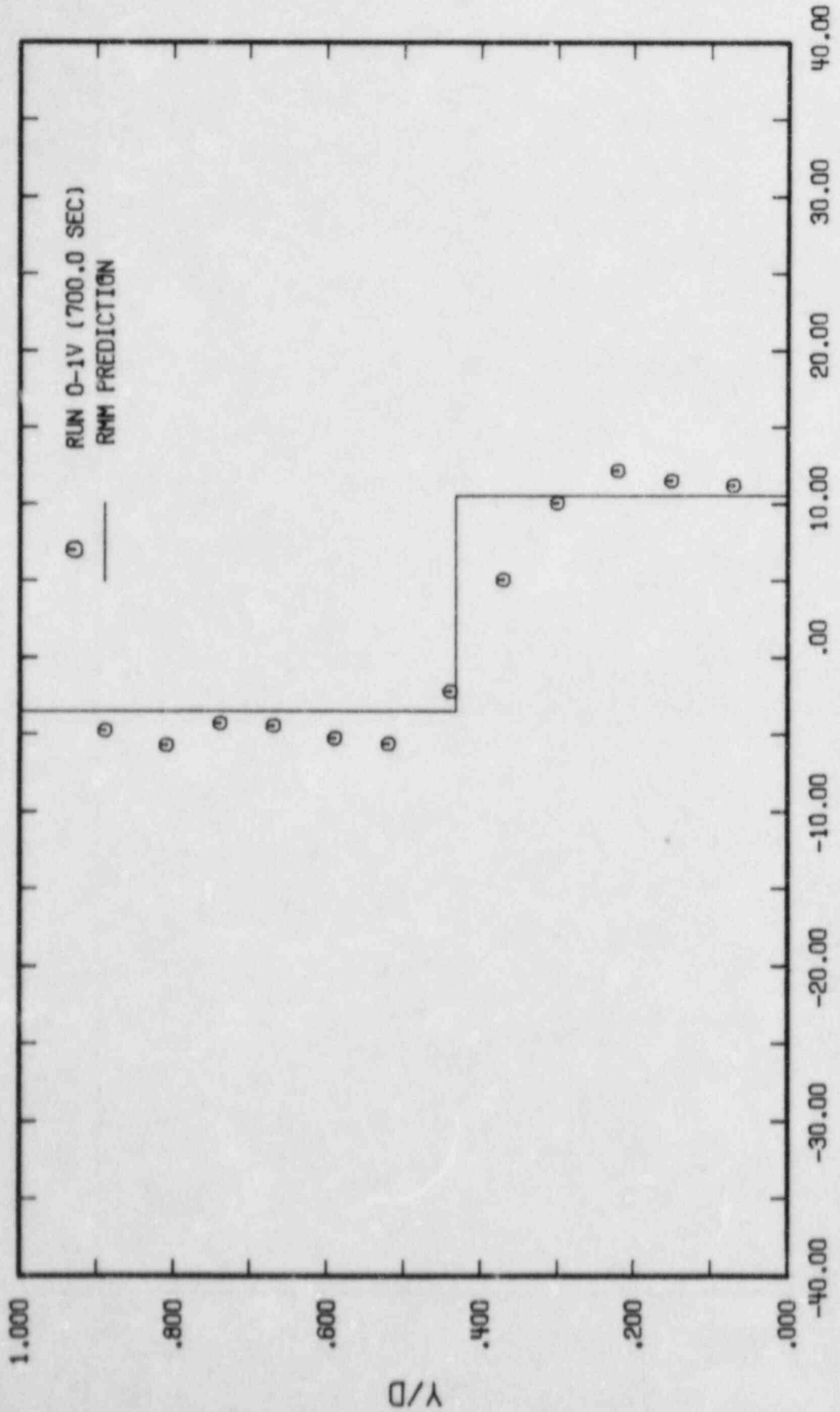
RUN 0-1V (700.0 SEC)
RMM PREDICTION
1.000
.800
.600
.400
.200
.000
Y/D
-40.00
-30.00
-20.00
-10.00
.00
10.00
20.00
30.00
40.00
VELOCITY (CM/S)

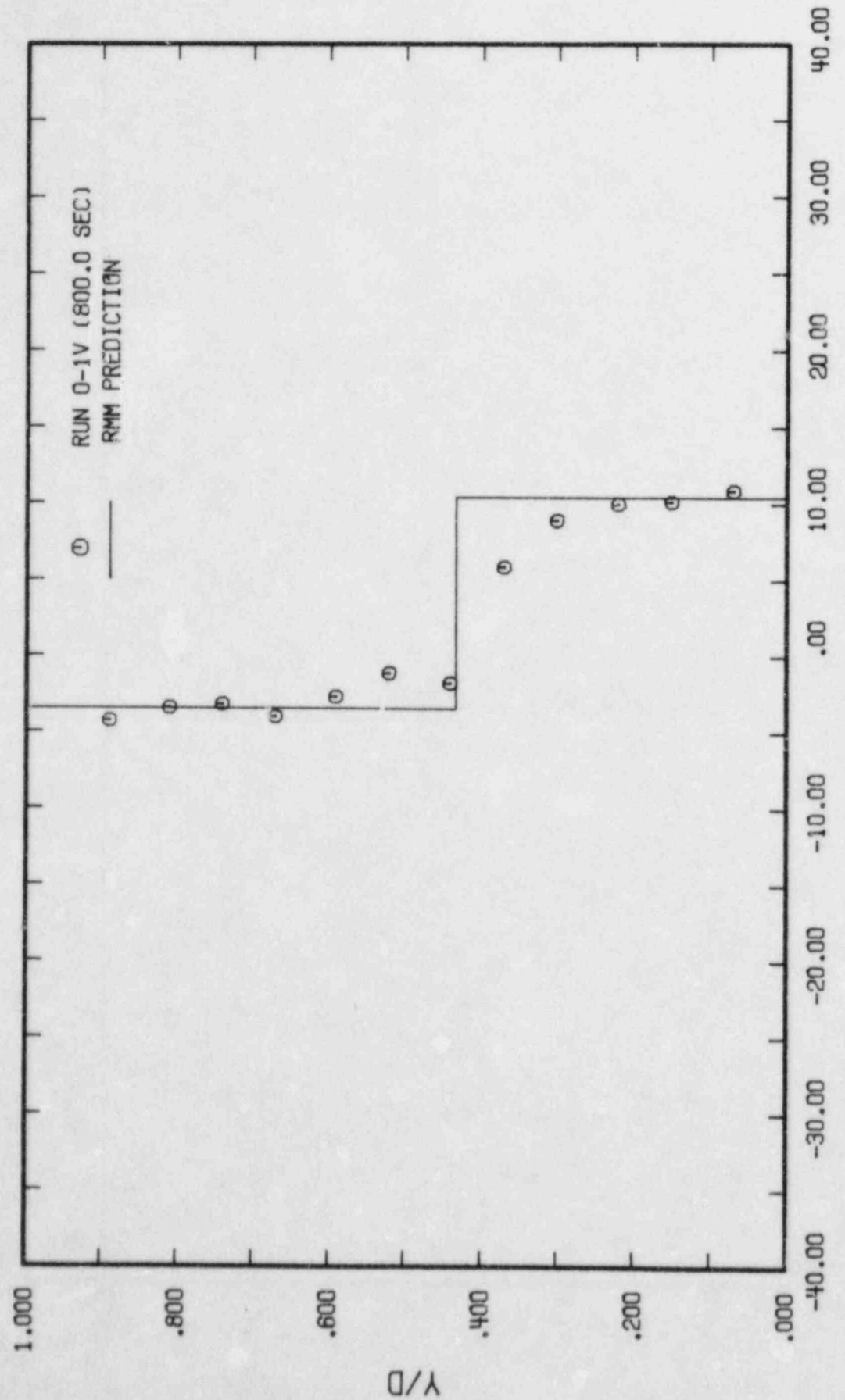
RUN 0-1V (800.0 SEC)
RMM PREDICTION
Y/D
1.000
.800
.600
.400
.200
.000
-40.00
-30.00
-20.00
-10.00
.00
10.00
20.00
30.00
40.00
VELOCITY (CM/S)

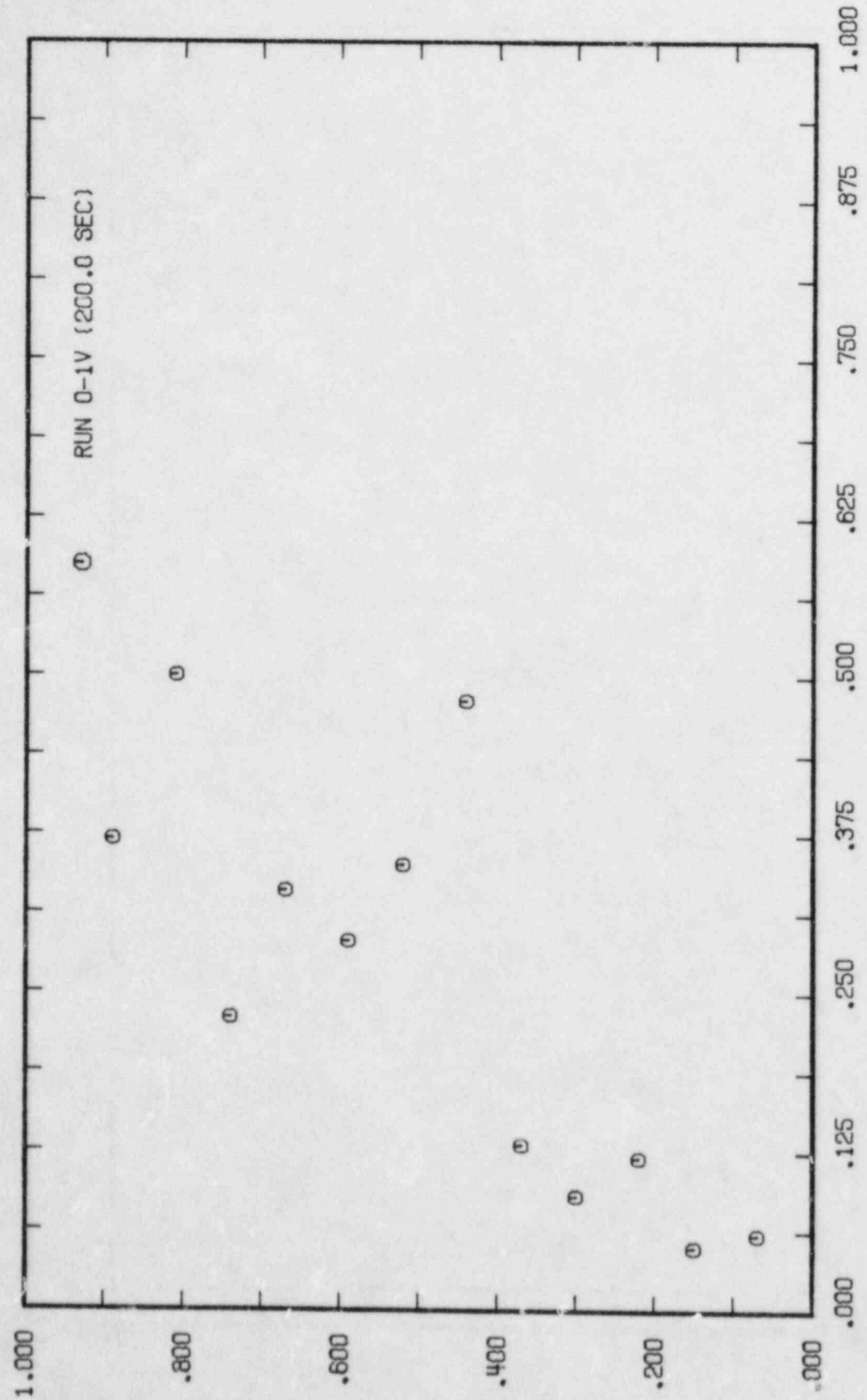
RUN 0-1V (200.0 SEC)
Y/D
VELOCITY INTENSITY
.000
.200
.400
.600
.800
1.000
.000
.125
.250
.375
.500
.625
.750
.875
1.000

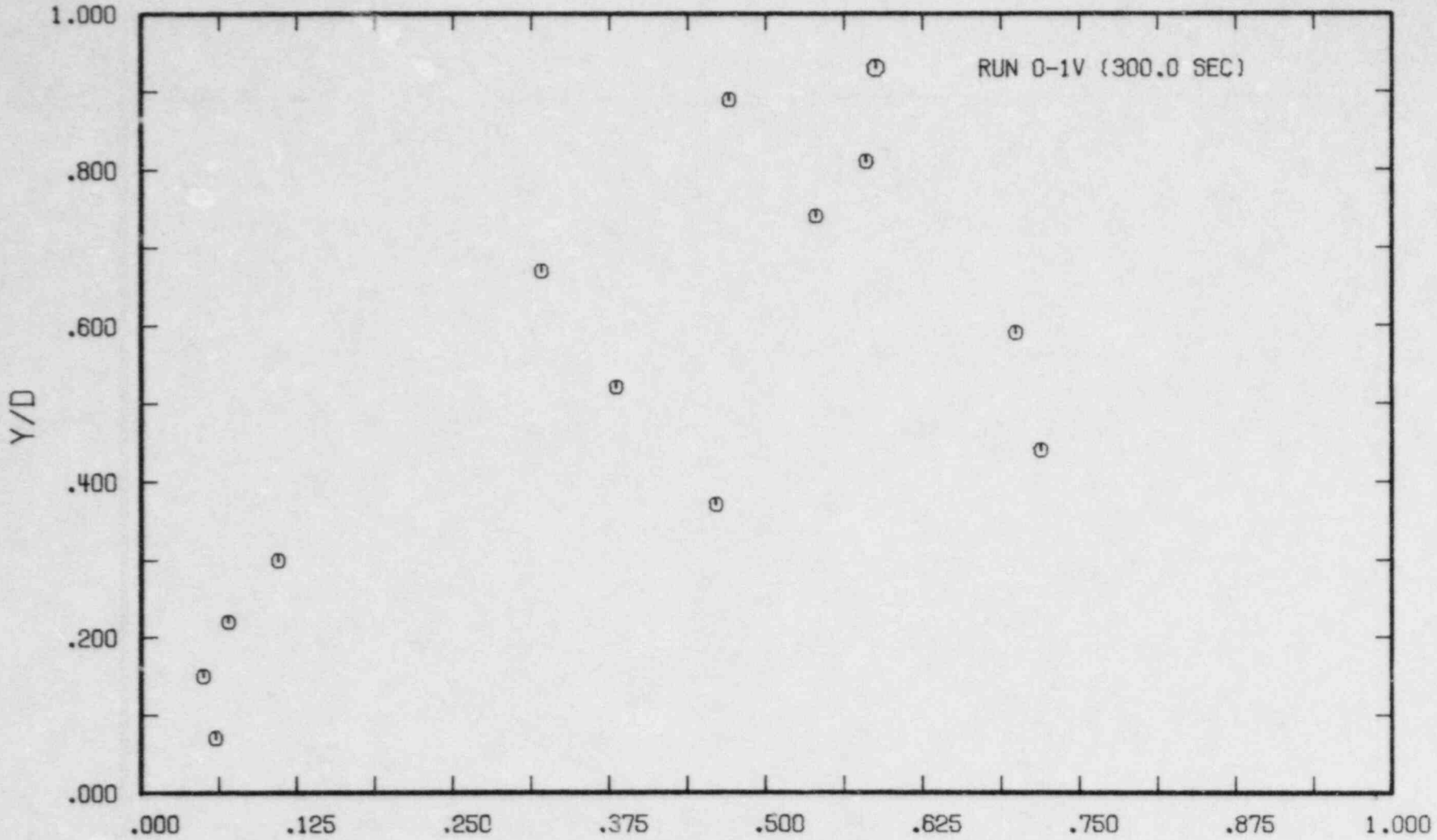
RUN 0-1V (300.0 SEC)
1.000
.800
.600
.400
.200
.000
Y/D
.000
.125
.250
.375
.500
.625
.750
.875
1.000
VELOCITY INTENSITY

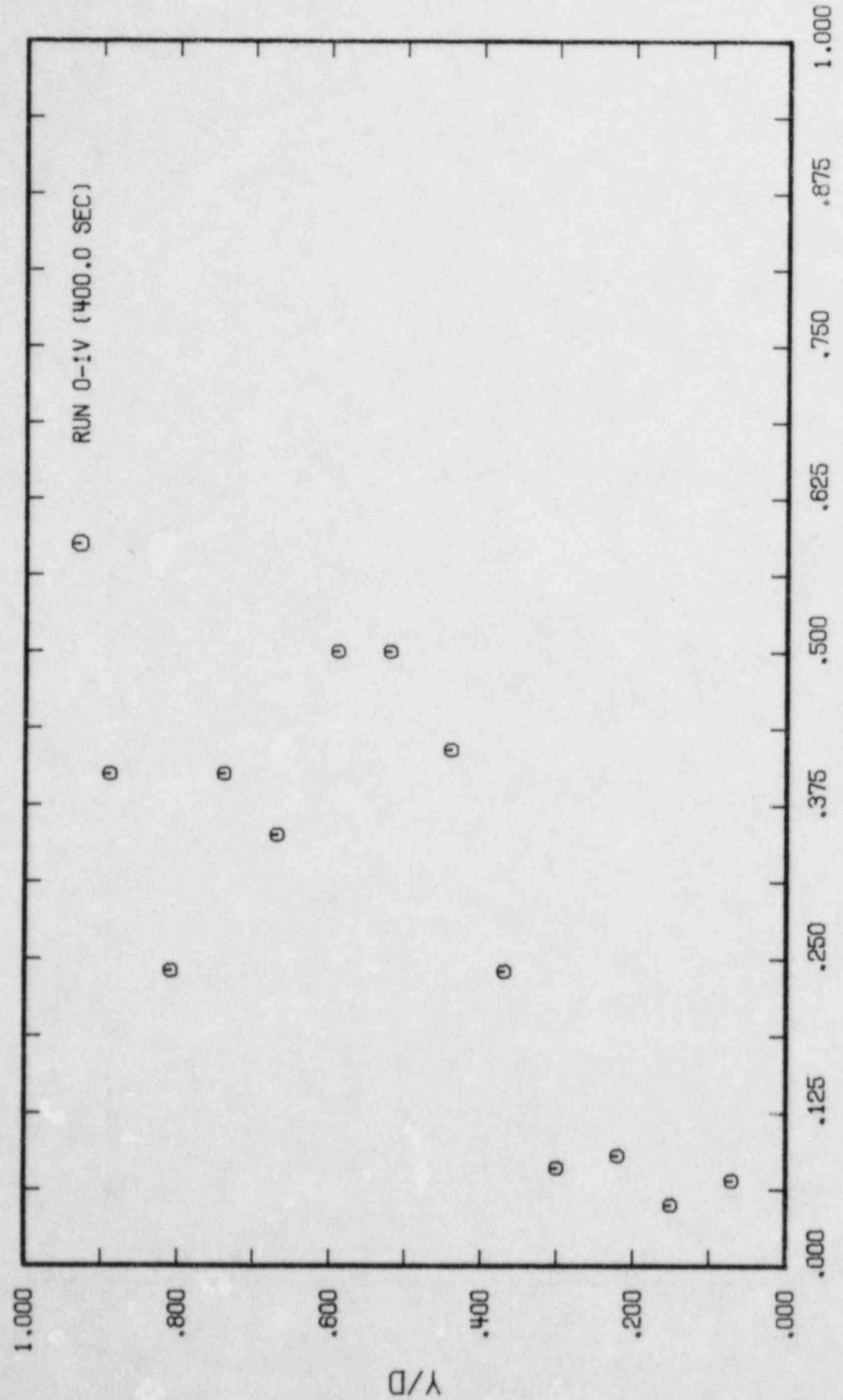
RUN 0-1V (400.0 SEC)
1.000
.800
.600
.400
.200
.000
Y/D
.000
.125
.250
.375
.500
.625
.750
.875
1.000
VELOCITY INTENSITY

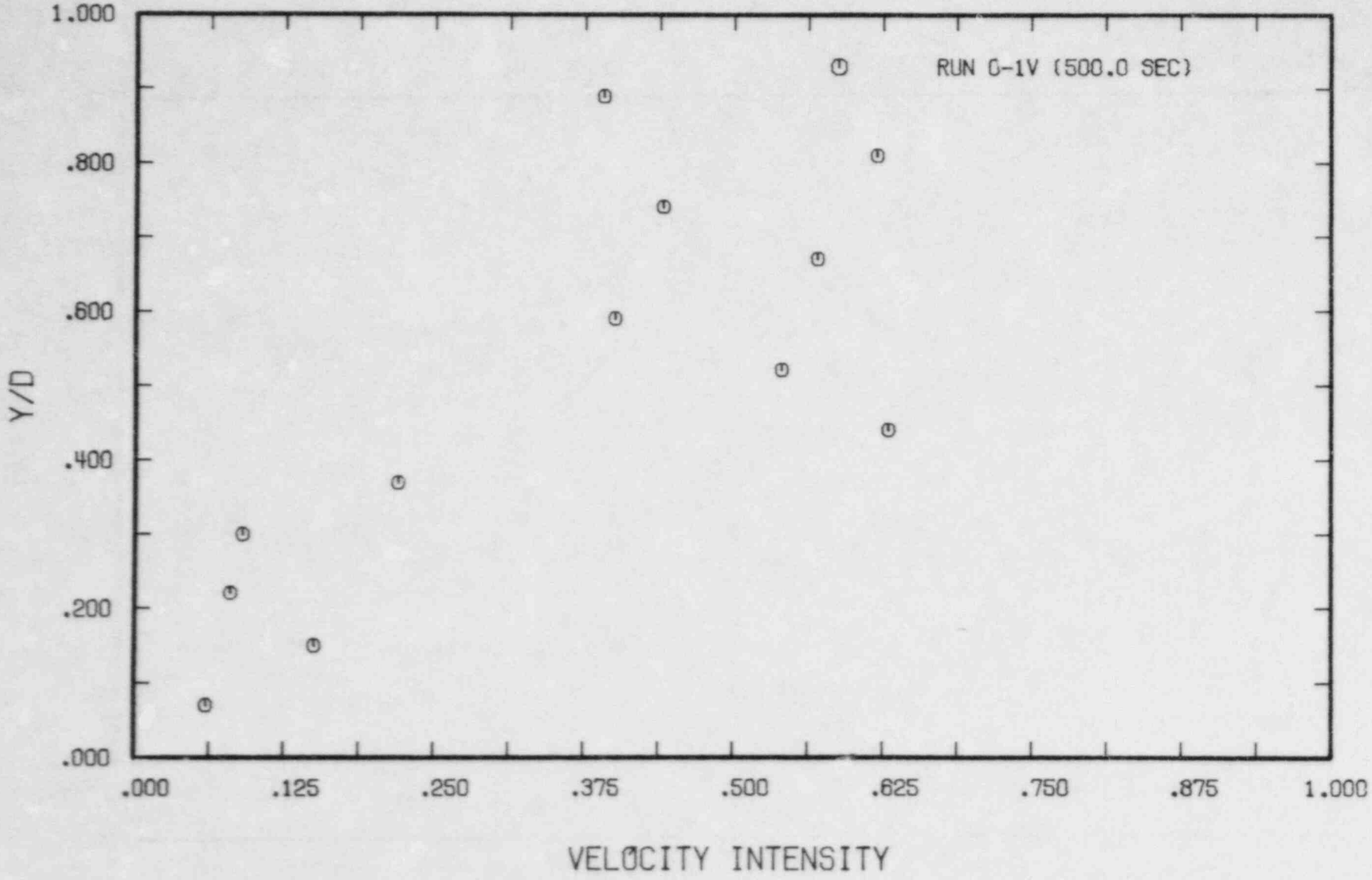
RUN 0-1V (500.0 SEC)
1.000
.800
.600
.400
.200
.000
Y/D
.000
.125
.250
.375
.500
.625
.750
.875
1.000
VELOCITY INTENSITY

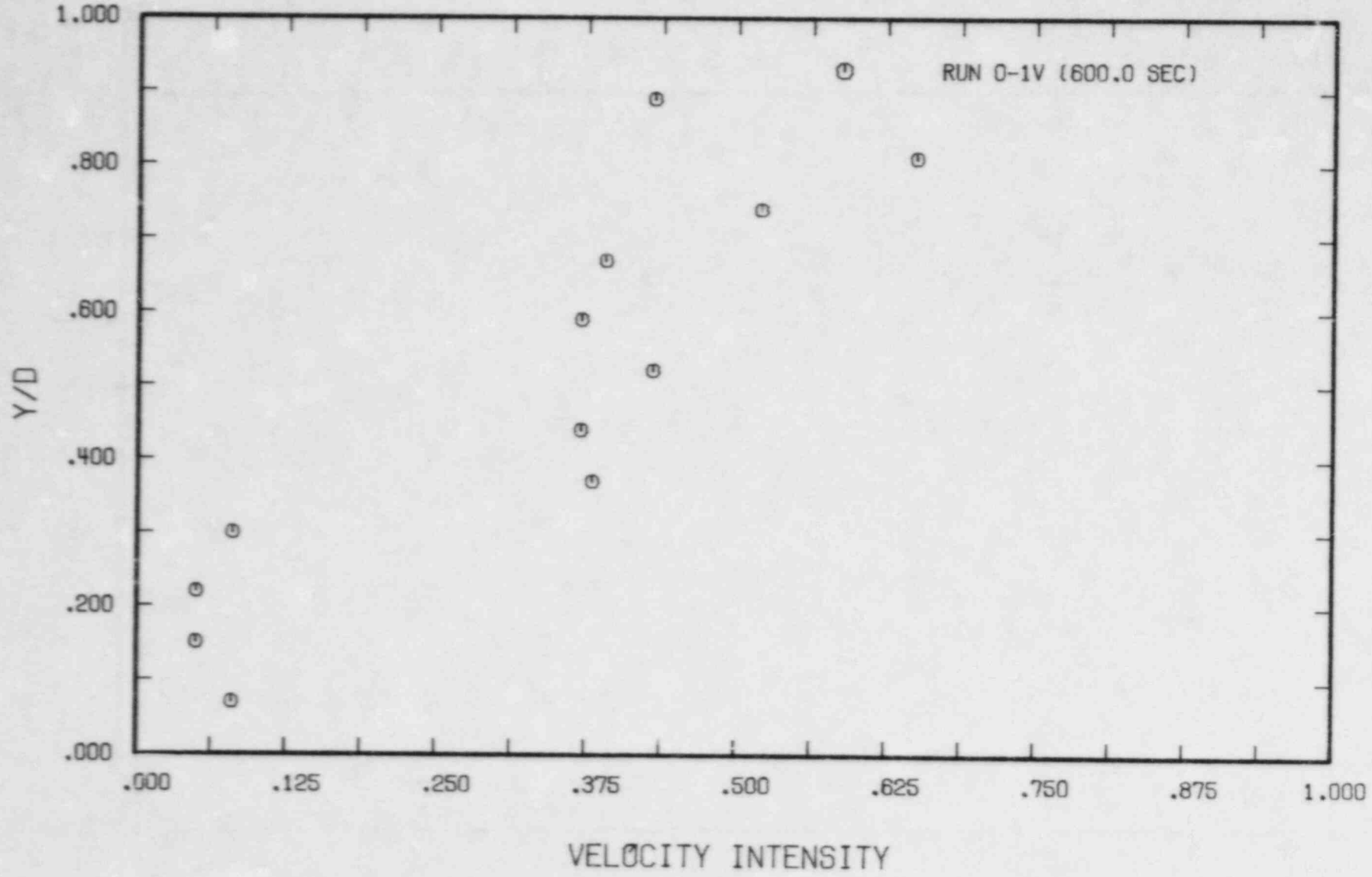
RUN 0-1V (600.0 SEC)
1.000
.800
.600
.400
.200
.000
Y/D
.000
.125
.250
.375
.500
.625
.750
.875
1.000
VELOCITY INTENSITY

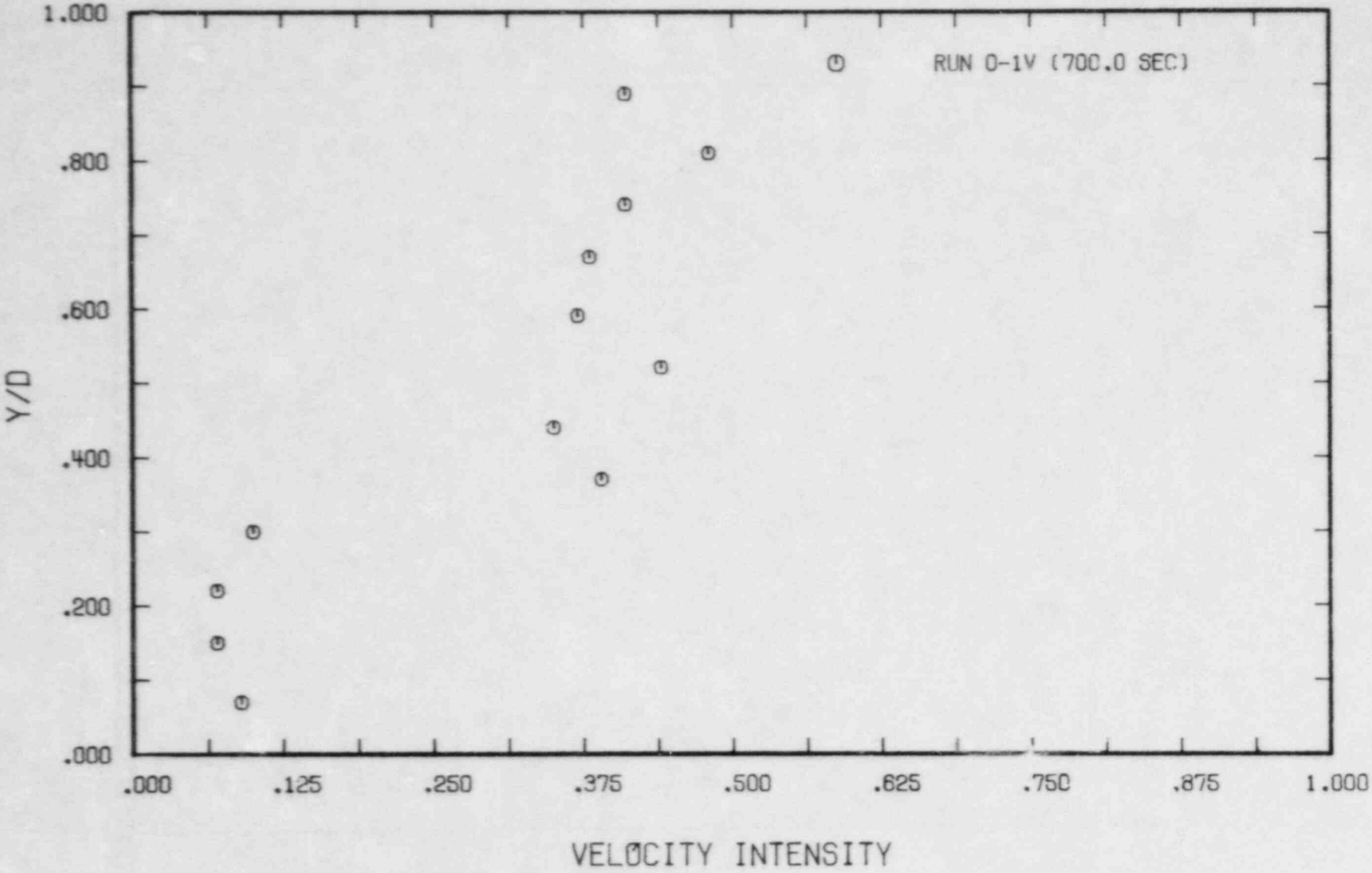
RUN 0-1V (700.0 SEC)
1.000
.800
.600
.400
.200
.000
Y/D
.000
.125
.250
.375
.500
.625
.750
.875
1.000
VELOCITY INTENSITY

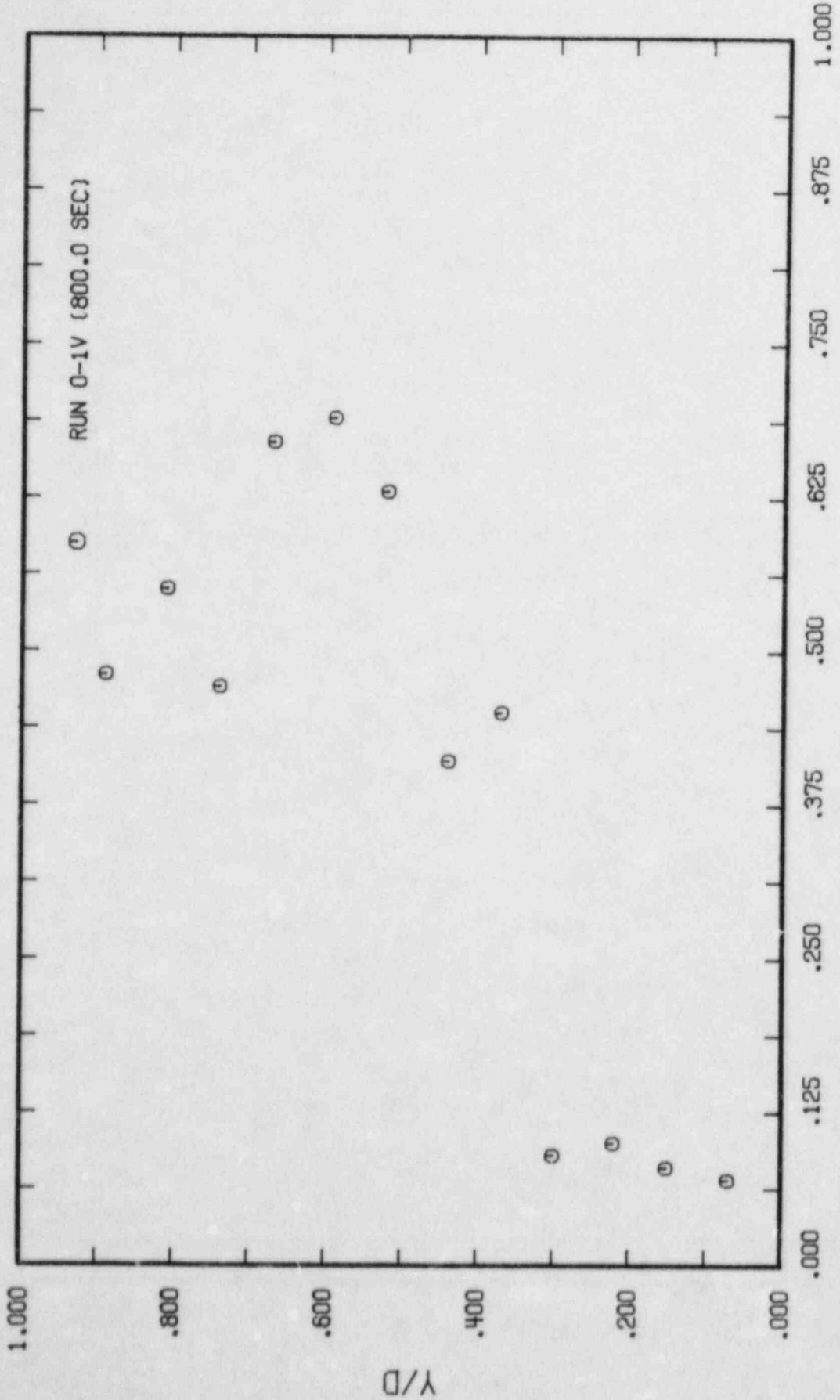
RUN 0-1V (800.0 SEC)
1.000
.800
.600
.400
.200
.000
Y/D
.000
.125
.250
.375
.500
.625
.750
.875
1.000
VELOCITY INTENSITY

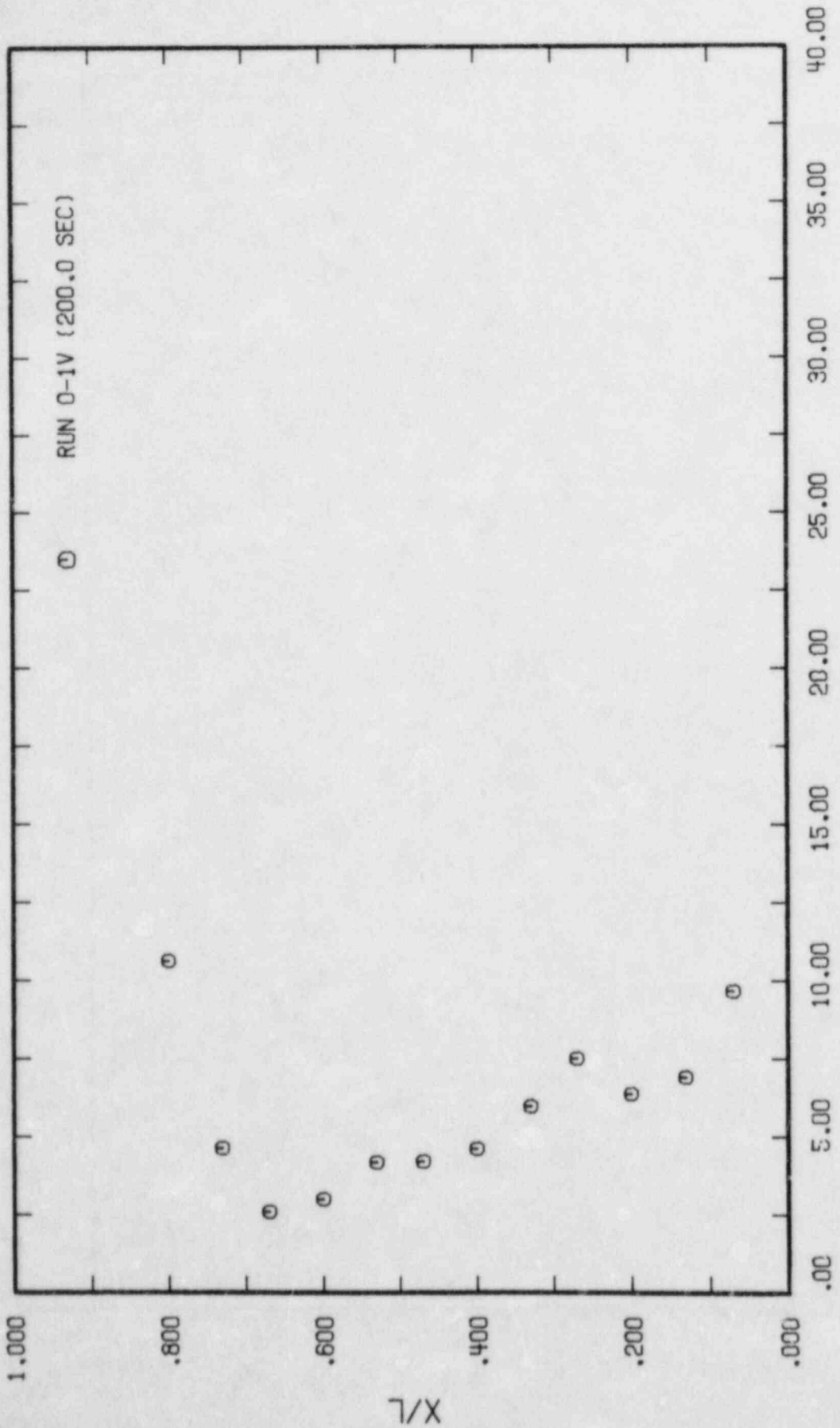
RUN 0-1V (200.0 SEC)
1.000
.800
.600
.400
.200
.000
X/L
.00
5.00
10.00
15.00
20.00
25.00
30.00
35.00
40.00
VELOCITY (CM/S)

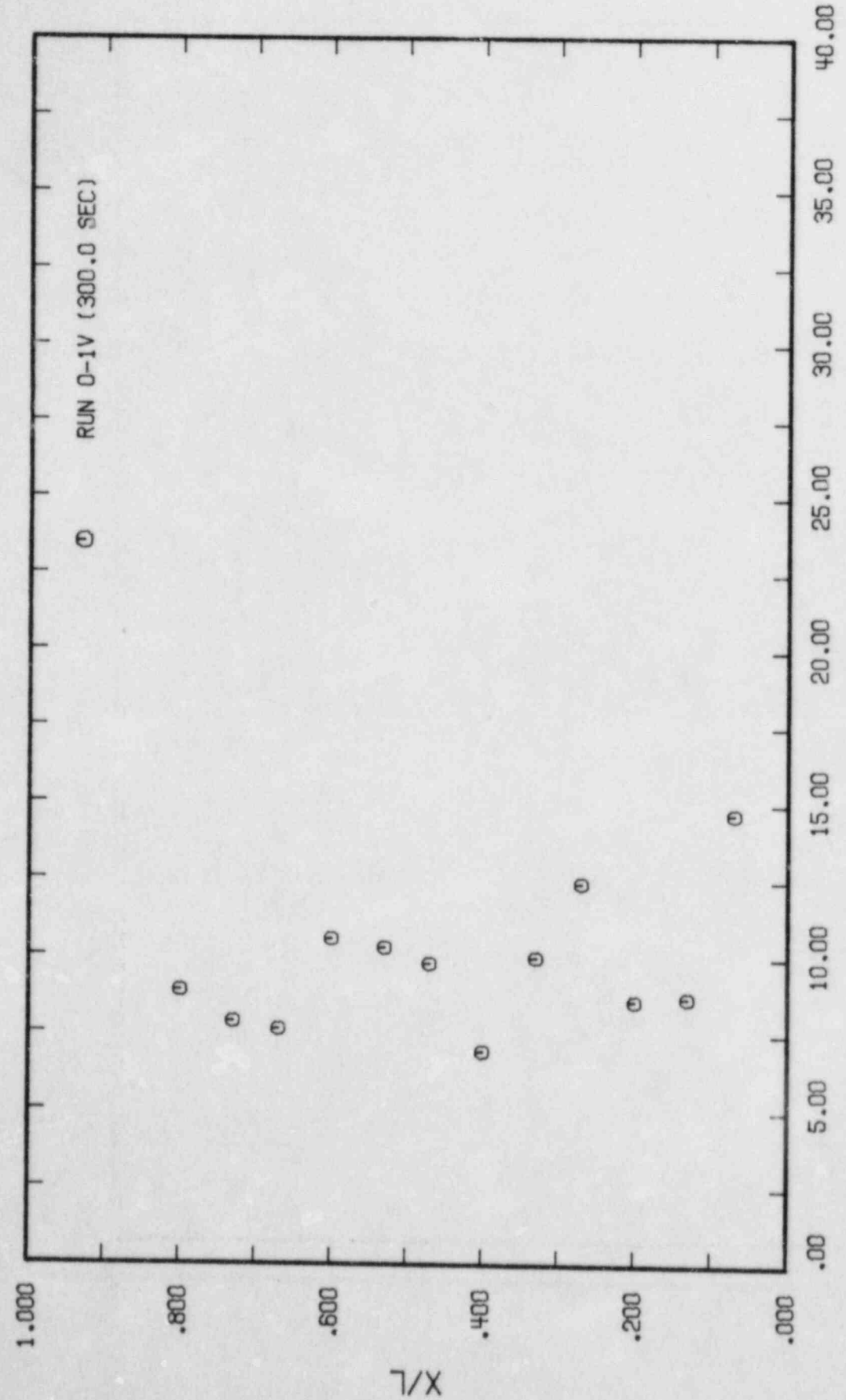
RUN 0-1V (300.0 SEC)
X/L
1.000
.800
.600
.400
.200
.000
.00
5.00
10.00
15.00
20.00
25.00
30.00
35.00
40.00
VELOCITY (CM/S)

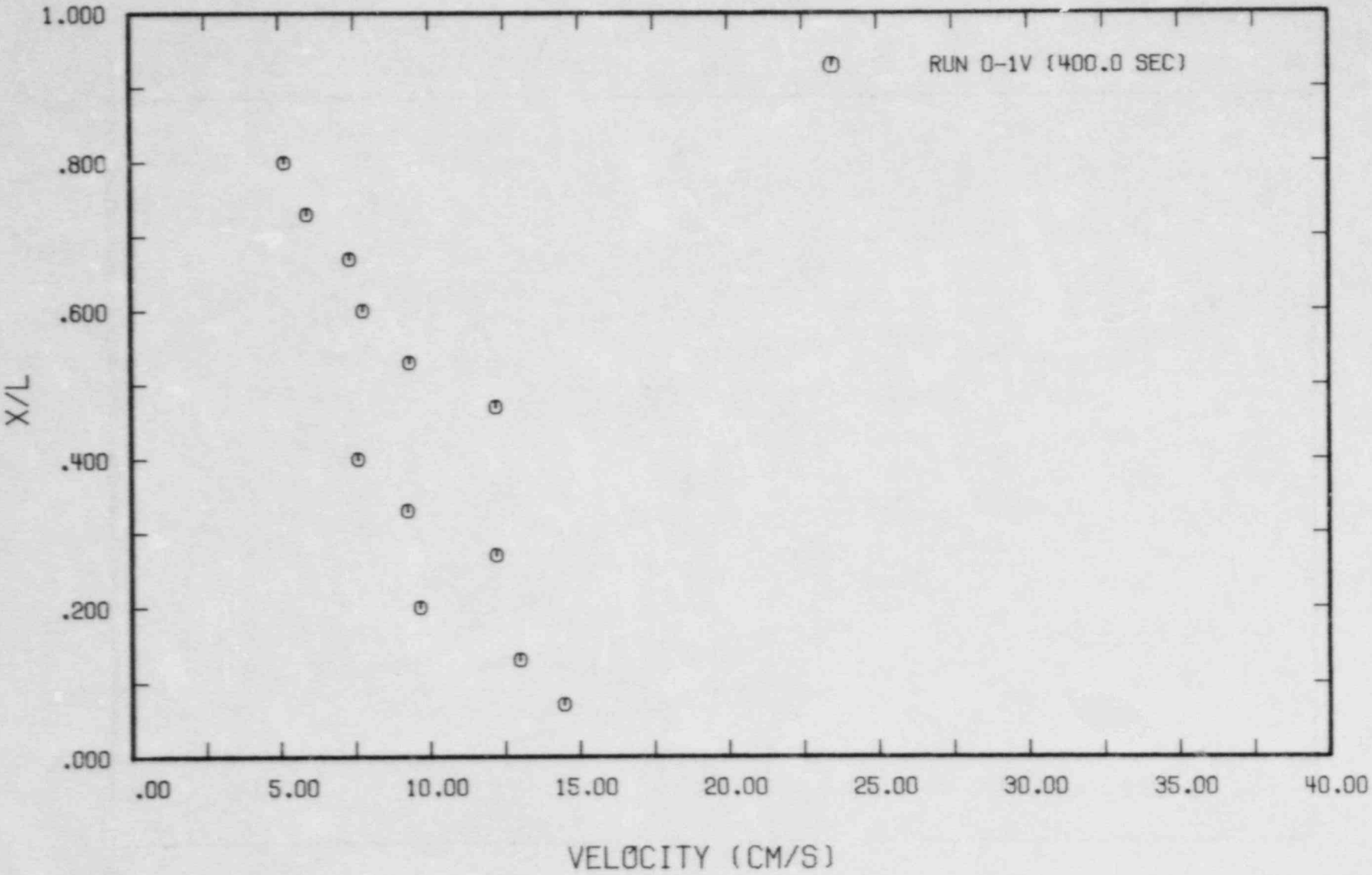
RUN 0-1V (400.0 SEC)
1.000
.800
.600
.400
.200
.000
X/L
.00
5.00
10.00
15.00
20.00
25.00
30.00
35.00
40.00
VELOCITY (CM/S)

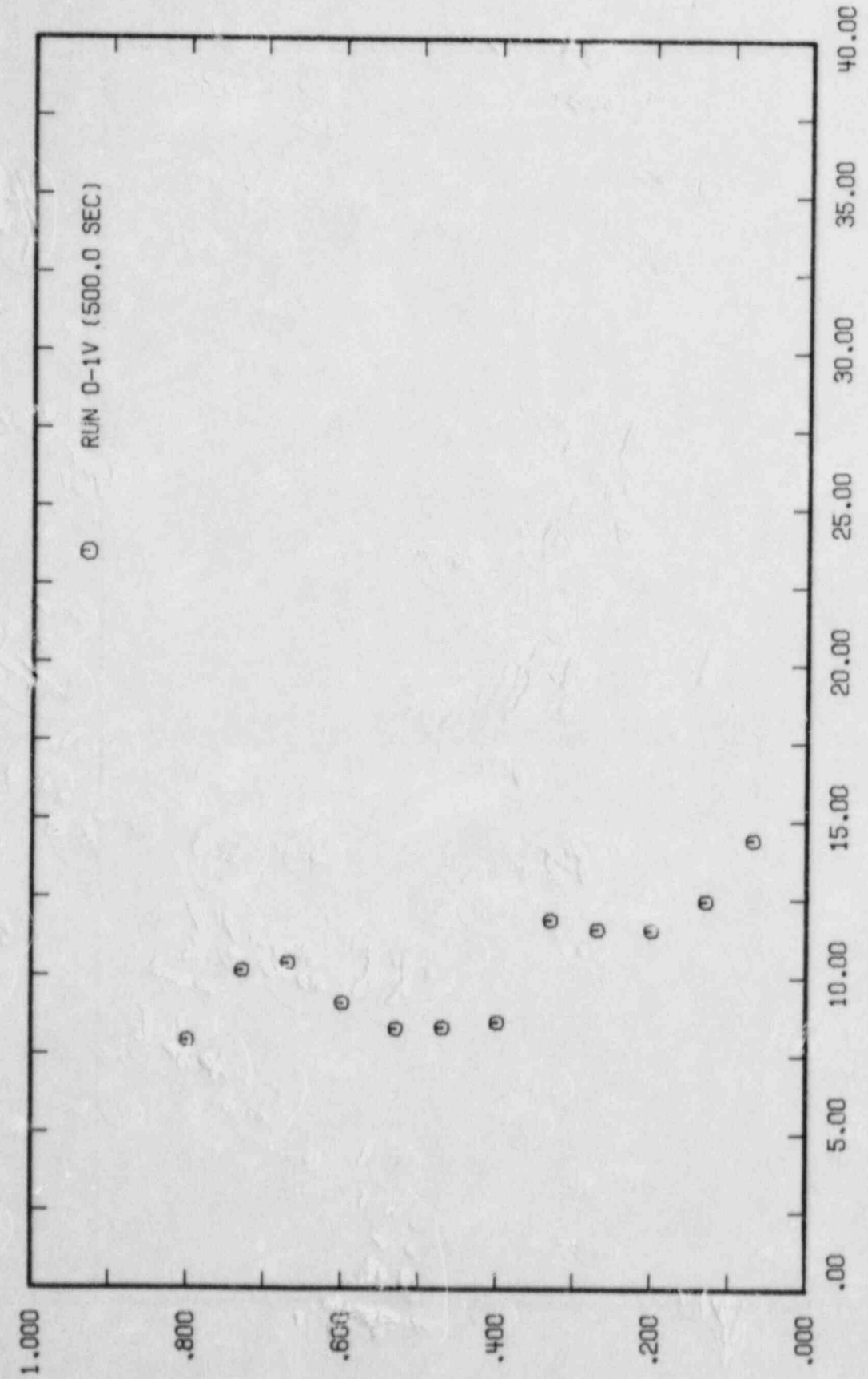
RUN 0-1V (500.0 SEC)
X/L
1.000
.800
.600
.400
.200
.000
.00
5.00
10.00
15.00
20.00
25.00
30.00
35.00
40.00
VELOCITY (CM/S)

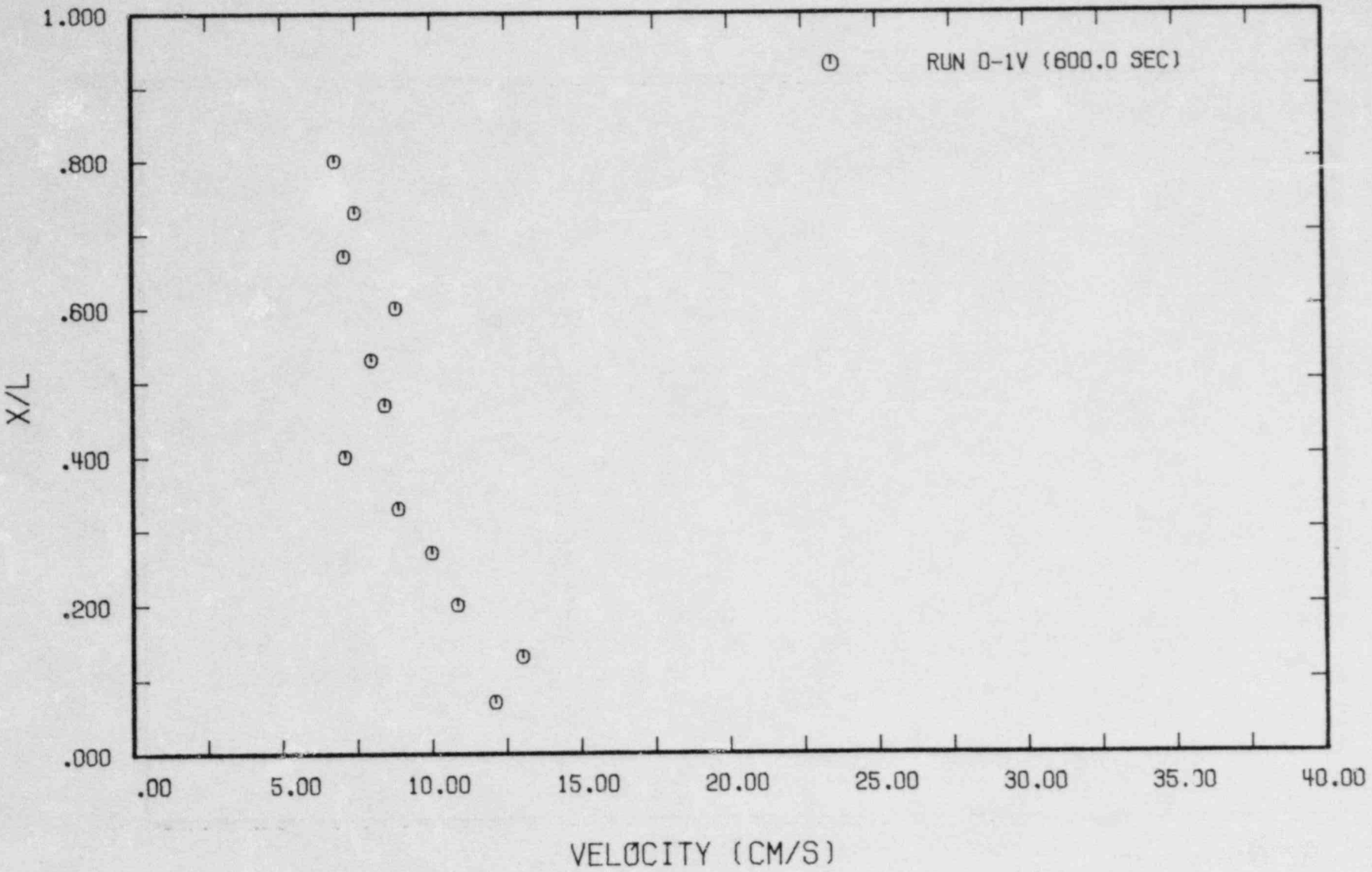
RUN 0-1V (600.0 SEC)
1.000
.800
.600
.400
.200
.000
X/L
.00
5.00
10.00
15.00
20.00
25.00
30.00
35.00
40.00
VELOCITY (CM/S)

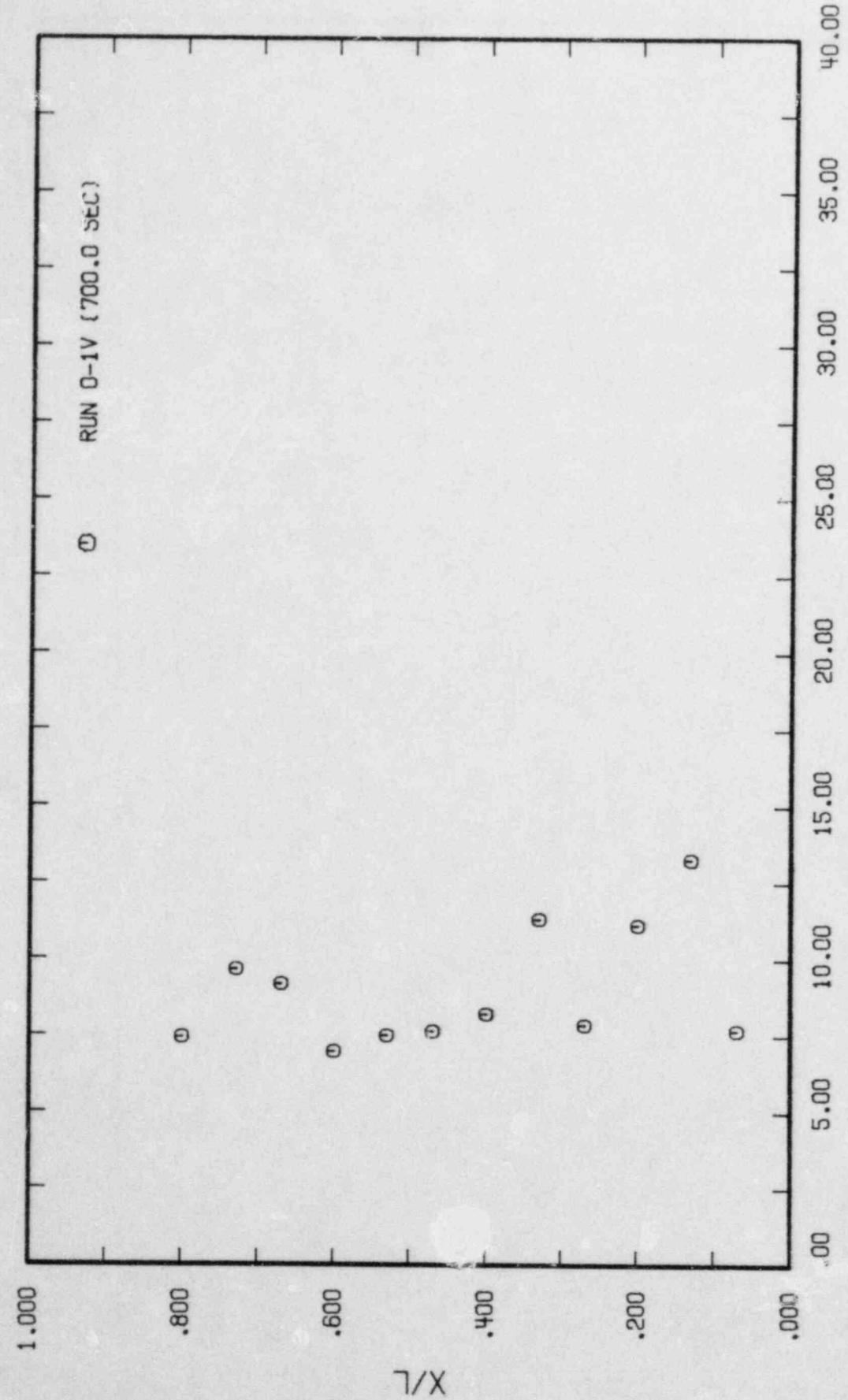
RUN 0-1V (700.0 SEC)
1.000
.800
.600
.400
.200
.000
X/L
.00
5.00
10.00
15.00
20.00
25.00
30.00
35.00
40.00
VELOCITY (CM/S)

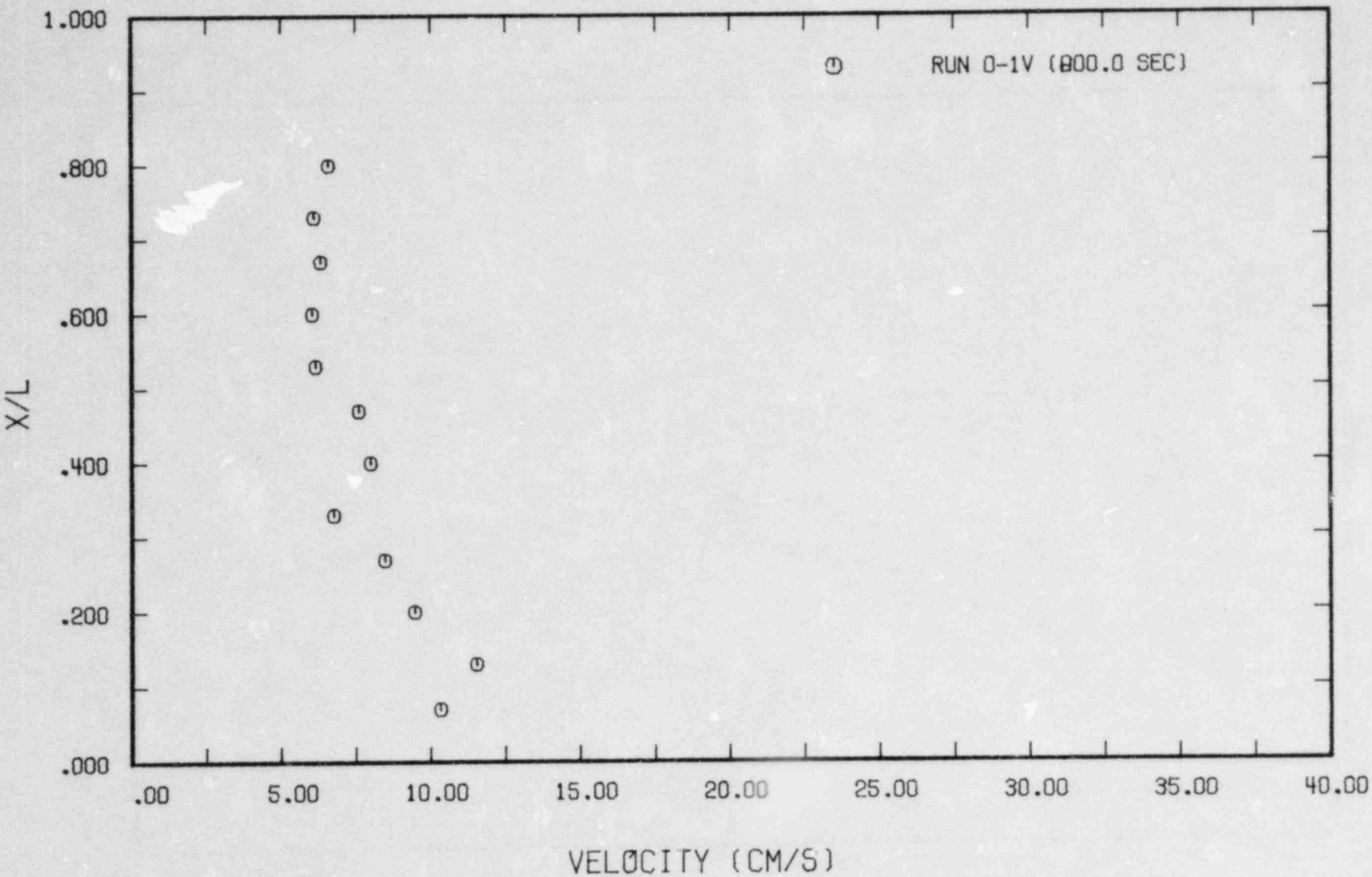
RUN 0-1V (800.0 SEC)
1.000
.800
.600
.400
.200
.000
X/L
.00
5.00
10.00
15.00
20.00
25.00
30.00
35.00
40.00
VELOCITY (CM/S)

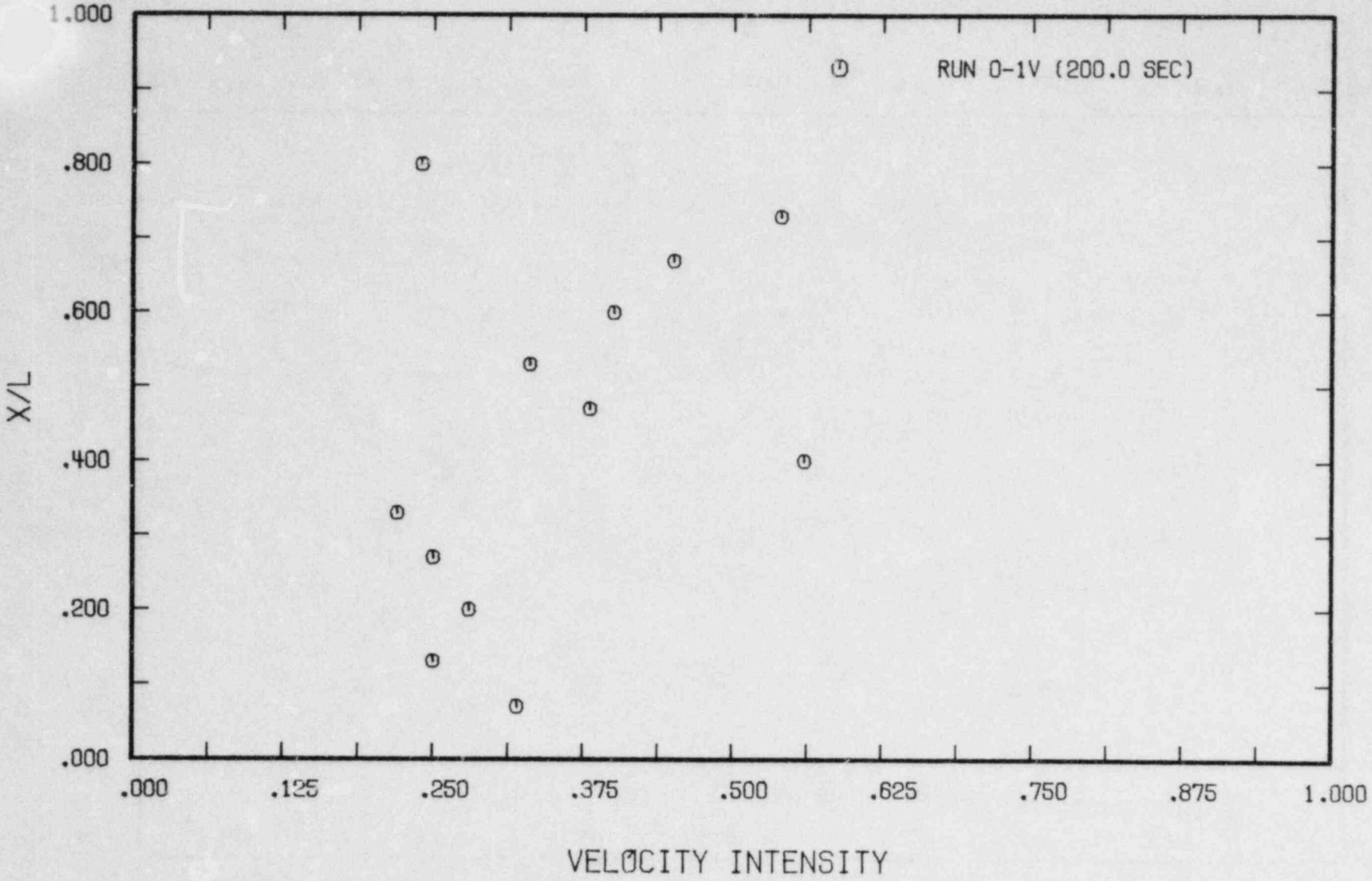
RUN 0-1V (200.0 SEC)
1.000
.800
.600
.400
.200
.000
X/L
.000
.125
.250
.375
.500
.625
.750
.875
1.000
VELOCITY INTENSITY

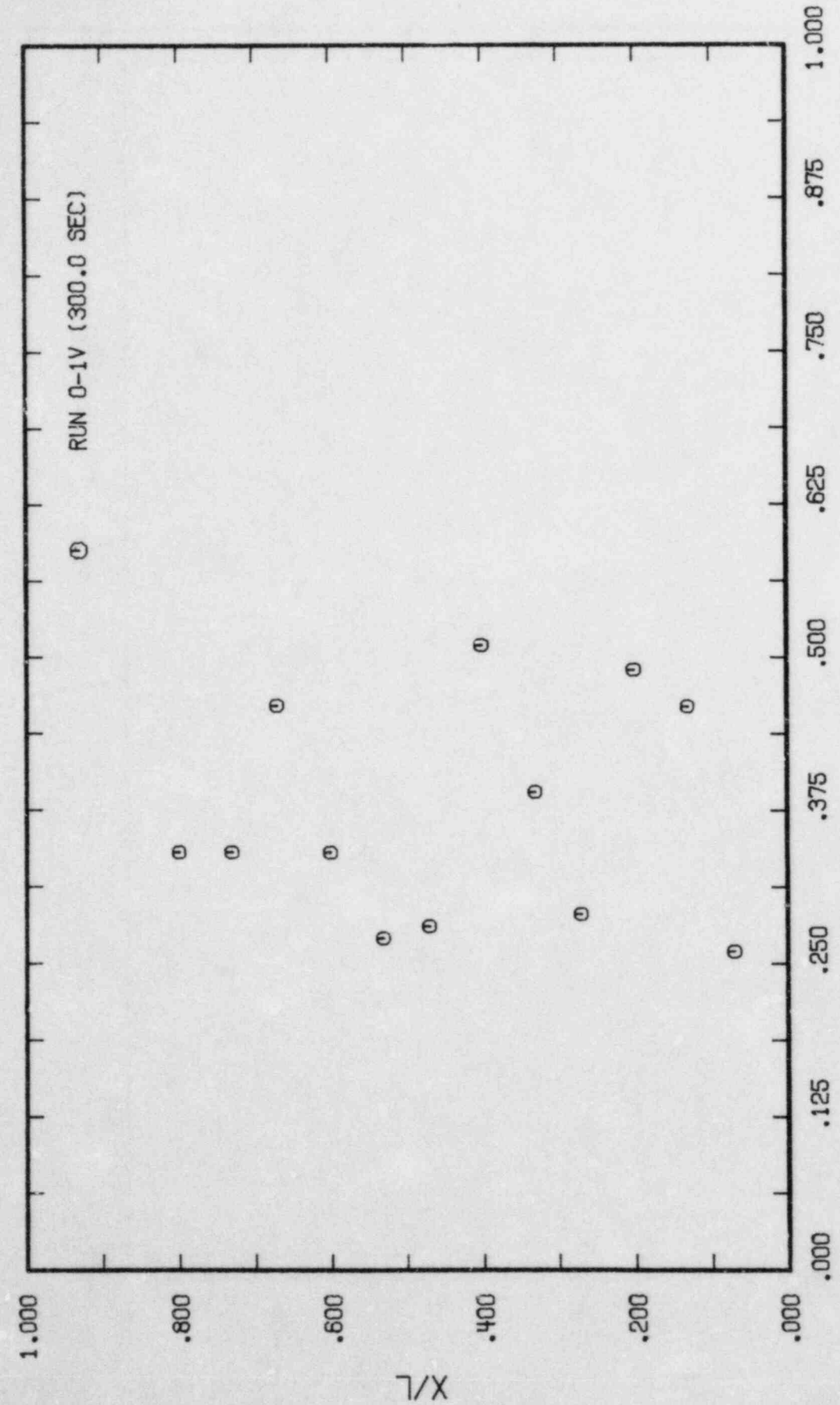
RUN 0-1V (300.0 SEC)
1.000
.800
.600
.400
.200
.000
X/L
.000
.125
.250
.375
.500
.625
.750
.875
1.000
VELOCITY INTENSITY

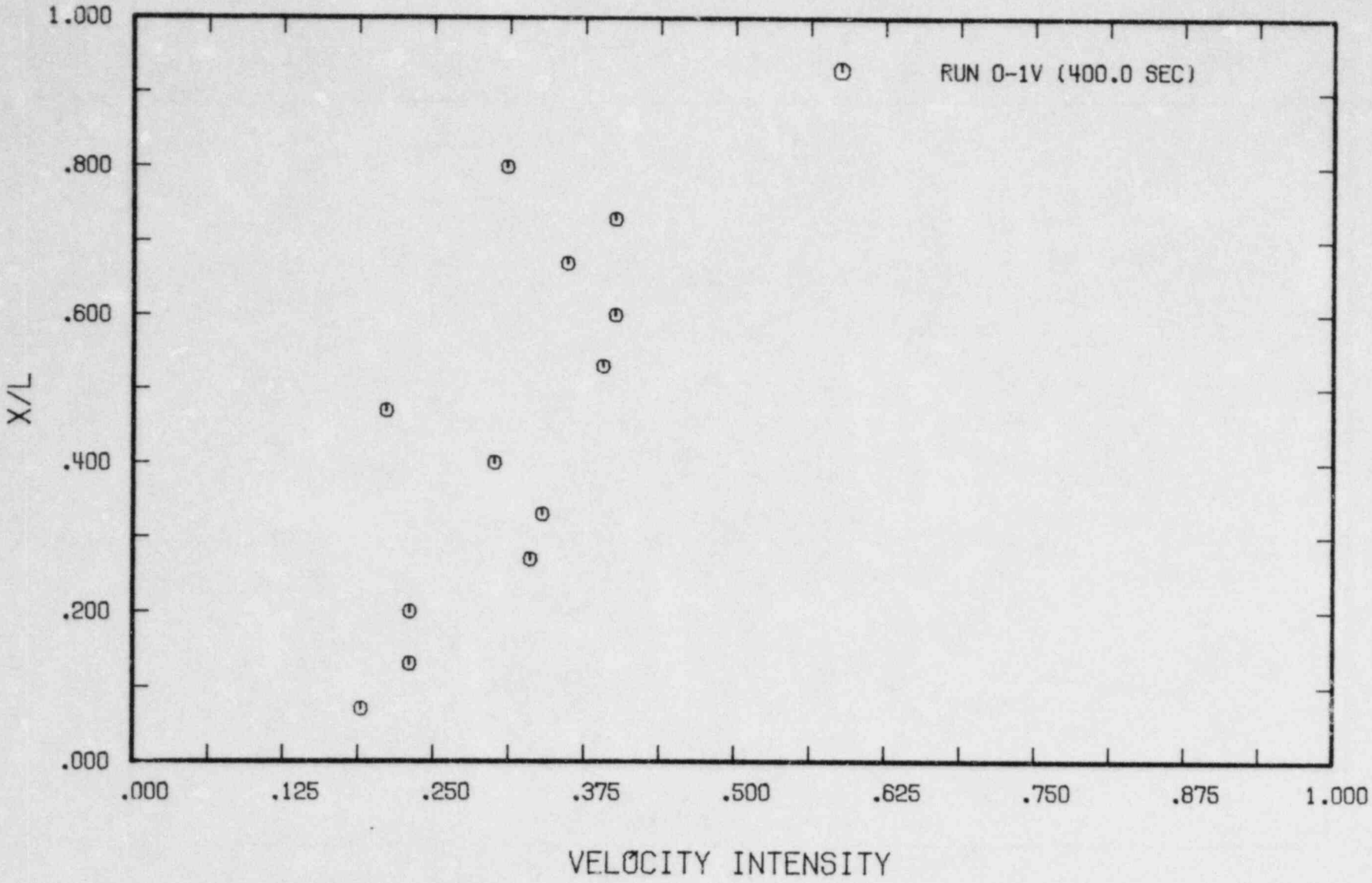
RUN 0-1V (400.0 SEC)
1.000
.800
.600
.400
.200
.000
X/L
.000
.125
.250
.375
.500
.625
.750
.875
1.000
VELOCITY INTENSITY

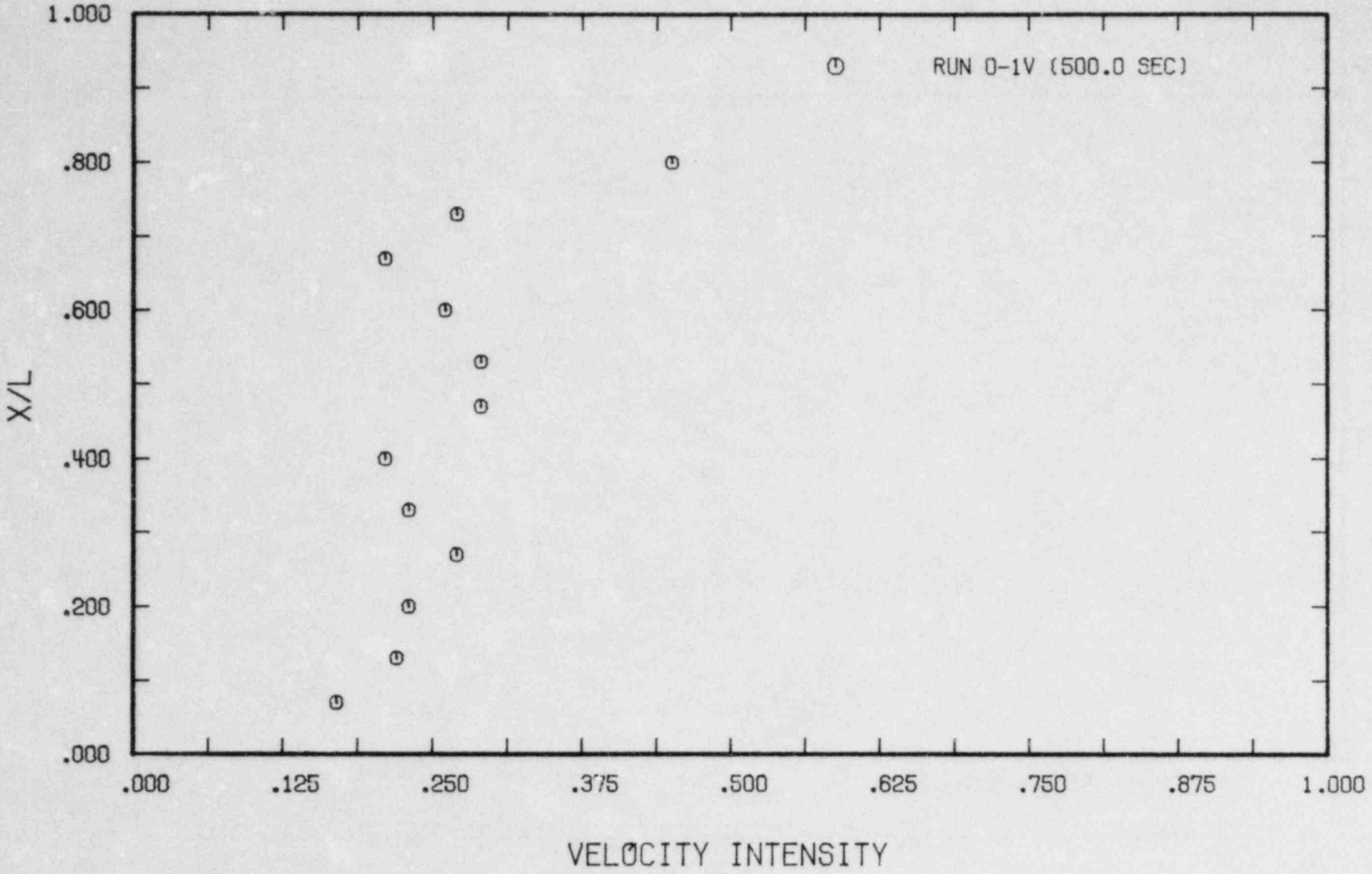
RUN 0-1V (500.0 SEC)
1.000
.800
.600
.400
.200
.000
X/L
.000
.125
.250
.375
.500
.625
.750
.875
1.000
VELOCITY INTENSITY

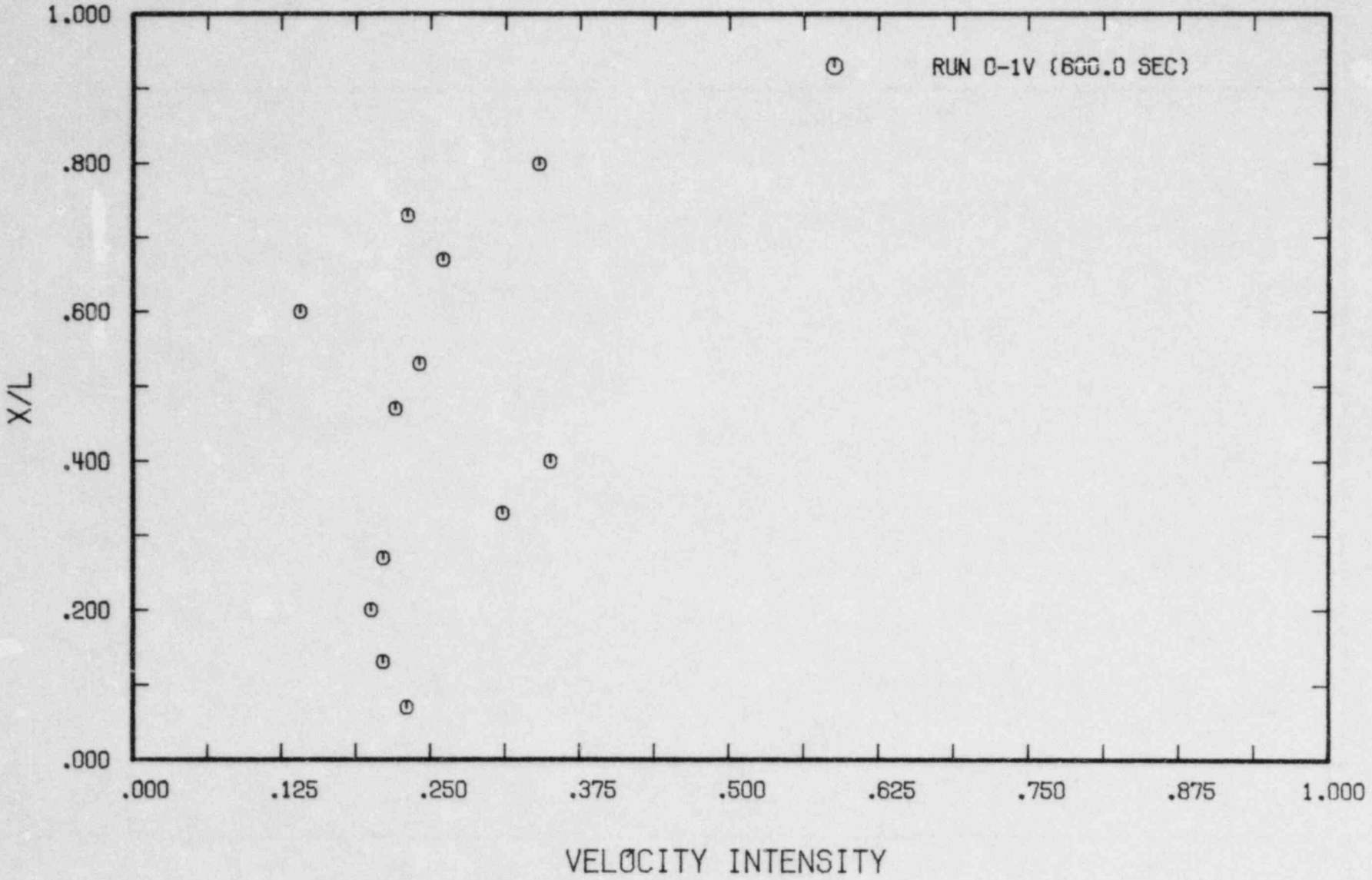
RUN 0-1V (600.0 SEC)
1.000
.800
.600
.400
.200
.000
X/L
.000
.125
.250
.375
.500
.625
.750
.875
1.000
VELOCITY INTENSITY

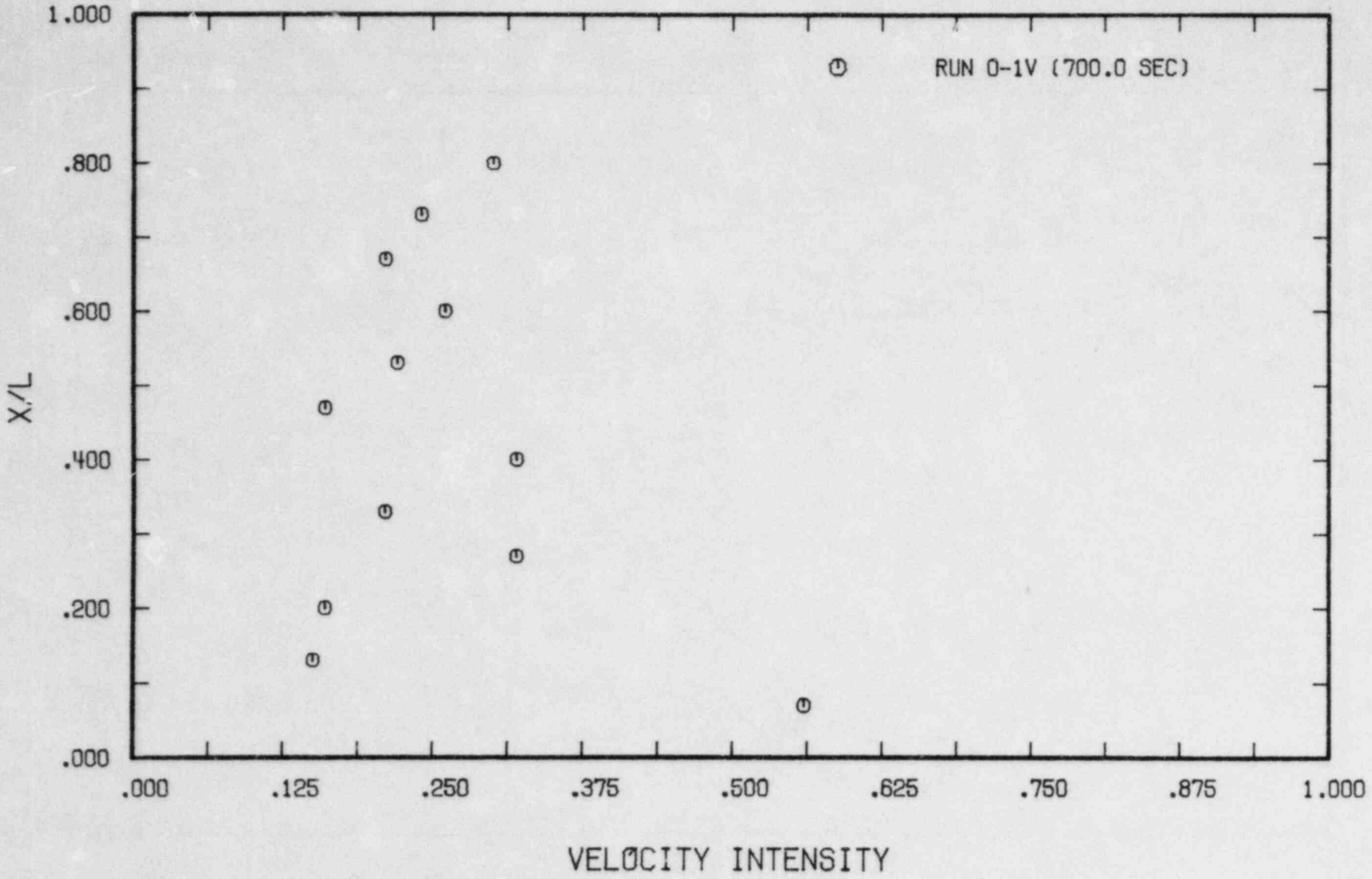
RUN 0-1V (700.0 SEC)
1.000
.800
.600
.400
.200
.000
X/L
.000
.125
.250
.375
.500
.625
.750
.875
1.000
VELOCITY INTENSITY

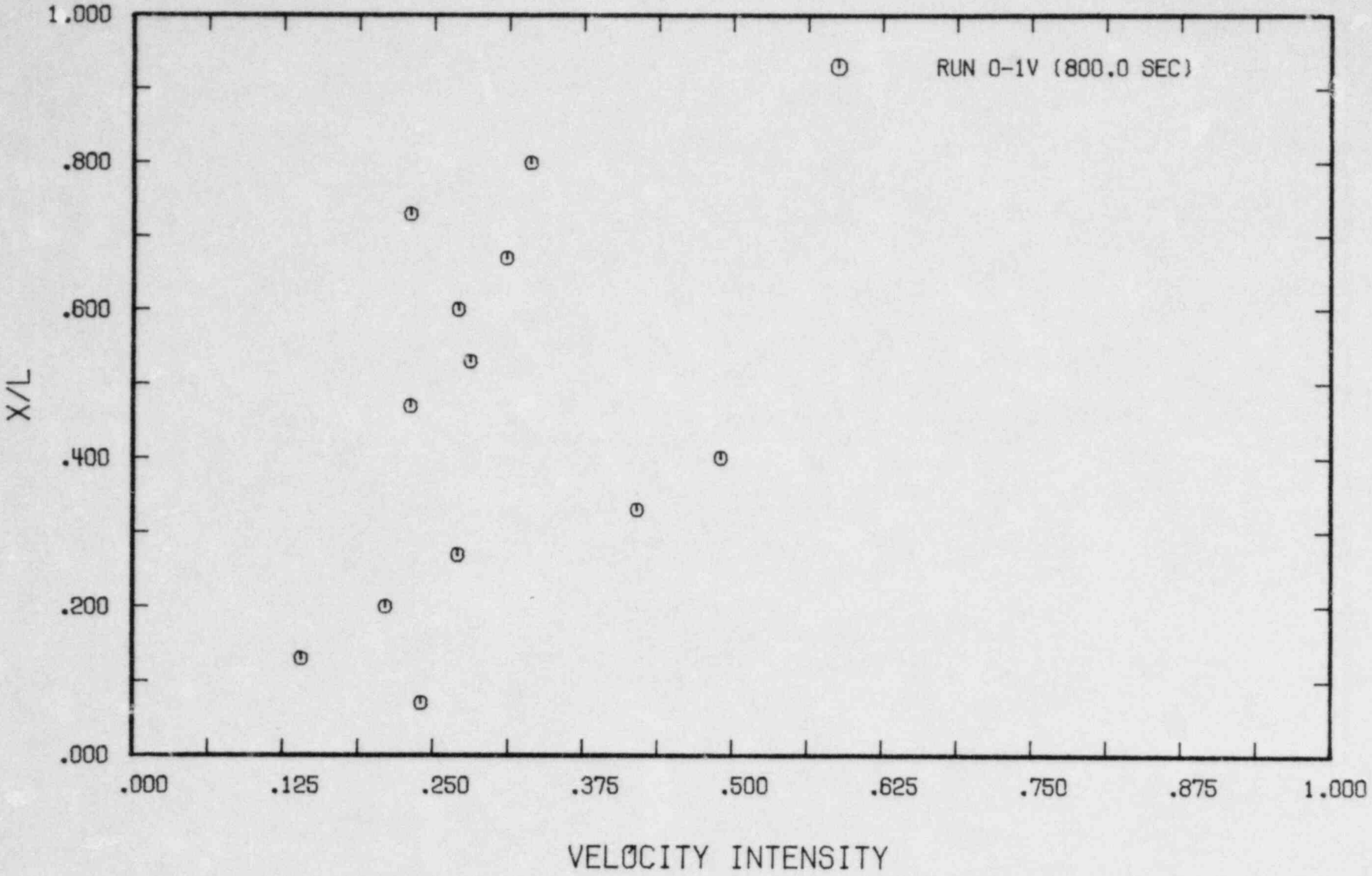
RUN 0-1V (800.0 SEC)
1.000
.800
.600
.400
.200
.000
X/L
.000
.125
.250
.375
.500
.625
.750
.875
1.000
VELOCITY INTENSITY

Run 0-2C

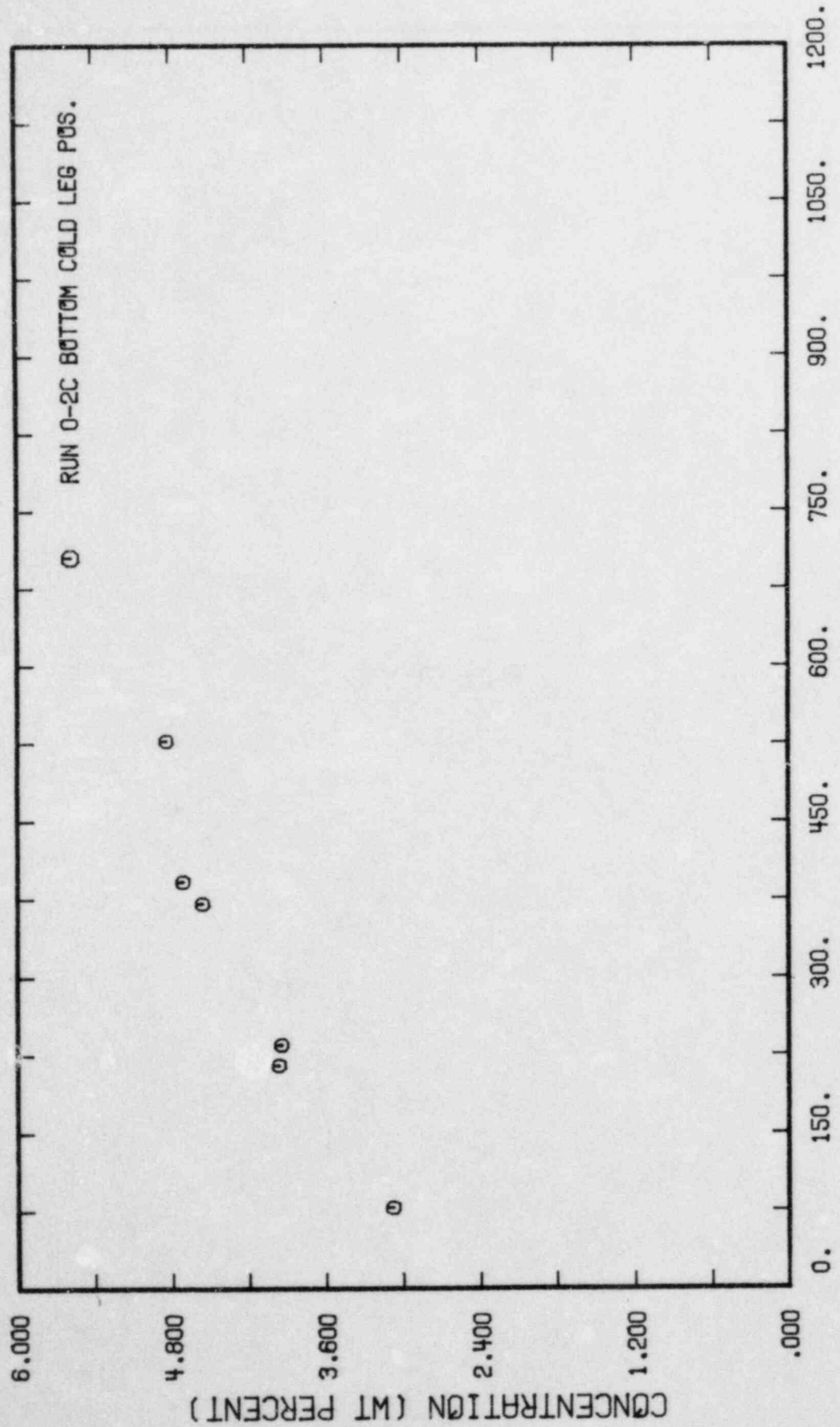
RUN 0-2C BOTTOM COLD LEG POS.
CONCENTRATION (WT PERCENT)
6.000
4.800
3.600
2.400
1.200
.000
0.
150.
300.
450.
600.
750.
900.
1050.
1200.
TIME (SEC)

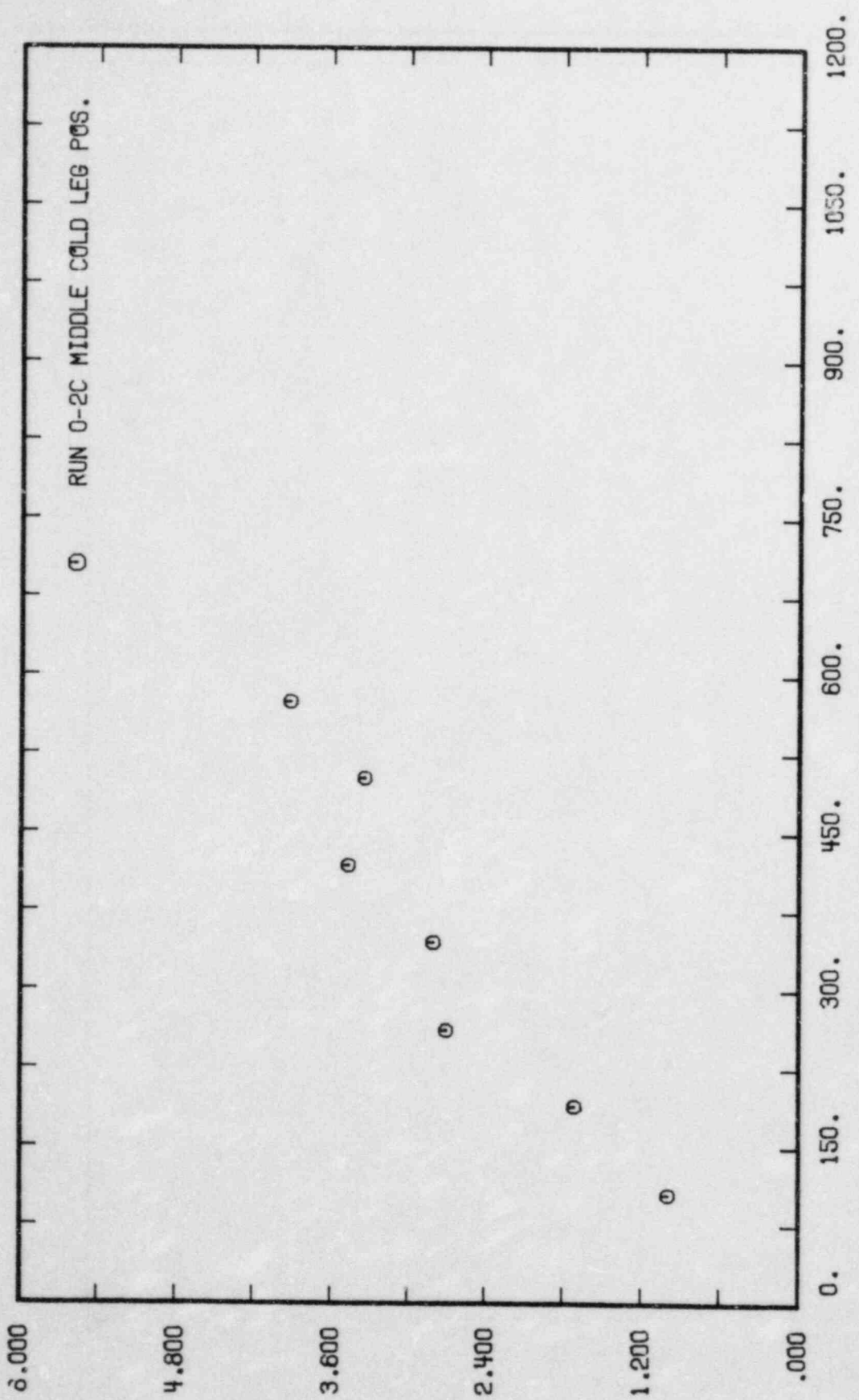
RUN 0-2C MIDDLE COLD LEG POS.
CONCENTRATION (WT PERCENT)
6.000
4.800
3.600
2.400
1.200
.000
0.
150.
300.
450.
600.
750.
900.
1050.
1200.
TIME (SEC)

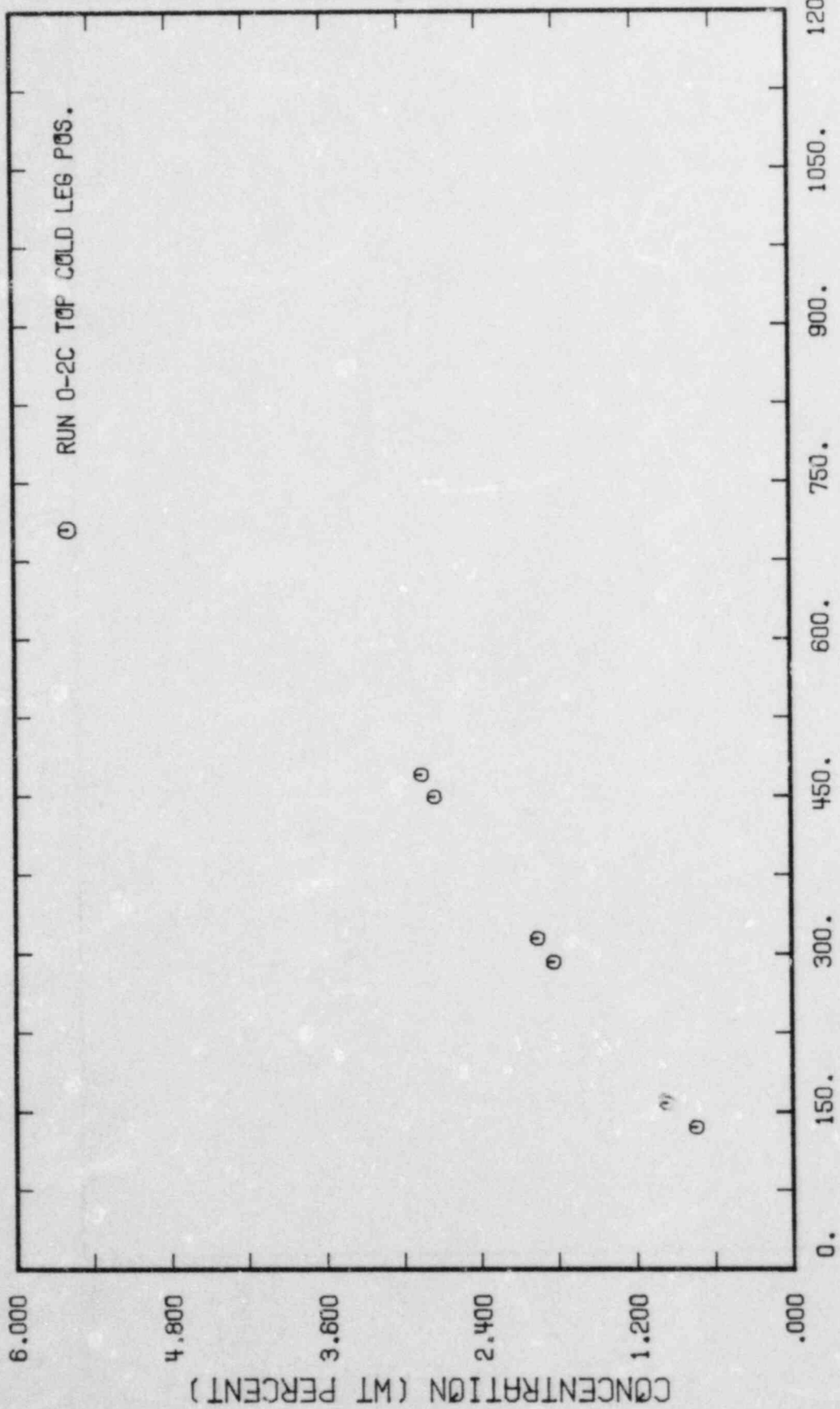
RUN 0-2C TOP COLD LEG POS.
CONCENTRATION (WT PERCENT)
6.000
4.800
3.600
2.400
1.200
.000
0.
150.
300.
450.
600.
750.
900.
1050.
1200.
TIME (SEC)

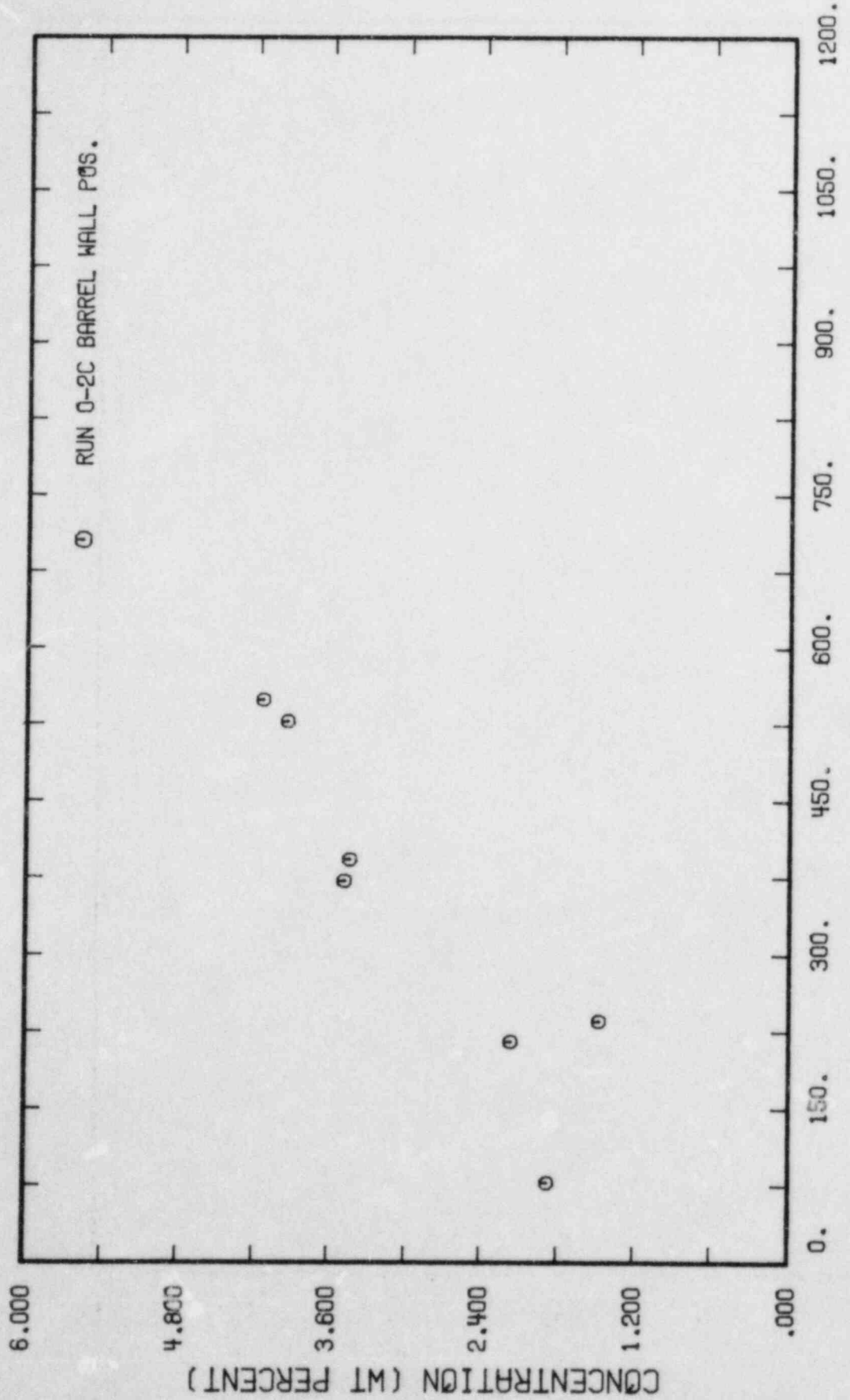
RUN 0-2C BARREL WALL POS.
CONCENTRATION (WT PERCENT)
6.000
4.800
3.600
2.400
1.200
.000
0.
150.
300.
450.
600.
750.
900.
1050.
1200.
TIME (SEC)

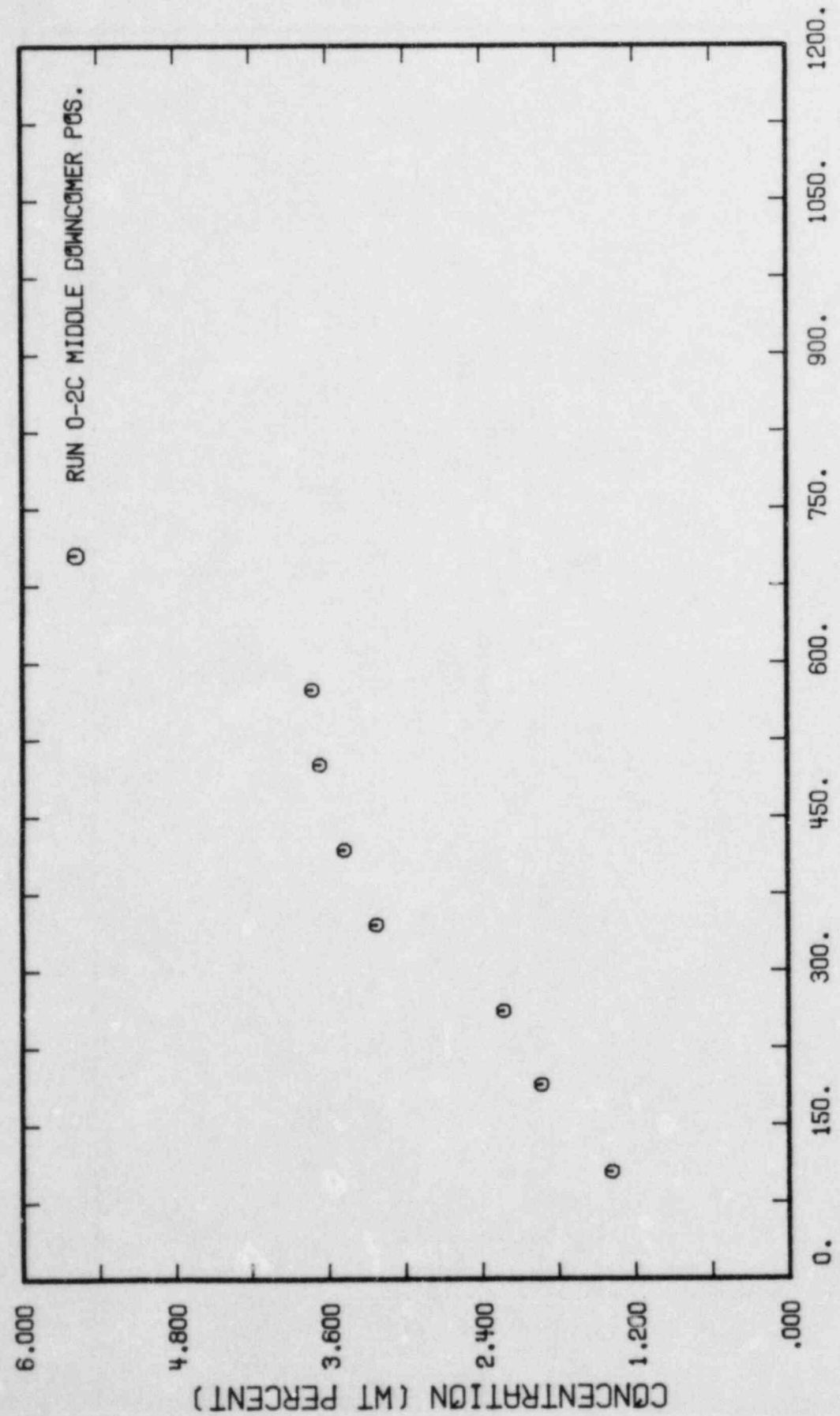
RUN 0-2C MIDDLE DOWNCOMER POS.
CONCENTRATION (WT PERCENT)
6.000
4.800
3.600
2.400
1.200
.000
0.
150.
300.
450.
600.
750.
900.
1050.
1200.
TIME (SEC)

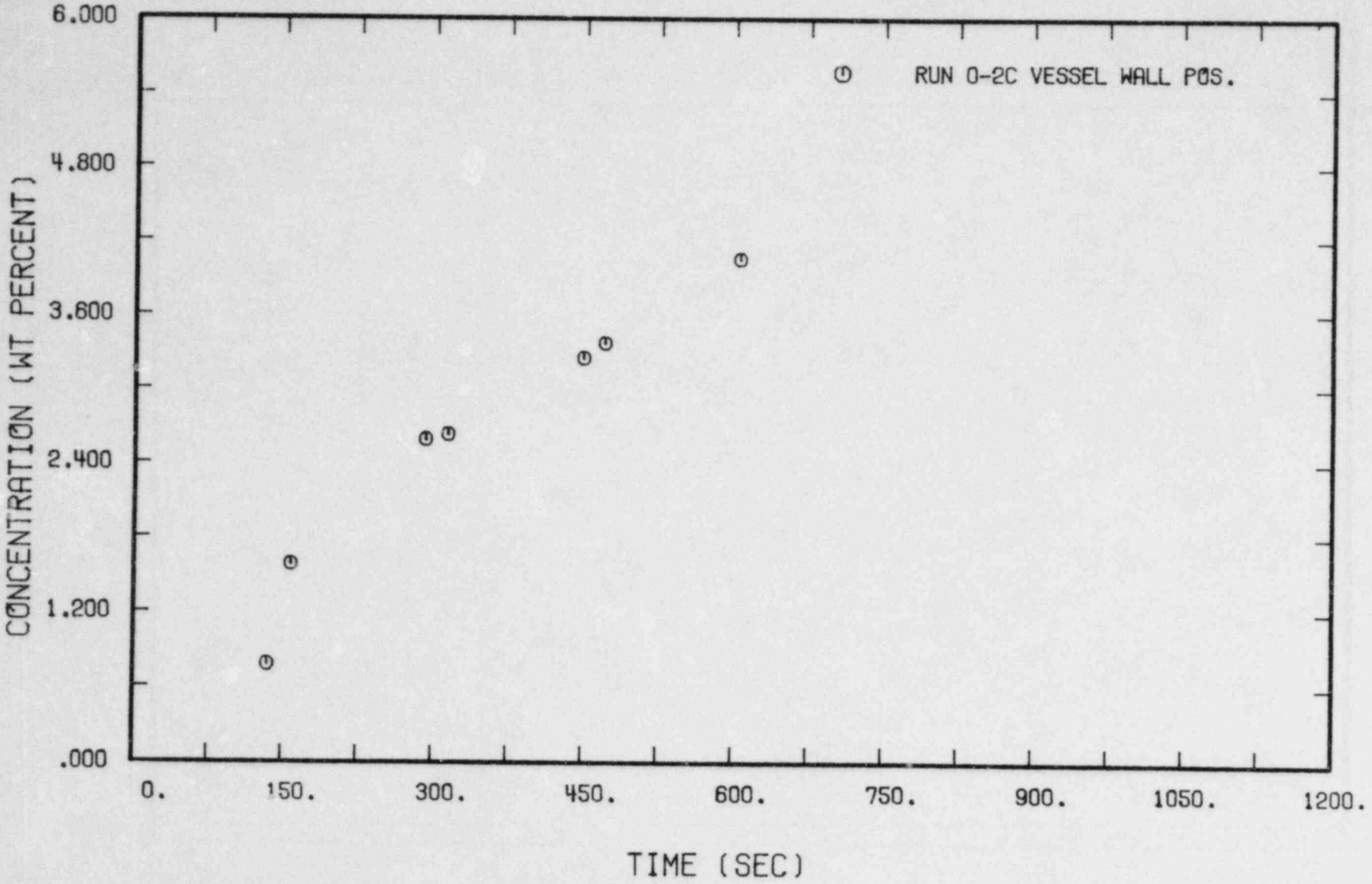
RUN 0-2C VESSEL WALL POS.
CONCENTRATION (WT PERCENT)
6.000
4.800
3.600
2.400
1.200
.000
0.
150.
300.
450.
600.
750.
900.
1050.
1200.
TIME (SEC)

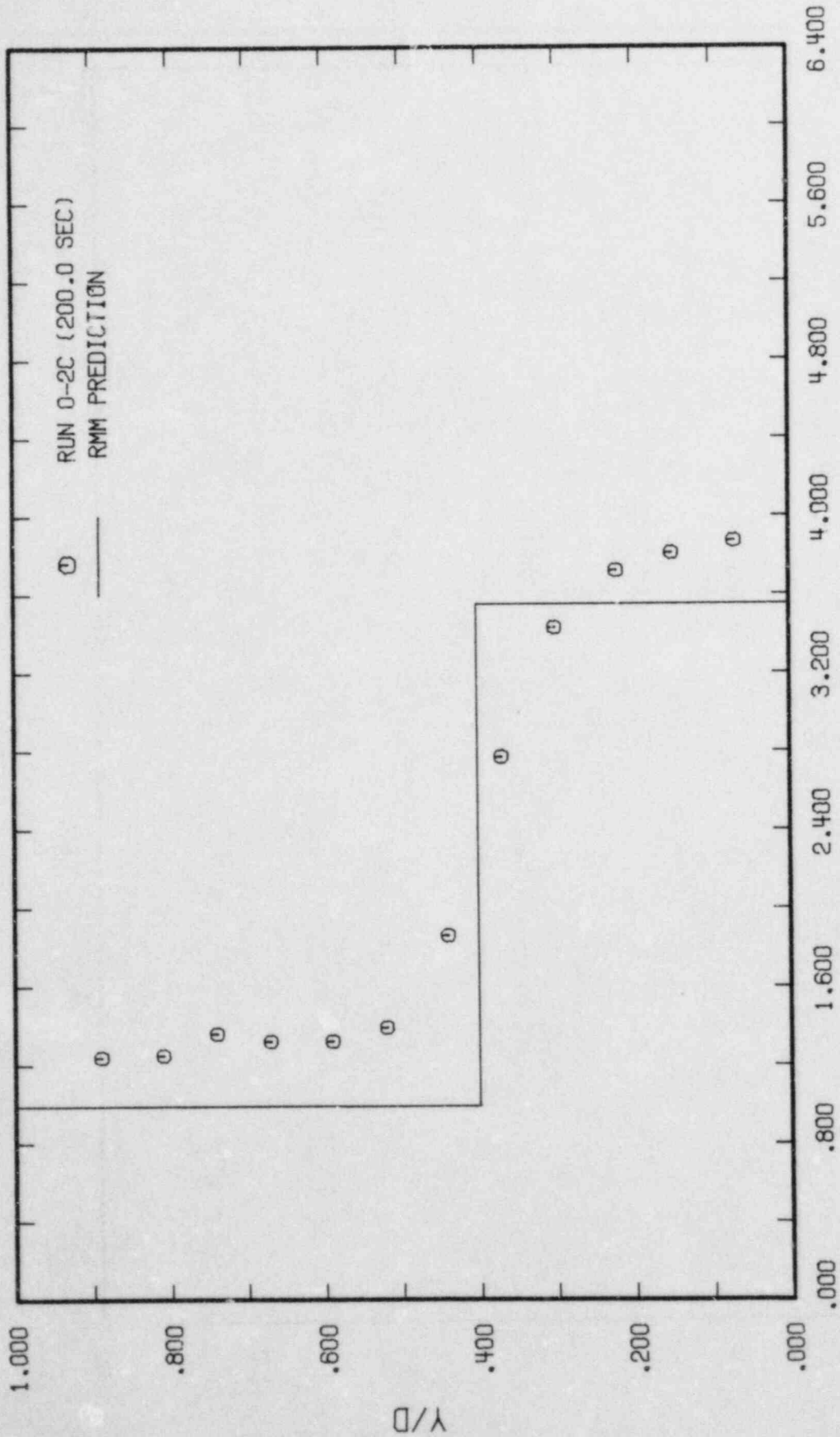
RUN 0-2C (200.0 SEC)
RMM PREDICTION
Y/D
1.000
.800
.600
.400
.200
.000
.000
.800
1.600
2.400
3.200
4.000
4.800
5.600
6.400
CONCENTRATION (WT PERCENT)

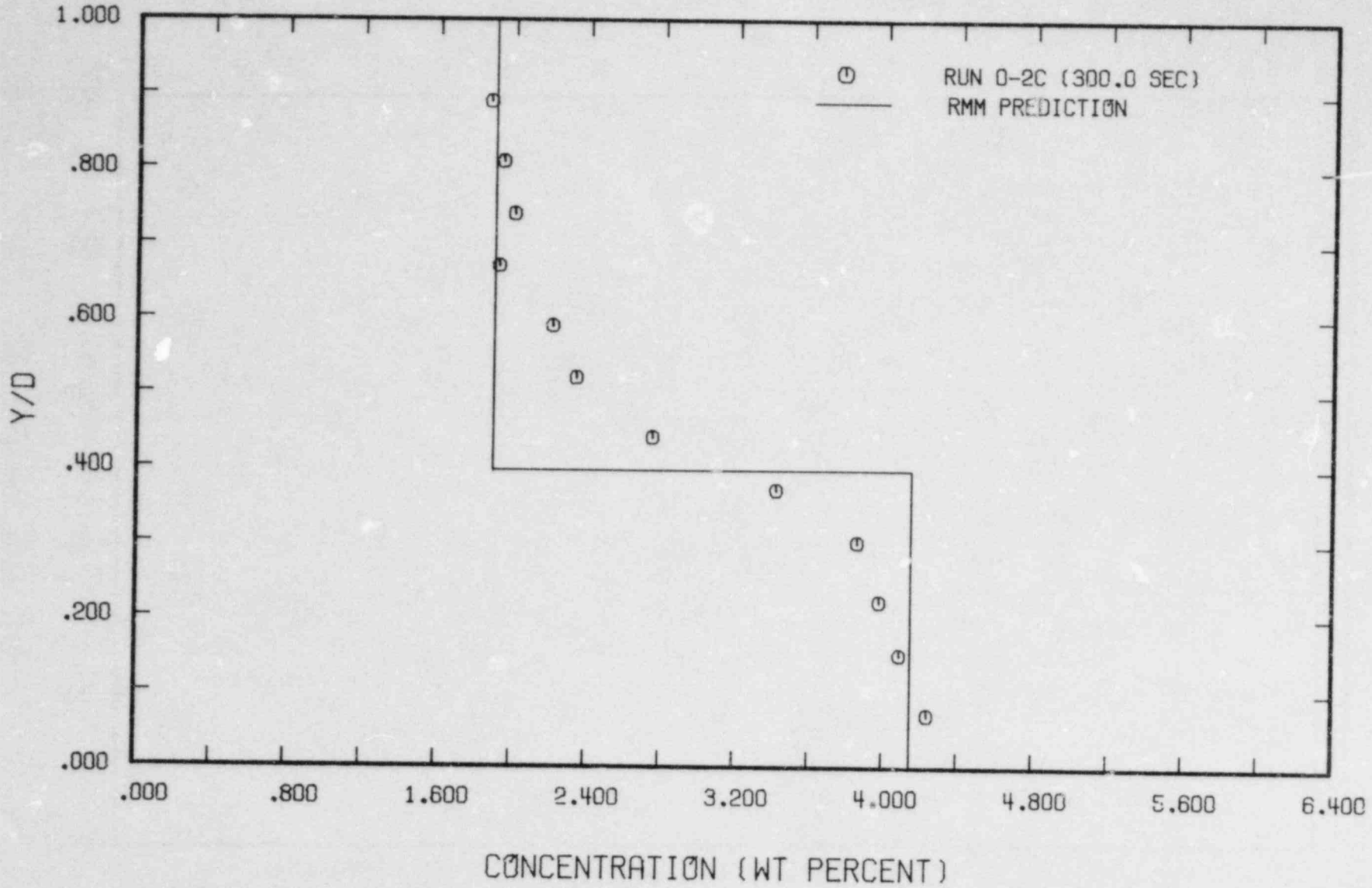
RUN 0-2C (300.0 SEC)
RMM PREDICTION
Y/D
1.000
.800
.600
.400
.200
.000
.000
.800
1.600
2.400
3.200
4.000
4.800
5.600
6.400
CONCENTRATION (WT PERCENT)

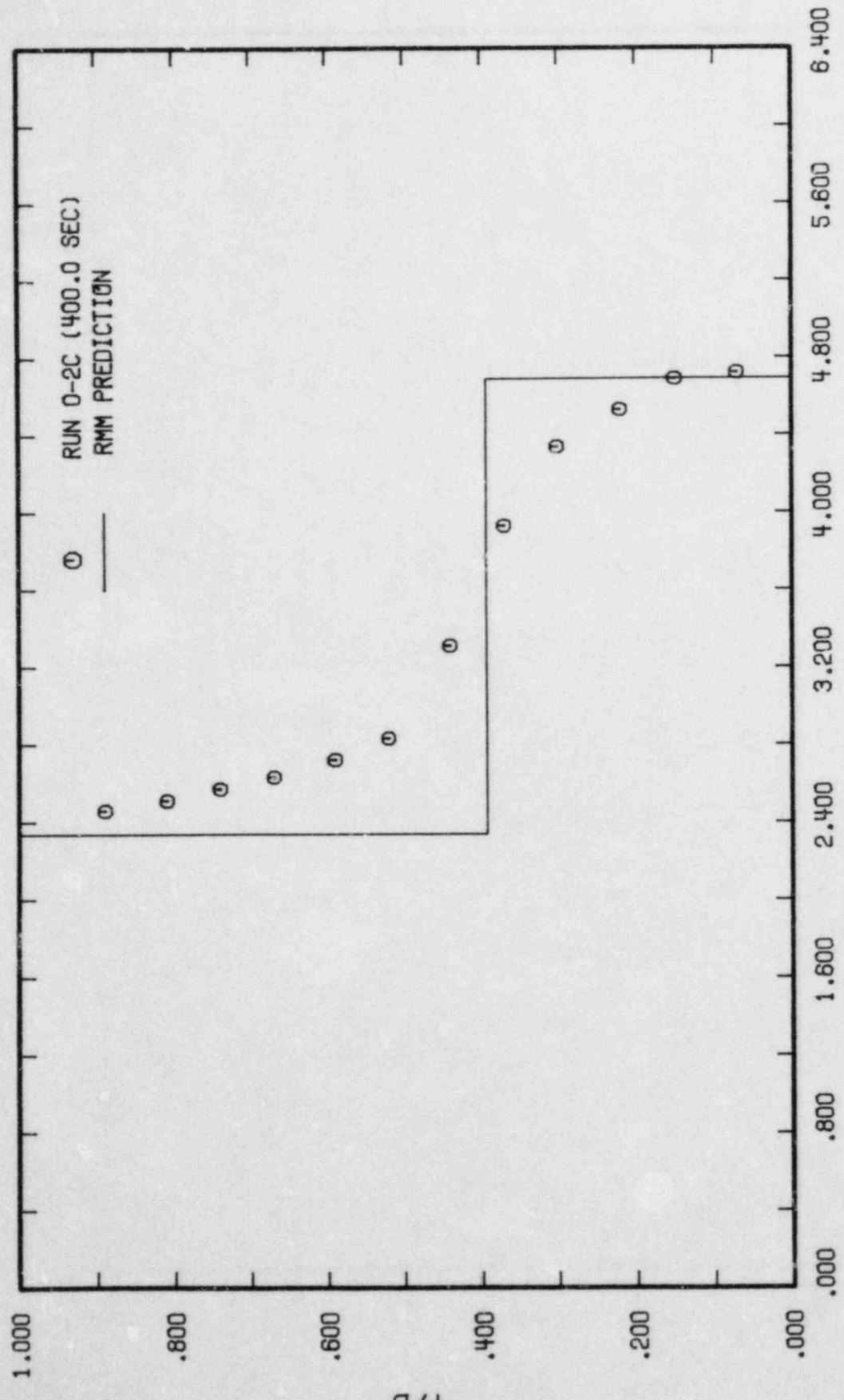
RUN 0-2C (400.0 SEC)
RMM PREDICTION
Y/D
1.000
.800
.600
.400
.200
.000
.000
.800
1.600
2.400
3.200
4.000
4.800
5.600
6.400
CONCENTRATION (WT PERCENT)

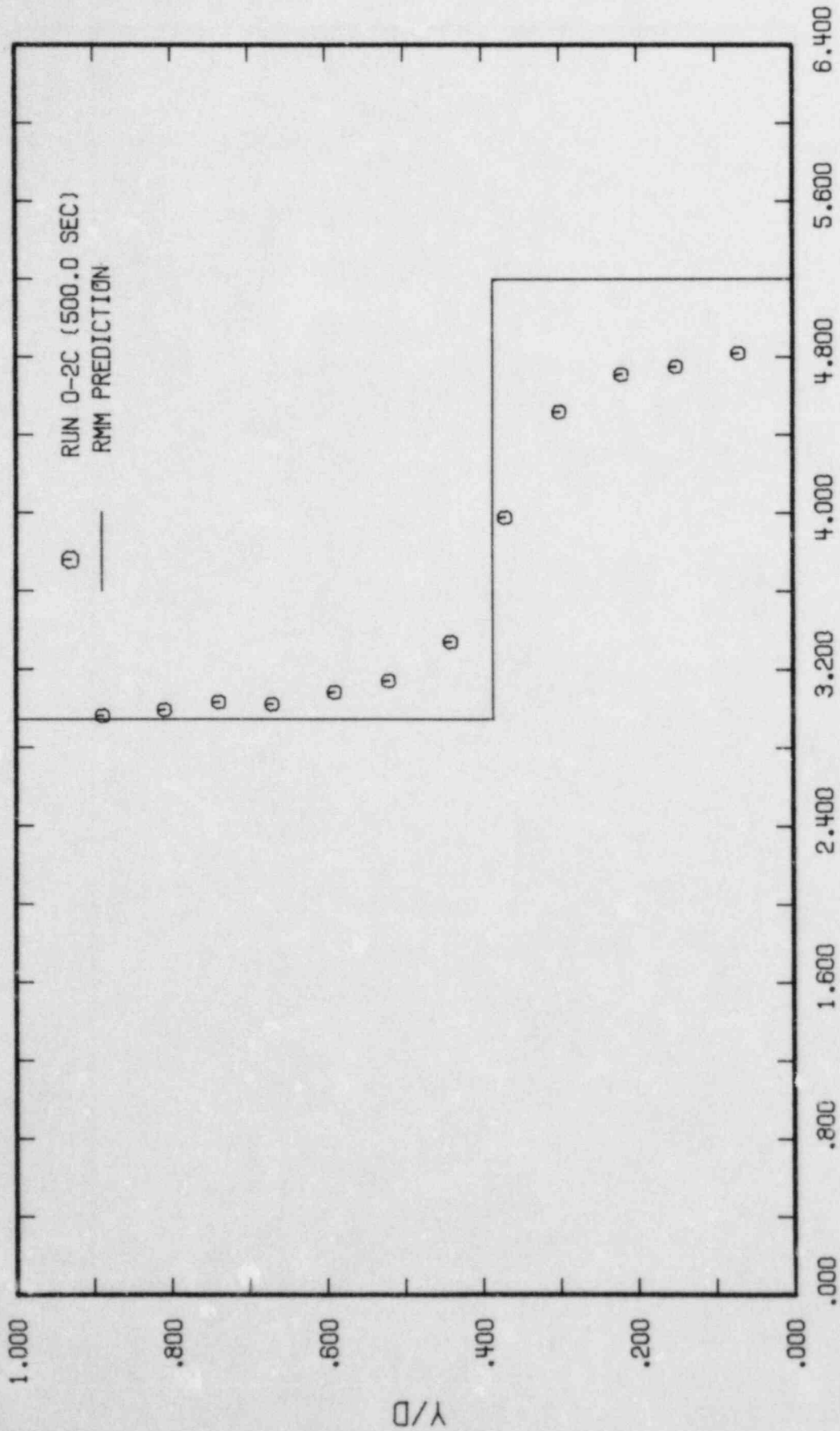
RUN 0-2C (500.0 SEC)
RMM PREDICTION
Y/D
1.000
.800
.600
.400
.200
.000
.000
.800
1.600
2.400
3.200
4.000
4.800
5.600
6.400
CONCENTRATION (WT PERCENT)

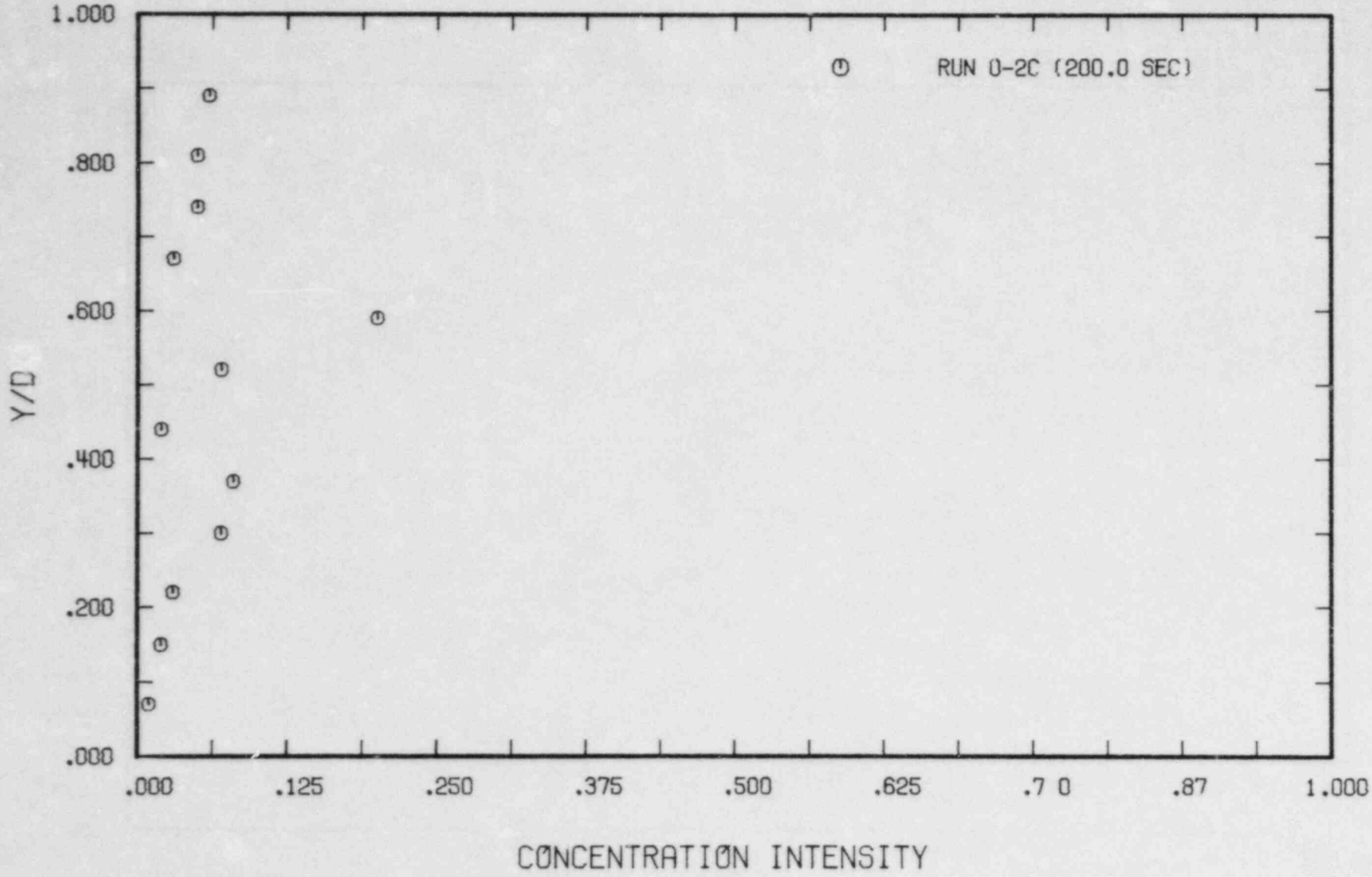
RUN 0-2C (200.0 SEC)
1.000
.800
.600
.400
.200
.000
Y/D
.000
.125
.250
.375
.500
.625
.7 0
.87
1.000
CONCENTRATION INTENSITY

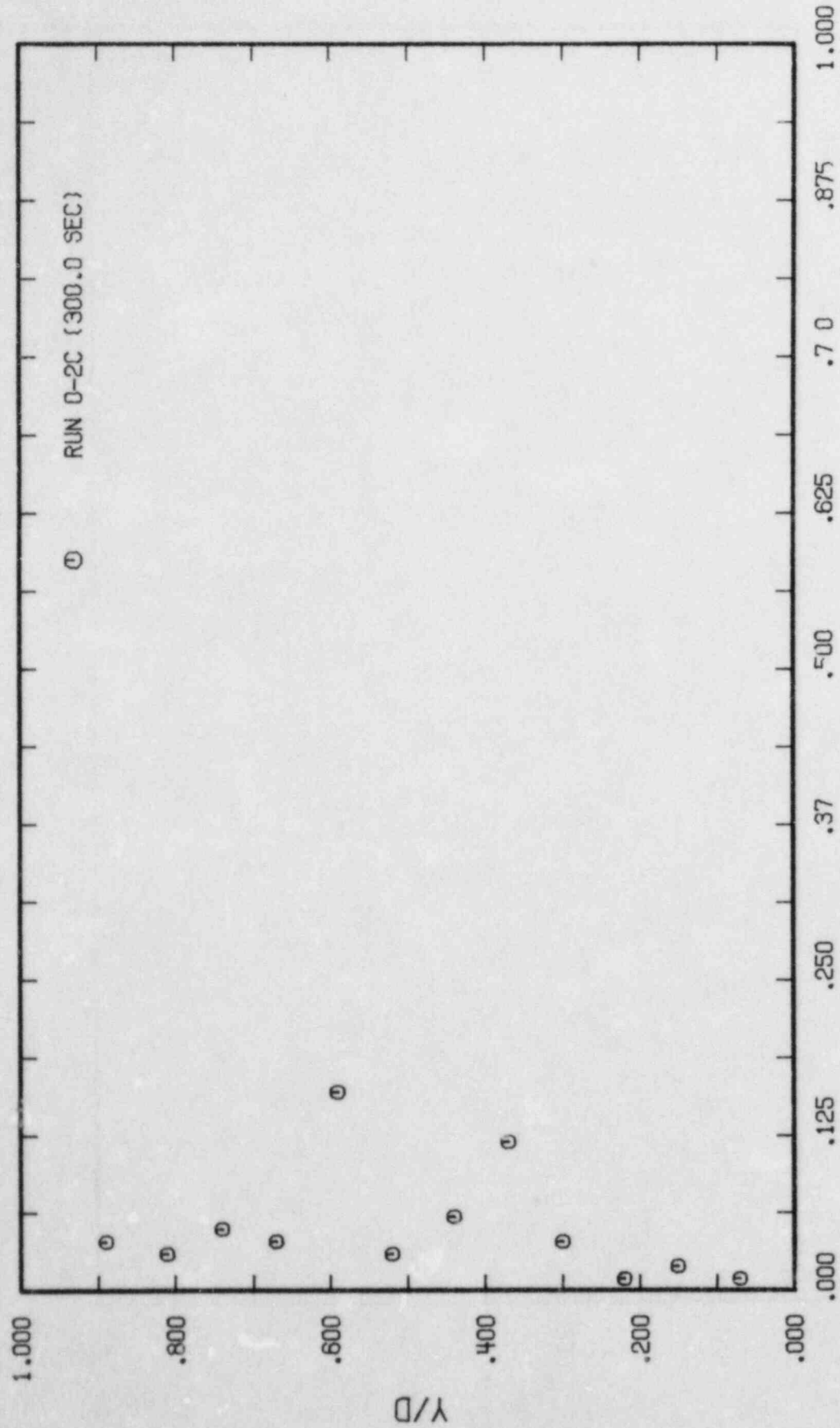
RUN 0-2C (300.0 SEC)
Y/D
1.000
.800
.600
.400
.200
.000
.000
.125
.250
.37
.500
.625
.7 0
.875
1.000
CONCENTRATION INTENSITY

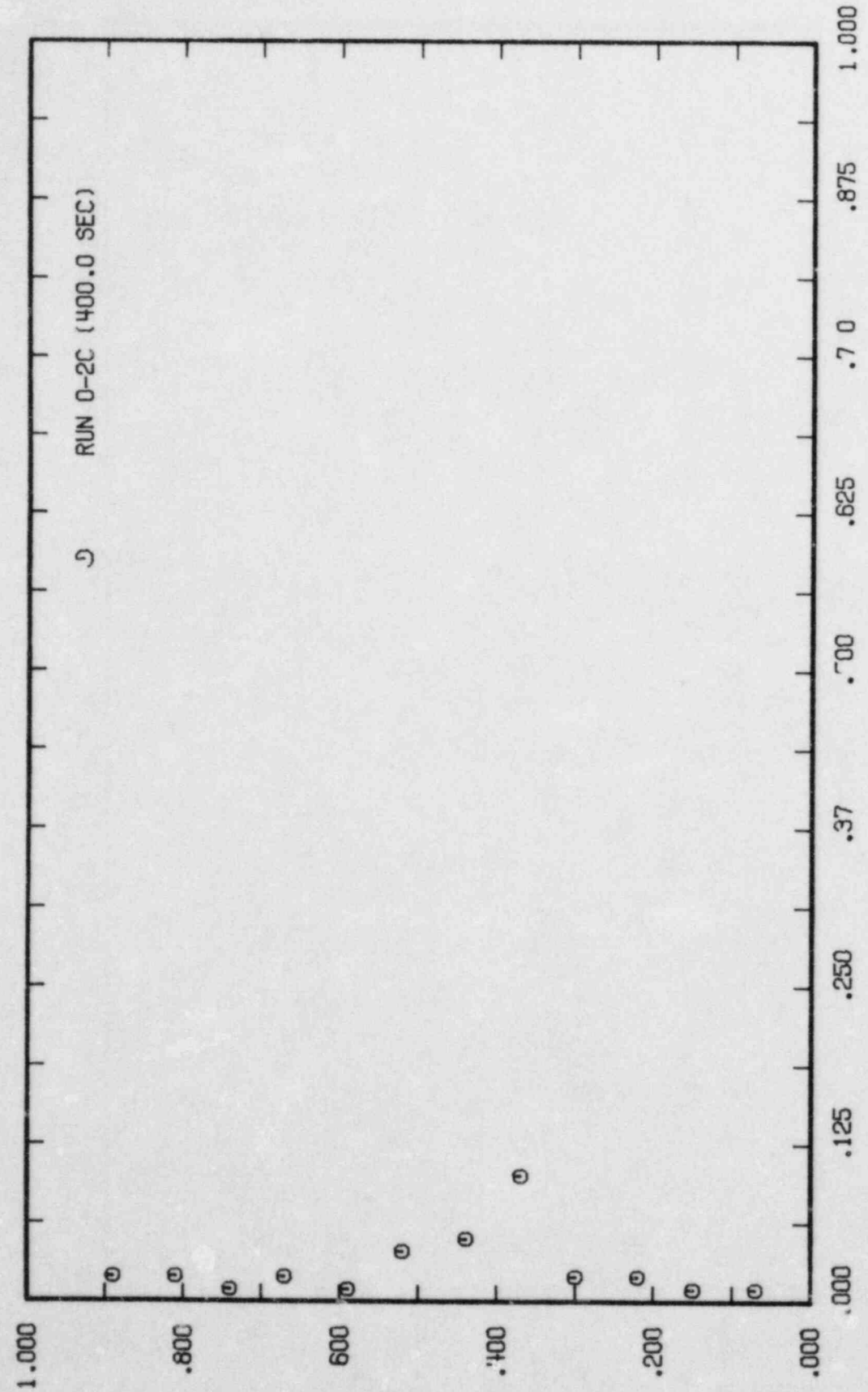
RUN 0-2C (400.0 SEC)
Y/D
1.000
.800
.600
.400
.200
.000
.000
.125
.250
.37
.700
.625
.875
1.000
CONCENTRATION INTENSITY

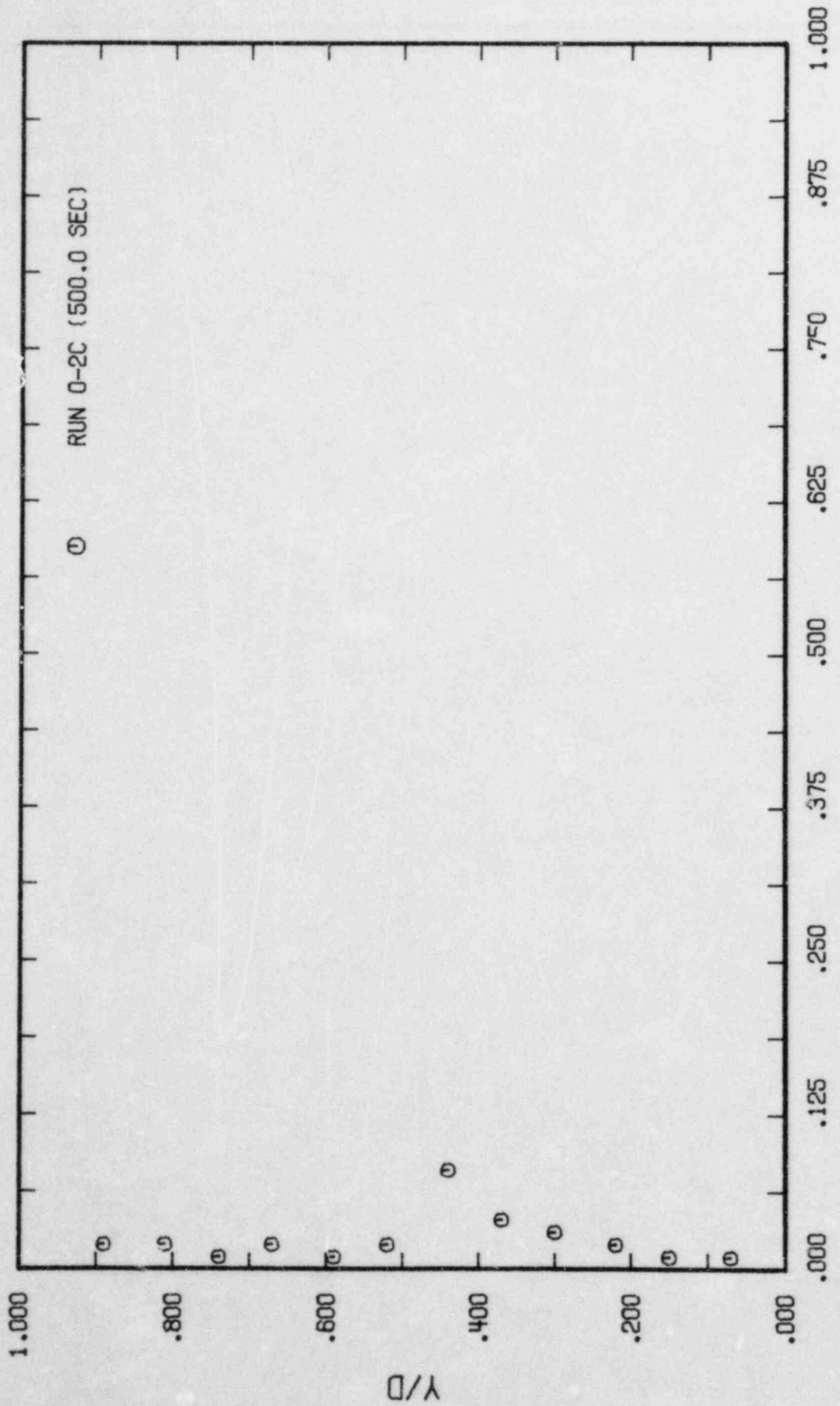
RUN 0-2C (500.0 SEC)
Y/D
1.000
.800
.600
.400
.200
.000
.000
.125
.250
.375
.500
.625
.750
.875
1.000
CONCENTRATION INTENSITY

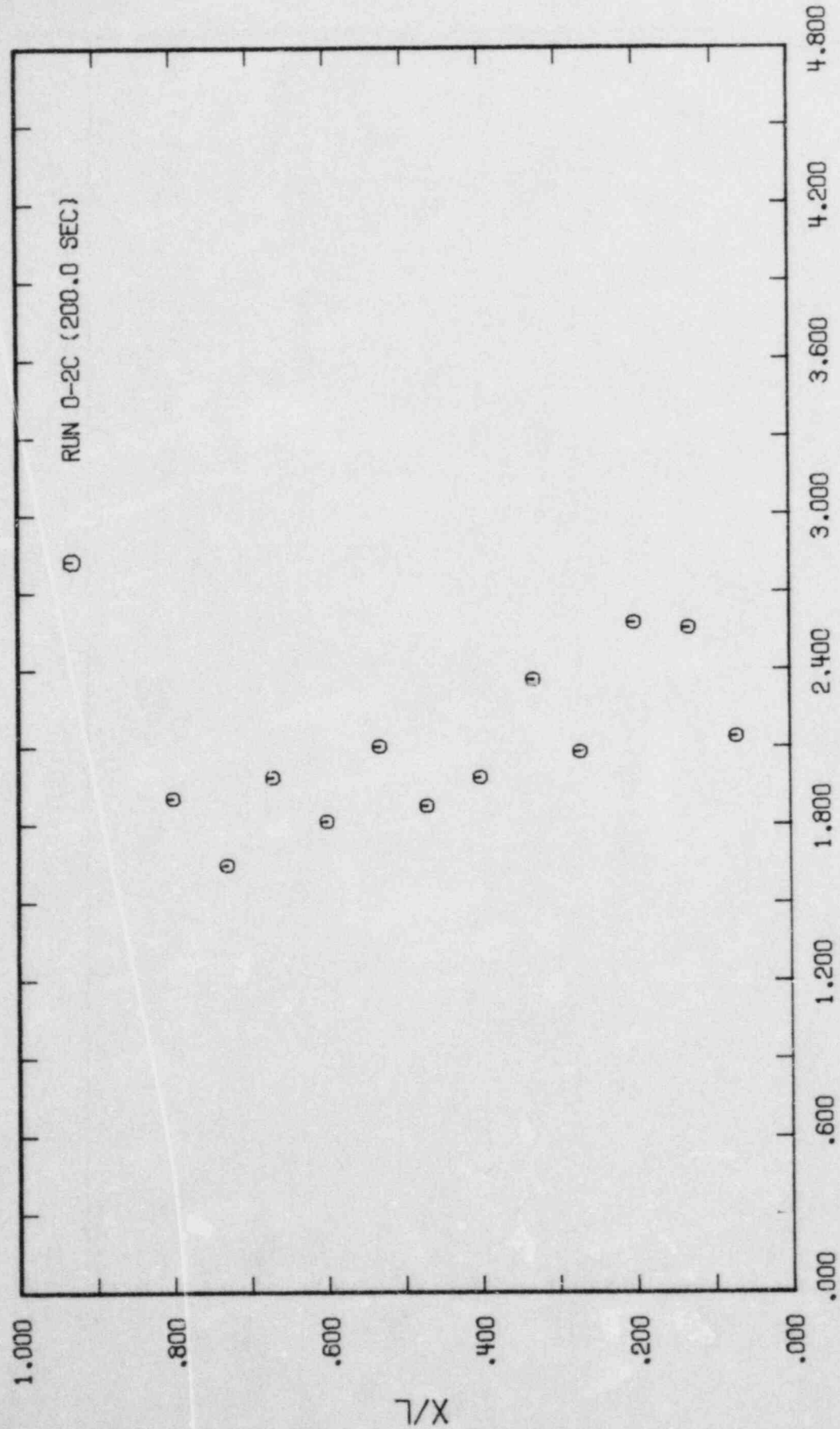
RUN 0-2C (200.0 SEC)
X/L
1.000
.800
.600
.400
.200
.000
.000
.600
1.200
1.800
2.400
3.000
3.600
4.200
4.800
CONCENTRATION (WT PERCENT)

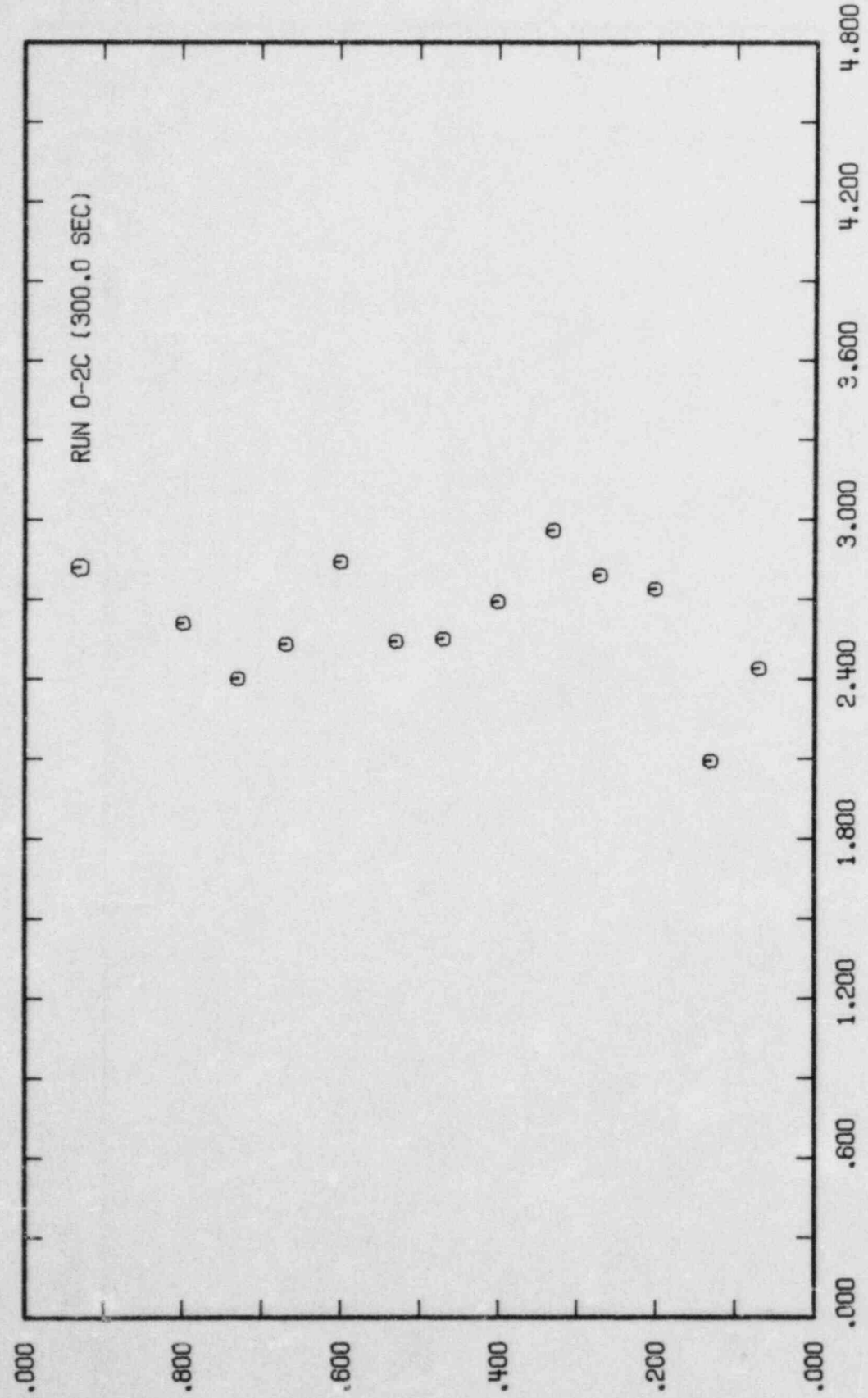
RUN 0-2C (300.0 SEC)
X/L
1.000
.800
.600
.400
.200
.000
.000
.600
1.200
1.800
2.400
3.000
3.600
4.200
4.800
CONCENTRATION (WT PERCENT)

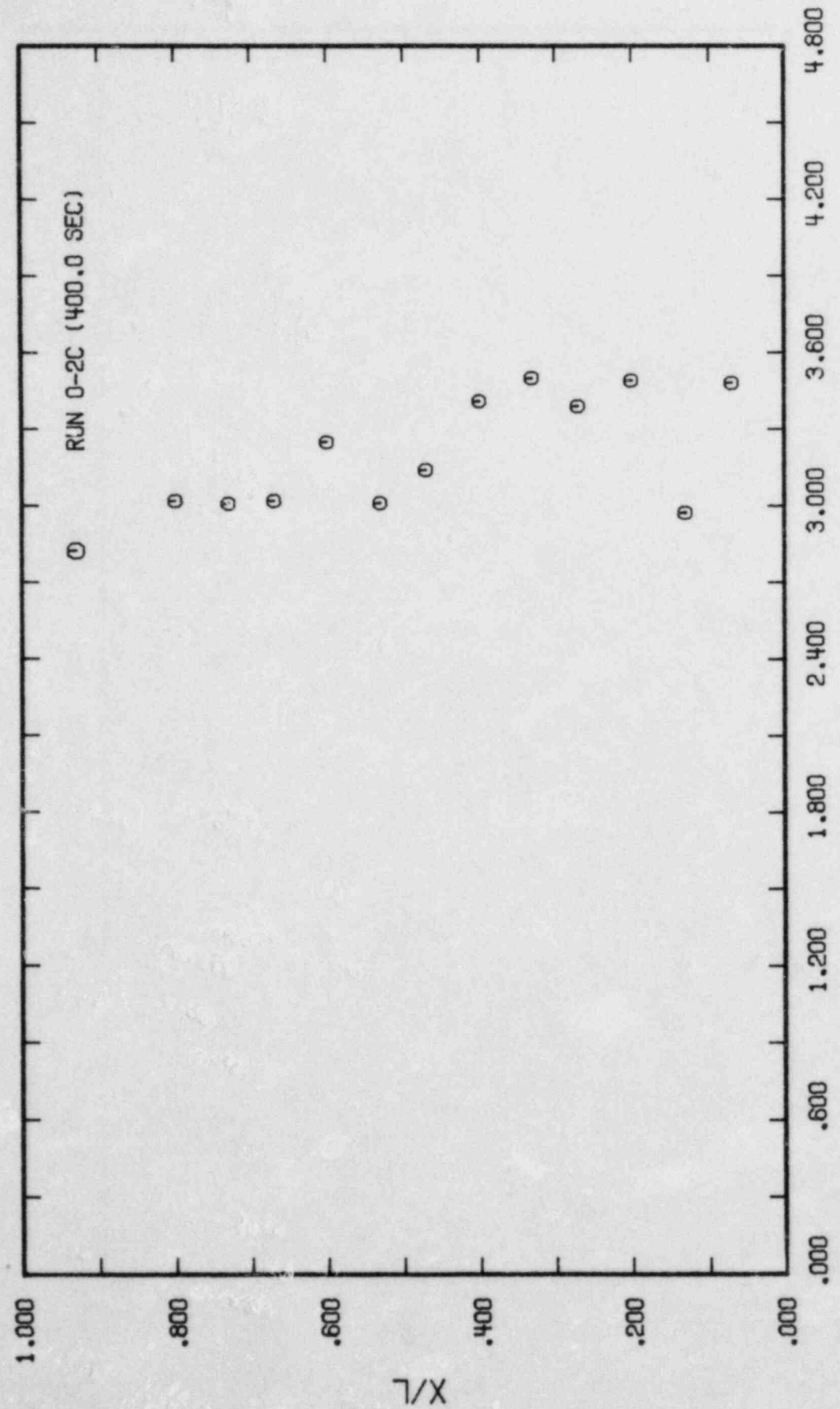
RUN 0-2C (400.0 SEC)
X/L
1.000
.800
.600
.400
.200
.000
.000
.600
1.200
1.800
2.400
3.000
3.600
4.200
4.800
CONCENTRATION (WT PERCENT)

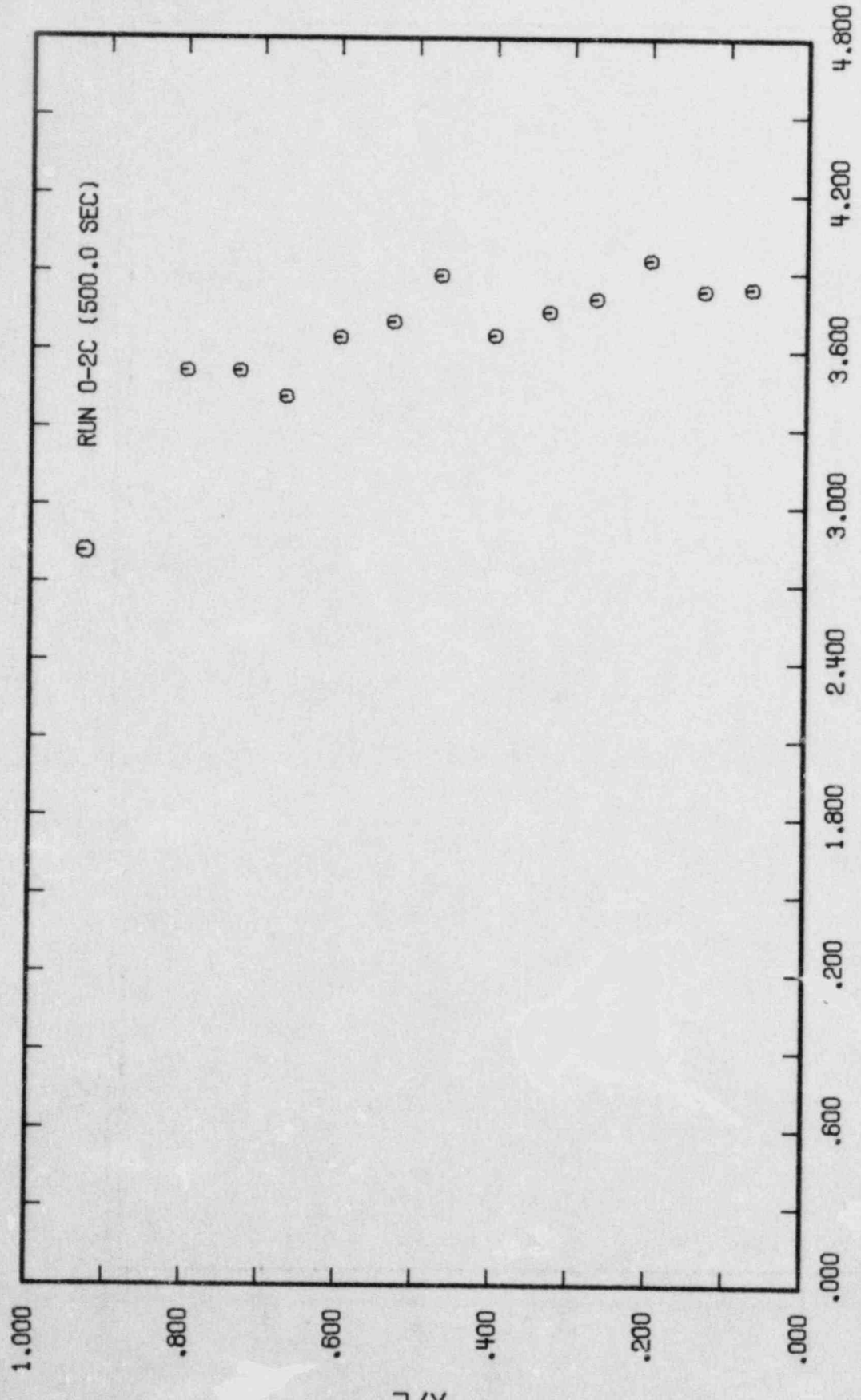
RUN 0-2C (500.0 SEC)
X/L
1.000
.800
.600
.400
.200
.000
.000
.600
.200
1.800
2.400
3.000
3.600
4.200
4.800
CONCENTRATION (WT PERCENT)

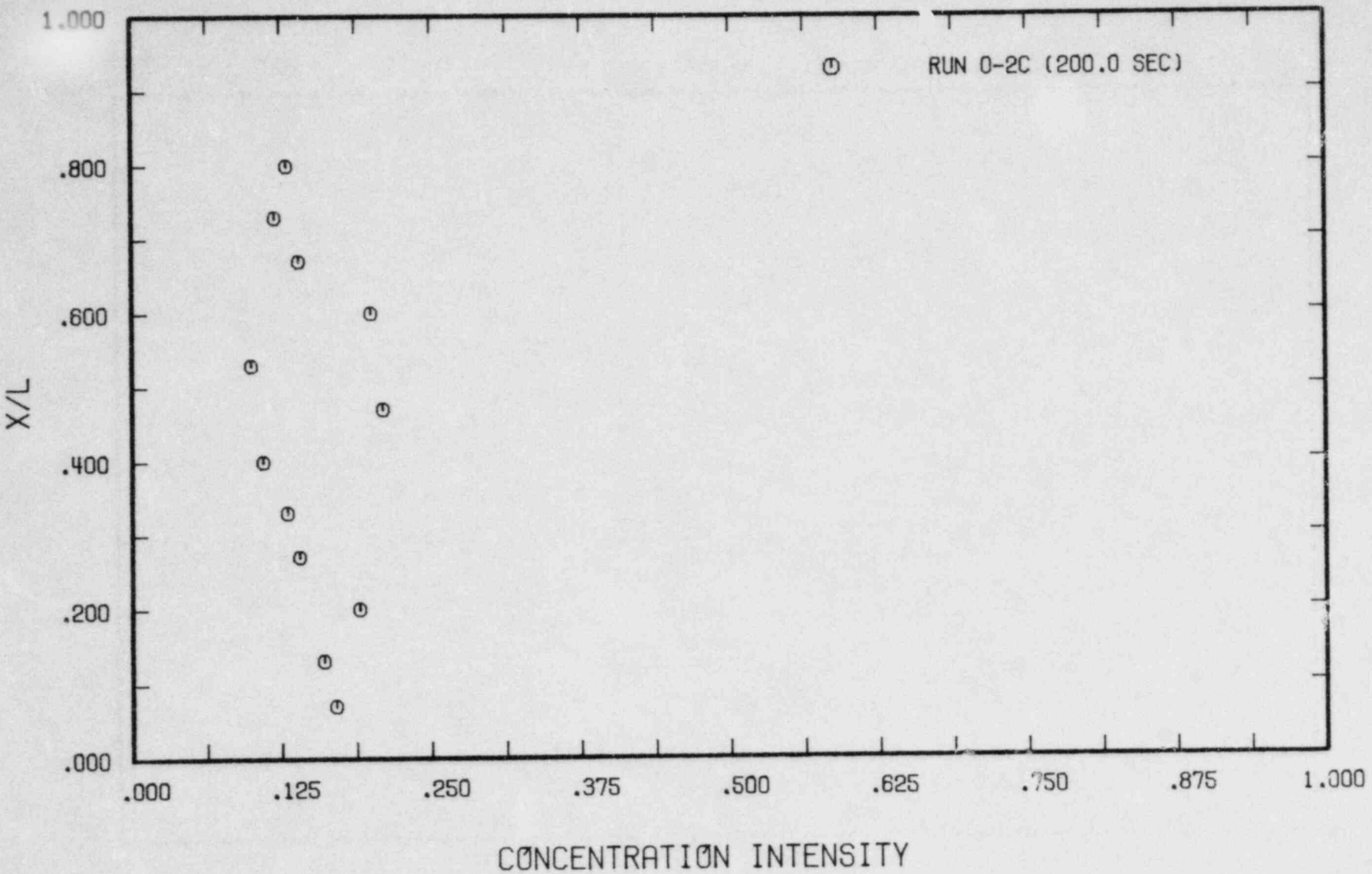
RUN 0-2C (200.0 SEC)
1.000
.800
.600
.400
.200
.000
X/L
.000
.125
.250
.375
.500
.625
.750
.875
1.000
CONCENTRATION INTENSITY

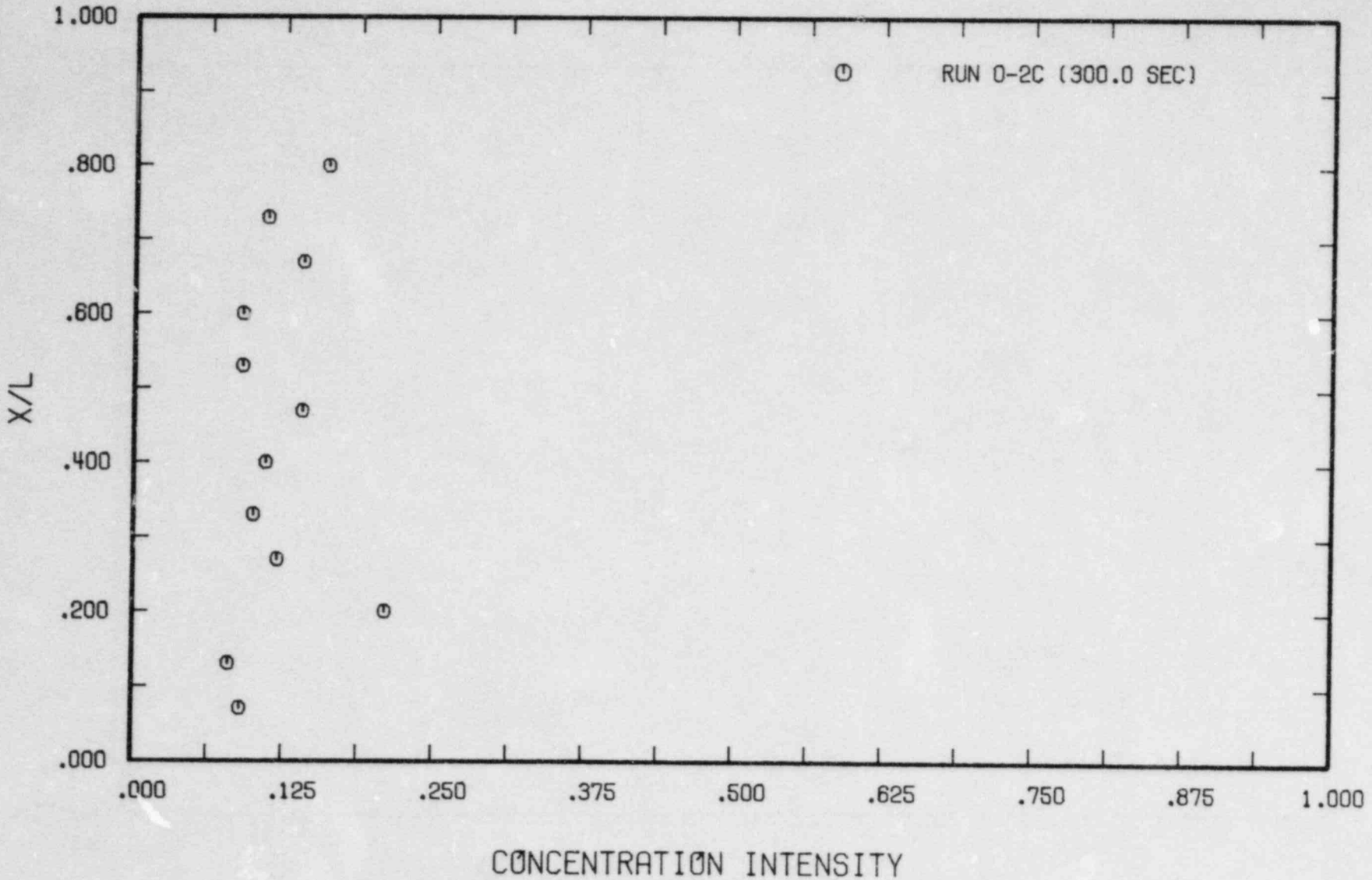
RUN 0-2C (300.0 SEC)
1.000
.800
.600
.400
.200
.000
X/L
.000
.125
.250
.375
.500
.625
.750
.875
1.000
CONCENTRATION INTENSITY

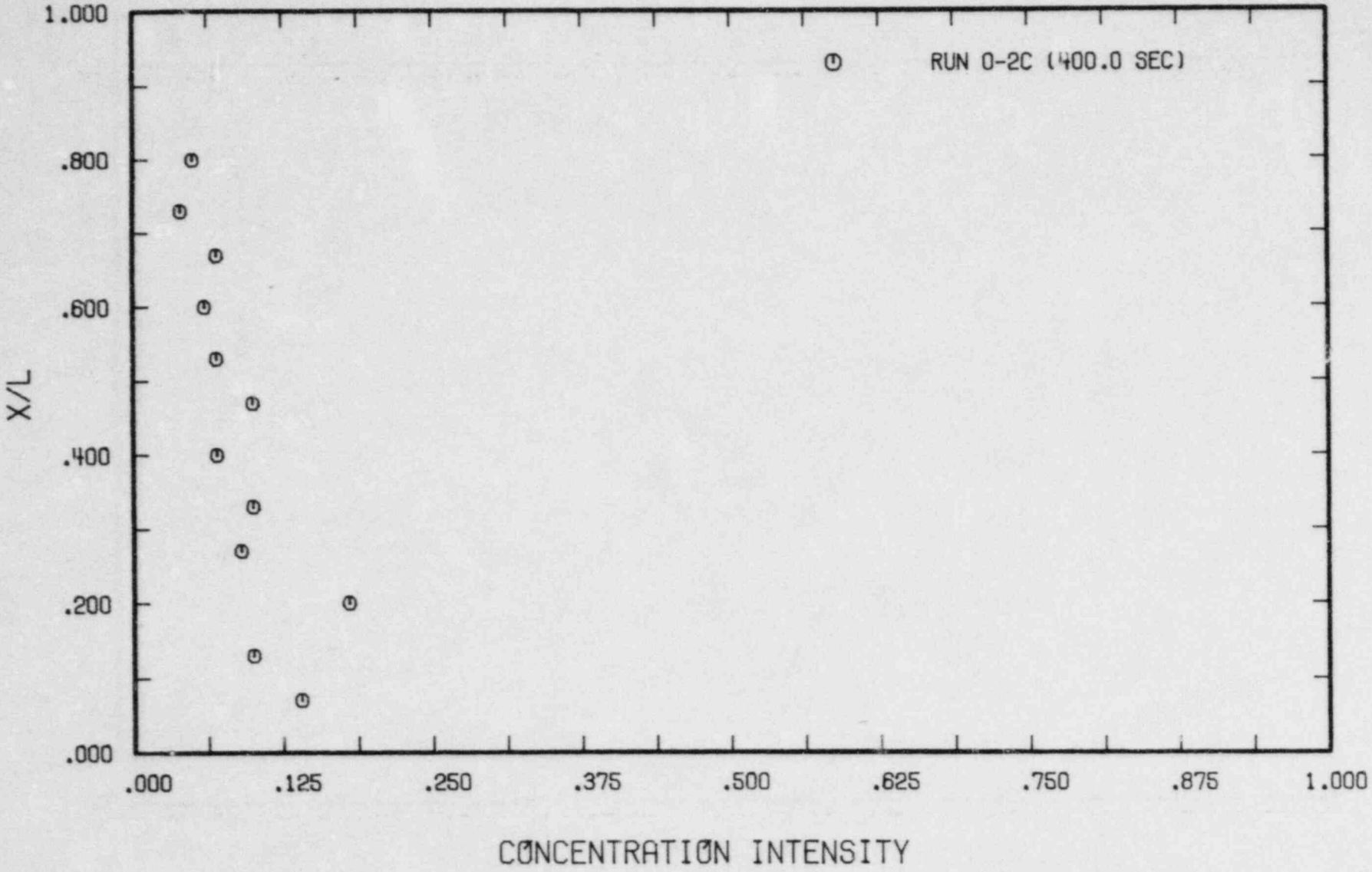
RUN 0-2C (400.0 SEC)
1.000
.800
.600
.400
.200
.000
X/L
.000
.125
.250
.375
.500
.625
.750
.875
1.000
CONCENTRATION INTENSITY

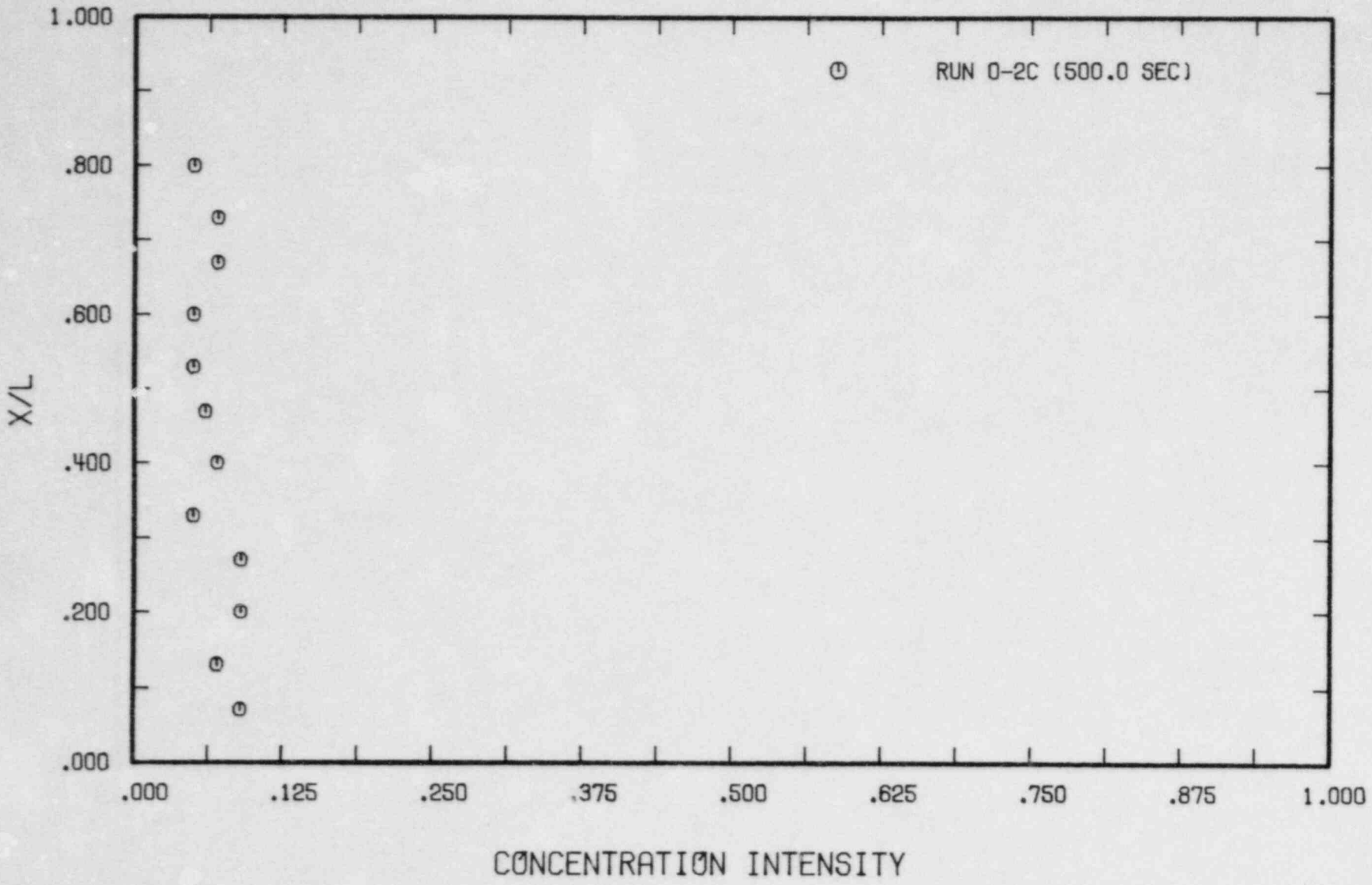
RUN 0-2C (500.0 SEC)
1.000
.800
.600
.400
.200
.000
X/L
.000
.125
.250
.375
.500
.625
.750
.875
1.000
CONCENTRATION INTENSITY

Run 0-2V

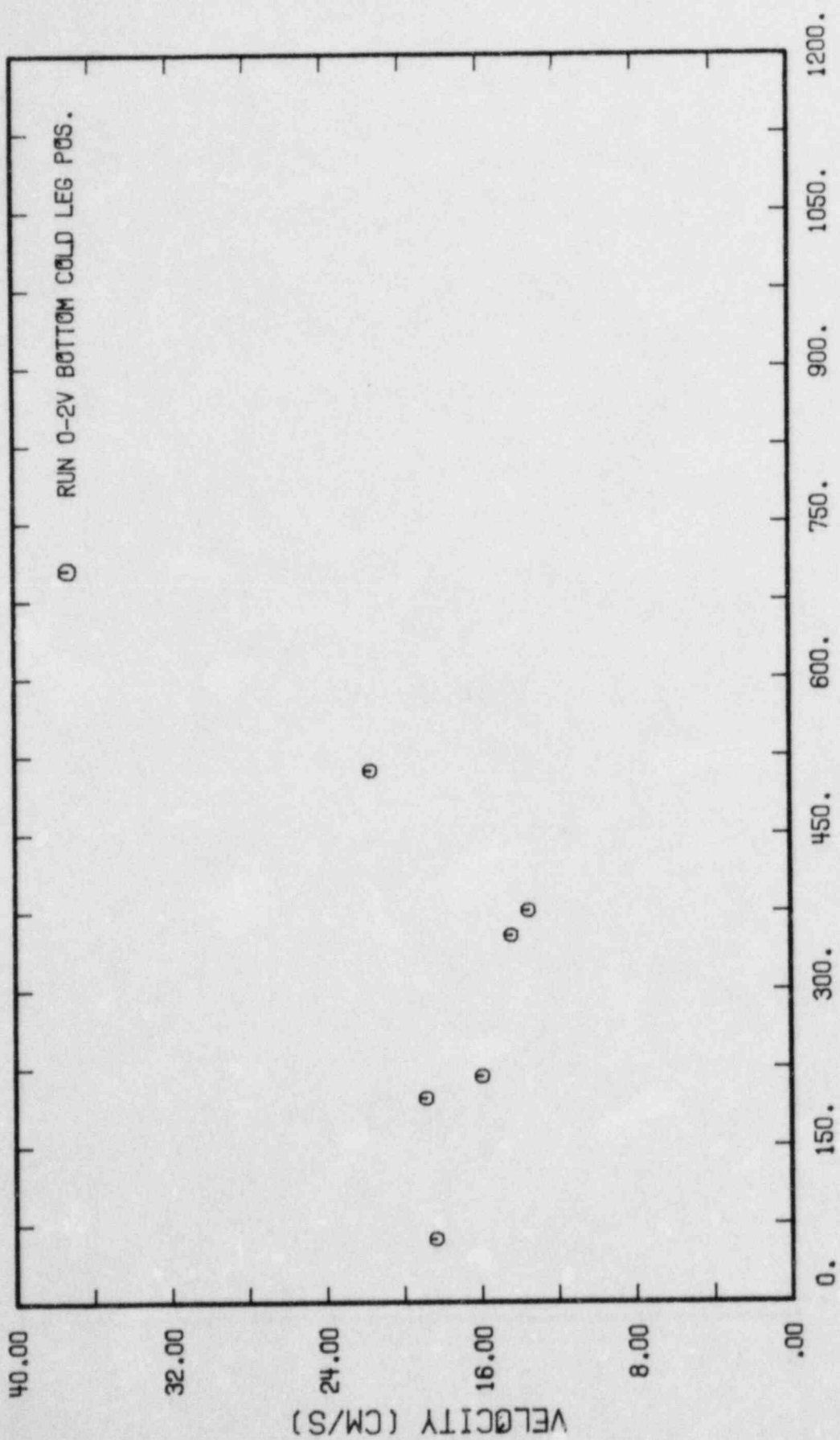
RUN 0-2V BOTTOM COLD LEG POS.
VELOCITY (CM/S)
40.00
32.00
24.00
16.00
8.00
.00
0.
150.
300.
450.
600.
750.
900.
1050.
1200.
TIME (SEC)

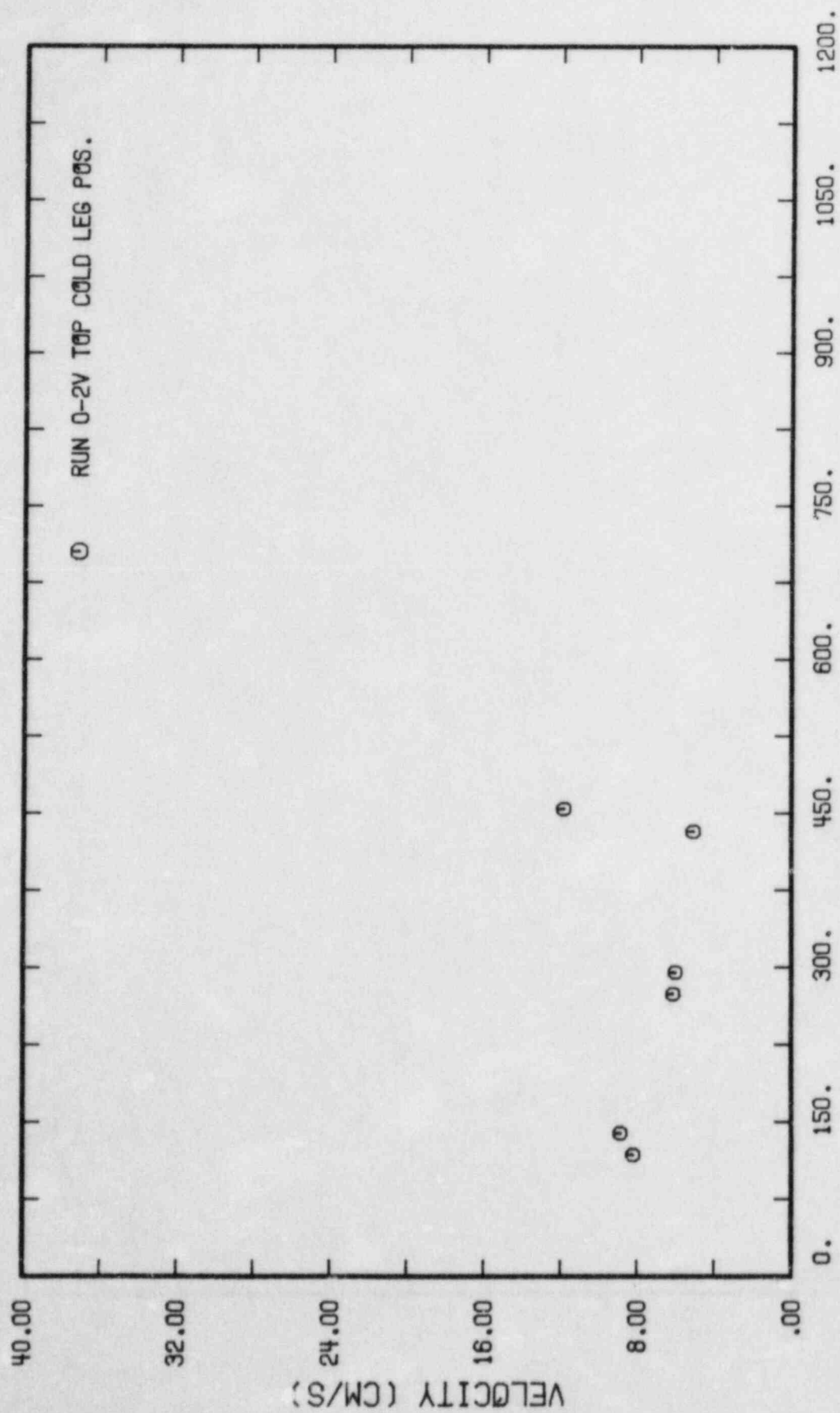
RUN 0-2V TOP COLD LEG POS.
VELOCITY (CM/S)
40.00
32.00
24.00
16.00
8.00
.00
0.
150.
300.
450.
600.
750.
900.
1050.
1200.
TIME (SEC)

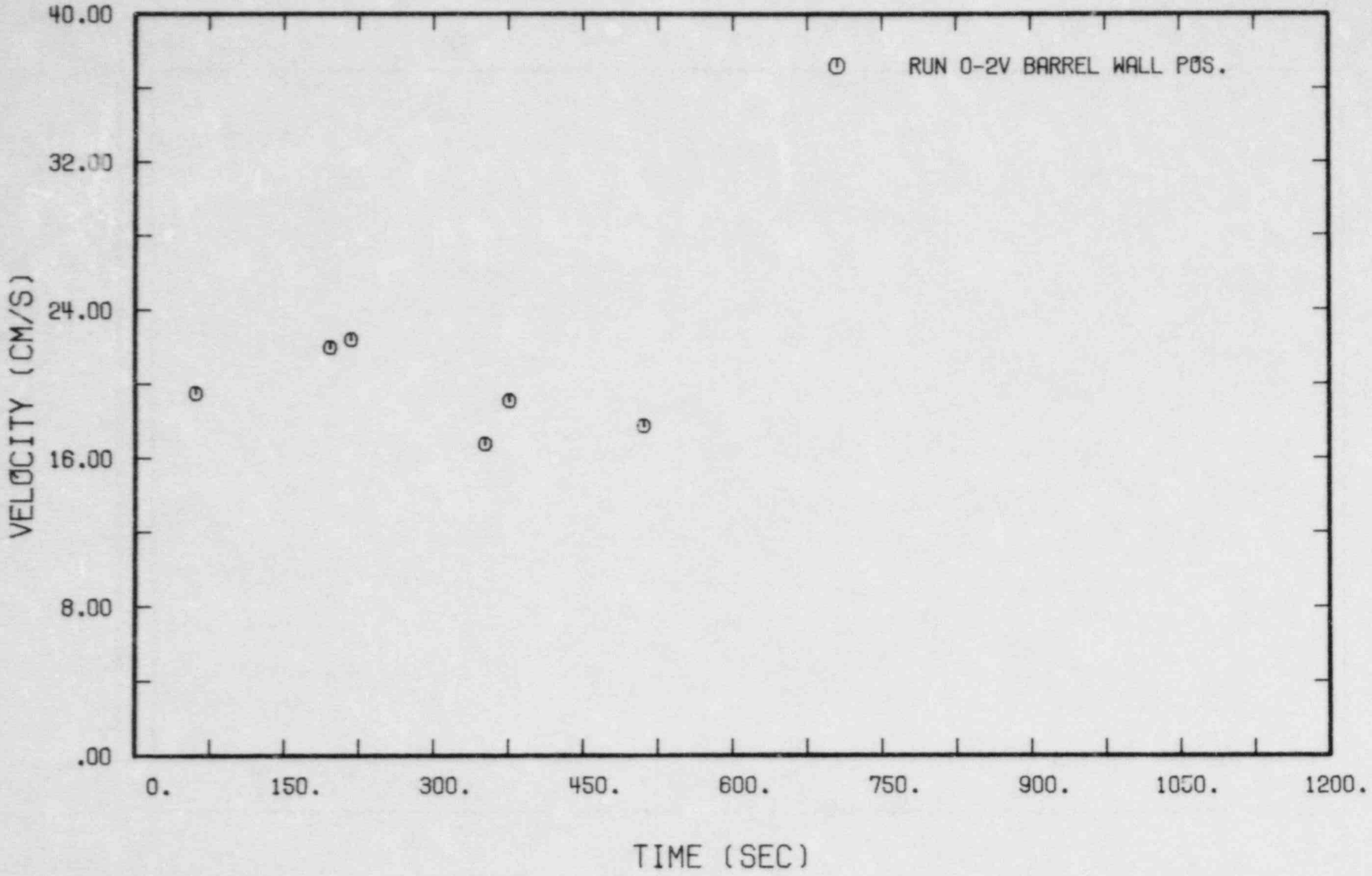
RUN 0-2V BARREL WALL POS.
VELOCITY (CM/S)
40.00
32.00
24.00
16.00
8.00
.00
0.
150.
300.
450.
600.
750.
900.
1050.
1200.
TIME (SEC)

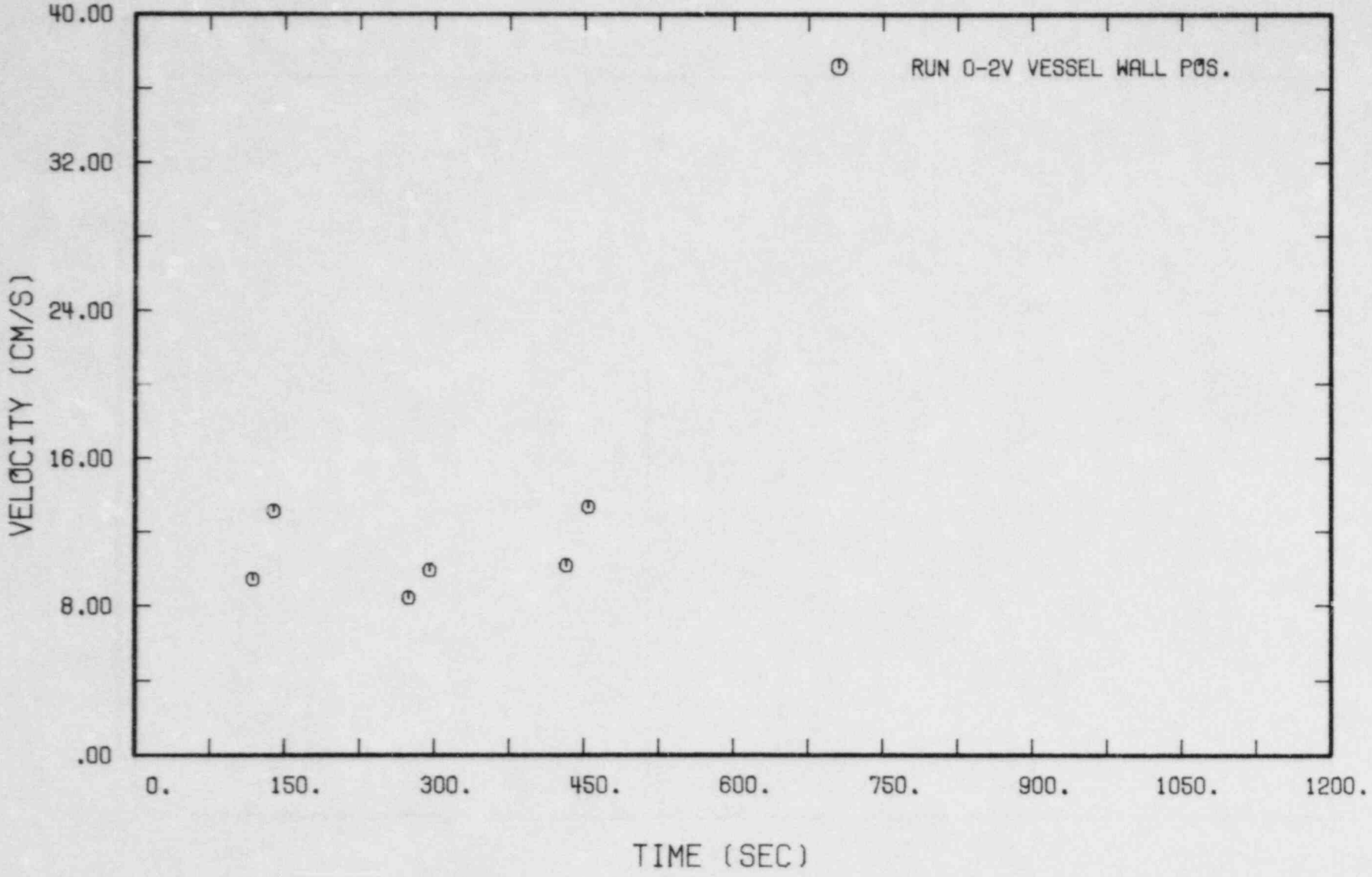
RUN 0-2V VESSEL WALL POS.
VELOCITY (CM/S)
40.00
32.00
24.00
16.00
8.00
.00
0.
150.
300.
450.
600.
750.
900.
1050.
1200.
TIME (SEC)

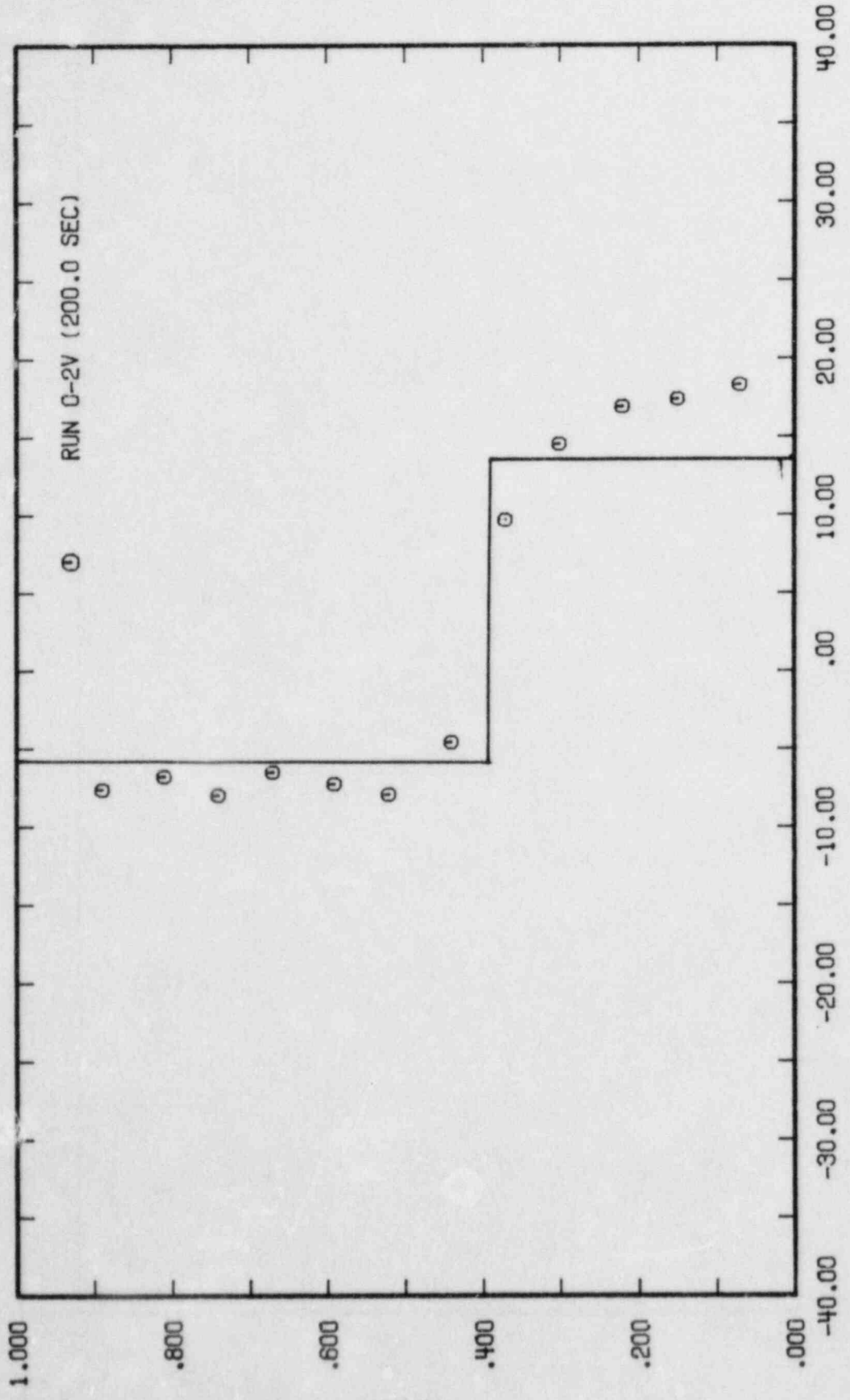
RUN 0-2V (200.0 SEC)
1.000
.800
.600
.400
.200
.000
Y/D
-40.00
-30.00
-20.00
-10.00
.00
10.00
20.00
30.00
40.00
VELOCITY (CM/S)

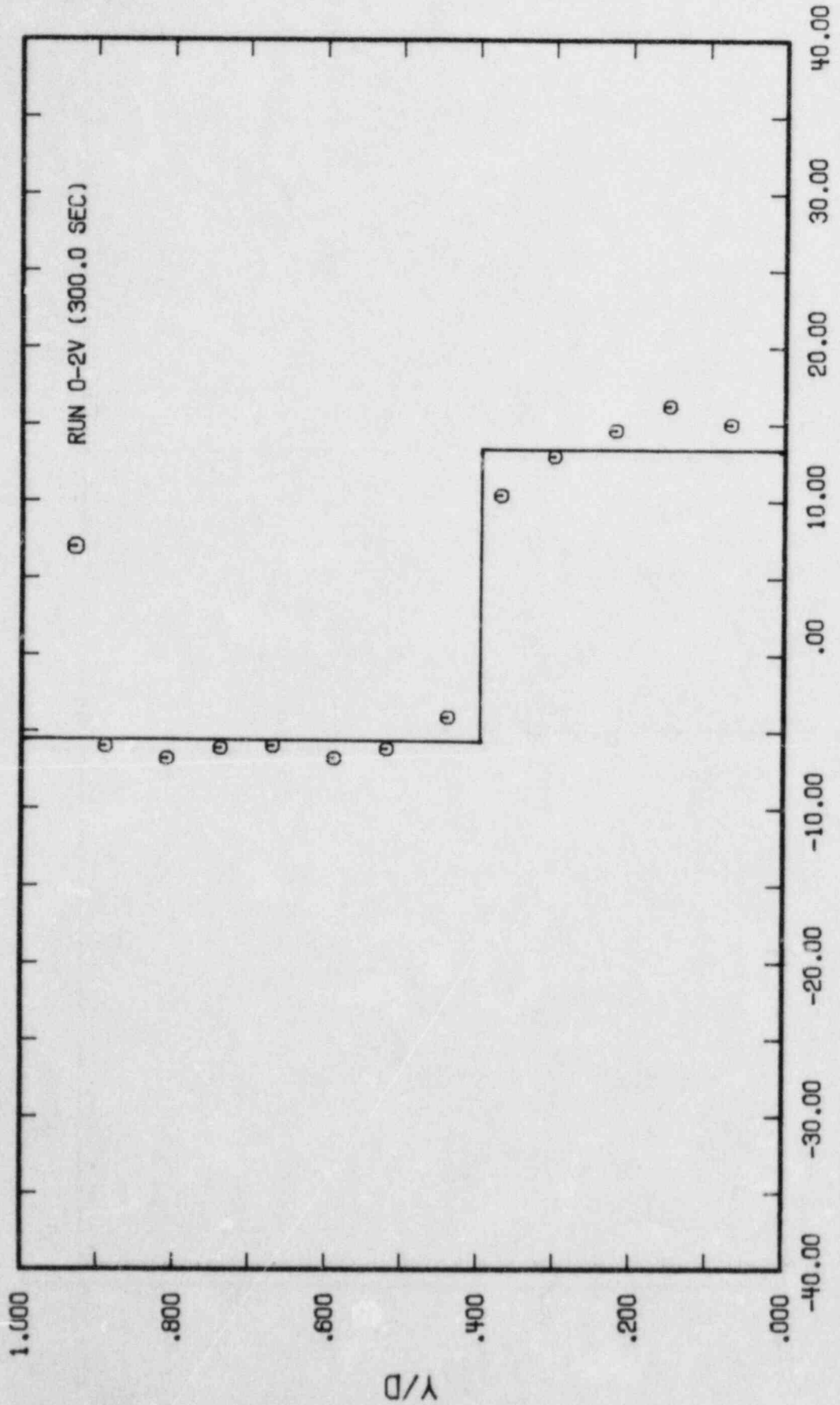
RUN 0-2V (300.0 SEC)
1.000
.800
.600
.400
.200
.000
Y/D
-40.00
-30.00
-20.00
-10.00
.00
10.00
20.00
30.00
40.00
VELOCITY (CM/S)

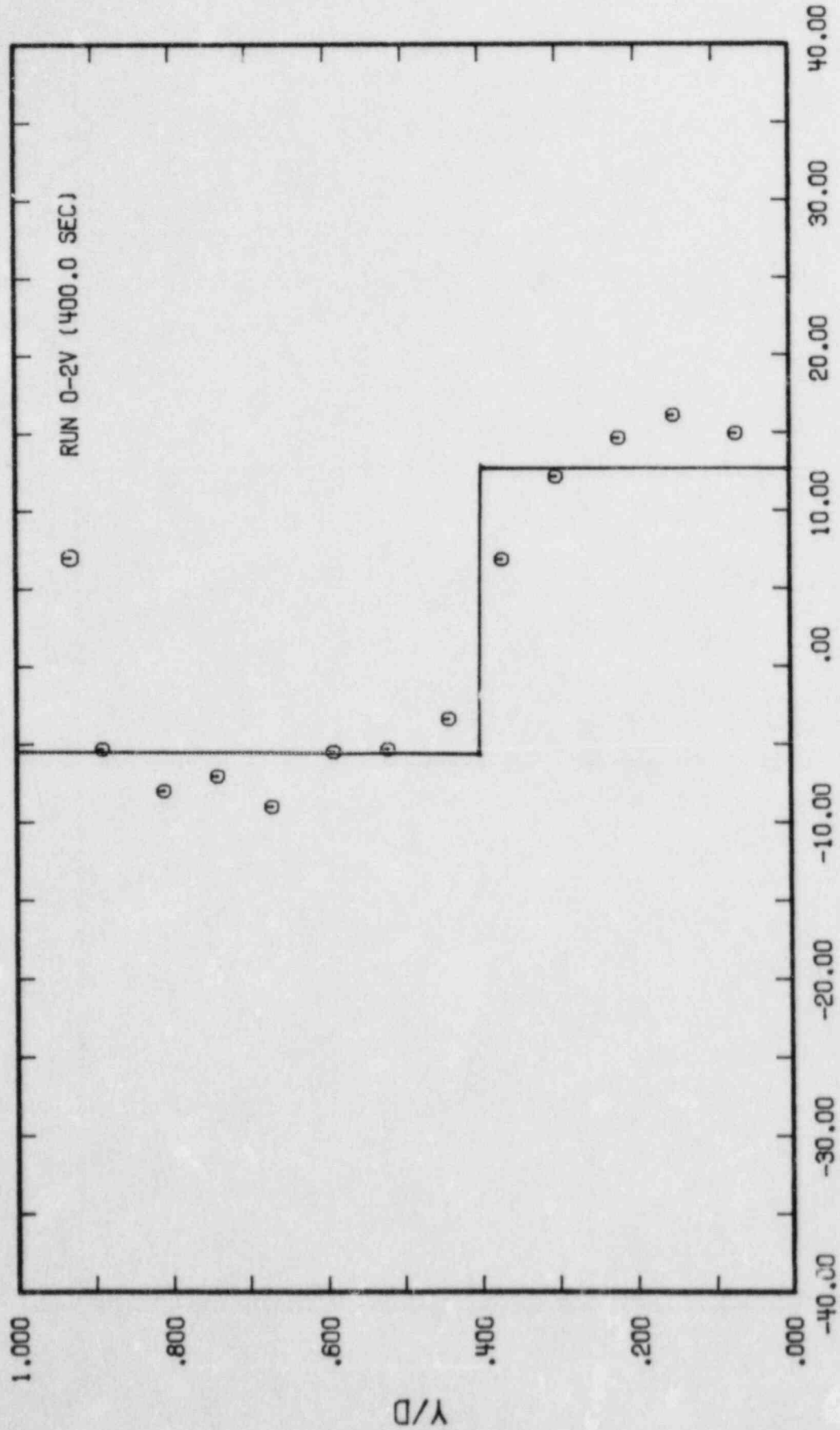
RUN 0-2V (400.0 SEC)
1.000
.800
.600
.400
.200
.000
Y/D
-40.00
-30.00
-20.00
-10.00
.00
10.00
20.00
30.00
40.00
VELOCITY (CM/S)

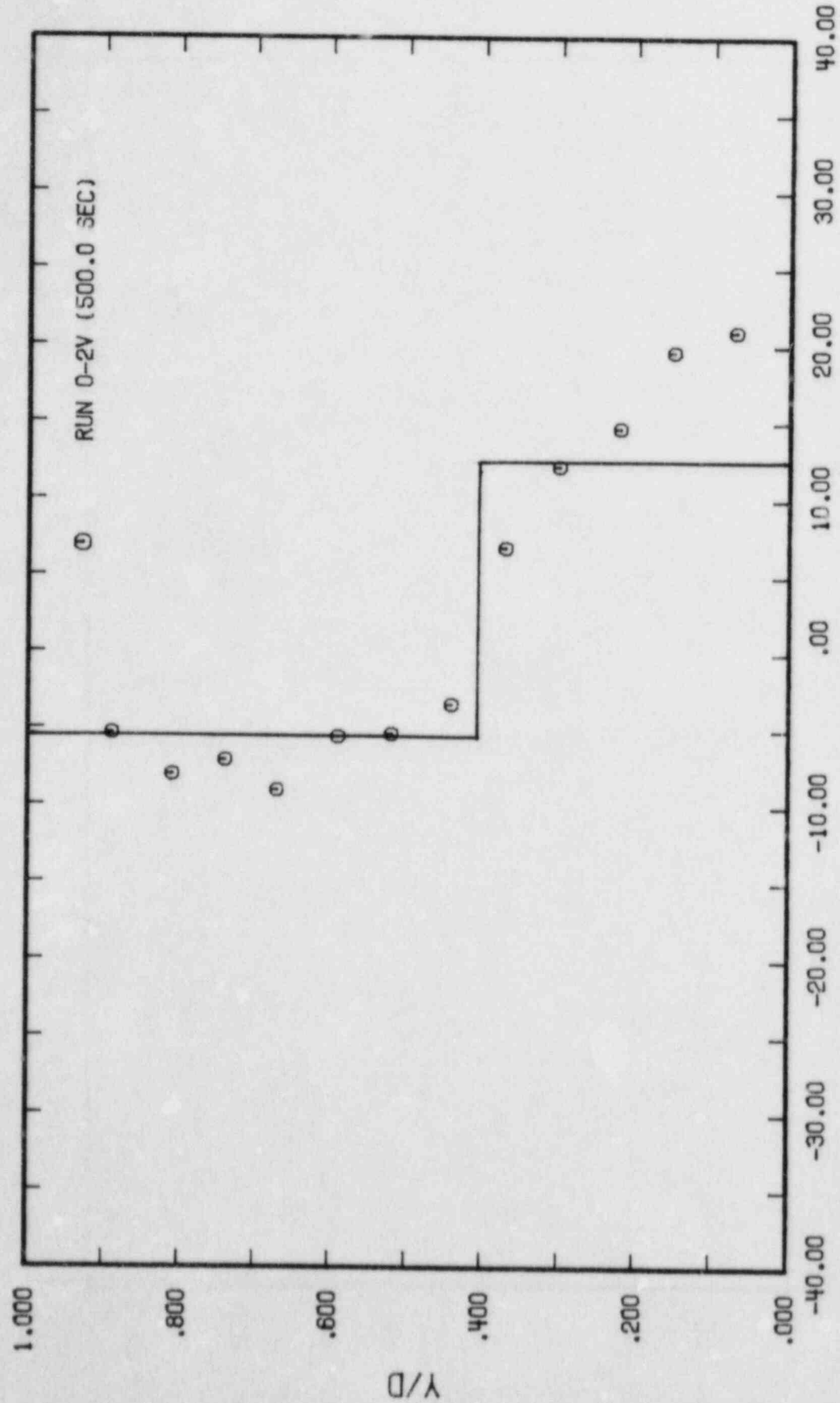
RUN 0-2V (500.0 SEC)
Y/D
1.000
.800
.600
.400
.200
.000
-40.00
-30.00
-20.00
-10.00
.00
10.00
20.00
30.00
40.00
VELOCITY (CM/S)

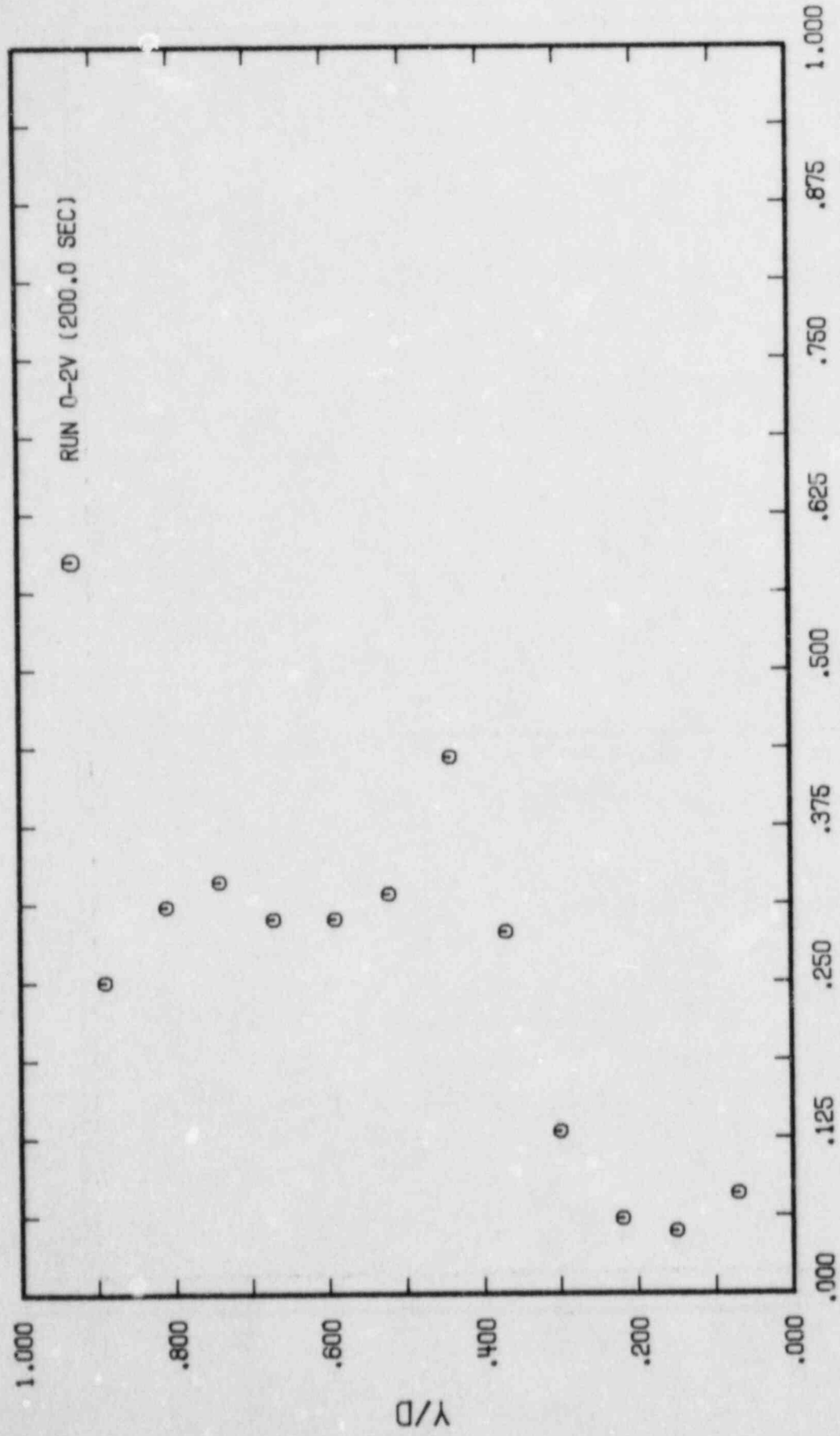
RUN 0-2V (200.0 SEC)
Y/D
VELOCITY INTENSITY
1.000
.800
.600
.400
.200
.000
.000
.125
.250
.375
.500
.625
.750
.875
1.000

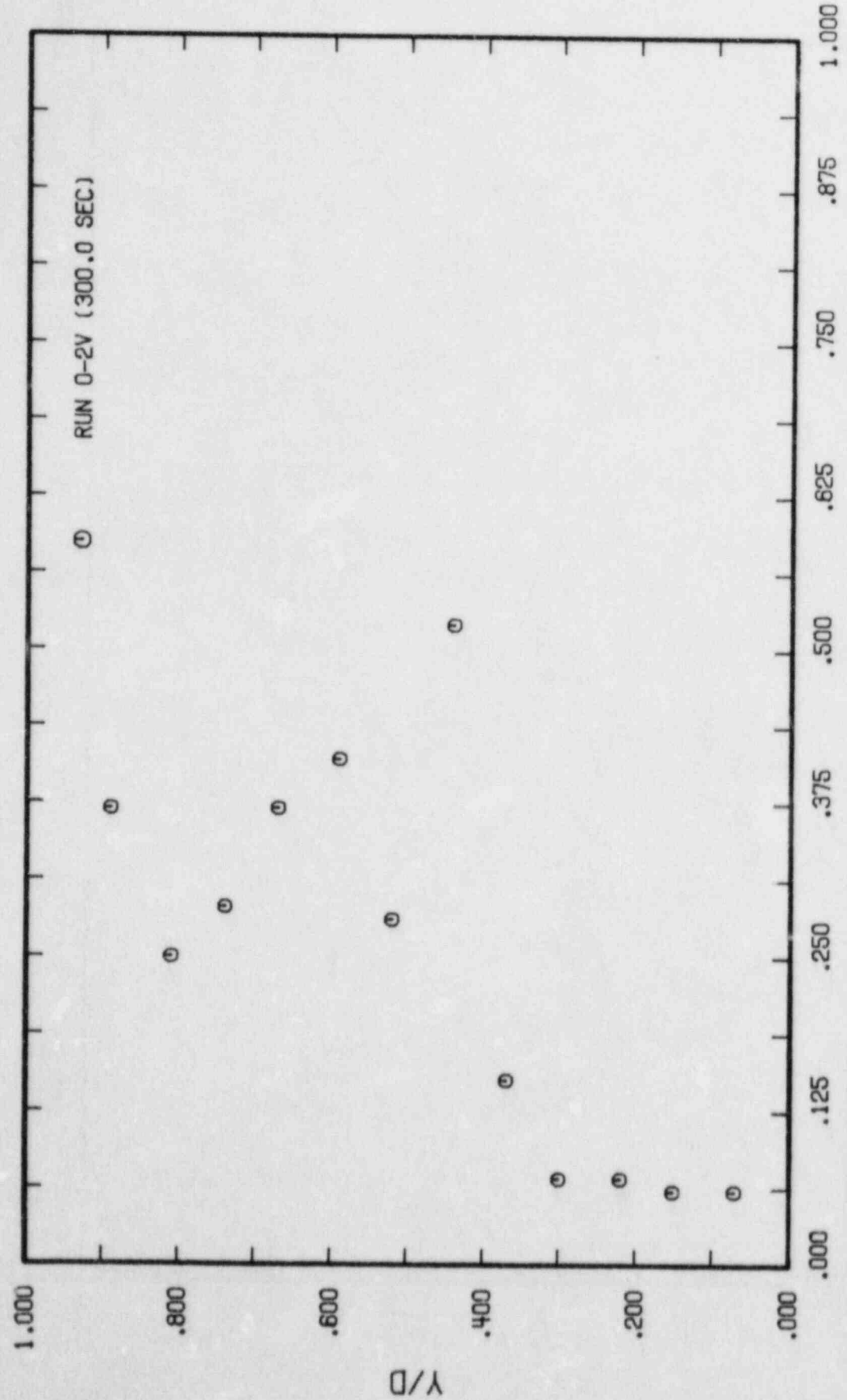
RUN 0-2V (300.0 SEC)
Y/D
1.000
.800
.600
.400
.200
.000
.000
.125
.250
.375
.500
.625
.750
.875
1.000
VELOCITY INTENSITY

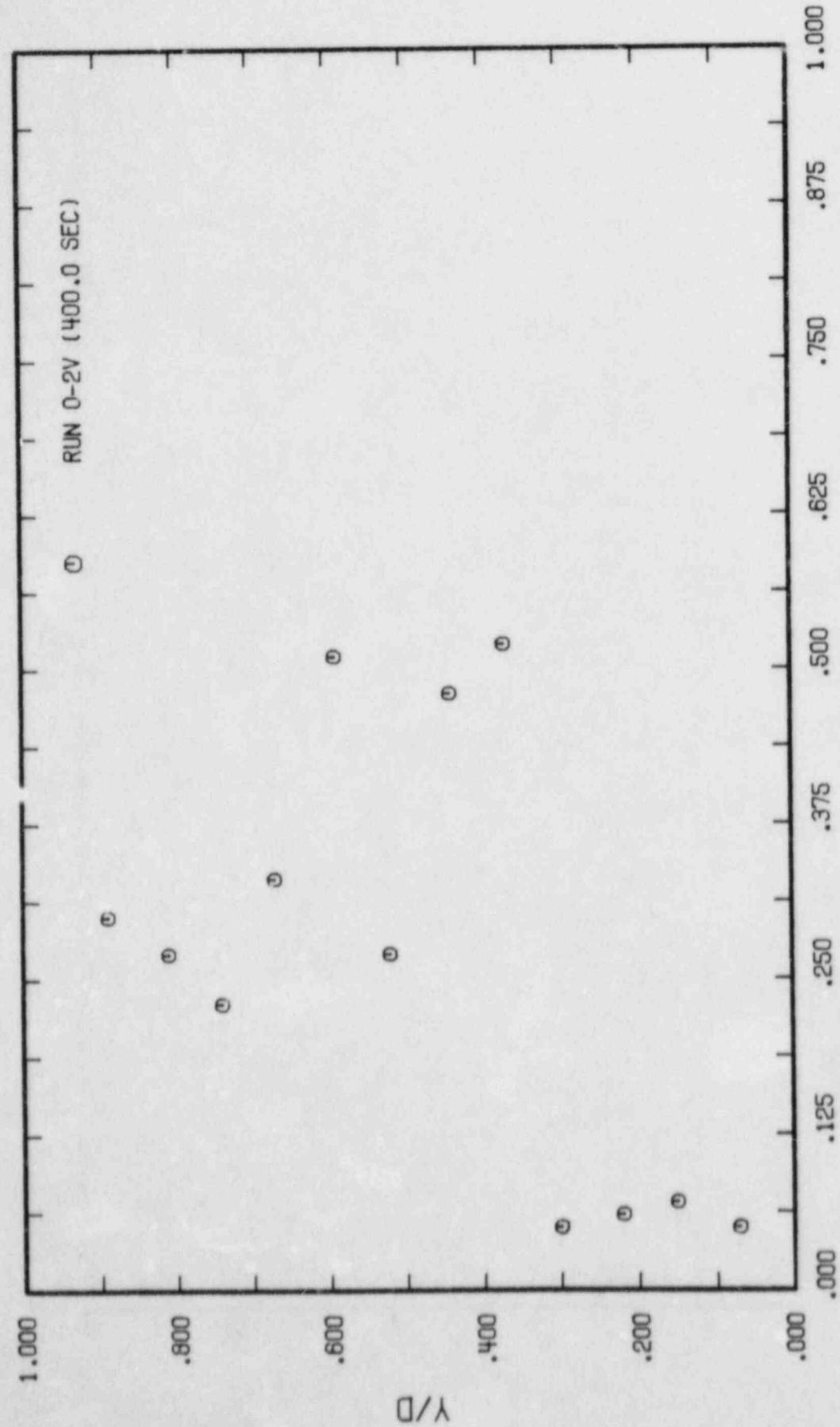
RUN 0-2V (400.0 SEC)
Y/D
VELOCITY INTENSITY
1.000
.800
.600
.400
.200
.000
.000
.125
.250
.375
.500
.625
.750
.875
1.000

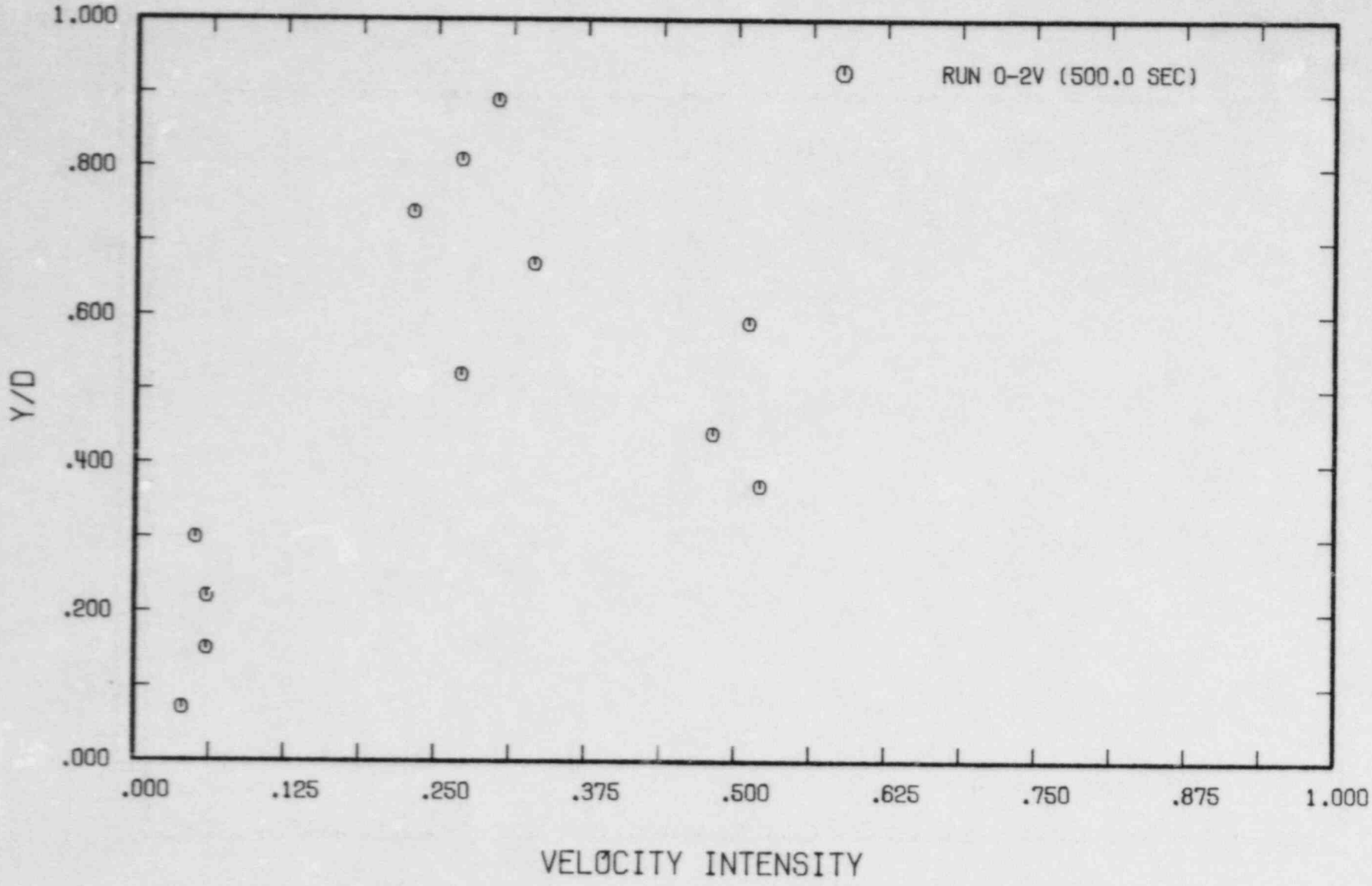
RUN 0-2V (500.0 SEC)
1.000
.800
.600
.400
.200
.000
Y/D
.000
.125
.250
.375
.500
.625
.750
.875
1.000
VELOCITY INTENSITY

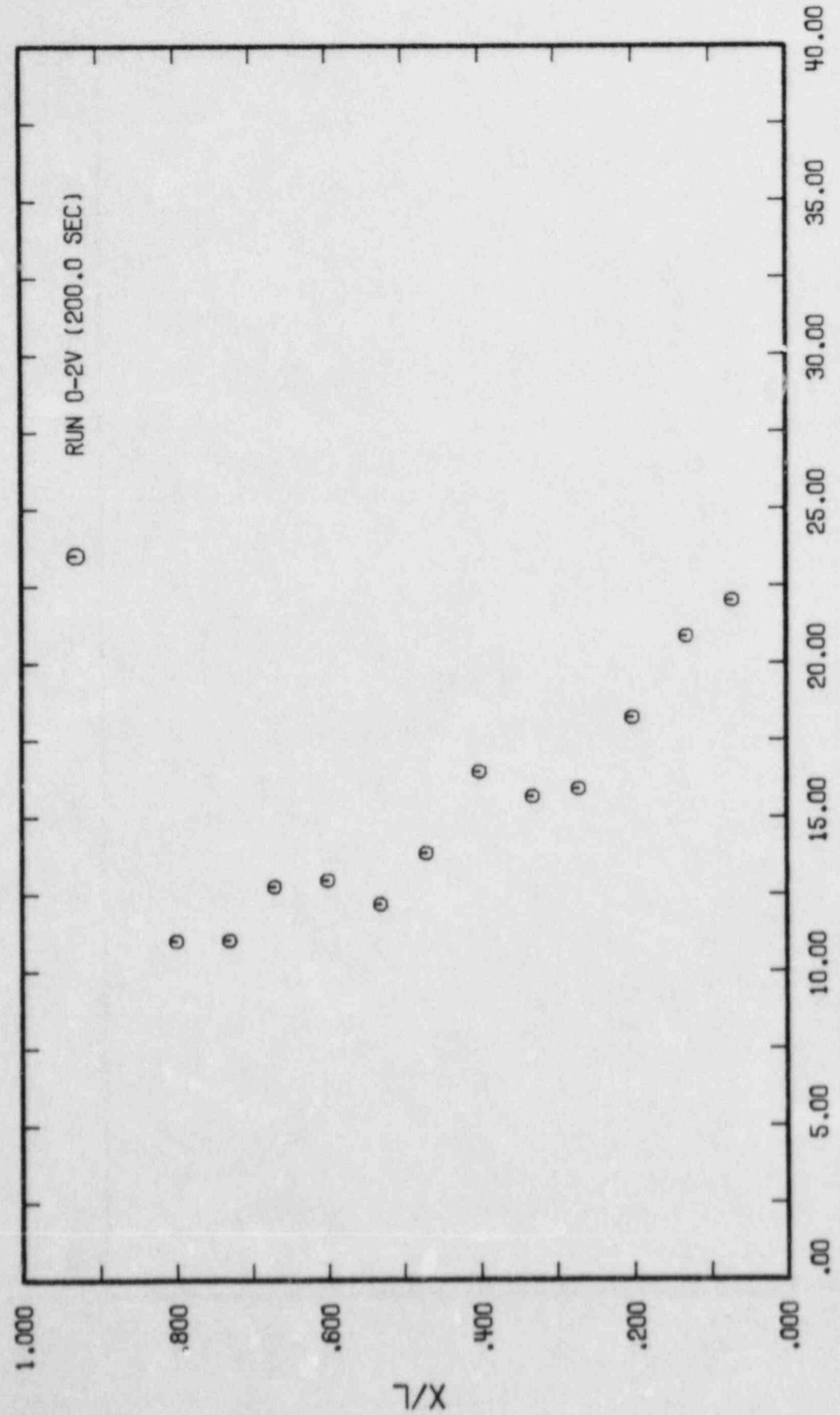
RUN 0-2V (200.0 SEC)
1.000
.800
.600
.400
.200
.000
X/L
.00
5.00
10.00
15.00
20.00
25.00
30.00
35.00
40.00
VELOCITY (CM/S)

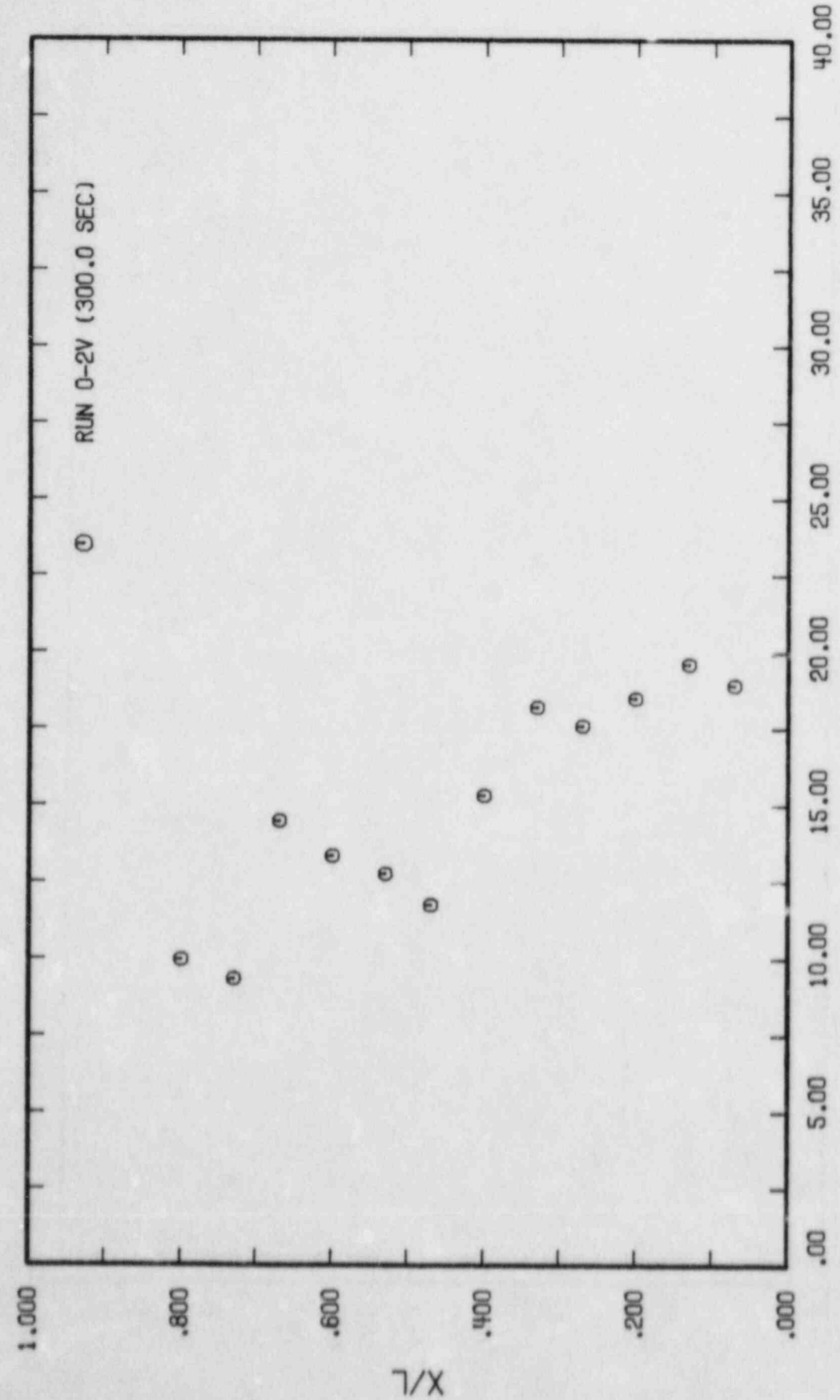
RUN 0-2V (300.0 SEC)
1
X/L
1.000
.800
.600
.400
.200
.000
.00
5.00
10.00
15.00
20.00
25.00
30.00
35.00
40.00
VELOCITY (CM/S)

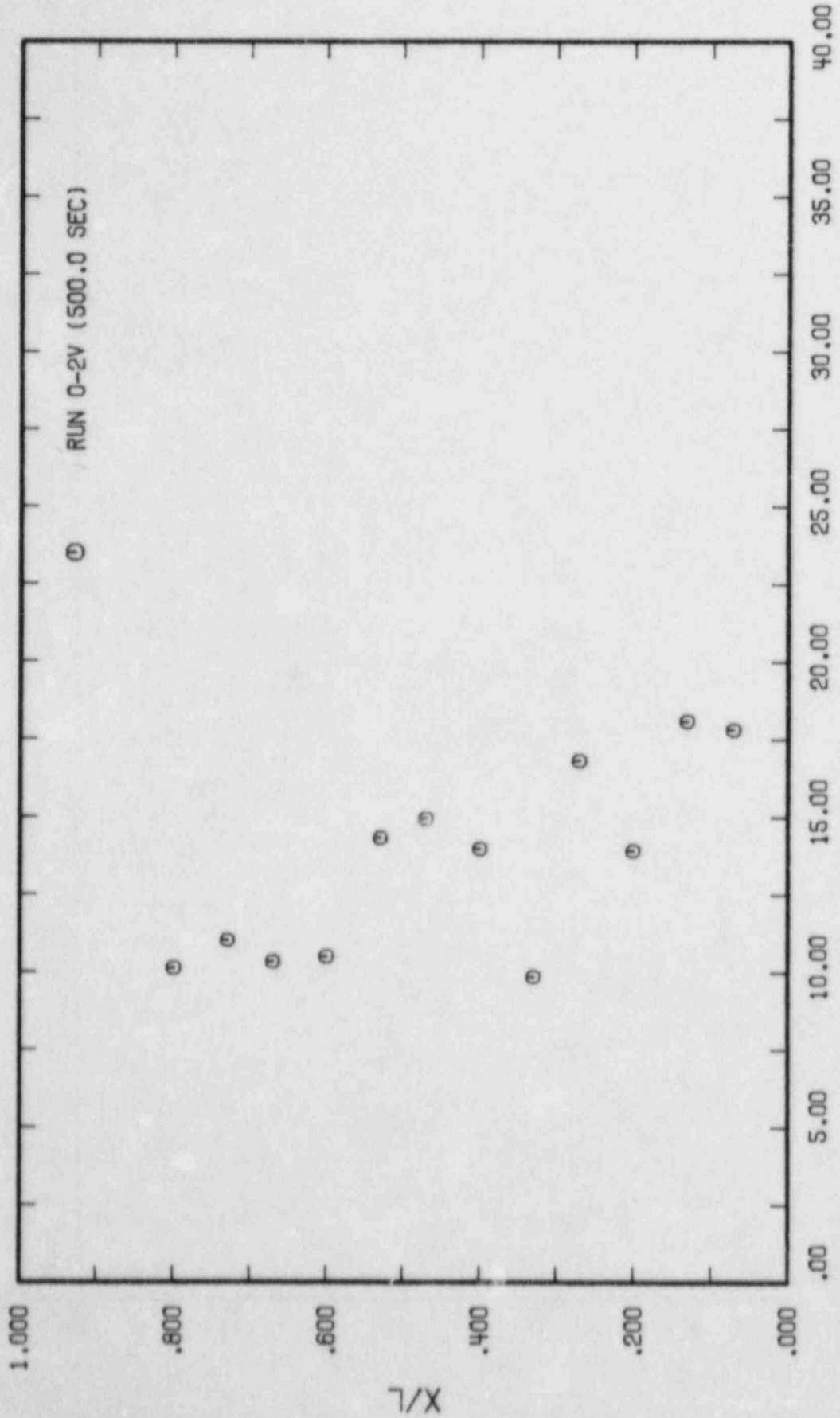
RUN 0-2V (500.0 SEC)
X/L
1.000
.800
.600
.400
.200
.000
.00
5.00
10.00
15.00
20.00
25.00
30.00
35.00
40.00
VELOCITY (CM/S)

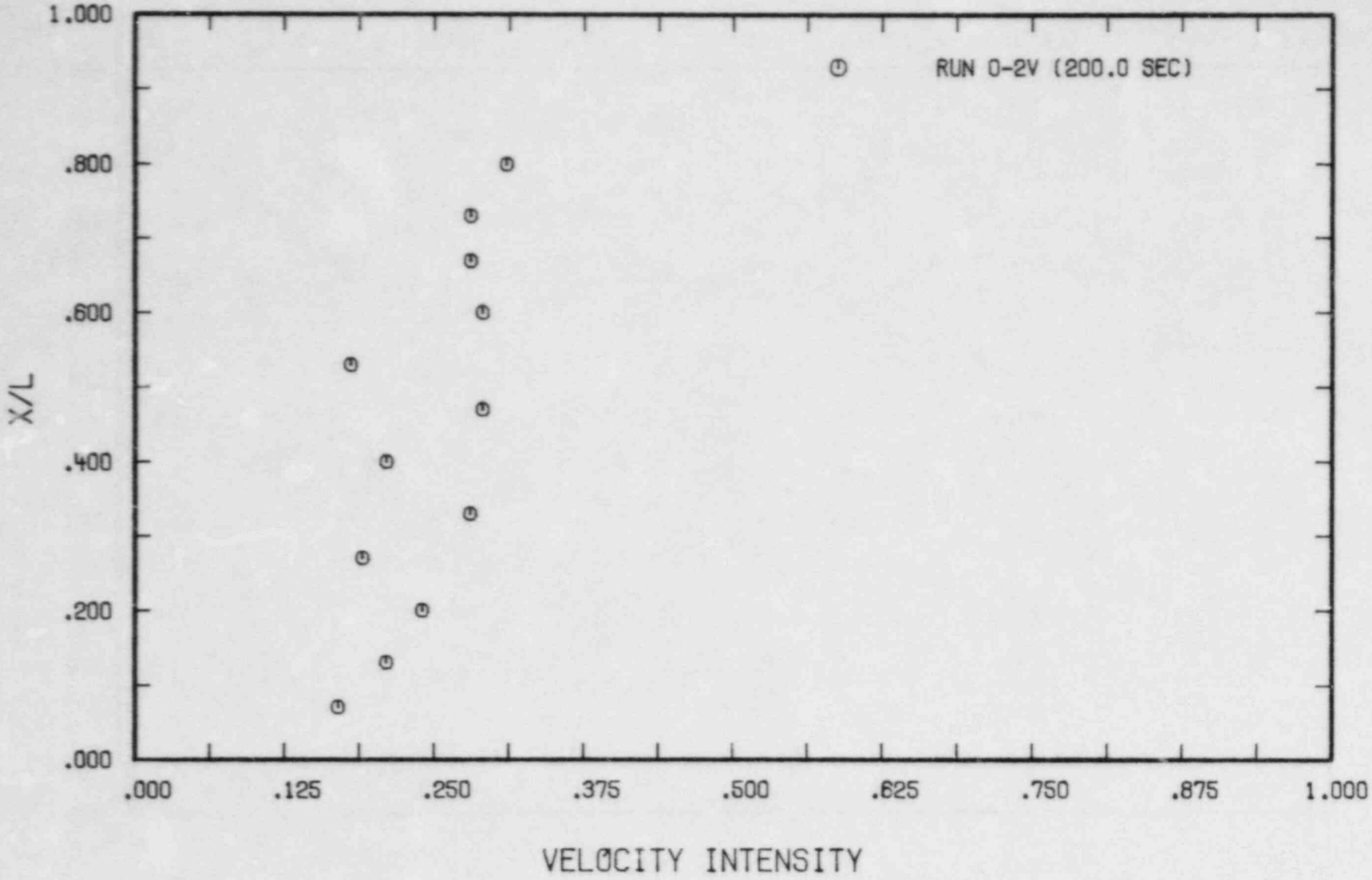
RUN 0-2V (200.0 SEC)
1.000
.800
.600
.400
.200
.000
X/L
.000
.125
.250
.375
.500
.625
.750
.875
1.000
VELOCITY INTENSITY

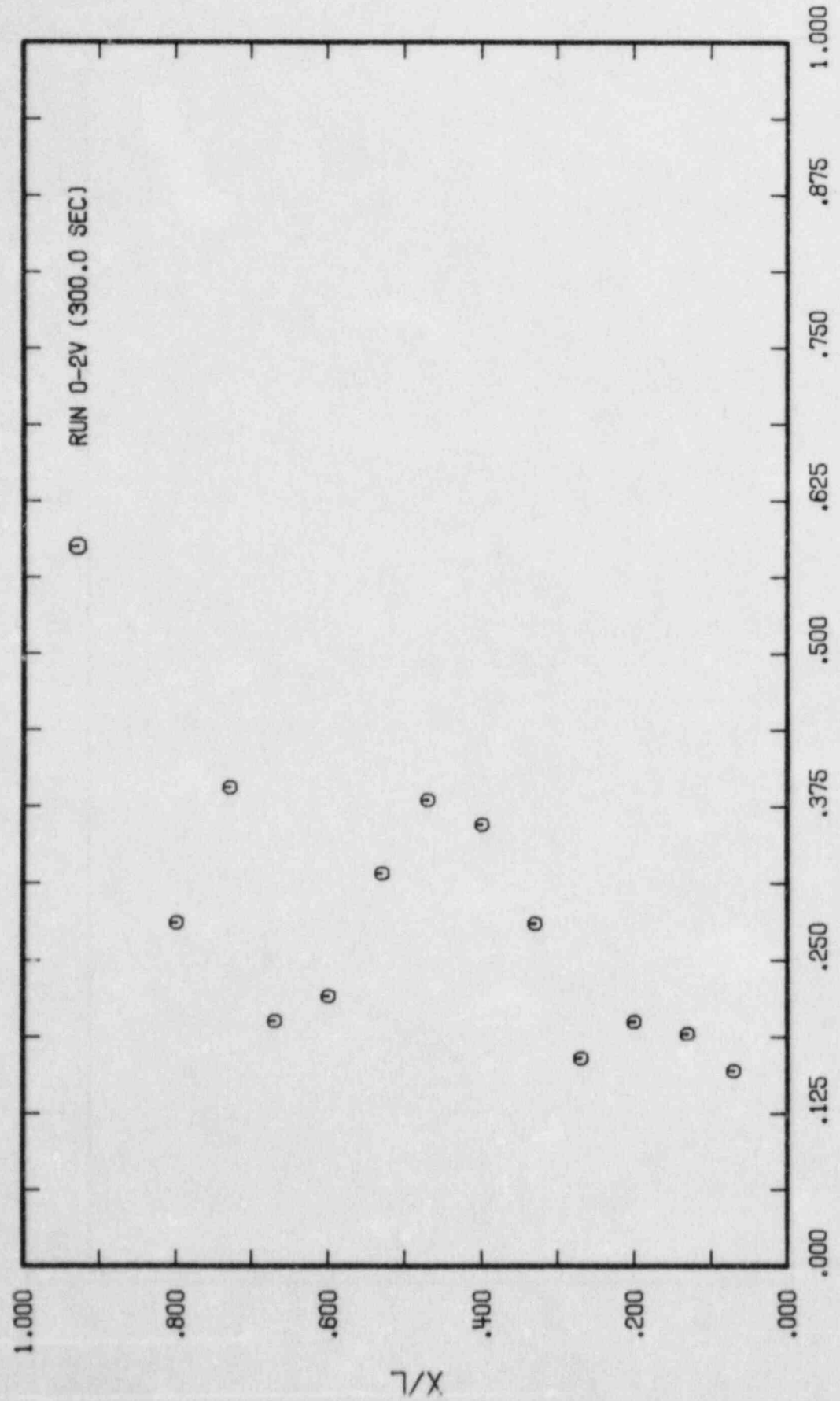
RUN 0-2V (300.0 SEC)
1.000
.800
.600
.400
.200
.000
X/L
.000
.125
.250
.375
.500
.625
.750
.875
1.000
VELOCITY INTENSITY

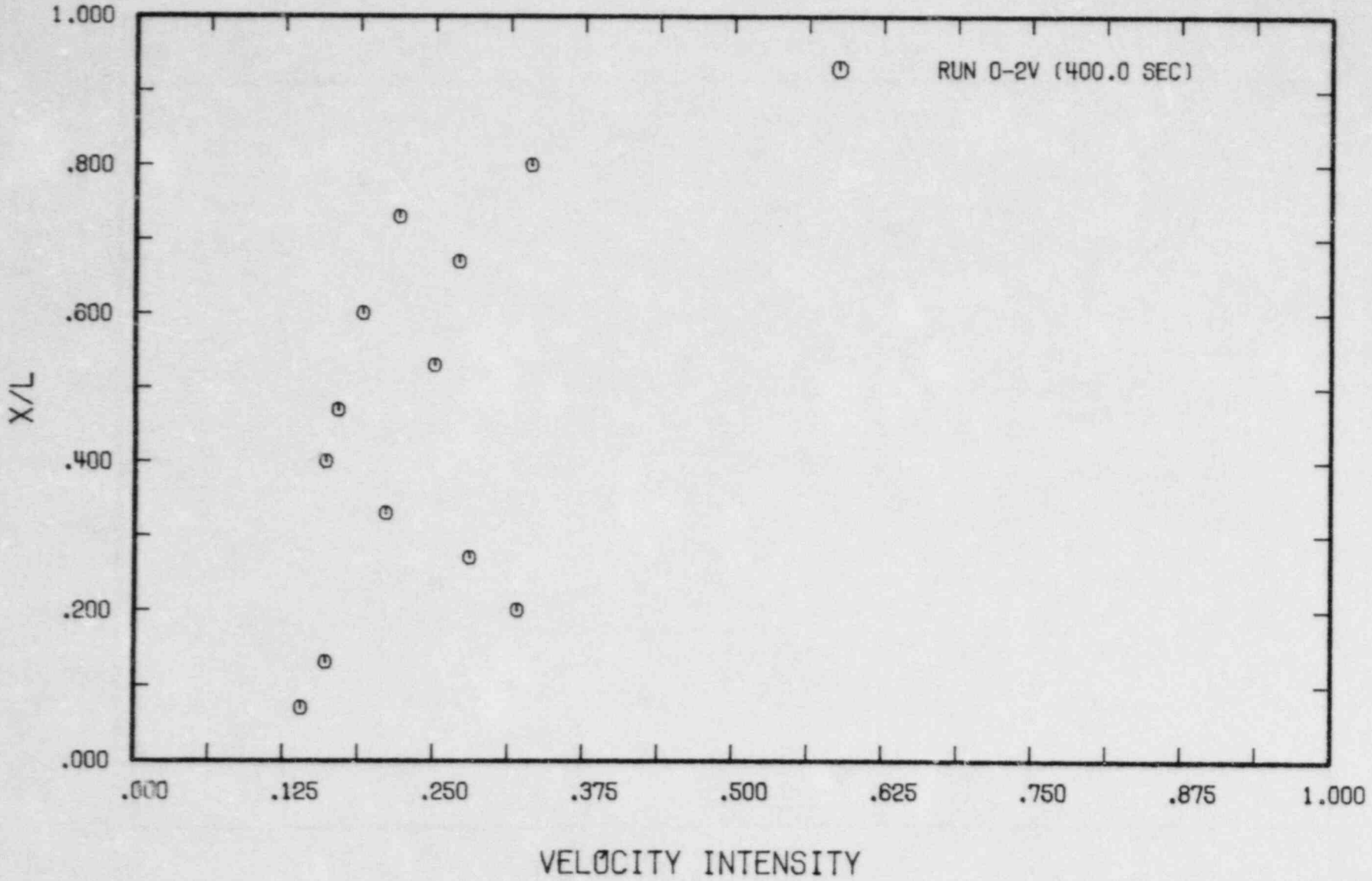
RUN 0-2V (400.0 SEC)
1.000
.800
.600
.400
.200
.000
X/L
.000
.125
.250
.375
.500
.625
.750
.875
1.000
VELOCITY INTENSITY

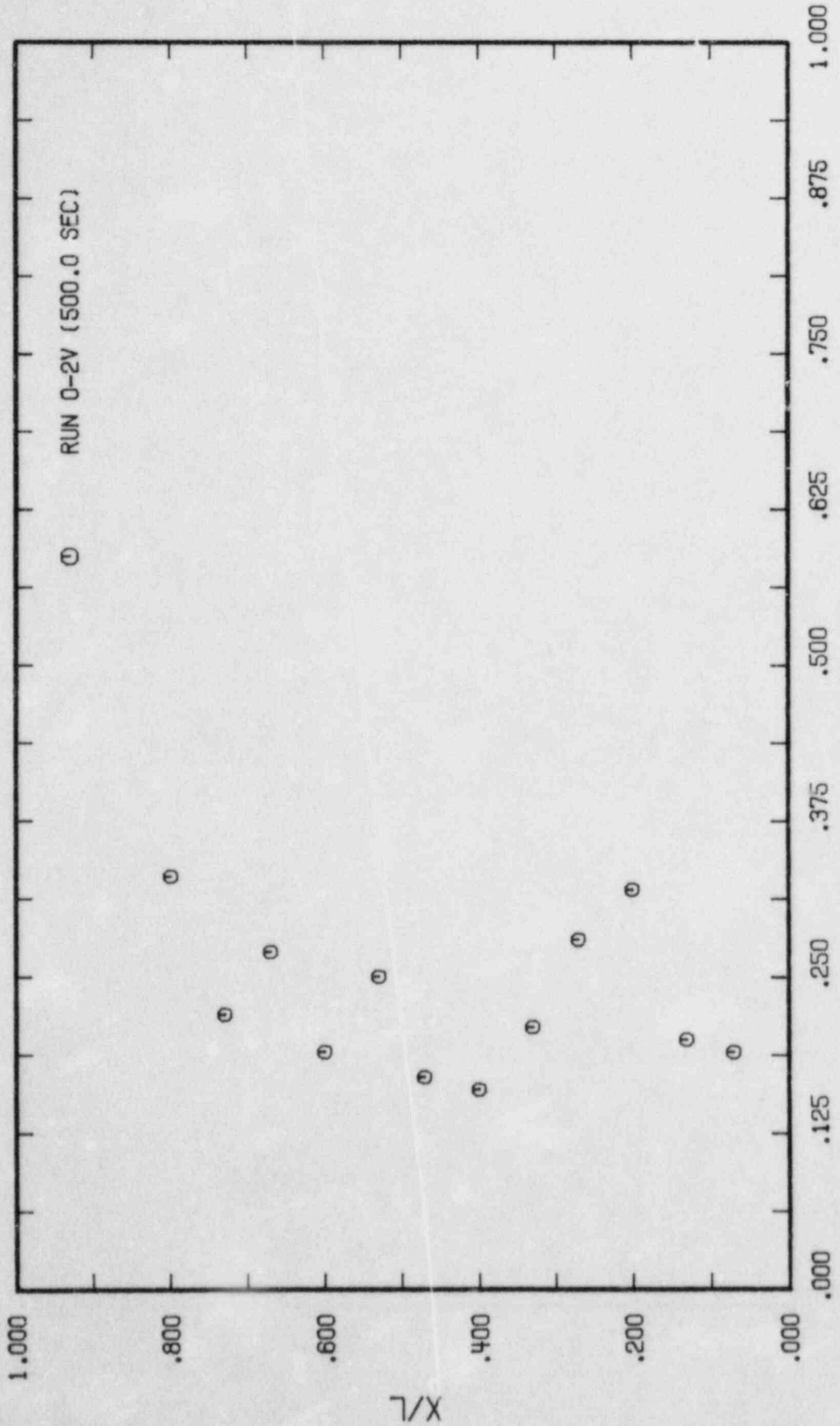
RUN 0-2V (500.0 SEC)
X/L
1.000
.800
.600
.400
.200
.000
.000
.125
.250
.375
.500
.625
.750
.875
1.000
VELOCITY INTENSITY

APPENDIX B: TABULATED DATA

LIST OF TABLES

Run 0-1C

DATA FROM TRAVERSE NR. : 1 RUN: 0 - 1C

		COLD LEG (TR1)				DOWNCOMER (TR2)				AMBIENT (ST1)		
TIME	FLOW	Y/D	C1	CPR1	CPR/C	X/L	C2	CPR2	CPR/C	C3	CPR3	CPR/C
SEC.	GPM.		%	%			%	%		%	%	
88.	10.182	0.074	1.924	0.064	0.033	0.167	1.021	0.229	0.225	0.057	0.080	1.410
94.	10.182	0.148	1.827	0.057	0.031	0.233	1.084	0.225	0.207	0.152	0.035	0.230
99.	10.182	0.222	1.786	0.064	0.036	0.300	1.026	0.149	0.145	0.165	0.038	0.231
104.	10.182	0.296	1.664	0.095	0.057	0.367	1.041	0.113	0.109	0.186	0.033	0.176
109.	10.139	0.370	1.528	0.081	0.053	0.433	0.843	0.135	0.160	0.293	0.022	0.073
114.	10.139	0.444	1.346	0.083	0.062	0.500	0.720	0.165	0.229	0.242	0.015	0.062
119.	10.139	0.519	1.030	0.218	0.212	0.567	0.909	0.221	0.244	0.250	0.020	0.080
125.	10.052	0.593	1.135	0.209	0.184	0.633	0.865	0.158	0.183	0.306	0.007	0.021
130.	10.052	0.667	0.581	0.267	0.460	0.700	0.365	0.381	1.042	0.352	0.024	0.068
135.	10.052	0.741	0.225	0.058	0.256	0.767	0.926	0.425	0.459	0.414	0.024	0.058
140.	10.052	0.815	0.039	0.091	2.346	0.833	0.909	0.240	0.264	0.372	0.013	0.035
145.	10.052	0.889	0.137	0.125	0.910	0.900	0.716	0.298	0.416	0.409	0.017	0.041

DATA FROM TRAVERSE NR. : 2 RUN: 0 - 1C

		COLD LEG (TR1)				DOWNCOMER (TR2)				AMBIENT (ST1)		
TIME	FLOW	Y/D	C1	CPR1	CPR/C	X/L	C2	CPR2	CPR/C	C3	CPR3	CPR/C
SEC.	GPM.		%	%			%	%		%	%	
164.	9.922	0.889	0.080	0.095	1.184	0.900	1.359	0.197	0.145	0.491	0.019	0.038
169.	9.965	0.815	0.185	0.043	0.235	0.833	1.285	0.118	0.092	0.487	0.008	0.017
175.	9.965	0.741	0.542	0.221	0.407	0.767	1.046	0.277	0.265	0.478	0.008	0.016
180.	9.965	0.667	1.178	0.063	0.054	0.700	1.100	0.357	0.324	0.465	0.006	0.014
185.	9.965	0.593	1.224	0.043	0.035	0.633	0.862	0.328	0.381	0.500	0.043	0.087
190.	9.922	0.519	1.273	0.063	0.049	0.567	0.418	0.122	0.291	0.579	0.007	0.013
195.	9.965	0.444	1.272	0.095	0.074	0.500	1.286	0.228	0.177	0.610	0.015	0.025
200.	9.879	0.370	1.827	0.186	0.102	0.433	1.066	0.334	0.313	0.784	0.086	0.109
206.	9.879	0.296	2.250	0.069	0.031	0.367	1.039	0.554	0.533	0.830	0.038	0.046
211.	9.835	0.222	2.424	0.060	0.025	0.300	1.342	0.300	0.224	0.823	0.029	0.036
216.	9.792	0.148	2.592	0.036	0.014	0.233	1.074	0.279	0.260	0.950	0.033	0.034
221.	9.792	0.074	2.768	0.036	0.013	0.167	1.485	0.224	0.151	0.892	0.024	0.027

DATA FROM TRAVERSE NR. : 3 RUN: 0 - 1C

		COLD LEG (TR1)				DOWNCOMER (TR2)				AMBIENT (ST1)		
TIME	FLOW	Y/D	C1	CPR1	CPR/C	X/L	C2	CPR2	CPR/C	C3	CPR3	CPR/C
SEC.	GPM.		%	%			%	%		%	%	
242.	9.792	0.074	2.580	0.064	0.025	0.167	0.727	0.460	0.633	1.019	0.050	0.050
248.	9.792	0.148	2.616	0.053	0.020	0.233	1.636	0.185	0.113	1.083	0.009	0.008
253.	9.792	0.222	2.491	0.047	0.019	0.300	1.590	0.302	0.190	1.113	0.011	0.009
258.	9.748	0.296	2.486	0.067	0.027	0.367	1.480	0.298	0.201	1.120	0.006	0.005
263.	9.748	0.370	2.206	0.157	0.071	0.433	1.712	0.171	0.100	1.109	0.003	0.003
268.	9.705	0.444	1.450	0.161	0.111	0.500	1.314	0.110	0.084	1.112	0.003	0.003
274.	9.705	0.519	1.283	0.051	0.039	0.567	1.375	0.204	0.149	1.145	0.029	0.026
279.	9.748	0.593	1.148	0.067	0.058	0.633	1.353	0.101	0.075	1.210	0.019	0.016
284.	9.705	0.667	1.213	0.069	0.057	0.700	1.177	0.057	0.049	1.186	0.026	0.022
289.	9.662	0.741	1.152	0.046	0.040	0.767	1.300	0.148	0.114	1.171	0.008	0.007
294.	9.662	0.815	1.017	0.122	0.120	0.833	1.377	0.261	0.189	1.174	0.004	0.004
299.	9.618	0.889	0.822	0.088	0.108	0.900	1.512	0.233	0.154	1.184	0.006	0.005

DATA FROM TRAVERSE NR. : 4 RUN: 0 - 1C

		COLD LEG (TR1)				DOWNCOMER (TR2)				AMBIENT (ST1)		
TIME	FLOW	Y/D	C1	CPR1	CPR/C	X/L	C2	CPR2	CPR/C	C3	CPR3	CPR/C
SEC.	GPM.		%	%			%	%		%	%	
322.	9.575	0.889	1.126	0.047	0.041	0.900	1.538	0.185	0.120	1.286	0.006	0.004
328.	9.575	0.815	1.108	0.031	0.028	0.833	1.629	0.177	0.109	1.273	0.007	0.005
333.	9.575	0.741	1.133	0.015	0.013	0.767	1.576	0.115	0.073	1.286	0.008	0.006
338.	9.575	0.667	1.232	0.087	0.071	0.700	1.553	0.221	0.142	1.297	0.003	0.002
343.	9.531	0.593	1.424	0.080	0.056	0.633	1.655	0.224	0.136	1.319	0.015	0.012
348.	9.488	0.519	1.374	0.062	0.045	0.567	1.701	0.296	0.174	1.410	0.037	0.026
354.	9.488	0.444	1.686	0.210	0.125	0.500	1.865	0.299	0.160	1.484	0.013	0.009
359.	9.488	0.370	2.310	0.198	0.086	0.433	1.673	0.166	0.099	1.428	0.005	0.004
364.	9.575	0.296	2.532	0.036	0.014	0.367	1.704	0.167	0.098	1.425	0.021	0.015
369.	9.531	0.222	2.734	0.054	0.020	0.300	1.905	0.223	0.117	1.487	0.013	0.009
374.	9.531	0.148	2.825	0.017	0.006	0.233	1.958	0.219	0.112	1.438	0.013	0.009
379.	9.488	0.074	2.843	0.038	0.013	0.167	1.925	0.228	0.119	1.440	0.007	0.005

DATA FROM TRAVERSE NR. : 5 RUN: 0 - 1C

		COLD LEG (TR1)				DOWNCOMER (TR2)				AMBIENT (ST1)		
TIME	FLOW	Y/D	C1	CPR1	CPR/C	X/L	C2	CPR2	CPR/C	C3	CPR3	CPR/C
SEC.	GPM.		%	%			%	%		%	%	
402.	9.445	0.074	3.006	0.031	0.010	0.167	2.248	0.182	0.081	1.545	0.020	0.013
407.	9.488	0.148	2.852	0.036	0.013	0.233	2.171	0.196	0.090	1.593	0.029	0.018
412.	9.488	0.222	2.812	0.034	0.012	0.300	1.951	0.263	0.135	1.594	0.015	0.009
417.	9.445	0.296	2.749	0.046	0.017	0.367	1.430	0.063	0.044	1.600	0.011	0.007
422.	9.401	0.370	2.575	0.088	0.034	0.433	1.562	0.088	0.056	1.600	0.004	0.003
428.	9.358	0.444	2.166	0.113	0.052	0.500	2.155	0.190	0.088	1.611	0.015	0.010
433.	9.401	0.519	1.904	0.148	0.078	0.567	2.126	0.156	0.073	1.632	0.004	0.003
438.	9.445	0.593	2.035	0.124	0.061	0.633	1.875	0.326	0.174	1.639	0.004	0.002
443.	9.488	0.667	1.904	0.077	0.040	0.700	1.999	0.191	0.096	1.703	0.034	0.020
448.	9.662	0.741	1.505	0.123	0.082	0.767	1.706	0.209	0.123	1.739	0.027	0.016
453.	9.748	0.815	1.533	0.039	0.025	0.833	2.023	0.121	0.060	1.685	0.005	0.003
459.	9.835	0.889	1.581	0.043	0.027	0.900	1.984	0.204	0.103	1.739	0.042	0.024

DATA FROM TRAVERSE NR. : 6 RUN: 0 - 1C

		COLD LEG (TR1)				DOWNCOMER (TR2)				AMBIENT (ST1)		
TIME	FLOW	Y/D	C1	CPR1	CPR/C	X/L	C2	CPR2	CPR/C	C3	CPR3	CPR/C
SEC.	GPM.		%	%			%	%		%	%	
479.	10.182	0.869	1.619	0.037	0.023	0.900	2.247	0.174	0.077	1.755	0.010	0.006
484.	10.22[illegible]	0.815	1.748	0.068	0.039	0.833	1.985	0.227	0.115	1.768	0.007	0.004
489.	10.226	0.741	1.808	0.091	0.050	0.767	1.880	0.282	0.150	1.797	0.010	0.006
494.	10.139	0.667	1.972	0.140	0.071	0.700	2.237	0.142	0.063	1.823	0.024	0.013
499.	10.269	0.593	2.050	0.196	0.096	0.633	2.365	0.199	0.084	1.952	0.017	0.009
505.	10.443	0.519	2.442	0.129	0.053	0.567	2.098	0.183	0.087	1.945	0.013	0.007
510.	10.356	0.444	2.507	0.166	0.066	0.500	1.920	0.062	0.032	1.918	0.008	0.004
515.	10.226	0.370	2.955	0.100	0.034	0.433	1.886	0.075	0.040	1.896	0.019	0.010
520.	10.269	0.296	3.055	0.029	0.010	0.367	2.232	0.394	0.177	1.896	0.016	0.008
525.	10.356	0.222	3.186	0.026	0.008	0.300	2.486	0.254	0.102	1.925	0.005	0.003
531.	10.312	0.148	3.337	0.049	0.015	0.233	2.049	0.252	0.123	1.928	0.005	0.003
536.	10.182	0.074	3.471	0.065	0.019	0.167	1.829	0.102	0.056	1.918	0.004	0.002

DATA FROM TRAVERSE NR. : 7 RUN: 0 - 1C

		COLD LEG (TR1)				DOWNCOMER (TR2)				AMBIENT (ST1)		
TIME	FLOW	Y/D	C1	CPR1	CPR/C	X/L	C2	CPR2	CPR/C	C3	CPR3	CPR/C
SEC.	GPM.		%	%			%	%		%	%	
556.	10.182	0.074	3.389	0.037	0.011	0.167	2.706	0.172	0.064	1.991	0.014	0.007
561.	10.182	0.148	3.347	0.033	0.010	0.233	2.118	0.323	0.153	2.091	0.068	0.033
567.	10.226	0.222	3.287	0.054	0.017	0.300	2.480	0.278	0.112	2.148	0.013	0.006
572.	10.226	0.296	3.283	0.060	0.018	0.367	2.179	0.069	0.032	2.132	0.008	0.004
577.	10.095	0.370	3.193	0.024	0.008	0.433	2.242	0.219	0.097	2.124	0.005	0.002
582.	10.009	0.444	3.038	0.133	0.044	0.500	2.491	0.229	0.092	2.122	0.006	0.003
587.	10.009	0.519	2.580	0.072	0.028	0.567	2.697	0.102	0.038	2.131	0.005	0.002
592.	10.139	0.593	2.188	0.145	0.066	0.633	2.663	0.185	0.069	2.134	0.005	0.002
598.	10.139	0.667	2.160	0.058	0.027	0.700	2.487	0.403	0.162	2.125	0.005	0.002
603.	10.182	0.741	2.018	0.083	0.041	0.767	2.025	0.210	0.104	2.125	0.008	0.004
608.	10.182	0.815	2.041	0.048	0.024	0.833	2.680	0.320	0.120	2.150	0.006	0.003
613.	10.182	0.889	2.098	0.032	0.015	0.900	2.688	0.199	0.074	2.267	0.049	0.022

DATA FROM TRAVERSE NR. : 8 RUN: 0 - 1C

		COLD LEG (TR1)				DOWNCOMER (TR2)				AMBIENT (ST1)		
TIME	FLOW	Y/D	C1	CPR1	CPR/C	X/L	C2	CPR2	CPR/C	C3	CPR3	CPR/C
SEC.	GPM.		%	%			%	%		%	%	
698.	10.095	0.889	2.351	0.032	0.013	0.900	2.583	0.037	0.014	2.566	0.014	0.005
703.	10.095	0.815	2.417	0.024	0.010	0.833	2.643	0.093	0.035	2.545	0.008	0.003
709.	10.052	0.741	2.388	0.061	0.026	0.767	2.702	0.108	0.040	2.545	0.006	0.002
714.	10.052	0.667	2.377	0.022	0.009	0.700	2.614	0.133	0.051	2.556	0.011	0.004
719.	10.052	0.593	2.560	0.095	0.037	0.633	2.900	0.205	0.071	2.598	0.006	0.002
724.	10.052	0.519	2.618	0.118	0.045	0.567	2.765	0.084	0.030	2.609	0.007	0.003
729.	10.095	0.444	2.951	0.075	0.026	0.500	2.721	0.136	0.050	2.593	0.007	0.003
735.	10.052	0.370	3.366	0.103	0.031	0.433	2.953	0.276	0.094	2.591	0.005	0.002
740.	10.052	0.296	3.465	0.044	0.013	0.367	3.047	0.290	0.095	2.595	0.007	0.003
745.	10.009	0.222	3.653	0.047	0.013	0.300	2.824	0.147	0.052	2.660	0.033	0.012
750.	10.009	0.148	3.736	0.033	0.009	0.233	3.076	0.286	0.093	2.727	0.024	0.009
755.	10.052	0.074	3.793	0.032	0.008	0.167	2.811	0.224	0.080	2.743	0.007	0.003

DATA FROM TRAVERSE NR. : 9 RUN: 0 - 1C

		COLD LEG (TR1)				DOWNCOMER (TR2)				AMBIENT (ST1)		
TIME	FLOW	Y/D	C1	CPR1	CPR/C	X/L	C2	CPR2	CPR/C	C3	CPR3	CPR/C
SEC.	GPM.		%	%			%	%		%	%	
778.	10.139	0.074	3.818	0.043	0.011	0.167	3.247	0.160	0.049	2.748	0.013	0.005
784.	10.095	0.148	3.823	0.027	0.007	0.233	2.883	0.168	0.058	2.774	0.019	0.007
789.	10.009	0.222	3.752	0.039	0.010	0.300	2.573	0.083	0.032	2.838	0.016	0.006
794.	10.009	0.296	3.633	0.096	0.027	0.367	2.861	0.398	0.139	2.847	0.009	0.003
799.	10.009	0.370	3.517	0.044	0.012	0.433	3.115	0.157	0.050	2.835	0.005	0.002
804.	10.009	0.444	3.121	0.188	0.060	0.500	2.919	0.324	0.111	2.843	0.010	0.003
810.	10.009	0.519	2.961	0.096	0.032	0.567	2.590	0.075	0.029	2.854	0.025	0.009
815.	9.922	0.593	2.746	0.033	0.012	0.633	2.959	0.246	0.083	2.895	0.016	0.005
820.	9.922	0.667	2.717	0.036	0.013	0.700	3.153	0.092	0.029	2.890	0.007	0.002
825.	10.009	0.741	2.748	0.042	0.015	0.767	3.051	0.149	0.049	2.889	0.008	0.003
830.	10.052	0.815	2.794	0.058	0.021	0.833	2.941	0.115	0.039	2.887	0.008	0.003
835.	10.052	0.889	2.807	0.024	0.009	0.900	2.921	0.175	0.060	2.938	0.067	0.023

DATA FROM TRAVERSE NR. : 10 RUN: 0 - 1C

		COLD LEG (TR1)				DOWNCOMER (TR2)				AMBIENT (ST1)		
TIME	FLOW	Y/D	C1	CPR1	CPR/C	X/L	C2	CPR2	CPR/C	C3	CPR3	CPR/C
SEC.	GPM.		%	%			%	%		%	%	
857.	10.052	0.889	2.769	0.028	0.010	0.900	3.141	0.164	0.052	3.040	0.009	0.003
862.	10.009	0.815	2.782	0.037	0.013	0.833	3.031	0.141	0.046	3.047	0.026	0.009
867.	9.965	0.741	2.777	0.021	0.008	0.767	2.905	0.107	0.037	3.036	0.017	0.005
872.	9.922	0.667	2.843	0.060	0.021	0.700	2.898	0.157	0.054	3.058	0.005	0.002
878.	9.965	0.593	2.881	0.046	0.016	0.633	3.229	0.065	0.020	3.072	0.012	0.004
883.	10.052	0.519	2.862	0.074	0.026	0.567	3.153	0.129	0.041	3.101	0.009	0.003
888.	10.009	0.444	3.335	0.201	0.060	0.500	3.312	0.155	0.047	3.074	0.014	0.004
893.	10.052	0.370	3.735	0.100	0.027	0.433	3.283	0.158	0.048	3.095	0.009	0.003
898.	10.052	0.296	3.839	0.027	0.007	0.367	3.484	0.191	0.055	3.096	0.014	0.005
904.	10.009	0.222	3.954	0.030	0.008	0.300	3.505	0.160	0.046	3.099	0.013	0.004
909.	9.965	0.148	4.008	0.021	0.005	0.233	3.327	0.145	0.044	3.197	0.026	0.008
914.	9.879	0.074	4.018	0.021	0.005	0.167	3.276	0.167	0.051	3.179	0.021	0.007

Run 0-1V

DATA FROM TRAVERSE NR. : 1 RUN: 0 - 1V

		COLD LEG (TR1)				DOWNCOMER (TR2)			
TIME	FLOW	Y/D	U1	UPR1	UPR/U	X/L	U2	UPR2	UPR/U
SEC.	GPM.		CM/S	CM/S			CM/S	CM/S	
92.	10.052	0.074	19.243	0.691	0.036	0.167	16.173	1.799	0.111
97.	10.052	0.148	18.087	0.698	0.039	0.233	16.335	1.689	0.103
102.	10.009	0.222	17.550	0.647	0.037	0.300	12.758	3.071	0.241
107.	9.922	0.296	16.830	0.520	0.031	0.367	14.760	2.116	0.143
113.	10.009	0.370	14.069	1.665	0.118	0.433	9.002	3.759	0.418
118.	9.922	0.444	6.459	2.435	0.377	0.500	8.541	2.623	0.307
123.	9.922	0.519	7.798	2.713	0.348	0.567	8.291	3.784	0.456
128.	10.009	0.593	6.891	2.398	0.348	0.633	10.125	2.564	0.253
133.	9.965	0.667	7.053	2.792	0.396	0.700	5.176	1.191	0.230
138.	9.922	0.741	7.330	4.459	0.608	0.767	5.248	1.713	0.326
144.	9.965	0.815	6.296	3.150	0.500	0.833	5.432	1.373	0.253
149.	9.922	0.889	2.263	1.192	0.527	0.900	6.210	2.307	0.371

DATA FROM TRAVERSE NR. : 2 RUN: 0 - 1V

		COLD LEG (TR1)				DOWNCOMER (TR2)			
TIME	FLOW	Y/D	U1	UPR1	UPR/U	X/L	U2	UPR2	UPR/U
SEC.	GPM.		CM/S	CM/S			CM/S	CM/S	
171.	9.922	0.889	5.976	2.120	0.355	0.900	11.108	2.455	0.221
176.	9.879	0.815	8.277	4.084	0.493	0.833	3.822	2.448	0.641
181.	9.835	0.741	10.836	2.252	0.208	0.767	1.624	0.724	0.446
187.	9.835	0.667	9.754	3.234	0.332	0.700	1.995	0.879	0.441
192.	9.965	0.593	9.658	2.728	0.282	0.633	3.651	1.260	0.345
197.	9.922	0.519	6.079	2.100	0.345	0.567	4.029	1.581	0.392
202.	9.879	0.444	4.488	2.155	0.480	0.500	4.512	2.582	0.572
207.	9.922	0.370	6.524	0.881	0.135	0.433	5.724	1.133	0.198
212.	9.922	0.296	7.146	0.797	0.112	0.367	6.559	1.831	0.279
218.	9.922	0.222	10.513	1.472	0.140	0.300	5.188	1.570	0.303
223.	9.879	0.148	11.304	0.663	0.059	0.233	4.778	1.725	0.361
228.	9.965	0.074	11.815	0.804	0.068	0.167	7.967	3.397	0.426

DATA FROM TRAVERSE NR. : 3 RUN: 0 - 1V

		COLD LEG (TR1)				DOWNCOMER (TR2)			
TIME	FLOW	Y/D	U1	UPR1	UPR/U	X/L	U2	UPR2	UPR/U
SEC.	GPM.		CM/S	CM/S			CM/S	CM/S	
259.	9.835	0.074	10.862	0.603	0.056	0.167	14.737	4.160	0.282
264.	9.879	0.148	11.178	0.623	0.056	0.233	7.039	4.286	0.609
269.	9.922	0.222	10.234	0.556	0.054	0.300	8.397	5.030	0.599
274.	9.835	0.296	8.109	1.036	0.128	0.367	12.636	3.319	0.263
279.	9.705	0.370	3.911	2.269	0.580	0.433	10.248	3.942	0.385
285.	9.705	0.444	1.705	1.479	0.868	0.500	7.059	3.739	0.530
290.	9.922	0.519	3.567	1.360	0.381	0.567	9.214	2.633	0.286
295.	9.879	0.593	2.090	1.600	0.766	0.633	10.342	2.647	0.256
300.	9.792	0.667	3.945	1.278	0.324	0.700	10.560	3.597	0.341
305.	9.705	0.741	3.614	2.122	0.587	0.767	7.868	3.612	0.459
310.	9.705	0.815	4.443	2.635	0.593	0.833	8.196	2.695	0.329
316.	9.705	0.889	3.962	1.939	0.489	0.900	8.598	3.107	0.361

DATA FROM TRAVERSE NR. : 4 RUN: 0 - 1V

		COLD LEG (TR1)				DOWNCOMER (TR2)			
TIME	FLOW	Y/D	U1	UPR1	UPR/U	X/L	U2	UPR2	UPR/U
SEC.	GPM.		CM/S	CM/S			CM/S	CM/S	
336.	9.835	0.889	7.248	3.289	0.454	0.900	5.040	1.808	0.359
341.	9.792	0.815	11.257	1.977	0.176	0.833	6.456	2.392	0.370
347.	9.748	0.741	6.209	2.747	0.442	0.767	4.705	2.212	0.470
352.	9.835	0.667	10.054	2.935	0.292	0.700	5.574	2.243	0.402
357.	10.139	0.593	7.915	4.119	0.520	0.633	9.617	4.597	0.478
362.	10.356	0.519	3.850	1.378	0.358	0.567	13.188	3.094	0.235
367.	10.356	0.444	3.728	1.549	0.415	0.500	6.310	2.438	0.386
373.	10.312	0.370	6.398	1.259	0.197	0.433	9.053	3.591	0.397
378.	10.269	0.296	10.443	0.766	0.073	0.367	11.727	4.531	0.386
383.	10.182	0.222	10.994	1.199	0.109	0.300	9.052	2.132	0.236
388.	10.269	0.148	11.832	0.617	0.052	0.233	12.738	3.267	0.257
393.	10.269	0.074	10.288	0.709	0.069	0.167	14.631	2.895	0.198

DATA FROM TRAVERSE NR. : 5 RUN: 0 - 1V

		COLD LEG (TR1)				DOWNCOMER (TR2)			
TIME	FLOW	Y/D	U1	UPR1	UPR/U	X/L	U2	UPR2	UPR/U
SEC.	GPM.		CM/S	CM/S			CM/S	CM/S	
414.	10.269	0.074	9.810	0.615	0.063	0.167	14.129	2.490	0.176
420.	10.226	0.148	10.147	0.601	0.059	0.233	13.416	2.494	0.186
425.	10.226	0.222	9.173	0.593	0.065	0.300	10.537	2.458	0.233
430.	10.269	0.296	7.697	0.803	0.104	0.367	12.887	3.338	0.259
435.	10.269	0.370	5.737	1.777	0.310	0.433	9.492	2.482	0.261
440.	10.226	0.444	2.013	0.857	0.426	0.500	9.141	2.089	0.229
446.	10.269	0.519	3.357	2.319	0.691	0.567	10.997	1.996	0.181
451.	10.312	0.593	5.910	2.788	0.472	0.633	8.950	2.423	0.271
456.	10.269	0.667	5.867	2.797	0.477	0.700	10.318	4.126	0.400
461.	10.269	0.741	4.354	1.446	0.332	0.767	10.320	3.093	0.300
466.	10.269	0.815	2.721	1.475	0.542	0.833	5.276	2.320	0.440
471.	10.269	0.889	4.848	1.526	0.315	0.900	5.285	1.375	0.260

DATA FROM TRAVERSE NR. : 6 RUN: 0 - 1V

		COLD LEG (TR1)				DOWNCOMER (TR2)			
TIME	FLOW	Y/D	U1	UPR1	UPR/U	X/L	U2	UPR2	UPR/U
SEC.	GPM.		CM/S	CM/S			CM/S	CM/S	
492.	10.226	0.889	5.842	2.277	0.390	0.900	8.028	3.703	0.461
497.	10.269	0.815	3.169	1.959	0.618	0.833	10.256	2.761	0.269
503.	10.182	0.741	1.901	0.878	0.462	0.767	10.401	2.151	0.207
508.	10.182	0.667	3.738	2.229	0.596	0.700	8.915	2.024	0.227
513.	10.139	0.593	4.976	1.851	0.372	0.633	8.141	2.392	0.294
518.	10.226	0.519	1.886	0.842	0.446	0.567	7.468	2.578	0.345
523.	10.226	0.444	1.754	1.269	0.723	0.500	8.302	1.719	0.207
529.	10.139	0.370	4.384	0.723	0.165	0.433	12.849	2.890	0.225
534.	10.052	0.296	6.281	0.479	0.076	0.367	10.857	3.001	0.276
539.	10.095	0.222	7.585	0.677	0.089	0.300	12.008	2.820	0.235
544.	10.226	0.148	7.843	1.625	0.207	0.233	11.894	2.906	0.244
549.	10.182	0.074	9.960	0.520	0.052	0.167	14.554	2.336	0.160

DATA FROM TRAVERSE NR. : 7 RUN: 0 - 1V

		COLD LEG (TR1)				DOWNCOMER (TR2)			
TIME	FLOW	Y/D	U1	UPR1	UPR/U	X/L	U2	UPR2	UPR/U
SEC.	GPM.		CM/S	CM/S			CM/S	CM/S	
574.	10.182	0.074	11.822	0.942	0.080	0.167	13.256	2.395	0.181
579.	10.182	0.148	12.421	0.645	0.052	0.233	12.976	2.819	0.217
584.	10.182	0.222	11.549	0.504	0.044	0.300	10.783	2.264	0.210
589.	10.182	0.296	11.119	0.877	0.079	0.367	10.251	2.074	0.202
594.	10.182	0.370	5.758	2.198	0.382	0.433	8.632	2.764	0.320
599.	10.226	0.444	1.512	0.566	0.374	0.500	7.086	2.452	0.346
605.	10.226	0.519	3.348	1.435	0.429	0.567	8.498	1.853	0.218
610.	10.182	0.593	4.040	1.497	0.370	0.633	7.978	1.894	0.237
615.	10.139	0.667	4.441	1.620	0.365	0.700	8.792	1.145	0.130
620.	10.182	0.741	2.056	1.103	0.536	0.767	6.398	1.744	0.273
625.	10.182	0.815	2.472	1.616	0.654	0.833	6.775	1.418	0.209
631.	10.182	0.889	2.074	0.942	0.454	0.900	6.430	1.947	0.303

DATA FROM TRAVERSE NR. : 8 RUN: 0 - 1V

		COLD LEG (TR1)				DOWNCOMER (TR2)			
TIME	FLOW	Y/D	U1	UPR1	UPR/U	X/L	U2	UPR2	UPR/U
SEC.	GPM.		CM/S	CM/S			CM/S	CM/S	
651.	10.182	0.889	5.377	1.887	0.351	0.900	7.307	2.351	0.322
657.	10.095	0.815	6.099	2.916	0.478	0.833	9.588	2.595	0.271
662.	10.095	0.741	4.284	1.701	0.397	0.767	11.227	2.006	0.179
667.	10.095	0.667	4.756	1.478	0.311	0.700	7.483	1.736	0.232
672.	10.095	0.593	6.615	2.295	0.347	0.633	6.871	1.531	0.223
677.	10.139	0.519	7.362	3.148	0.428	0.567	6.991	1.047	0.150
682.	10.095	0.444	2.339	0.716	0.306	0.500	8.599	2.442	0.284
688.	10.095	0.370	4.993	1.698	0.340	0.433	12.398	2.269	0.183
693.	10.139	0.296	10.075	1.094	0.109	0.367	7.707	2.523	0.327
698.	10.095	0.222	12.257	0.857	0.070	0.300	11.208	1.814	0.162
703.	10.095	0.148	11.504	0.802	0.070	0.233	13.263	1.980	0.149
708.	10.139	0.074	11.159	1.004	0.090	0.167	7.330	4.403	0.601

DATA FROM TRAVERSE NR. : 9 RUN: 0 - 1V

		COLD LEG (TR1)				DOWNCOMER (TR2)			
TIME	FLOW	Y/D	U1	UPR1	UPR/U	X/L	U2	UPR2	UPR/U
SEC.	GPM.		CM/S	CM/S			CM/S	CM/S	
730.	10.139	0.074	10.644	0.846	0.079	0.167	8.723	3.424	0.392
736.	10.182	0.148	10.878	0.897	0.083	0.233	11.184	1.779	0.159
741.	10.139	0.222	10.589	1.047	0.099	0.300	9.029	1.887	0.209
746.	10.095	0.296	10.016	0.513	0.051	0.367	8.696	2.496	0.287
751.	10.182	0.370	5.374	3.138	0.584	0.433	6.657	3.007	0.452
756.	10.182	0.444	1.863	0.962	0.516	0.500	6.911	3.179	0.460
762.	10.095	0.519	1.016	0.718	0.707	0.567	9.326	1.612	0.173
767.	10.052	0.593	2.095	1.203	0.574	0.633	8.952	2.036	0.227
772.	10.095	0.667	3.781	2.134	0.564	0.700	5.820	2.033	0.349
777.	10.052	0.741	4.315	1.842	0.427	0.767	4.979	1.812	0.364
782.	10.095	0.815	4.956	2.327	0.470	0.833	9.734	1.801	0.185
787.	10.095	0.889	3.630	2.039	0.562	0.900	7.638	2.029	0.266

DATA FROM TRAVERSE NR. : 10 RUN: 0 - 1V

		COLD LEG (TR1)				DOWNCOMER (TR2)			
TIME	FLOW	Y/D	U1	UPR1	UPR/U	X/L	U2	UPR2	UPR/U
SEC.	GPM.		CM/S	CM/S			CM/S	CM/S	
809.	10.182	0.889	4.727	2.099	0.444	0.900	6.412	2.426	0.378
814.	10.182	0.815	2.256	1.535	0.681	0.833	5.935	1.693	0.285
819.	10.095	0.741	2.308	1.218	0.528	0.767	7.229	2.040	0.282
824.	10.139	0.667	4.221	3.176	0.753	0.700	7.468	1.647	0.221
829.	10.139	0.593	3.265	2.487	0.762	0.633	7.777	2.527	0.325
835.	10.095	0.519	1.288	0.731	0.568	0.567	7.642	2.304	0.301
840.	10.095	0.444	1.730	0.542	0.313	0.500	4.610	2.393	0.519
845.	10.052	0.370	6.300	2.207	0.350	0.433	5.964	2.357	0.395
850.	10.052	0.296	7.903	1.087	0.138	0.367	8.283	2.100	0.253
855.	10.095	0.222	9.419	1.000	0.106	0.300	9.859	2.006	0.203
860.	10.095	0.148	9.423	0.762	0.081	0.233	11.860	1.427	0.120
866.	10.139	0.074	11.036	0.600	0.054	0.167	11.837	1.591	0.134

DATA FROM TRAVERSE NR. : 11 RUN: 0 - 1V

		COLD LEG (TR1)				DOWNCOMER (TR2)			
TIME	FLOW	Y/D	U1	UPR1	UPR/U	X/L	U2	UPR2	UPR/U
SEC.	GPM.		CM/S	CM/S			CM/S	CM/S	
887.	10.052	0.074	10.424	1.736	0.167	0.167	11.192	2.187	0.195
892.	10.095	0.148	12.051	0.610	0.051	0.233	10.615	2.095	0.197
898.	10.139	0.222	12.528	0.564	0.045	0.300	8.295	1.525	0.184
903.	10.139	0.296	11.536	0.994	0.086	0.367	8.473	1.574	0.186
908.	10.095	0.370	6.239	1.355	0.217	0.433	6.874	1.371	0.199
913.	10.052	0.444	2.925	1.349	0.461	0.500	8.721	2.229	0.256
918.	10.095	0.519	3.934	1.146	0.291	0.567	7.573	2.326	0.307
924.	10.052	0.593	6.012	2.576	0.428	0.633	5.605	1.709	0.305
929.	10.009	0.667	3.178	1.304	0.411	0.700	5.490	2.164	0.394
934.	10.052	0.741	2.817	1.154	0.410	0.767	5.938	1.975	0.333
939.	10.095	0.815	3.514	0.844	0.240	0.833	6.179	1.825	0.295
944.	10.095	0.889	2.113	0.765	0.362	0.900	6.677	2.181	0.327

DATA FROM TRAVERSE NR. : 12 RUN: 0 - 1V

		COLD LEG (TR1)				DOWNCOMER (TR2)			
TIME	FLOW	Y/D	U1	UPR1	UPR/U	X/L	U2	UPR2	UPR/U
SEC.	GPM.		CM/S	CM/S			CM/S	CM/S	
966.	10.052	0.889	4.449	1.214	0.273	0.900	4.718	1.964	0.416
972.	10.052	0.815	3.113	1.174	0.377	0.833	5.376	2.112	0.393
977.	10.052	0.741	5.347	2.287	0.428	0.767	6.525	1.816	0.278
982.	10.052	0.667	4.877	1.893	0.388	0.700	8.486	2.654	0.313
987.	10.095	0.593	3.620	1.678	0.464	0.633	9.224	2.177	0.236
992.	10.139	0.519	4.365	1.172	0.269	0.567	8.072	1.618	0.200
997.	10.052	0.444	2.751	0.614	0.223	0.500	7.466	1.845	0.247
1003.	10.052	0.370	4.906	0.581	0.118	0.433	9.484	1.782	0.188
1008.	10.139	0.296	9.869	1.452	0.147	0.367	8.562	2.199	0.257
1013.	10.139	0.222	13.126	1.374	0.105	0.300	8.141	1.744	0.214
1018.	10.095	0.148	13.657	1.643	0.120	0.233	12.268	1.722	0.140
1023.	10.052	0.074	11.388	0.484	0.043	0.167	10.484	2.305	0.220

Run 0-2C

DATA FROM TRAVERSE NR. : 1 RUN: 0 - 2C

		COLD LEG (TR1)				DOWNCOMER (TR2)				AMBIENT (ST1)		
TIME	FLOW	Y/D	C1	CPR1	CPR/C	X/L	C2	CPR2	CPR/C	C3	CPR3	CPR/C
SEC.	GPM.		%	%			%	%		%	%	
78.	20.638	0.074	3.083	0.053	0.017	0.167	1.882	0.315	0.167	0.694	0.038	0.055
83.	20.551	0.148	3.111	0.039	0.012	0.233	1.734	0.282	0.163	0.644	0.042	0.065
88.	20.551	0.222	3.028	0.072	0.024	0.300	1.169	0.340	0.291	0.653	0.021	0.032
93.	20.638	0.296	2.858	0.122	0.043	0.367	1.156	0.347	0.300	0.788	0.053	0.068
98.	20.594	0.370	2.517	0.294	0.117	0.433	1.309	0.193	0.147	0.919	0.071	0.078
104.	20.551	0.444	0.986	0.456	0.463	0.500	1.377	0.316	0.229	1.023	0.045	0.044
109.	20.464	0.519	1.095	0.104	0.095	0.567	1.694	0.253	0.149	0.901	0.023	0.026
114.	20.464	0.593	0.557	0.273	0.489	0.633	1.453	0.336	0.231	1.053	0.040	0.038
119.	20.421	0.667	0.354	0.131	0.369	0.700	1.958	0.401	0.205	1.084	0.012	0.011
124.	20.377	0.741	0.548	0.048	0.088	0.767	1.558	0.412	0.264	1.066	0.012	0.011
130.	20.421	0.815	0.461	0.115	0.250	0.833	1.295	0.091	0.070	1.257	0.071	0.057
135.	20.421	0.889	0.736	0.125	0.169	0.900	0.773	0.280	0.363	1.284	0.039	0.030

DATA FROM TRAVERSE NR. : 2 RUN: 0 - 2C

		COLD LEG (TR1)				DOWNCOMER (TR2)				AMBIENT (ST1)		
TIME	FLOW	Y/D	C1	CPR1	CPR/C	X/L	C2	CPR2	CPR/C	C3	CPR3	CPR/C
SEC.	GPM.		%	%			%	%		%	%	
158.	20.334	0.889	0.974	0.089	0.091	0.900	1.584	0.112	0.070	1.377	0.006	0.004
163.	20.941	0.815	1.019	0.058	0.057	0.833	1.330	0.145	0.109	1.330	0.016	0.012
168.	21.288	0.741	1.166	0.049	0.042	0.767	1.778	0.255	0.143	1.424	0.071	0.050
173.	21.288	0.667	1.189	0.050	0.042	0.700	1.537	0.407	0.264	1.463	0.009	0.006
178.	21.115	0.593	1.131	0.091	0.081	0.633	1.916	0.204	0.106	1.495	0.009	0.006
183.	21.115	0.519	1.202	0.174	0.145	0.567	1.724	0.394	0.229	1.494	0.008	0.005
189.	21.158	0.444	1.706	0.186	0.109	0.500	1.930	0.179	0.093	1.551	0.020	0.013
194.	21.158	0.370	2.691	0.245	0.091	0.433	2.306	0.307	0.133	1.611	0.033	0.020
199.	21.115	0.296	3.424	0.142	0.042	0.367	2.066	0.278	0.135	1.654	0.010	0.006
204.	21.115	0.222	3.746	0.070	0.019	0.300	2.630	0.488	0.186	1.696	0.055	0.033
209.	21.245	0.148	3.866	0.071	0.018	0.233	2.621	0.417	0.159	1.819	0.028	0.015
215.	21.158	0.074	3.972	0.029	0.007	0.167	2.168	0.377	0.174	1.965	0.070	0.035

DATA FROM TRAVERSE NR. : 3 RUN: 0 - 2C

		COLD LEG (TR1)				DOWNCOMER (TR2)				AMBIENT (ST1)		
TIME	FLOW	Y/D	C1	CPR1	CPR/C	X/L	C2	CPR2	CPR/C	C3	CPR3	CPR/C
SEC.	GPM.		%	%			%	%		%	%	
235.	21.202	0.074	3.948	0.043	0.011	0.167	1.477	0.116	0.078	1.997	0.030	0.015
240.	21.115	0.148	3.906	0.075	0.019	0.233	1.536	0.115	0.075	2.070	0.025	0.012
246.	21.072	0.222	3.791	0.037	0.010	0.300	2.511	0.849	0.338	2.084	0.052	0.025
251.	20.941	0.296	3.756	0.051	0.014	0.367	2.784	0.443	0.159	2.125	0.027	0.013
256.	20.247	0.370	3.496	0.091	0.026	0.433	2.837	0.266	0.094	2.068	0.015	0.007
261.	20.074	0.444	2.708	0.432	0.159	0.500	2.228	0.397	0.178	2.099	0.078	0.037
266.	20.030	0.519	2.136	0.103	0.048	0.567	2.434	0.342	0.140	2.243	0.011	0.005
271.	20.074	0.593	1.932	0.201	0.104	0.633	2.700	0.209	0.077	2.265	0.038	0.017
277.	19.944	0.667	1.712	0.071	0.041	0.700	2.595	0.201	0.077	2.313	0.063	0.027
282.	19.900	0.741	1.846	0.058	0.031	0.767	2.497	0.315	0.126	2.256	0.028	0.012
287.	19.944	0.815	1.805	0.034	0.019	0.833	2.363	0.325	0.137	2.338	0.029	0.013
292.	19.987	0.889	1.826	0.034	0.018	0.900	2.589	0.532	0.205	2.419	0.017	0.007

DATA FROM TRAVERSE NR. : 4 RUN: 0 - 2C

		COLD LEG (TR1)				DOWNCOMER (TR2)				AMBIENT (ST1)		
TIME	FLOW	Y/D	C1	CPR1	CPR/C	X/L	C2	CPR2	CPR/C	C3	CPR3	CPR/C
SEC.	GPM.		%	%			%	%		%	%	
314.	20.074	0.889	1.955	0.072	0.037	0.900	2.633	0.232	0.088	2.582	0.022	0.009
319.	19.944	0.815	2.142	0.057	0.026	0.833	2.453	0.167	0.068	2.555	0.026	0.010
324.	19.857	0.741	2.195	0.050	0.023	0.767	2.573	0.416	0.162	2.610	0.007	0.003
329.	19.900	0.667	2.192	0.227	0.103	0.700	3.153	0.347	0.110	2.583	0.020	0.008
334.	19.900	0.593	2.546	0.069	0.027	0.633	2.362	0.251	0.106	2.548	0.005	0.002
339.	19.813	0.519	2.584	0.126	0.049	0.567	2.692	0.362	0.135	2.543	0.007	0.003
345.	19.900	0.444	2.807	0.191	0.068	0.500	3.223	0.201	0.062	2.645	0.049	0.018
350.	19.857	0.370	3.331	0.199	0.060	0.433	3.099	0.313	0.101	2.685	0.051	0.019
355.	19.944	0.296	3.984	0.093	0.023	0.367	2.802	0.185	0.066	2.819	0.013	0.005
360.	19.900	0.222	4.184	0.105	0.025	0.300	3.004	0.293	0.098	2.808	0.030	0.011
365.	19.944	0.148	4.281	0.097	0.023	0.233	2.680	0.209	0.078	2.828	0.011	0.004
371.	19.813	0.074	4.565	0.028	0.006	0.167	3.492	0.356	0.102	2.834	0.006	0.002

DATA FROM TRAVERSE NR. : 5 RUN: 0 - 2C

		COLD LEG (TR1)				DOWNCOMER (TR2)				AMBIENT (ST1)		
TIME	FLOW	Y/D	C1	CPR1	CPR/C	X/L	C2	CPR2	CPR/C	C3	CPR3	CPR/C
SEC.	GPM.		%	%			%	%		%	%	
392.	19.813	0.074	4.714	0.044	0.009	0.167	3.452	0.506	0.147	2.871	0.012	0.004
397.	19.857	0.148	4.693	0.034	0.007	0.233	2.948	0.307	0.104	2.922	0.020	0.007
403.	19.857	0.222	4.553	0.081	0.018	0.300	3.526	0.647	0.183	2.993	0.028	0.009
408.	19.770	0.296	4.402	0.042	0.009	0.367	3.494	0.321	0.092	3.098	0.024	0.008
413.	19.727	0.370	4.092	0.253	0.062	0.433	3.603	0.358	0.099	3.135	0.013	0.004
418.	19.770	0.444	3.472	0.236	0.068	0.500	3.473	0.237	0.068	3.085	0.010	0.003
423.	19.857	0.519	2.919	0.064	0.022	0.567	3.305	0.290	0.088	3.165	0.016	0.005
428.	19.987	0.593	2.800	0.025	0.009	0.633	3.283	0.191	0.058	3.159	0.006	0.002
434.	20.074	0.667	2.841	0.073	0.026	0.700	3.297	0.123	0.037	3.290	0.074	0.022
439.	20.117	0.741	2.756	0.015	0.005	0.767	3.242	0.109	0.034	3.360	0.016	0.005
444.	20.117	0.815	2.709	0.029	0.011	0.833	3.312	0.105	0.032	3.352	0.014	0.004
449.	20.117	0.889	2.745	0.027	0.010	0.900	3.245	0.098	0.030	3.364	0.006	0.002

DATA FROM TRAVERSE NR. : 6 RUN: 0 - 2C

		COLD LEG (TR1)				DOWNCOMER (TR2)				AMBIENT (ST1)		
TIME	FLOW	Y/D	C1	CPR1	CPR/C	X/L	C2	CPR2	CPR/C	C3	CPR3	CPR/C
SEC.	GPM.		%	%			%	%		%	%	
470.	20.117	0.889	2.851	0.015	0.005	0.900	3.368	0.200	0.059	3.487	0.042	0.012
475.	20.074	0.815	2.894	0.044	0.015	0.833	3.404	0.253	0.074	3.469	0.022	0.006
481.	19.987	0.741	2.950	0.020	0.007	0.767	3.303	0.265	0.080	3.463	0.011	0.003
486.	19.987	0.667	2.960	0.025	0.009	0.700	3.601	0.174	0.048	3.577	0.075	0.021
491.	20.117	0.593	3.052	0.024	0.008	0.633	3.705	0.196	0.053	3.622	0.027	0.007
496.	20.117	0.519	3.129	0.050	0.016	0.567	3.896	0.240	0.062	3.647	0.020	0.005
501.	20.377	0.444	3.342	0.059	0.018	0.500	3.663	0.241	0.066	3.633	0.006	0.002
507.	20.421	0.370	3.968	0.282	0.071	0.433	3.758	0.189	0.050	3.674	0.035	0.010
512.	20.551	0.296	4.537	0.076	0.017	0.367	3.838	0.354	0.092	3.708	0.020	0.005
517.	20.464	0.222	4.733	0.038	0.008	0.300	4.021	0.307	0.076	3.755	0.013	0.004
522.	20.551	0.148	4.765	0.026	0.006	0.233	4.017	0.250	0.062	3.807	0.008	0.002
527.	20.551	0.074	4.845	0.049	0.010	0.167	3.941	0.298	0.076	3.817	0.012	0.003

Run 0-2V

DATA FROM TRAVERSE NR. : 1 RUN: 0 - 2V

		COLD LEG (TR1)				DOWNCOMER (TR2)			
TIME	FLOW	Y/D	U1	UPR1	UPR/U	X/L	U2	UPR2	UPR/U
SEC.	GPM.		CM/S	CM/S			CM/S	CM/S	
61.	20.334	0.074	19.994	1.137	0.057	0.167	19.455	4.273	0.220
66.	20.334	0.148	17.097	1.263	0.074	0.233	19.474	3.304	0.170
71.	20.334	0.222	18.325	1.039	0.057	0.300	15.299	2.732	0.179
76.	20.204	0.296	15.989	1.145	0.072	0.367	13.421	4.769	0.355
82.	20.247	0.370	9.777	3.597	0.368	0.433	9.808	3.980	0.406
87.	20.247	0.444	2.354	0.800	0.340	0.500	15.820	2.890	0.183
92.	20.204	0.519	4.859	2.086	0.429	0.567	14.934	3.404	0.228
97.	20.161	0.593	4.308	2.168	0.503	0.633	11.839	1.853	0.156
102.	20.074	0.667	4.354	2.275	0.523	0.700	12.885	4.585	0.356
107.	20.117	0.741	10.264	3.185	0.310	0.767	11.809	4.531	0.384
113.	20.204	0.815	5.518	2.953	0.535	0.833	10.305	2.402	0.233
118.	20.117	0.889	6.705	3.485	0.520	0.900	9.437	2.281	0.242

DATA FROM TRAVERSE NR. : 2 RUN: 0 - 2V

		COLD LEG (TR1)				DOWNCOMER (TR2)			
TIME	FLOW	Y/D	U1	UPR1	UPR/U	X/L	U2	UPR2	UPR/U
SEC.	GPM.		CM/S	CM/S			CM/S	CM/S	
139.	20.161	0.889	7.513	2.845	0.379	0.900	13.143	3.594	0.273
144.	20.161	0.815	5.140	2.902	0.564	0.833	12.366	3.282	0.265
149.	20.117	0.741	8.542	4.774	0.559	0.767	12.657	4.701	0.371
154.	19.944	0.667	5.300	2.449	0.462	0.700	13.774	3.929	0.285
160.	19.944	0.593	6.348	3.487	0.549	0.633	13.455	2.526	0.188
165.	20.508	0.519	3.813	2.792	0.732	0.567	13.358	3.898	0.292
170.	21.158	0.444	2.929	2.010	0.686	0.500	16.884	3.246	0.192
175.	21.288	0.370	10.044	3.705	0.369	0.433	15.084	3.786	0.251
180.	20.421	0.296	16.687	2.658	0.159	0.367	14.890	2.618	0.176
186.	20.117	0.222	19.620	1.053	0.054	0.300	17.604	4.416	0.251
191.	20.594	0.148	19.394	0.699	0.036	0.233	20.903	4.408	0.211
196.	20.725	0.074	20.451	1.523	0.074	0.167	21.877	3.552	0.162

DATA FROM TRAVERSE NR. : 3 RUN: 0 - 2V

		COLD LEG (TR1)				DOWNCOMER (TR2)			
TIME	FLOW	Y/D	U1	UPR1	UPR/U	X/L	U2	UPR2	UPR/U
SEC.	GPM.		CM/S	CM/S			CM/S	CM/S	
217.	20.725	0.074	17.608	0.920	0.052	0.167	22.283	3.894	0.175
222.	20.768	0.148	18.230	0.943	0.052	0.233	20.587	3.969	0.193
227.	20.291	0.222	16.559	0.870	0.053	0.300	19.411	3.997	0.206
233.	20.464	0.296	14.794	1.112	0.075	0.367	17.704	3.785	0.214
238.	20.725	0.370	7.910	4.743	0.600	0.433	16.575	5.323	0.321
243.	20.811	0.444	2.020	1.510	0.747	0.500	16.002	3.889	0.243
248.	20.681	0.519	10.707	3.753	0.350	0.567	14.546	4.299	0.296
253.	20.681	0.593	4.206	2.066	0.491	0.633	10.531	1.930	0.183
259.	20.681	0.667	3.448	2.155	0.625	0.700	11.936	3.415	0.286
264.	20.594	0.741	4.122	2.066	0.501	0.767	12.902	2.271	0.176
269.	20.594	0.815	4.330	2.019	0.466	0.833	9.390	2.856	0.304
274.	20.594	0.889	3.995	2.354	0.589	0.900	8.429	3.173	0.376

DATA FROM TRAVERSE NR. : 4 RUN: 0 - 2V

		COLD LEG (TR1)				DOWNCOMER (TR2)			
TIME	FLOW	Y/D	U1	UPR1	UPR/U	X/L	U2	UPR2	UPR/U
SEC.	GPM.		CM/S	CM/S			CM/S	CM/S	
295.	20.551	0.889	3.902	2.428	0.622	0.900	9.951	2.791	0.281
301.	20.334	0.815	4.659	2.057	0.441	0.833	9.324	3.664	0.393
306.	20.334	0.741	3.860	1.896	0.491	0.767	14.745	3.062	0.208
311.	20.464	0.667	4.035	2.498	0.619	0.700	13.729	2.789	0.203
316.	20.464	0.593	5.209	4.188	0.804	0.633	13.507	4.731	0.350
321.	20.421	0.519	2.083	1.145	0.550	0.567	10.605	4.488	0.423
327.	20.551	0.444	2.290	2.110	0.921	0.500	14.989	6.166	0.411
332.	20.377	0.370	11.522	1.191	0.103	0.433	18.999	4.842	0.255
337.	20.421	0.296	13.715	1.342	0.098	0.367	17.581	2.522	0.143
342.	20.508	0.222	16.036	1.197	0.075	0.300	17.938	3.471	0.193
347.	20.508	0.148	17.668	0.923	0.052	0.233	18.965	3.488	0.184
352.	20.551	0.074	15.949	1.149	0.072	0.167	16.813	2.313	0.138

DATA FROM TRAVERSE NR. : 5 RUN: 0 - 2V

		COLD LEG (TR1)				DOWNCOMER (TR2)			
TIME	FLOW	Y/D	U1	UPR1	UPR/U	X/L	U2	UPR2	UPR/U
SEC.	GPM.		CM/S	CM/S			CM/S	CM/S	
454.	19.076	0.889	4.870	2.696	0.554	0.900	13.367	2.737	0.205
459.	18.989	0.815	2.284	1.488	0.651	0.833	12.096	3.851	0.318
464.	18.989	0.741	2.585	1.592	0.616	0.767	14.018	3.193	0.228
469.	19.076	0.667	3.515	1.806	0.514	0.700	11.842	2.762	0.233
474.	19.033	0.593	2.818	1.565	0.555	0.633	10.633	2.649	0.249
480.	18.989	0.519	2.151	1.149	0.534	0.567	10.210	4.241	0.415
485.	19.033	0.444	1.458	0.949	0.651	0.500	15.214	3.307	0.217
490.	19.119	0.370	3.162	1.157	0.366	0.433	15.023	2.531	0.168
495.	19.076	0.296	10.592	1.231	0.116	0.367	16.649	3.675	0.221
500.	18.946	0.222	11.352	0.731	0.064	0.300	15.324	2.800	0.183
505.	18.902	0.148	11.209	1.016	0.091	0.233	17.976	3.503	0.195
511.	18.989	0.074	12.802	0.792	0.062	0.167	17.698	3.501	0.198

NRC FORM 335 (2 84) NRCM 1102, 3201, 3202

U.S. NUCLEAR REGULATORY COMMISSION

BIBLIOGRAPHIC DATA SHEET

SEE INSTRUCTIONS ON THE REVERSE

1. REPORT NUMBER (Assigned by TIDC, add Vol. No., if any)
NUREG/CR-3700

2. TITLE AND SUBTITLE
Decay of Buoyancy Driven Stratified Layers With Application to Pressurized Thermal Shock (PTS)

3. LEAVE BLANK

4. DATE REPORT COMPLETED
MONTH: February YEAR: 1984

5. AUTHOR(S)
T.G. Theofanous, H.R. Nourbakhsh, P. Gherson, K. Iyer

6. DATE REPORT ISSUED
MONTH: May YEAR: 1984

7. PERFORMING ORGANIZATION NAME AND MAILING ADDRESS (Include Zip Code)
School of Nuclear Engineering
Purdue University
West Lafayette, IN 47907

8. PROJECT/TASK/WORK UNIT NUMBER

9. FIN OR GRANT NUMBER
G1047
Grant No. NRC-G-04-83-003

10. SPONSORING ORGANIZATION NAME AND MAILING ADDRESS (Include Zip Code)
Division of Accident Evaluation
Office of Nuclear Regulatory Research
U.S. Nuclear Regulatory Commission
Washington, DC 20555

11a. TYPE OF REPORT

b. PERIOD COVERED (Inclusive dates)

12. SUPPLEMENTARY NOTES

13. ABSTRACT (200 words or less)

This report consists of two parts. In Part I physically based calculational models are proposed for predicting (a) conditions for stratification due to HPI in a circulating reactor loop (stratification model) and (b) cooldown transients due to HPI in a stagnated primary reactor fluid (thermal mixing model). The integral aspects of these models are confirmed by comparison to the CREARE 1/5-scale data. In part II the thermal mixing model is assessed in an integral as well as in a local sense by comparison to the first round of data from Purdue's 1/2-scale facility. These data are the only available large-scale data at this time and they are an important complement to CREARE's 1/5-scale results in constructing a basis for scale-up to reactor conditions. Facility construction, instrumentation, data reduction techniques and detailed experimental results are also included in Part II.

14. DOCUMENT ANALYSIS – a. KEYWORDS/DESCRIPTORS
Pressurized Thermal Shock
Stratification Criteria
Axisymmetric Jets (Plumes)
Froude Number

b. IDENTIFIERS/OPEN-ENDED TERMS

15. AVAILABILITY STATEMENT
Unlimited

16. SECURITY CLASSIFICATION
(This page) Unclassified
(This report) Unclassified

17. NUMBER OF PAGES

18. PRICE